



Numéro National de Thèse : 2018LYSEN033

THESE de DOCTORAT DE L'UNIVERSITE DE LYON

opérée par
l'Ecole Normale Supérieure de Lyon
en cotutelle avec
University of Nottingham

Ecole Doctorale N°340
Biologie Moléculaire, Intégrative et Cellulaire

Spécialité de doctorat : Biologie des plantes
Discipline : Sciences de la Vie

Soutenue publiquement le 28.09.2018, par :
Jekaterina TRUSKINA

The role of auxin in cell differentiation in meristems

Rôle de l'auxine dans la différenciation des cellules au sein des méristèmes

---

Devant le jury composé de :

Mme **Catherine BELLINI**, Professeure, Umeå Plant Science Center	Rapporteure
Mme **Zoe WILSON**, Professeure, University of Nottingham	Rapporteure
M. **Joop EM VERMEER**, Professeur, University of Zurich	Examinateur
M. **Renaud DUMAS**, Directeur de recherche, Université Grenoble Alpes	Examinateur
M. **Teva VERNOUX**, Directeur de recherche, ENS de Lyon	Directeur de thèse
M. **Anthony BISHOPP**, Chercheur, University of Nottingham	Co-tuteur de thèse

Thesis

submitted to the

University of Nottingham

for joint examination with the

ENS de Lyon

for the degree of

Doctor of Philosophy

by

Jekaterina Truskina

The role of auxin in cell differentiation in meristems

Rôle de l'auxine dans la différenciation des cellules au sein des méristèmes

---

Date of submission : 11.06.2018
Date of public defence : 28.09.2018

The thesis jury is composed of :

Mme **Catherine Bellini**, Professor, Umeå Plant Science Center	Reporter
Mme **Zoe Wilson**, Professor, University of Nottingham	Reporter
M. **Joop EM Vermeer**, Professor, University of Zurich	Examiner
M. **Renaud Dumas**, Research Director, Université Grenoble Alpes	Examiner
M. **Teva Vernoux**, Research Director, ENS de Lyon	Thesis director
M. **Anthony Bishopp**, University Research Fellow, University of Nottingham	Thesis co-director

Abstract

Auxin regulates plant growth and development through the transcription factors of the AUXIN RESPONSE FACTOR (ARF) gene family. Most notably in *Arabidopsis thaliana* ARF5, 6, 7, 8 and 19 activate expression of target genes in response to auxin. These five ARF activators control both variable and overlapping processes during plant development including regulation of growth at the root and the shoot apical meristems, lateral root and axillary shoot formation.

Each of the five ARF activators shows unique tissue-specific expression patterns in the root and the shoot associated with their distinct functions. This tissue-specific expression is likely derived from the differences in the control of ARF activator transcription. In this study the upstream regulators of ARF5, 6, 7, 8 and 19 transcription were identified. This was achieved by utilizing a high-throughput yeast one-hybrid (Y1H) method. The transient protoplast assay revealed that each ARF activator is controlled by specific transcriptional regulators and that the majority of these regulators are repressors of ARF transcription *in planta*. Mutants of the regulatory transcription factors were utilized to additionally investigate the interactions *in planta*. These mutants display auxin-related developmental phenotypes in the root and the shoot including alternations in growth kinetics, emergence of lateral organs, responses to auxin and altered expression of ARF activators.

Furthermore, this study additionally focuses on cross-talk between the auxin and cytokinin signaling pathways and its role in root and shoot development. One of the interactions identified in the Y1H screen is a repression of ARF7 by CRF10, a member of the Cytokinin Response Factors gene family. The importance of this interaction in maintaining architecture of the root apical meristem, in leaf senescence and in the phototropic response to blue light in hypocotyls is studied.

Résumé

L'auxine régule la croissance et le développement des plantes grâce aux facteurs de transcription de la famille des "*AUXIN RESPONSE FACTOR*" (*ARF*). Chez *Arabidopsis thaliana* en particulier, ARF5, 6, 7, 8 et 19 activent l'expression de gènes cibles en réponse à l'auxine. Ces cinq ARF activateurs contrôlent de façon plus ou moins redondante des processus divers au cours du développement de la plante, notamment la régulation des croissances au niveau des méristèmes racinaires et aériens ainsi que la formation des racines latérales ou des méristèmes axillaires.

Chacun de ces cinq ARF activateurs présente des patrons d'expression uniques dans chacun des tissus racinaires et aériens, en association avec leurs fonctions particulières. Il est probable que cette expression tissu-spécifique trouve son origine dans un contrôle différencié de leur transcription. Dans cette étude, des régulateurs amonts de la transcription de *ARF5, 6, 7, 8* et *19* ont été identifiés par une méthode haut-débit de crible simple hybride en levure (Y1H). Une procédure d'expression transitoire en protoplastes a permis de confirmer que l'expression de chaque ARF activateur est contrôlée par des régulateurs spécifiques, dont la majorité se comportent comme des répresseurs de la transcription des ARF *in planta*. Parmi les régulateurs identifiés, les facteurs de transcription ont été étudiés grâce à des mutants pour préciser les interactions *in planta*. Ces mutants montrent des phénotypes développementaux typiques de perturbations de l'auxine dans les racines et les tiges : altérations des cinétiques de croissance, de l'émergence des organes latéraux ou de réponses à l'auxine et modification de l'expression des ARF activateurs.

Par ailleurs, ce travail aborde également les dialogues entre les voies de signalisation de l'auxine et des cytokinines, et en particulier le rôle de ces interactions dans le développement des racines et des tiges. Une des interactions identifiées dans le crible Y1H est la répression de *ARF7* par *CRF10*, un gène membre de la famille des "Cytokinin Response Factors". Nous avons mis en évidence l'importance de cette interaction pour le maintien de l'architecture du méristème apical racinaire, pour la sénescence des feuille et pour la réponse phototropique à la lumière bleue dans les hypocotyles.

Acknowledgments

Teva and Tony, my most incredible supervisors, I own great gratitude to you both. You changed my life when you offered me this PhD position and since then, I spend awesome four years learning from you how to do science. When it comes to science your advices were always full of wisdom and experience guiding me through my thesis. I had amazing support from you both in my work but also in my life. I felt it from the start when you took this incredible effort to go through a huge pile of paperwork to organize this joint PhD. I felt it even more during my thesis when I was able to come up to any of you with my problems or difficulties at any time of the day, and you would always help me. Your kindness and friendliness made me feel great being a part of this project and I hope, both of you have become truly my friends.

Tony, with your incredible patience, enthusiasm and kindness you are a perfect mentor that anyone can wish for. I felt your support throughout the whole thesis starting from the first day when you helped me to get to Sutton Bonington campus and all the way through. You had a young new team consisting of PhD students just starting their thesis, all fresh and inexperience like me, and it was great to see how everyone in the team had a very happy successful PhD thanks to your great supervision. Thank you for everything, Tony!

Teva, it's your endless energy, dedication and kindness that made you the amazing mentor. You are a very busy person managing a whole laboratory, and yet you always found time for me as much as I needed. I learned so much from you and your experienced team of researchers. You have such a great team and it was amazing to feel a part of it. Thanks for everything, Teva!

Throughout my thesis I met many great people from all over the world and some of them became my friends.

In Nottingham, I was part of a great PhD student community with John, George, Ben and Nicky. Thanks a lot guys for your support! Especially, a great thank you to Nicky with whom we shared great times as friends. I also would like to thank Kamal for your friendliness and help during my stay in the lab. Jingyi, thank you for helping me with experiments, I wish you a good start on your PhD thesis with Tony, I am sure it

will be great! I would like to thank Malcolm for your kindness and gentle personality; you treat every person, even simple student like me, with such respect and patience, making them feel welcomed and a part of the great scientific community. Finally, I would like to thank all people from the lab for the friendly atmosphere.

In Lyon, I felt a true part of an incredible team. Carlos, thank you for all the great advices you gave me; you inspire everyone in the lab with your enthusiasm for science and your ingenious ideas. Stephanie, it was wonderfull to work with you together as a team. Antoine, Fabfab, Geraldine, Bihai, Jo and Guillaume, I thank you for all your support, great advices and friendliness during my thesis. I would like to thank also my friends from RDP Lucie and Claudia; the gardeners Alexis, Patrice and Justin for keeping my plants alive and well, and all the rest of the RDP for the friendly atmosphere.

My big gratitude is to my family who supported me throughout these four years, coping with me being away across the world in foreign countries. To my mom, my dad, my brother and my sister, I love you so much! And to my cat Frodo.

The biggest thank you is for one other person; you know who you are. You changed my life and supported me on this road to PhD. You made me happy like never before. I love you so much!

Finally, I would like to thank all the member of my thesis jury: Catherine Bellini, Zoe Wilson, Joop Vermeer and Renaud Dumas. You took a lot of effort to come on my defense, travelling from almost the North Pole (Umea), from England, from Switzerland and France. Thanks a lot!

Table of Contents

Abstract ... 2

Résumé ... 3

Acknowledgments ... 4

Abbreviations ... 10

Introduction ... 13

Plant embryonic development ... 14

Root growth and the root apical meristem ... 16

Root apical meristem morphology ... 16

Regulation of root apical meristem development ... 20

Lateral root development ... 24

Shoot apical meristem ... 27

The plant hormone auxin ... 32

The TIR1/AFB family of auxin receptors ... 37

The AUX/IAA repressors of auxin signalling ... 37

ARF transcription factors ... 38

ARF5 ... 40

ARF6 and ARF8 ... 43

ARF7 and ARF19 ... 43

The plant hormone cytokinin ... 45

Cytokinin signalling pathway ... 45

Cytokinin Response Factors (CRFs) ... 46

Aims of the thesis ... 49

Chapter I: The tissue-specific expression of ARF activators during growth and development in the RAM and the SAM ... 51

Introduction ... 51

Results ... 53

ARF activators are differentially expressed in the root and the shoot ... 53

ARF7 expression in the RAM is regulated at the first intron ... 61

ARF activator distribution can be post-transcriptionally regulated ... 64

Discussion ... 68

Tissue-specific expression of ARF activators provides insights into specificity and redundancy of their functions in plant development ... 68
Expression patterns of ARF activators fits their well-studied functions and suggests new potential functions ... 71
Which elements are important to correctly recapitulate expression patterns of genes? ... 73
Post-transcriptional movement or degradation of ARF proteins provides another level of control in the auxin signaling pathway ... 75
Material and methods ... 77
Cloning and generation of ARF reporter lines ... 77
Root microscopy ... 78
Shoot microscopy ... 79
Supplementary information ... 80
Chapter II: Auxin Response Factor (ARF) activators are transcriptionally regulated by gene-specific repressor network ... 84
Introduction ... 84
Results ... 92
Yeast one-hybrid assay revealed an elaborate network of transcription factors controlling expression of ARF activators ... 92
The majority of the ARF activator transcriptional regulators act as repressors ... 99
Publically available databases can be used to further validate and explore the interactions ... 104
Mutants of the regulatory transcription factors indicate co-regulation of multiple ARF activators ... 110
Expression of the several transcription factors is regulated by auxin ... 115
Mutants of the regulatory transcription factors show auxin-related defects in root and shoot development ... 117
Discussion ... 121
Does the yeast one-hybrid gene regulatory network reflect *in planta* gene interactions? ... 121
ARF activator expression is predominantly regulated by transcriptional repressors ... 123
Regulation of ARF8 by multiple transcription factors might indicate its special significance in auxin signaling ... 125
Gene regulatory network motifs describe regulations that could be important during development ... 128
Expression of ARF activators is co-regulated *in planta* ... 132
Material and methods ... 133
Plant material ... 133
Y1H assay ... 133
Transient expression in *Arabidopsis thaliana* protoplasts ... 134

Expression analysis with qRT-PCR 136
Expression analysis of crosses between ARF transcriptional reporter lines and T-DNA mutants 137
Shoot phenotype analysis of the TF mutants 137
Root phenotype analysis of the TF mutants 137
Growth on NPA for shoot phenotype analysis 138
Supplementary information 139
Chapter III: Cytokinin Response Factor 10 regulates ARF7 expression to control plant development 154
Introduction 154
Results 158
Genetic characterization of the *crf10* mutant 158
CRF10 is expressed in various tissues 162
crf10 mutant has an ARF7-dependant early senescence phenotype 165
crf10 mutant shows perturbation in hypocotyl response to blue light 169
crf10 mutant has a defect in root apical meristem morphology 170
Discussion 181
Is *crf10-1* a loss-of-function mutant? 181
Does CRF10 act in cytokinin signaling? 183
CRF10 and ARF7 antagonistically control leaf senescence 185
CRF10 and ARF7 are acting together in hypocotyl phototropic response 186
CRF10 and ARF7 are involved in the maintenance of the root apical meristem 187
Material and methods 191
Plant material 191
Analysis of the conserved regions within the CRF10 protein across *A. thaliana* ecotypes 191
Genetic analysis of the *crf10-1* mutant 191
Expression analysis with qRT-PCR 191
Cloning and generation of transgenic lines 192
Root microscopy 193
Shoot microscopy 193
Shoot phenotype analysis 194
Early senescence phenotype analysis 194
Chlorophyll measurement 194
Hypocotyl phototropism assay 194
Root phenotype analysis 195

Supplementary information 196

General discussion 200

ARF activators in control of plant development 200

ARF activators diversify and specialize during evolution 204

Component of auxin signaling pathway show specificity in expression patterns 208

ARF activator expression is predominantly regulated by gene repression mechanism 209

Auxin and cytokinin interactions regulate many aspects of plant development 210

Appendix 212

Overview of primers used in this study 212

List of primers 214

References 228

Abbreviations

2,4-D	2,4-dichlorophenoxyacetic acid
4-Cl-IAA	4-chloroindole-3-acetic acid
A. thaliana	*Arabidopsis thaliana*
AHK	*Arabidopsis* histidine kinase
AHP	*Arabidopsis* histidine phosphotransfer protein
AM	Axillary meristem
AP2/ERF	APETALA2/ethylene response factor
Arabidopsis	*Arabidopsis thaliana*
ARF	Auxin response factor
ARR	*Arabidopsis* response regulator
AUX/IAA	AUXIN/INDOLE-3-ACETIC ACID
AUX/LAX	AUXIN1/LIKE AUX1
AuxRe	Auxin responsive element
bp	Base pair
C. elegans	*Caenorhabditis elegans*
CCR	C-terminal conserved region
CDF4	CYCLIC DOF FACTOR 4
CLE	CLAVATA3/EMBRYO SURROUNDING REGION-RELATED
CKX	Cytokinin oxidase/dehydrogenase
CLV3	CLAVATA3
CRF	Cytokinin response factor
CSC	Columella stem cells
DII	Domain II
DBD	DNA-binding domain
DD	Dimerization domain

Dicamba	3,6-dichloro-2-methoxybenzoic acid
DMAPP	Dimethylallyl pyrophosphate
DNA	Deoxyribonucleic acid
FD	Flanking domain
GFP	Green fluorescent protein
IAA	Indole-3-acetic acid
IME	intron mediated enhancement
IPT	Isopentenyltransferase
KAN1	KANADI 1
kb	kilobase pair
L1, L2, L3	Layers 1, 2 or 3 of the shoot apical meristem
LBD	Lateral organ boundaries domain
LHW	LONESOME HIGHWAY
LOG	LONELY GUY
LR	Lateral root
MP	MONOPTEROS
MR	Middle region
mRNA	Messenger RNA
mTQ2	mTurquoise2
NAA	1-naphthaleneacetic acid
NLS	Nuclear localization signal or sequence
NPA	1-N-Naphthylphthalamic acid
PAA	Phenylacetic acid
PB1	Phox and Bem1
pH	Potential of Hydrogen
Picloram	4-amino-3,5,6-trichloropicolinic acid
PIN	PIN-formed protein
PLT	PLETHORA

QC	Quiescent center
RAM	Root apical meristem
RNA	Ribonucleic acid
SAM	Shoot apical meristem
SCR	SCARECROW
SHR	SHORT ROOT
SMB	SOMBRERO
STM	SHOOT MERISTEMLESS
TAA	TRYPTOPHAN AMINOTRANSFERASE OF ARABIDOPSIS
TIR1/AFB	TRANSPORT INHIBITOR RESPONSE1/AUXIN SIGNALING F-BOX PROTEIN
TMO	TARGET OF MP
WOX5	WUSCHEL related homeobox 5
WUS	WUSCHEL

Introduction

Among the diverse groups of living organisms land plants constitute a unique branch. Unlike animals, plants generally spend the majority of their life immobilized and restricted to a small space where they gradually progress through each stage of their development starting from a small embryo and proceeding as an adult plant capable of reproduction. During this whole developmental cycle plants have to continually adapt themselves to the ever-changing environmental conditions. They are subjected to a variety of stresses from various abiotic factors such as changes in temperature, humidity, nutrient content of the soil as well as biotic factors including attacks by pathogens and herbivore animals. To overcome these difficulties plants continue to produce new organs and modify the existing organs postembryonically. For example, phosphorus deficiency in the soil causes plants to alter their root architecture by attenuating growth of the primary root, forming more lateral roots and root hairs and this allows for more efficient forging of the available space (Bates and Lynch 1996, Bates and Lynch 2001, Brown *et al.* 2012, Giehl and von Wiren 2014, Lopez-Bucio *et al.* 2002, Sanchez-Calderon *et al.* 2005, Williamson *et al.* 2001).

The constant growth and adaptation of the body structure throughout the entire life requires tight communication between various tissues to initiate or terminate the development of specific organs. On a cellular level this complex communication between tissues and cells is mediated by various mechanisms involving plant hormones, mobile transcription factors, small mobile peptides and small RNAs (Chaiwanon *et al.* 2016, Van Norman *et al.* 2011). Among the plant hormones, auxin and cytokinin control a large number of developmental processes in either an antagonistic or synergistic manner. For example, auxin inhibits formation of axillary branches while cytokinin acts in opposition promoting growth of axillary branches (Muller and Leyser 2011, Shimizu-Sato *et al.* 2009). Similarly, antagonistic interactions between auxin and cytokinin control specification of vasculature tissues in the root (Bishopp *et al.* 2011, Vaughan-Hirsch *et al.* 2018).

Auxin and cytokinin appear to be key factors that regulate the formation and maintenance of the root and the shoot apical meristems (Su *et al.* 2011). The root and the shoot apical meristems are important sites of growth in the plant. They contain a pool of pluripotent stem cells that are able to divide, grow and differentiate

into various specific cell types (Heidstra and Sabatini 2014). In the root apical meristem (RAM) located at the root tip the primary root tissues are produced (Petricka *et al.* 2012). Shoot apical meristem (SAM) is found at the shoot apex; here all new flowers, leaves and axillary shoots are formed (Barton 2010, Murray *et al.* 2012). How auxin and cytokinin controls plant growth in the RAM and the SAM remains a subject of intensive research with key signalling pathways being discovered in the last 20 years. Nevertheless, many aspects of auxin and cytokinin involvement in growth regulation at the RAM and the SAM still remain to be explored.

This thesis focuses on genes involved in the auxin signalling pathway and their involvement in the root and shoot growth as well as on the crosstalk between auxin and cytokinin signalling pathways. For these reasons, this introduction will start with the detailed description of the plant development focusing on the growth of the root and the shoot, followed by description of the auxin and cytokinin signalling pathways. A stronger emphasis will be given to knowledge obtained using *Arabidopsis thaliana*, the model plant that was used in this study.

Plant embryonic development

Plants start their development from the zygote, a single totipotent cell. In *Arabidopsis thaliana*, the zygote undergoes a series of highly ordered cell divisions followed by cell differentiation that results in formation of the basic tissue types found in the mature plants including epidermis, vasculature, stem-cells and the ground tissue (Esau 1977). Several more specific tissue types develop post-embryonically including adventitious and lateral roots (Bellini *et al. 2*014), trichomes (Pattanaik *et al.* 2014) and root hair (Grierson *et al.* 2014).

The embryogenesis starts with an asymmetric division of the zygote cell producing the small apical and the elongated basal cells (Fig. In-1) (ten Hove *et al.* 2015). The apical cell will eventually give rise to the majority of the cells of the embryo whereas the lower basal cell will generate only a few specific cell types of the primary root: columella and the quiescent center (QC).

Following the initial asymmetric division, the upper apical cell will continue to divide; these divisions will partition the original cell volume without substantial cell expansion (Yoshida *et al.* 2014) (Fig. In-1). The lower basal cell will divide as well forming the suspensor domain (Fig. In-1). Together these divisions will form the globular stage

embryo with the roughly spherical shaped apical domain and the lower suspensor domain that looks like a vertical string of cells (Fig. In-1) (ten Howe *et al.* 2015).

During this stage, the uppermost suspensor cell called hypophysis is specified to become the root apical meristem founder cell (Dolan *et al.* 1993). The hypophysis divides to produce two daughter cells: the upper cell becomes the quiescent centre cell (QC) and the lower cell gives rise to columella initials and columella proper (Yoshida *et al.* 2013). The QC is a part of the root stem cell niche which incorporates mitotically inactive cells (Dubrovsky and Barlow 2015). Therefore the QC and the columella cell layers below it are derived from hypophysis. On the other hand, the lower tier of the sphere-shaped apical domain eventually gives rise to the rest of the root tissues including root vasculature, cortex, endodermis and epidermis layers (Fig. In-1) (ten Hove *et al.* 2015; Petricka *et al.* 2012, Yoshida *et al.* 2013).

The outer cells of the sphere-shaped apical domain divide anticlinally to form the epidermal tissue. On the other hand, the inner cells divide longitudinally to produce the vasculature and the ground tissues (Fig. In-1) (ten Hove *et al.* 2015). The increased number of cells leads to morphological transformation from the globular to the heart-stage embryo (ten Hove *et al.* 2015). At this stage the future cotyledons become distinguishable as two bulges. The shoot stem cell niche forms between the emerging cotyledon primordia (Zhang *et al.* 2017).

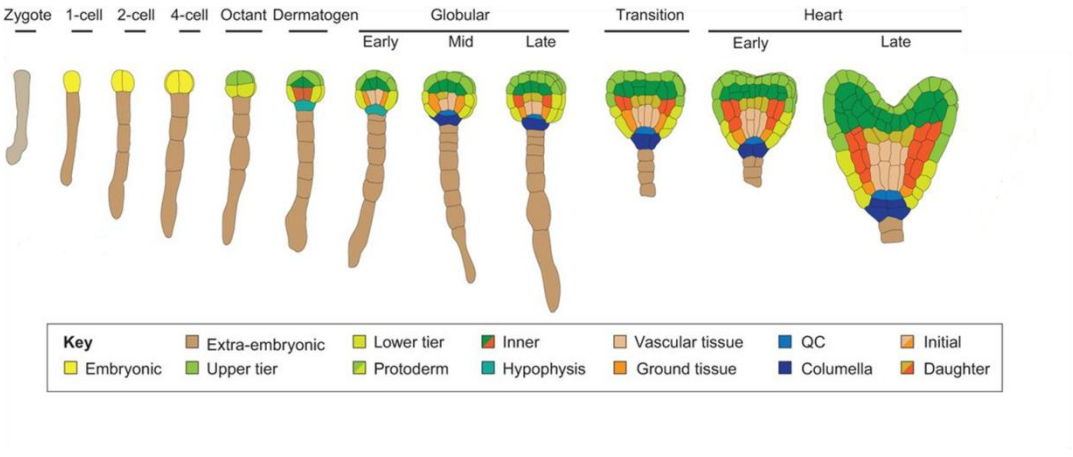

Fig. In-1. A schematic of embryonic development in *Arabidopsis thaliana* (ten Hove *et al.* 2015).

The shoot- and the root stem-cell niches are already established at the heart-stage embryo and are maintained in the mature plant where they function to produce new tissues and organs. After the heart-stage embryo, the provascular tissues within the cotyledons are formed, the hypocotyl and the root cellular organization is established, and the SAM acquired the three layer structure (Capron *et al.* 2009). The structural complexity of the fully-formed embryo equals that of the plant seedling (Capron *et al.* 2009). At the end of embryogenesis the cell divisions are arrested and the mature embryo remains inside the seed through a period of dormancy until the germination phase is initiated (Bentsink and Koornneef 2008).

Root growth and the root apical meristem

Root apical meristem morphology

As pointed out earlier, roots are dynamic structures that undergo developmental changes. Studies in various plant species reveal that the root growth is not indeterminate and that the growth rate of the root is not identical throughout its development. Postembryonically, the young primary root grows at accelerated rate for the first 1-2 weeks of the seedling growth (Chapman *et al.* 2002, Zhu *et al.* 1998). This growth acceleration is followed by a period of constant growth rate with a steady increase in root length. Later, the root undergoes gradual deceleration of the growth rate which finally results in cessation of the growth altogether when the root reaches its final size (Chapman *et al.* 2002; Gladish and Rost 1993; Reinhardt and Rost 1995; Zhu *et al.* 1998). The precise final length of the root depends on growth conditions such as the temperature (Gladish and Rost 1993).

The root growth is sustained by the root apical meristem (RAM) which contains undifferentiated stem cells called initials. The cells in the RAM are able to divide and differentiate producing other tissues of the root (Petricka *et al.* 2012). Morphological patterns of the RAM can substantially vary depending on plant species (Heimsch and Seago 2008). In addition, root morphology undergoes changes as the root ages and in response to environmental conditions (De Tullio *et al.* 2010; Rost 2011). Three different types of RAM organisation have been reported: closed, intermediate and open (Groot *et al.* 2004). The differences between these RAM types lie in the organization of the stem cell niche consisting of the initial cells and QC. Initial cells are able to divide and differentiate into specific cell types. In the closed RAM each

cell layer (cortex, epidermis etc.) can be traced back to specific separate tiers of initials. The opposite root organization is the open type which lacks well-defined tiers of initials; here all initials look morphologically identical. The intermediate type displays to some extent organization especially for the epidermis/cortex lineage but still lacks apparent tiers of initials (Rost 2011). In many species with the closed types of RAMs the meristem structure was shown to gradually change from a well-organized closed type to a less organized structure resembling an intermediate type as the root became older and reached its final root length (Chapman *et al.* 2002). In some species the overall size of the root meristem reduces as the root ages (Chapman *et al.* 2002). These changes in RAM architecture over the lifespan of the root were speculated to be due to reduction or cessation of RAM function in the old root and were linked to reduced cell to cell communication evident by the reduction of plasmodesmata (Zhu *et al.* 1998).

As previously mentioned, this thesis has been focused on the plant model species *Arabidopsis thaliana*. The root apical meristem of *Arabidopsis thaliana* has a closed meristem with a very precise organization of cells that remains remarkably unchanged under different growth conditions and between individual plants. As with other species, this organization undergoes changes to a more intermediate type as the root ages, although these changes are limited (Baum *et al.* 2002).

The root tip of *Arabidopsis* can be separated into well-defined zones: the meristematic, the elongation and the differentiation zones (Fig. In-2A) (Petricka *et al.* 2012). The meristematic zone is made of actively dividing cells and is located above QC. In the meristematic zone cells undergo rapid divisions. The cells stop dividing, start to elongate and to increase in length when they reach the elongation zone. The area between the meristematic and the elongation zones is known as the transition zone. Finally, in the differentiation zone the cells complete their maturation (Fig. In-2A) (Dolan *et al.* 1993; Heidstra and Sabatini 2014; Petricka *et al.* 2012).

The architecture of the RAM is well-described (Fig. In-2B). The QC located at the tip of the root contains cells that divide slowly (Clowes 1956, Dubrovsky and Barlow 2015). The function of the QC is to inhibit differentiation of the surrounding initials (van den Berg *et al.* 1997). The QC therefore acts as an organizing center maintaining organization of the root stem cell niche. In roots younger than one week old there are 4-8 QC cells. In the 3 week old plants the QC structure changes: some

QC cells can divide forming a partial two-layered QC structure. In a 4-5 week old plants the QC becomes more disorganized (Baum *et al.* 2002).

Surrounding the QC are the initials that are the precursor cells of the cell types composing the root. Rootwards from QC is a single cell file of columella initials (also known as columella stem cells) followed by a few layers of mature columella cells. Shootwards from QC are vasculature initials that later produce xylem, phloem and procambium tissues. Initials of endodermis, cortex, epidermis and lateral root cap are found laterally to the QC (Fig. In-2B) (Petricka *et al.* 2012).

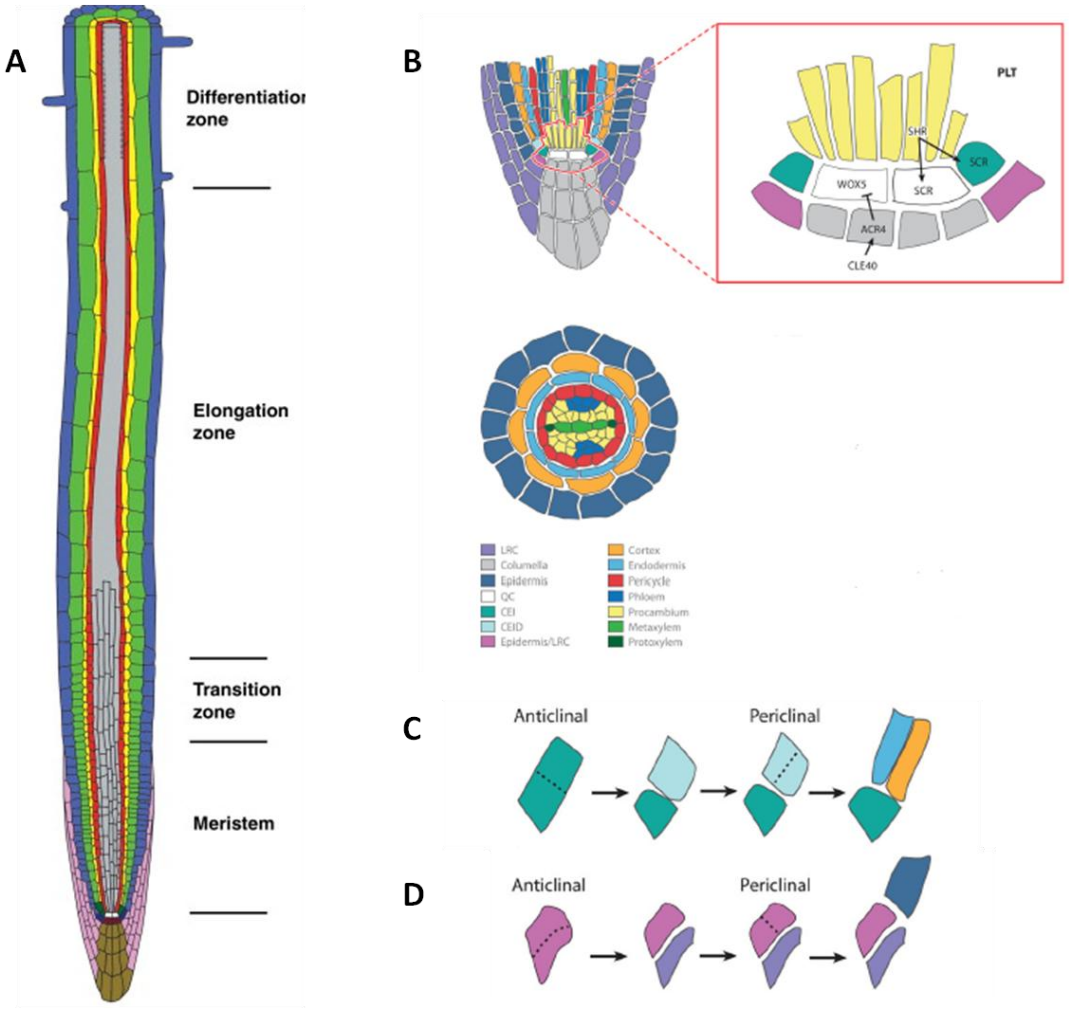

Fig. In-2. Structure of the mature primary root in *Arabidopsis thaliana*. **(A)** Zones at the root apex (Ubeda-Thomas *et al.* 2012). **(B)** Patterning at the root apical meristem (RAM). **(C)** Cell divisions of the cortex/endodermal initials. **(D)** Cell divisions of the epidermal/lateral root cap initials (Petricka *et al.* 2012).

The origin of each tissue type can be easily traced to specific initials. As mentioned above columella cells originate from the columella initials which divide periclinally (Dolan *et al.* 1993). The cortex initial cell located laterally to the QC undergoes first anticlinal division followed by a periclinal division that results in formation of two parallel cell layers: cortex and endodermis (Fig. In-2C) (Petricka *et al.* 2012). This pattern of divisions changes as the plant ages; in most plants older than 1 week the cortex initial divides periclinally without first dividing anticlinally which results in two new initials: the cortex initial and the endodermis initial. These two initials give rise to the respective cell layers: cortex and endodermis. Finally, in roots older than 3 week an additional second layer of cortex, the middle cortex, forms. The second layer of cortex is formed though a periclinal division of cortex initials (Baum *et al.* 2002).

The epidermis and lateral root cap layers are also derived from a single initial. This initial divides first anticlinally and then periclinally to produce these two cell layers (Fig. In-2D) (Petricka *et al.* 2012).

The vascular initials are located shootwards from the QC (Fig. In-2B). They gradually give rise to different cell types of the vasculature: the single pericycle layer, phloem, xylem and procambium (Baum *et al.* 2002).

The RAM structure in transverse view in a root less than 1 week old is very precise (Fig. In-2B) (Petricka *et al.* 2012). The root is surrounded by a single epidermis layer followed by single layers of cortex and endodermis. There are normally eight or nine cortical and endodermal cells (Baum *et al.* 2002). Next, a single layer of pericycle separates vasculature tissues from cortex. Xylem consists of 5 vessels which form a diarch pattern. There are two protoxylem vessels located adjacent to the pericycle layer as well as three metaxylem vessels. The two phloem sections are positioned perpendicularly to the xylem and adjacent to the pericycle layer. The vasculature cells located between the phloem and the xylem are called procambium (Fig. In-2B) (Baum *et al.* 2002; Dolan *et al.* 1993; Petricka *et al.* 2012).

The different cell types of the root originating from the root apical meristem have specific functions in the mature root. For example, xylem cells transport water and minerals upwards to the above-ground organs of the plant, whereas phloem cells transport nutrients from the sites of their synthesis into non-photosynthetic plant organs (Lucas *et al.* 2013). The columella cells are involved in gravity perception due to the presence of the starch-filled plastids in these cells (Blancaflor *et al.* 1998).

Overall, the structure of the RAM has been well described but the questions remain how this very precise structural organisation is achieved and maintained. New findings implement several hormone and various key genes involved in this process.

Regulation of root apical meristem development

The precise cell patterning of the root apical meristem is a result of cell division and differentiation processes which are tightly regulated by specific molecular mechanisms. Recently, a few major signals regulating these molecular mechanisms were characterized. These include auxin and cytokinin; together they manage patterning of the RAM in mostly antagonistic manner. In my thesis the focus lies on the role of auxin and, to a lesser extent, cytokinin in the growth of the root and the activity of the root apical meristem.

The levels of auxin and cytokinin signalling are relatively high in the root apical meristem, and this has been observed using appropriate *in planta* reporter constructs. Auxin itself and its signalling both have maximum in the QC, columella and xylem cells of the vasculature (Fig. In-3A and B) (Brunoud *et al.* 2012). On the other hand, cytokinin signalling is enriched in phloem and procambium domains of the vasculature as well as in the lateral root cap (Zurcher *et al.* 2013) (Fig. In-3C).

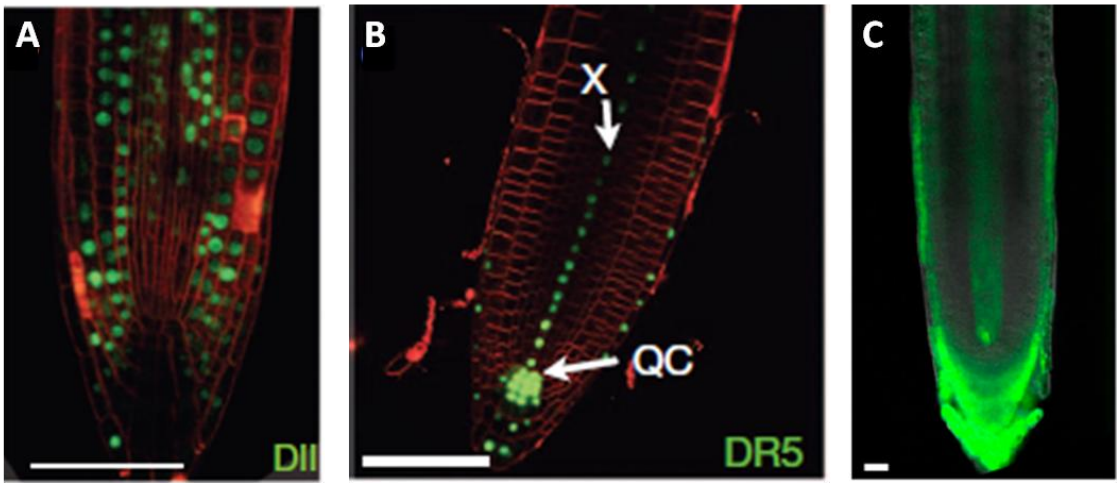

Fig. In-3 Auxin hormone accumulation **(A)** and signalling maxima **(B)** are visualized by the inverse auxin sensor DII-VENUS **(A)** and the auxin signalling output reporter DR5 **(B)** (Brunoud *et al.* 2012). Cytokinin signalling maxima are displayed using the TCSn reporter **(C)** (Zurcher *et al.* 2013).

Auxin modulates growth of the root already at the embryonic stage through the action of the Auxin Response Factor 5 (ARF5), an essential component of the auxin signalling pathway (see later for further details on auxin signalling). ARF5 mediates specification of the hypophysis through the direct activation of the mobile transcription factor TMO7 (Schlereth *et al.* 2010; Weijers *et al.* 2006). Likewise, the establishment of the root vascular cylinder during embryonic development and its maintenance post-embryonically is also controlled by auxin via ARF5. In this process ARF5 acts through activation of its target genes including TMO5 which form heterodimers with members of the LONESOME HIGHWAY (LHW) family transcription factors and together they regulate cell divisions in vasculature initials (De Rybel *et al.* 2013, Ohashi-Ito and Bergmann 2007). Interestingly, the TMO5/LHW heterodimers directly induce expression of genes involved in cytokinin biosynthesis (LOG3 and LOG4) and signalling (AHP6) in xylem precursor cells of the RAM (De Rybel *et al.* 2014, Ohashi-Ito *et al.* 2014). Cytokinins produced by the activity of LOG3 and LOG4 have been proposed to move from xylem precursors into adjacent vasculature cells where they promotes vascular cell divisions resulting in the growth of the vascular cylinder (De Rybel *et al.* 2014, Ohashi-Ito *et al.* 2014). On the other hand, AHP6, an inhibitor of cytokinin signalling, acts in the xylem precursor cells where it restricts cytokinin signalling and blocks additional cell divisions maintaining an invariable number of xylem cells (De Rybel *et al.* 2014, Mahonen *et al.* 2006, Ohashi-Ito *et al.* 2014).

In addition to cell division, auxin and cytokinin determine specification of vasculature cells into respective cell types: proto- and metaxylem, phloem and procambium which are organized in a strict pattern (Fig. In-2B). The patterning of the vasculature cylinder is possible due separation of the cylinder into two distinct spatial domains, one with high auxin signalling in the xylem surrounded by one with the high cytokinin signalling in the phloem and procambium. This separation is achieved by two key molecular actors. On one hand, cytokinin signalling is maintained at low level in xylem through the repressive action of the auxin-induced cytokinin signalling inhibitor AHP6. Simultaneously, auxin is actively directed into xylem cells though activity of several PIN proteins whose expression and subcellular localization are regulated by cytokinin. PIN proteins are auxin efflux carriers that are localized polarly in cells and control the direction of intracellular auxin fluxes (Adamowski and Friml 2015), thus allowing for the accumulation of auxin in xylem cells and for the formation and

maintenance of the two antagonistic hormone signalling domains. The hormonal signalling output within these domains then determines the cell fate of the vasculature initial daughter cells which will be specified to become either xylem, phloem or procambium cells (Bishopp *et al.* 2011, Mellor *et al.* 2017).

Besides vasculature formation and patterning, cytokinin and auxin determine the size of the root meristem and control transition from cell division in the meristematic zone to cell differentiation in the elongation zone. Application of cytokinin reduces the size of the meristem and promotes cell differentiation; likewise, the cytokinin biosynthesis and signalling mutants exhibit increased meristematic zone (Dello Ioio *et al.* 2007). On the contrary, auxin increases the size of the meristematic zone and promotes cell divisions (Blilou *et al.* 2005, Dello Ioio *et al.* 2007, Dello Ioio *et al.* 2008). Thus these hormones together establish a boundary between two domains with different cell responses: rapid cell divisions in the meristematic zone and cell growth in the elongation zone (Di Mambro *et al.* 2017).

Finally, cytokinin was shown to be important in regulation of the QC function. Cytokinin is able to promote cell division in the mitotically inactive QC cells (Zhang *et al.* 2013). Application of cytokinin does not alter the expression pattern of the QC patterning marker lines such as QC46, SCR, WOX5 (Dello Ioio *et al.* 2007) but seems to reduce the expression levels of several of these markers (Zhang *et al.* 2013).

In addition to auxin and cytokinin, the RAM development is regulated by specific regulatory transcription factors. Among these is WOX5, which controls the development of the QC. WOX5 is expressed specifically in the QC starting already in the embryonic QC cell lineage (Sarkar *et al.* 2007). The *wox5* mutant has abnormally enlarged QC and columella stem cells, reduced number of columella cells and ectopic cell divisions in the QC (Fig. In-4A and B) (Forzani *et al.* 2014; Sarkar *et al.* 2007). WOX5 is required for columella stem cell maintenance preventing their differentiation into mature columella cells (Sarkar *et al.* 2007). The WOX5 protein is able to move from QC into columella stem cell layer where it represses the transcription factor CDF4 thus maintaining columella stem cells in undifferentiated state (Pi *et al.* 2015).

The columella architecture is controlled by the two NAC-domain transcription factors SOMBRERO (SMB) and FEZ. *fez* mutants have a reduced number of columella

layers and lateral root cap cells whereas *smb* mutant has one additional columella layer. This control of the root cap patterning is independent from the other known RAM patterning regulators including WOX5, SHR, SCR or PLT genes. FEZ gene is expressed in the columella stem cells and columella proper whereas SMB is only expressed in mature columella cells. There is a negative feedback loop proposed between these two regulators: FEZ promotes cell divisions in columella stem cells and also activates SMB transcription in mature columella cells where SMB in turn represses FEZ function (Willemsen *et al.* 2008).

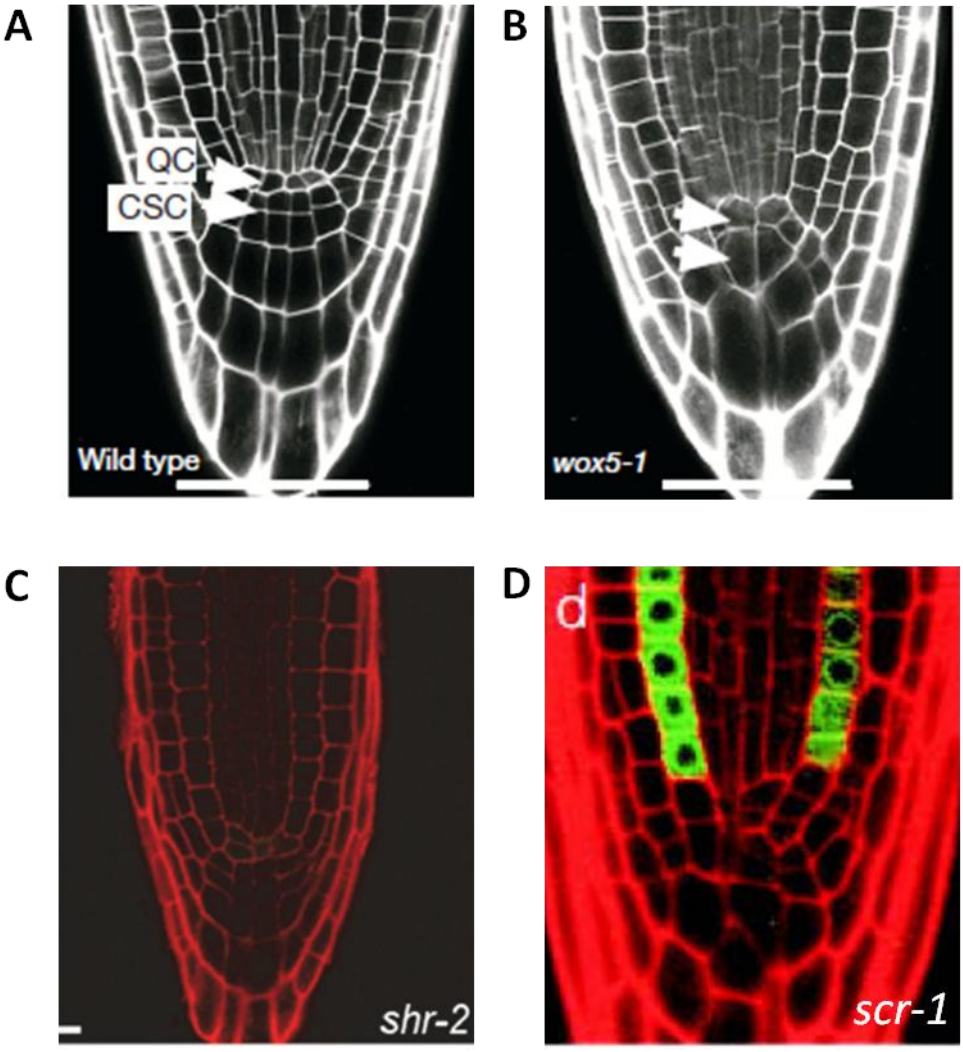

Fig. In-4. Phenotypes of mutants with defects in RAM architecture. **(A)** Root tip of the wild type (Sarkar *et al.* 2007), **(B)** *wox5-1* mutant (Sarkar *et al.* 2007), **(C)** *shr-2* mutant (Sebastian *et al.* 2015), **(D)** *scr-1* mutant (Sabatini *et al.* 2003). QC = quiescent center; CSC = columella stem cells.

A pair of transcription factors SHR and SCR is involved in two separate processes: they regulate both the specification of QC and the patterning of endodermis and cortex. In *scr* mutants the cortex/endodermis initials do not undergo asymmetric division, and this results in formation of a single cell layer with mixed cortex/endodermis identity; additionally, the QC cells have abnormal shapes and function which causes loss of meristematic activity and premature termination of root growth (Fig. In-4D) (Sabatini *et al.* 2003). *shr* mutant also shows abnormal morphology in the QC and columella regions leading to premature termination of root growth; the mutant is characterized by the presence of a single layer of ground tissue with cortex identity instead of cortex and endodermis layers (Fig. In-4C) (Helariutta *et al.* 2000). Both *scr* and *shr* are required for correct QC function but the precise mechanism of this regulation is yet to be determined (Sabatini *et al.* 2003). SHR mRNA is found specifically in the stele tissues of the root but the SHR protein moves from the stele to the endodermis where it activates SCR (Cui *et al.* 2007; Helariutta *et al.* 2000; Nakajima *et al.* 2001). SCR and SHR interact with each other to regulate a number of common target genes (Cui *et al.* 2007, Levesque *et al.* 2006).

Stem cell activity in the root meristem is also controlled by members of the PLETHORA (PLT) gene family. *plt1* mutants have increased number of columella tiers and extra cells in tier 2 of the columella. *plt2* mutants have more subtle phenotypes showing increased columella cell numbers. The *plt1 plt2* double mutant displays severe defects in root development. PLT1 and PLT2 genes are AP2-domain transcription factors and their expression is induced by auxin. PLT1 and PLT2 are required for stem cell niche maintenance independently from SCR/SHR (Aida *et al.* 2004).

Overall, it appears that the key transcription factors such as WOX5, SCR, SHR and PLT act together with the plant hormones auxin and cytokinin to establish the RAM during embryogenesis and to regulate its functions post-embryonically.

Lateral root development

The primary root is established during embryonic development and continues to grow for a certain period post-embryonically. The origin of every cell in the root is traced back to the meristematic cells in the root apical meristem. Nevertheless, adult plants have to establish additional new roots post-embryonically in order to increase the forging surface of their root system and thus adapt themselves to changes in nutrient

and water availability of the soil. There are several types of post-embryonic roots that do not originate from the root apical meristem but are produced *de novo*: the lateral roots, the adventitious roots and the crown roots (Bellini *et al.* 2014). Lateral roots start to grow on other roots whereas the adventitious roots develop on non-root organs (for example, on hypocotyls and stems).

In *Arabidopsis thaliana* lateral roots (LR) are initiated in the differentiation zone of the primary root from pericycle cells which lie adjacent to xylem poles. These lateral root founder cells consist of a cluster of several pericycle cells (ca. 11 cells on average), but only a few of these cells contribute to the majority of the future LR body (von Wangenheim *et al.* 2016). The pericycle founder cells divide anticlinally to form a single file of several cells (stage I of LR formation in Fig. In-5). The sequence of these first cell divisions is strictly controlled (von Wangenheim *et al.* 2016). Next, the cells undergo periclinal divisions resulting in a two-layer lateral root primordium (stage II of LR formation in Fig. In-5). Subsequently, the primordium continues to divide anticlinally and periclinally creating a dome-shaped structure (stages III-VII of LR formation in Fig. In-5). The patterns of these subsequent cell divisions can vary between plants and do not follow a rigid sequence. The division planes often change depending on the cell geometry; the cells tend to divide along local minima of plane area (following the shortest wall principle) and prefer to alternate their division orientation plane between anticlinal and periclinal divisions for each subsequent

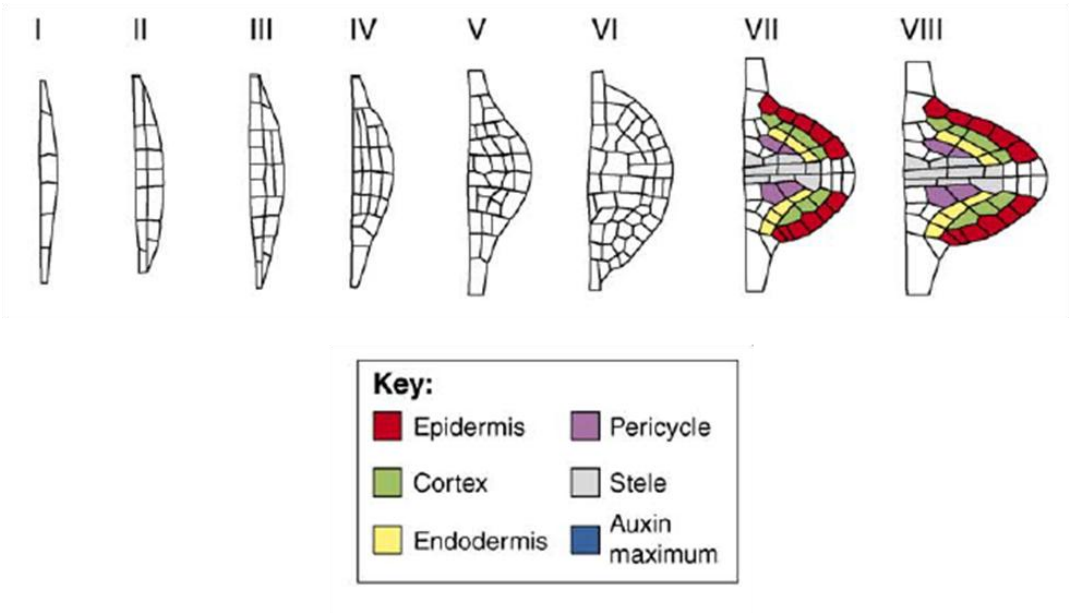

Fig. In-5. Developmental stages during lateral root development (Stages I to VIII) (Peret *et al.* 2009).

division round (von Wangenheim *et al.* 2016). Already at stage VI the lateral root primordium consists of distinctive cell types characteristic for a mature root tip including epidermis, cortex, endodermis and vasculature cells. At the final stage the primordium breaks through the root epidermal tissue, emerging as a new lateral root (stage VIII of LR formation in Fig. In-5) (Lavenus *et al.* 2013, Malamy and Benfley 1997, Peret *et al.* 2009, von Wangenheim *et al.* 2016).

The lateral roots positioning is strictly controlled: the lateral roots emerge at a regular spacing along the primary root in a left-right alternating pattern (De Smet *et al.* 2007). The temporal and spatial distribution of the lateral roots was argued to be regulated by an endogenous clock mechanism involving oscillating genes (Moreno-Risueno *et al.* 2010). Auxin was shown to additionally contribute as a signal which primes the xylem pericycle cells to become lateral root founder cells. The regular distribution of lateral roots correlates with an oscillating auxin signalling in the protoxylem cells which lie adjacent to the pericycle cells. When auxin response is maximum, the adjacent pericycle cells acquire a competence to divide and form a lateral root primordium (De Smet *et al.* 2007, Peret *et al.* 2009). The exact mechanism which choreographs these auxin signalling oscillations is still uncharacterized. Furthermore, exactly how an auxin signal is propagated from the xylem cells into the neighbouring pericycle cells remains undetermined.

Cytokinin appears to act antagonistically to auxin during lateral root initiation. Exogenous cytokinins perturb initiation of lateral root primordia at a very early stage by blocking asymmetric cell division in the xylem pericycle cells (Laplaze *et al.* 2007). This perturbation is achieved by arresting cell cycle at the G_2 to M transition phase (Li *et al.* 2006b). Additionally, at later stages, exogenous cytokinins induce a morphological disorganization in the emerging lateral root primordia particularly at the root tip (Laplaze *et al.* 2007). Cytokinin signalling is repressed in the xylem pericycle cells in which lateral root primordia priming and initiation occurs. On the contrary, cytokinin signalling was detected in xylem pericycle cells which lie between two existing lateral root primordia where no further lateral roots are initiated (Bielach *et al.* 2012). Therefore cytokinin appears be a repressive signal preventing initiation of new lateral roots in close proximity to each other and thus regulating spatial distribution of lateral roots along the primary root.

The subsequent growth of the lateral root primordia appears to be regulated by auxin at all stages. Several mutants involved in auxin homeostasis, transport and signalling are impaired in lateral root growth (Peret *et al.* 2009). In particular, the Auxin Response Factors 7 and 19 (ARF7 and ARF19) as well as INDOLE-3-ACETIC ACID INDUCIBLE 28 and 14 (IAA28 and IAA14) are key auxin signalling pathway genes (see later for more details on auxin signalling) involved in lateral root formation at different stages (De Rybel *et al.* 2010; Fukaki *et al.* 2002; Okushima *et al.* 2005; Okushima *et al.* 2007). Auxin response is transmitted though the transcriptional activation of auxin-responsive gene by ARF7 and ARF19 transcription factors. Together ARF7 and ARF19 directly activate expression of several genes including the transcription factors Lateral Organ Boundaries Domain 16 and 29 (LBD16 and LBD29) (Okushima *et al.* 2007). Presumably, LBD16/LBD29 as well as other yet unidentified transcription factors are able to activate cell-specific programs in the developing lateral root primordia. These programs lead to coordinated cell divisions followed by cell specification and eventually formation of mature specialized tissues within the emerging lateral root. The *de novo* formed root apical meristem of the lateral root acts in the same way as the RAM of the primary root enabling post-emergence growth of the lateral root. Thus differentiated xylem pericycle cells eventually give rise to a multitude of root-specific tissues including undifferentiated stem cells.

Shoot apical meristem

The development of all above-ground organs relies almost entirely on the function of the shoot apical meristem (SAM). Two opposite processes occur in the SAM: the stem cell pool is constantly maintained and renewed whereas some cells accelerate their growth and division rate and eventually differentiate to become part of the newly forming organs (the leaves and flowers). The balance between these two processes is strictly controlled over the life of the plant and the location and timing of new organ emergence appears to be tightly regulated.

This regulation can be first seen from the organization of the SAM which is divided into functional zones with distinct cellular behaviours (division and expansion) and distinct cellular identities. In *Arabidopsis thaliana* the dome-shaped structure of the SAM is divided into the central, peripheral and rib zones (Fig. In-6A). The central zone is found at the apex and contains undifferentiated stem cells. The site of organ

primordia initiation occurs at the peripheral zone. The rib zone, situated below central and peripheral zones, produces the internal tissues of the stem. The SAM can be further divided into individual cell layers. The top two layers (L1 and L2; collectively referred as tunica) are able to divide only in one direction (anticlinally) whereas the deeper layers (L3 and further; collectively referred as corpus) are able to divide in any direction. This organization is largely similar in other higher plants with some variations in the number of tunica layers.

The cells in the functional zones of the SAM differ in their properties. For example, the cells in the central zone where the stem cells are located divide slower than the cells in the peripheral zone (Laufs *et al.* 1998; Reddy *et al.* 2004). The cells in the central zone frequently divide asymmetrically but maintain overall similar cell size within the zone. This is achieved by an adjustment of the cell growth rate and the

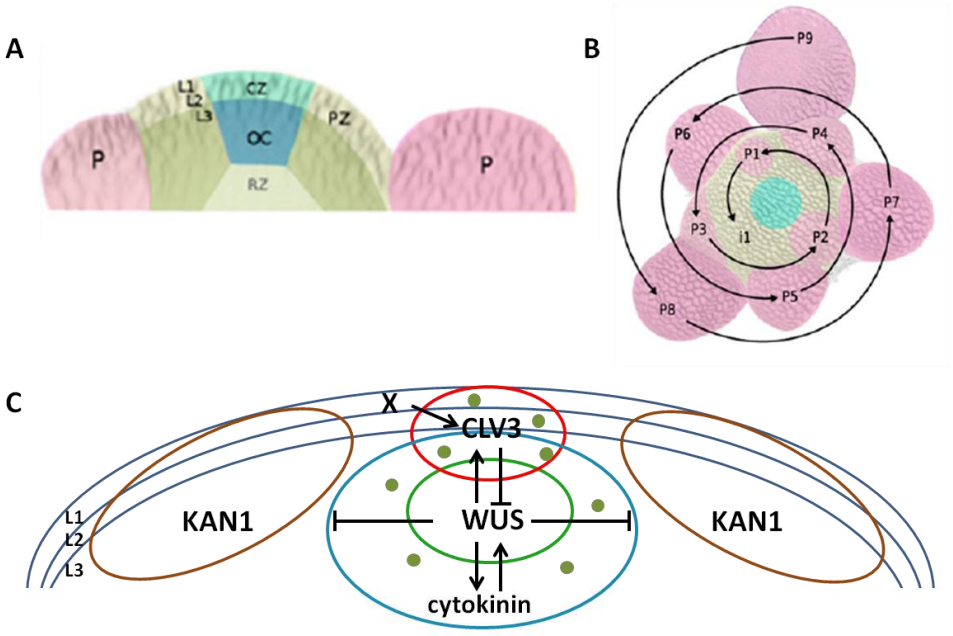

Fig. In-6. Organization of the shoot apical meristem. **(A)** The structure of the shoot apical meristem with functional zones: the central zone CZ, the peripheral zone PZ, the organizing center OC, the rib zone RZ and the organ primordia P. L1, L2 and L3 indicate the cell layers (Murray *et al.* 2012). **(B)** The order of new primordia initiation from the youngest P1 to the oldest P9. I1 marks the site of the next primordia initiation (Murray *et al.* 2012). **(C)** Minimal gene interaction network controlling SAM maintenance. Circles mark the expression domains of CLV3 (red), WUS (green), KAN1 (brown) and cytokinin maximum (blue). Green dots show localization of WUS protein. X stands for a hypothetical L1-devived signal which activated CLV3 (Truskina and Vernoux 2018).

cell cycle length following an asymmetric cell division illustrating the presence of a compensatory mechanism that allows the meristem to maintain the desired overall uniform structure (Jones *et al.* 2017; Serrano-Mislata *et al.* 2015; Willis *et al.* 2016). The local variability of cell growth rates in the meristem plays a key role in setting the geometry of the SAM (Uyttewaal *et al.* 2012), highlighting the importance of cell behavior in generating a specific shape. The division of the SAM into the central and peripheral zones also correlates with differences in mechanical properties: the central zone of the SAM is characterized by increased stiffness of the tissue compared to more peripheral regions (Milani *et al.* 2014, Milani *et al.* 2011, Kierzkowski *et al.* 2012) or organ primordia (Braybrook and Peaucelle 2013, Peaucelle *et al.* 2011). Similarly to the root, these patterns associated with the functional zones of the SAM are established by both cell-autonomous factors such as the cell-specific gene regulatory networks and non-cell autonomous factors including mobile proteins and hormones (Barton 2010; Murray *et al.* 2012).

The functional zones of the SAM are characterized by specific expression of master regulatory genes with CLV3 in the central zone (Fletcher *et al.* 1999), WUS in the organizing center (Mayer *et al.* 1998) and KAN1 in the boundary domain (Yadav *et al.* 2013) amongst many others. Several publications have attempted to model SAM maintenance based on expression patterns and interactions of these regulatory genes (Adibi *et al.* 2016, Fujita *et al.* 2011, Gruel *et al.* 2016, Yadav *et al.* 2013). Computer simulations attempted to define the minimal regulatory networks required for functioning of the SAM (Fig. In-6C). The models always include the well-described WUS-CLV3 feedback loop which dynamically maintains the size of stem cell niche (Brand *et al.* 2000, Lenhard and Laux 2003, Schoof *et al.* 2000; Yadav *et al.* 2011). Repression of the differentiation-promoting genes such as KAN1 by WUS contributes to the entry into differentiation (Gruel *et al.* 2016, Yadav *et al.* 2013). Furthermore, this modeling work emphasizes the importance of cytokinin signalling in SAM maintenance by showing that regulation of WUS expression by cytokinin (Chickarmane *et al.* 2012, Gordon *et al.* 2009) and activation of cytokinin signalling by WUS (Leibfried *et al.* 2005) are fundamental for correct positioning of WUS in the SAM. Recently an additional signalling network was identified which includes a movement of a CLE peptide produced in organ primordia to the center of the SAM where it regulates stem cell activity thus providing an extra feedback regulation from

developing organs on the stem cell niche and providing an interesting mechanisms for integrating stem cell maintenance and organogenesis (Je *et al.* 2016).

At the periphery of the SAM, new leaf or flower primordia are initiated at predictable positions and with regular time intervals between initiation events (Fig. In-6B). In *Arabidopsis thaliana* new organ primordia are initiated sequentially one after another following a whorled phyllotaxis pattern with an angle of approximately 137.5 degrees between each newly formed primordium (Bartlett and Thompson 2014, Galvan-Ampudia *et al.* 2016, Kuhlemeier 2007, Traas 2013). A long-standing theory postulates that the positioning and timing of organs at the growing shoot apex is determined by the presence of inhibitory signals around developing organ primordia, these inhibitory fields preventing initiation of new primordia. The current understanding of the molecular mechanisms behind organ initiation suggests that this inhibition results from auxin depletion in the regions surrounding a local auxin accumulation that drives organ primordia (Jönsson *et al.* 2006, Reinhardt *et al.* 2003, Smith *et al.* 2006, Stoma *et al.* 2008, Vernoux *et al.* 2011). The developing organ primordia are characterized by high auxin signalling in primordia of all stages (Fig. In-7A). On the other hand, the cytokinin signalling is highest in the young primordia but decreases rapidly in the older primordia; cytokinin signalling is also detected in the organizing center (Fig. In-7B). Auxin and cytokinin signalling is first switched on at the site of the next primordia initiation (Besnard *et al.* 2014). Auxin is transported

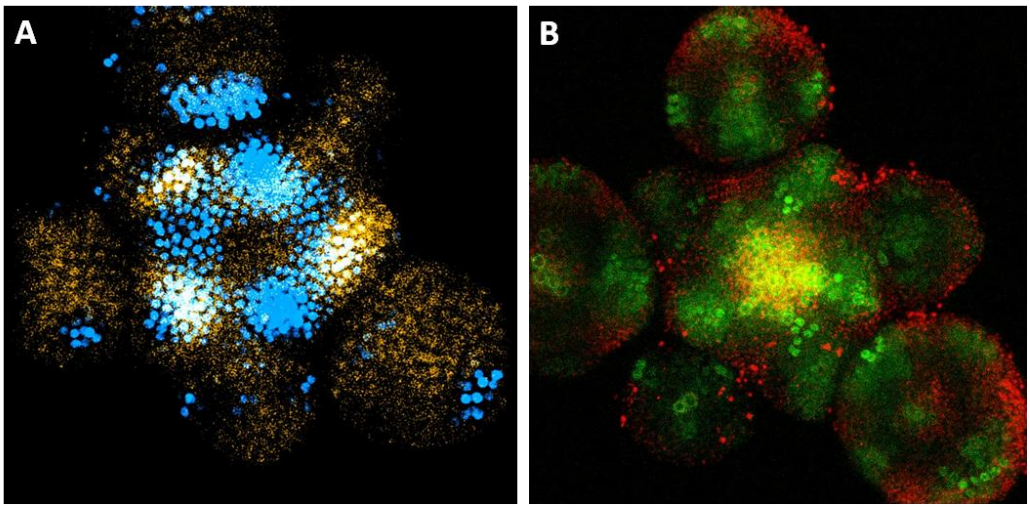

Fig. In-7. Auxin hormone accumulation and signalling maxima **(A)** are visualized by the inverse auxin sensor DII-VENUS (yellow) and the auxin signalling output reporter DR5 (blue) at the SAM (image from Carlos Galvan-Ampudia, ENS de Lyon). Cytokinin signalling maxima are displayed using the TCSn reporter at the SAM **(B)** (image from Fabrice Besnard, ENS de Lyon).

directionally towards these sites of the future organ primordia and this auxin accumulation leads to lateral organ initiation. The directional transport is achieved through the polar localization of the auxin efflux carriers from the PIN gene family, most notably PIN1 (Heisler *et al.* 2005, Reinhardt *et al.* 2003). The importance of the PIN1 for the shoot development is evident by the *pin1* mutant phenotype; the *pin1* mutants are unable to develop a functional inflorescence producing instead a “pin”-looking structure which lacks normal lateral organs (Galweiler *et al.* 1998). In addition to PINs, the auxin influx carriers from the AUX/LAX gene family also contribute to the spatiotemporal distribution of auxin in the SAM (Bainbridge *et al.* 2008, Reinhardt *et al.* 2003).

Recent findings indicate that the timing of primordia initiation is regulated by an interplay between auxin and cytokinin signalling (Besnard *et al.* 2014). This study focuses on the role of the AHP6 protein which production is induced by auxin and enriched in organ primordia and developing flowers. The AHP6 protein produced in the primordia is then able to move to the neighboring cells where it acts as an inhibitor of cytokinin signalling. The movement of AHP6 creates a differential in cytokinin signalling activity between sites of successive organ initiation that facilitates sequential initiation of organs and thus provides robustness to the timing of organ initiation.

Differential auxin patterns continue to regulate development following the initiation of the shoot organs. In particular, the developing leaf primordia require transient low auxin zone at the adaxial (upper) side for successful establishment of leaf polarity (Qi *et al.* 2014). The auxin depletion at the adaxial site is achieved by PIN1 auxin efflux transporter which moves auxin away from the adaxial site of the developing leaf primordia towards the meristem. The same mechanisms that pattern the meristem are thus also key in establishing the symmetry of the organs.

In addition to the SAM, axillary meristems (AM) are small stem cell niches located at the upper (adaxial) side of the newly formed leaf. The AM gives rise to axillary buds which are able to remain dormant or eventually produce an axillary shoot (Bennett and Leyser 2006, Yang and Jiao 2016). Each newly formed axillary shoot contains a functional shoot apical meristem capable of producing new organs. Thus plants can increase and diversify their architecture to adapt to the changing environmental conditions.

The formation of the axillary meristem appears to be tightly controlled by patterns of hormone signalling which presents a remarkable similarity to the mechanisms behind the pattern formation in the SAM proper. The process requires initial auxin depletion at the future AM initiation site in the leaf axil closely followed by a pulse of cytokinin signalling. This auxin depletion in the leaf axil is achieved well before AM initiation at the early stages of leaf primordia formation due to directed polar auxin transport mediated by PIN1 localization (Wang *et al.* 2014a, Wang *et al.* 2014b).

Lately, the axillary meristem was shown to be regulated by the same key genes as the main SAM. Specifically, the regulators of the shoot stem-cell niche WUS and CLV3 were dynamically induced one after another during initiation of the AM creating a two-step pattern of expression. Interestingly, CLV3 was initially induced in the WUS-specific central domain before the expression shifted to the expected L1 and L2 layers at the later stages of AM formation (Xin *et al.* 2017). In addition, the mobile stem-cell specific gene STM was shown to be important for AM initiation (Balkunde *et al.* 2017, Shi *et al.* 2016).

In summary, the key mechanism controlling organ initiation and maintenance of the stem-cell niche in the SAM is the contrasting hormone signalling between different regions in the SAM which results in tissue-specific gene expression patterns. In turn, the differentially expressed regulatory genes trigger cell-specific programs promoting cell fate determination. A strong emerging trend in recent research is that a similar set of signals and genes define a patterning module that is used in the SAM, the developing organs and to establish new meristems such as the AM. How this module is reused and how this allows to link organ and tissue development to the SAM activity is yet to be fully characterized but some of the key mechanisms have clearly been identified.

The plant hormone auxin

Auxin was shown to be involved in numerous developmental processes including cell division and cell expansion (Perrot-Rechenmann 2010), root and shoot growth (Overvoorde *et al.* 2010, Vernoux *et al.* 2010), phototropism (Fankhauser and Christie 2015), gravitropism (Band *et al.* 2012), leaf senescence (Ellis *et al.* 2005), response to pathogens (Kazan and Manners 2009, Fu and Wang 2011), abiotic stress (Bielach *et al.* 2017, Salopek-Sondi *et al.* 2017). The main type of auxin found

in plants is the indole-3-acetic acid (IAA) (Fig. In-8A) (Simon and Petrasek 2011). Other naturally occurring auxins include 4-chloroindole-3-acetic acid (4-Cl-IAA), and phenylacetic acid (PAA). In addition, several synthetic compounds such as 2,4-dichlorophenoxyacetic acid (2,4-D), 1-naphthaleneacetic acid (NAA), 3,6-dichloro-2-methoxybenzoic acid (dicamba), and 4-amino-3,5,6-trichloropicolinic acid (picloram) also induce auxin responses when applied externally on the plant or added to the growth medium (Fig. In-8A) (Sauer *et al.* 2013).

The metabolism of IAA is well-studied. IAA can be produced through two major routes using either the tryptophan (Trp)-dependent and the Trp-independent pathways (Fig. In-8B) (Korasick *et al.* 2013). Both these pathways might contribute to the regulation of IAA levels but the precise role of each pathway in *Arabidopsis thaliana* is unclear. The IPyA pathway where tryptophan is converted to IAA via the enzymes from the TRYPTOPHAN AMINOTRANSFERASE OF ARABIDOPSIS (TAA) family of Trp aminotransferases and the YUCCA (YUC) family of flavin monooxygenases seems to contribute the most to the active IAA (Korasick *et al.* 2013, Zhao 2012). Active auxins can be conjugated and transformed into inactive

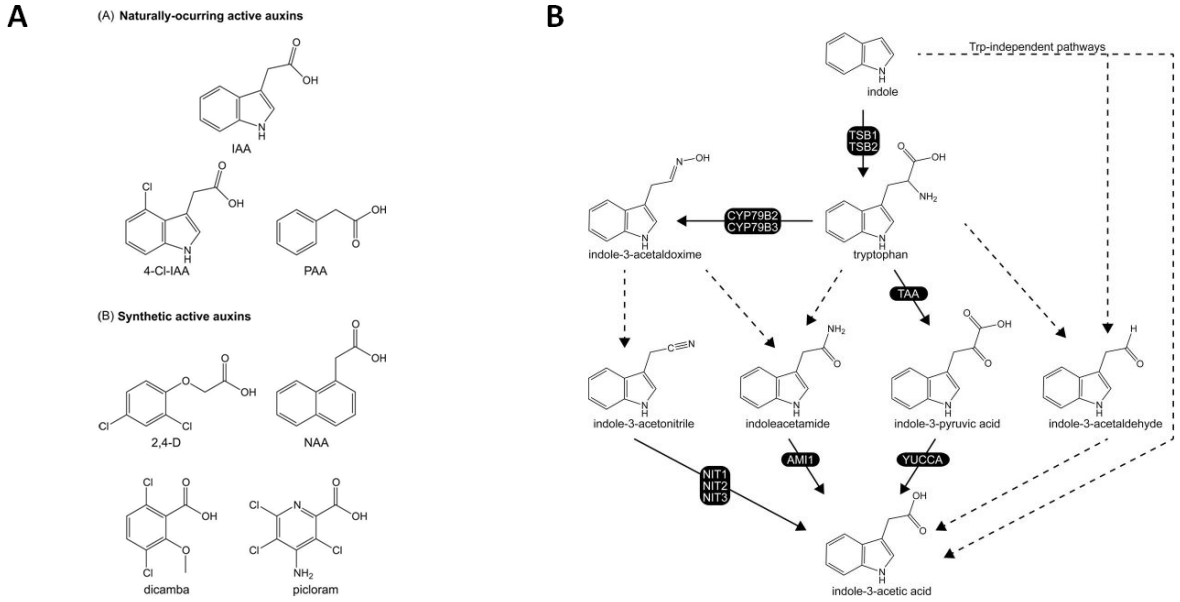

Fig. In-8. Auxin structure and biosynthesis pathways. **(A)** Naturally occurring and synthetic active auxins (Korasick *et al.* 2013). **(B)** Potential IAA biosynthetic pathways. Solid arrows indicate pathways for which all enzymes have been identified; dashed arrows indicate pathways for which not all enzymes have been identified (Korasick *et al.* 2013).

storage forms. In addition, inactive auxins can be reactivated (Korasick *et al.* 2013, Sauer *et al.* 2013).

Auxin is not synthesized ubiquitously throughout the plant; the main sites of auxin synthesis in *Arabidopsis thaliana* are the aerial plant parts especially the young developing leaves (Ljung *et al.* 2001) from which auxin is transported into the root tip though the stele (Michniewicz *et al.* 2007). But auxin is also synthesized in the root especially in the primary root meristem and in developing lateral roots (Ljung *et al.* 2005).

In addition to this, auxin is transported locally between the adjacent cells through the process of polar auxin transport. This well described process is based on the fact that IAA, as a weak organic acid, can exist in both protonated and deprotonated forms depending on the pH level of the environment (Raven 1975, Rubery and Sheldrake 1973, Rubery and Sheldrake 1974). Outside the cells, in the apoplast, the pH level is acidic which means that IAA is protonated and can diffuse into cells easily due to its neutral charge. Additionally the influx carriers of the AUX/LAX family actively pump IAA into the cells (Peret *et al.* 2012b). Inside the cells the pH is neutral which causes IAA to lose the proton and become electrically charged preventing it from diffusing

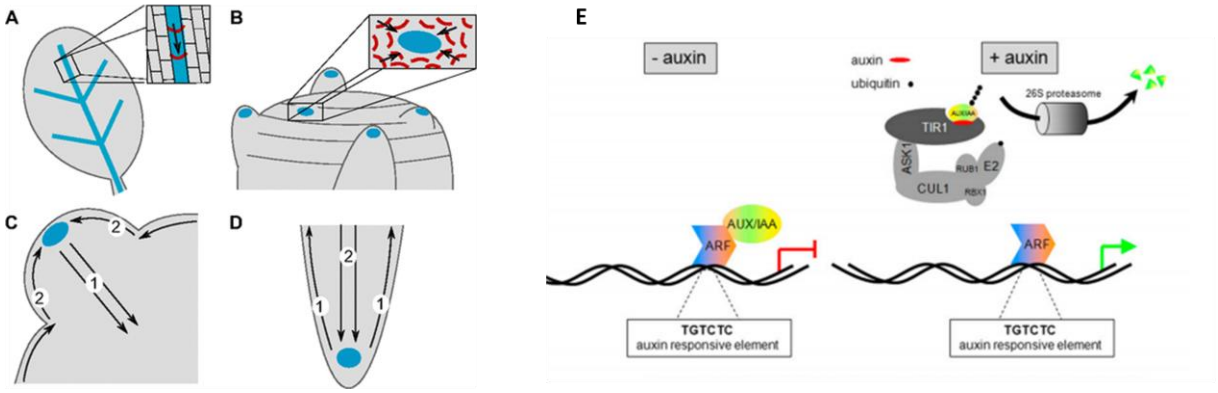

Fig. In-9. PIN distribution and auxin transport in the leaf **(A)**, the shoot apex **(B)**, in developing shoot primordium **(C)** and the root apex **(D)** (Berkel *et al.* 2013). Auxin is in blue and PIN proteins in red; arrows indicate the direction of auxin flux. **(E)** Scheme of the auxin signalling pathway in the absence or presence of auxin (Lau *et al.* 2008).

outside the cell (Goldsmith 1977). This charged IAA molecules can be actively transported outside through efflux carriers from the PIN-FORMED (PIN) family (Adamowski and Friml 2015). The PIN transporters are distributed asymmetrically on the plasma membrane with clear preferences for the transport into one or more specific directions (Galweiler *et al.* 1998, Friml *et al.* 2002a, b, Muller *et al.* 1998). As a result, auxin is transported directionally. In the leaves auxin is transported within the veins towards the base of the leaf (Fig. In-9A) (Berkel *et al.* 2013). In the shoot apex auxin is concentrated towards organ primordia (Fig. In-9B) where it flows in the upper layers towards the center of the primordium and then flows back though the vasculature creating a fountain-like flow pattern (Fig. In-9C) (Reinhardt *et al.* 2003). In the root tip auxin moves in a reverse fountain-like pattern with downwards movement though the vasculature towards the root tip and then the upwards movement along the outer epidermal layer (Fig. In-9D) (Blilou *et al.* 2005).

Auxin triggers cell or tissue specific responses though a well-studied signalling pathway. Inside the cell auxin is bound by the TRANSPORT INHIBITOR RESPONSE1/AUXIN SIGNALLING F-BOX PROTEIN (TIR1/AFB) receptors (Dharmasiri *et al.* 2005a,b, Kepinski and Leyser 2005). TIR1 proteins are F-box proteins and for this reason they can bind three different ligands: an SCF-TIR1 ubiquitin ligase complex, auxin and AUXIN/INDOLE-3-ACETIC ACID (AUX/IAA) proteins. The binding of all these three ligands at the same time triggers the ubiquitination of AUX/IAA proteins and their subsequent degradation by the 26S proteasome. AUX/IAA proteins repress the transcription of auxin-induced genes by building multimers with other AUX/IAA proteins and with AUXIN RESPONSE FACTOR (ARF) transcription factors. After the auxin-induced degradation of Aux/IAAs, ARF transcription factors are free to activate or repress the expression of genes to which promoters they are bound (Hayashi 2012; Lau *et al.* 2008). ARF proteins bind as higher-order multimers to the so-called auxin responsive element (AuxRe) in the promoters of the auxin-induced genes (Fig. In-9E) (Boer *et al.* 2014, Korasick *et al.* 2014, Nanao *et al.* 2014). The TIR1/AFB gene family consists of 6 members in *Arabidopsis thaliana* (Dharmasiri *et al.* 2005b), the AUX/IAA gene family contains 29 members (Remington *et al.* 2004) and the ARF gene family includes 23 transcription factors (Okushima *et al.* 2005). It can be speculated that the differential expression of these genes, their post-transcriptional regulation and the predisposition

towards oligomerization are of key importance in understanding the specificity of auxin-induced developmental changes (Vernoux *et al.* 2011).

Auxin can be detected on the cellular level within living tissues using auxin sensors. The DII-Venus auxin sensor utilizes the auxin-induced degradation of AUX/IAA proteins to detect the auxin content (Fig. In-3A, 7A). In this sensor, a DII domain of an AUX/IAA protein fused to a fluorescent reporter gene is constitutively produced in the plants and is degraded rapidly in response to elevated levels of auxin (Brunoud *et al.* 2012). The second auxin sensor, DR5, does not detect auxin as such but reports output of the auxin signalling pathway (Fig. In-3B, 7A). The DR5 reporter contains concatemerized repeats of AuxRE elements representing the binding sites of ARFs (Ulmasov *et al.* 1997). The AuxRe concatemers drive the expression of fluorescent proteins or GUS reporters thus providing information on ARF activity *in vivo* and on the activity of auxin signalling during developmental processes (Benkova *et al.* 2003, Friml *et al.* 2002a, Ulmasov *et al.* 1997).

The action of auxin is based on its ability to reprogram cellular responses through ARF-mediated changes in expression of auxin-inducible genes. The altered gene expression then leads to specific physiological responses. Fundamentally, auxin-induced growth responses involve cell division, cell expansion and cell differentiation. Auxin promotes cell division and controls cell-cycle progression (Perrot-Rechenmann 2010, Stals and Inze 2001, Trehin *et al.* 1998). The effect of auxin on the cell cycle machinery is based on transcriptional and post-transcriptional control of cell-cycle regulators (Perrot-Rechenmann 2010, Vanneste *et al.* 2005). Following division, cells undergo expansion accompanied by increase in size. This process is also regulated by auxin in a cell-type and concentration-specific manner (Perrot-Rechenmann 2010, Rayle *et al.* 1970). For example, auxin stimulates cell elongation by activating expression of cell-wall related genes which can modify cell wall composition and initiate cell wall loosening (Esmon *et al.* 2006, Majda and Robert 2018, Perrot-Rechenmann 2010). Auxin can trigger cell differentiation as shown for the root columella stem cells (Ding and Friml 2010). The auxin-induced cellular reprogramming requires flexibility to produce responses specific for a given developmental context. The involvement of multiple TIR1/AFB auxin receptors, AUX/IAA repressors and ARF transcription factors provides essential complexity to the auxin signalling pathway and allows specificity of auxin-induced developmental changes.

The TIR1/AFB family of auxin receptors

One key initial step in auxin signalling is the degradation of AUX/IAA repressors which triggers derepression of ARFs allowing auxin-regulated gene transcription. The degradation is initiated when AUX/IAA build a transient complex with the TIR1/AFB proteins, auxin and the members of the SCF complex (Salehin *et al.* 2015). There are 6 TIR1/AFBs in *Arabidopsis thaliana* genome: TIR1 and AFB1-5 (Dharmasiri *et al.* 2005b). The single mutants of TIR1/AFBs have only mild phenotypes (Dharmasiri *et al.* 2005b, Ruegger *et al.* 1998) whereas higher order mutants show auxin resistance phenotypes and strong developmental defects which can lead to complete growth arrest (Dharmasiri *et al.* 2005b).

TIR1 and AFB1-5 proteins function as auxin receptors (Dharmasiri *et al.* 2005a, b, Prigge *et al.* 2016). They share a similar structure with an F-BOX domain close to the N-terminus and 18 leucine-rich repeats (LRR) composing the rest of the protein. The AUX/IAA proteins interact with TIR1 through their F-box domain. Another domain or TIR1, the LRR, contains a binding pocket for auxin (Tan *et al.* 2007). It appears that auxin acts to stabilize interactions between TIR1 and AUX/IAA proteins (Calderon-Villalobos *et al.* 2010).

There are 6 TIR1/AFB receptors and 29 AUX/IAA repressors in *A. thaliana* which results in multiple possible combinations of the coreceptor complex. Indeed, different receptor-repressor combinations have variable affinities to auxin (Calderon-Villalobos *et al.* 2012, Winkler *et al.* 2017). In addition, the TIR1/AFB receptors and AUX/IAA proteins show tissue-specific expression patterns (Dharmasiri *et al.* 2005b, Vernoux *et a.* 2011) which adds another level of specificity to auxin signalling.

The AUX/IAA repressors of auxin signalling

AUX/IAA proteins consist of three conserved domain: domains I, II and the PB1 domain (previously known as domains III and IV). Among them, domain I is the repressor EAR domain which facilitates interaction between AUX/IAA protein and the plant co-repressor TOPLESS; this interaction is required for the repression of the ARF transcriptional activity (Szemenyei *et al.* 2008). Domain II is responsible for the interaction with TIR1/AFB auxin receptors (Kepinski *et al.* 2005). The PB1 domain allows for interactions between AUX/IAA repressors and ARFs, a majority of which share this domain (Guilfoyle 2015). The PB1 domain is a well-described protein interaction module found in fungi, amoebas, animals and plants that mediates

protein-protein interactions between PB1 domain-containing proteins (Sumimoto *et al.* 2007). The conserved residues in the N- and C-terminal ends of the PB1 domain confer electrostatic and hydrogen-bond interactions between two proteins with PB1 domains; these interactions are oriented front-to-back enabling formation of oligomers (Guilfoyle 2015, Korasick *et al.* 2014, Nanao *et al.* 2014).

At low auxin levels AUX/IAA build oligomers with ARFs and recruit the co-repressor TOPLESS to attenuate auxin signalling. At high auxin, TIR1/AFB and AUX/IAA proteins build a complex which results in ubiquitination and degradation of AUX/IAAs by 26S proteasome and the subsequent derepression of the auxin signalling pathway (Luo *et al.* 2018). Most of AUX/IAAs are short-lived proteins with half-life ca. 5-12 minutes (Abel *et al.* 1994).

Majority of the AUX/IAA proteins are able to interact with each other and with ARF activators (Vernoux *et al.* 2011). There are multiple possibilities to build variable oligomer complexes between AUX/IAA and ARFs (Korasick *et al.* 2014, Nanao *et al.* 2014). In addition, the tissue-specific expression of individual AUX/IAAs contributes to the complexity of ARF repression (Vernoux *et al.* 2011).

ARF transcription factors

Auxin Response Factors mediate auxin signalling by directly transmitting auxin response through the activation or repression of auxin-induced genes. Most of the ARFs share a similar structure with a B3 DNA-binding domain (B3 DBD) at the N-terminus which is responsible for the interactions with the AuxRe element in the promoters of their target genes (Fig. In-10A) (Tiwari *et al.* 2003). ARFs also contain a dimerization domain (DD) at the N-terminus which facilitates homodimerization of ARFs and allows cooperative binding of ARF dimers to their target AuxRe element; this domain consists of two parts surrounding the DNA-binding domain (Boer *et al.* 2014). The flanking domains (FD) are found adjacent to the DD at the N-terminus; the function of these domains remains unclear (Boer *et al.* 2014, Guilfoyle 2015). A variable middle region (MR) inside the ARF protein determines if the ARF is a transcriptional activator or a repressor (Tiwari *et al.* 2003). The C-terminal domain PB1 is involved in homo- and heterooligomerization between ARFs and AUX/IAAs (Fig. In-10A) (Korasick *et al.* 2014, Nanao *et al.* 2014).

The phylogenetical analysis of the ARF gene family leads to division of these genes into 3 classes (Fig. In-10B) (Okushima *et al.* 2005). Class II genes include ARF5, 6,

7, 8 and 19; it has been argued that these are transcriptional activators due to the presence of the Q-rich middle region located between the N-terminus and the C-terminus. This middle region was shown to act as an activator domain in carrot protoplast assays (Tiwari *et al.* 2003, Ulmasov *et al.* 1999). More recent data suggest that at least ARF5 is able to act as both transcriptional activator (Cole *et al.* 2009,

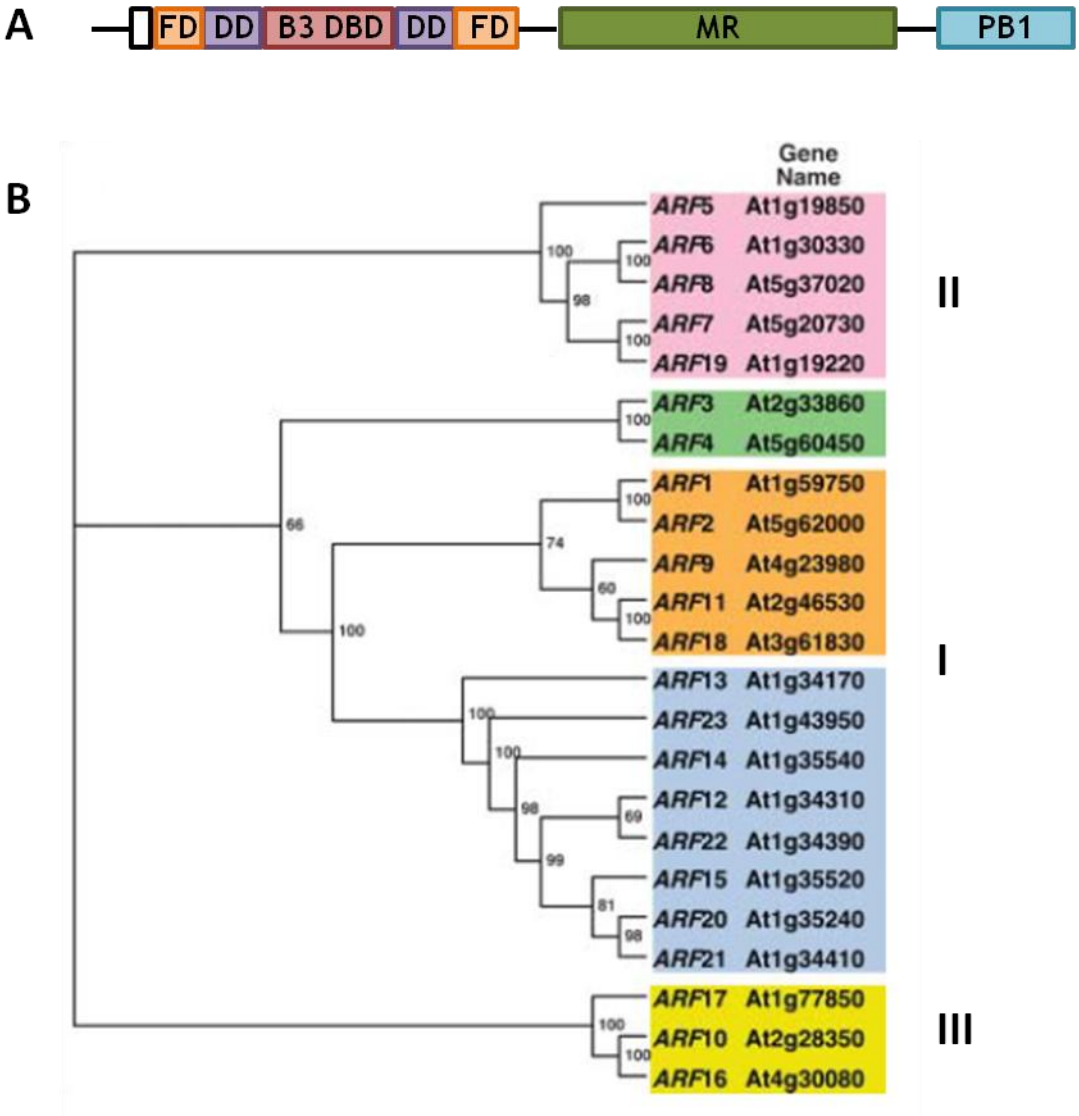

Fig. In-10. The structure of the auxin response factors (ARFs) with the B3 DNA-binding domain (B3 DBD), the dimerization domain (DD), the flanking domain (FD), the middle region (MR) and the PB1 domain **(A)** (Guilfoyle 2015). The ARF Gene Family of *Arabidopsis thaliana* **(B)** (Okushima *et al.* 2005).

Konishi *et al.* 2015, Schlereth *et al.* 2010, Yamaguchi *et al.* 2013) and transcriptional repressor (Zhang *et al.* 2014, Zhao *et al.* 2010). Several members of Class I (15 members) and Class III (3 members) were shown to act as transcriptional repressors (Tiwari *et al.* 2003, Ulmasov *et al.* 1999). The focus of my thesis lies in Class II ARFs in *Arabidopsis* and for this reason I will describe these ARFs in more details below.

ARF5

Among the Class II ARF family genes ARF5 (also called MONOPTEROS) is the most well studied. Loss of function mutations in the ARF5 gene result in severe phenotypes that include the inability to initiate root growth during embryonic development, variable arrangement of cotyledons and defects in vascular pattern in the leaves (Berleth and Jurgens 1993, Hardtke and Berleth 1998). The *arf5* mutant seedlings show defects in the embryonic development already at the triangular stage where the lower tier of cells show erratic patterns of cell division leading to incorrect development of suspensor cells. Consequently, the hypocotyl and the primary root are missing in the mutant seedling (Fig. In-11A) (Berleth and Jurgens 1993).

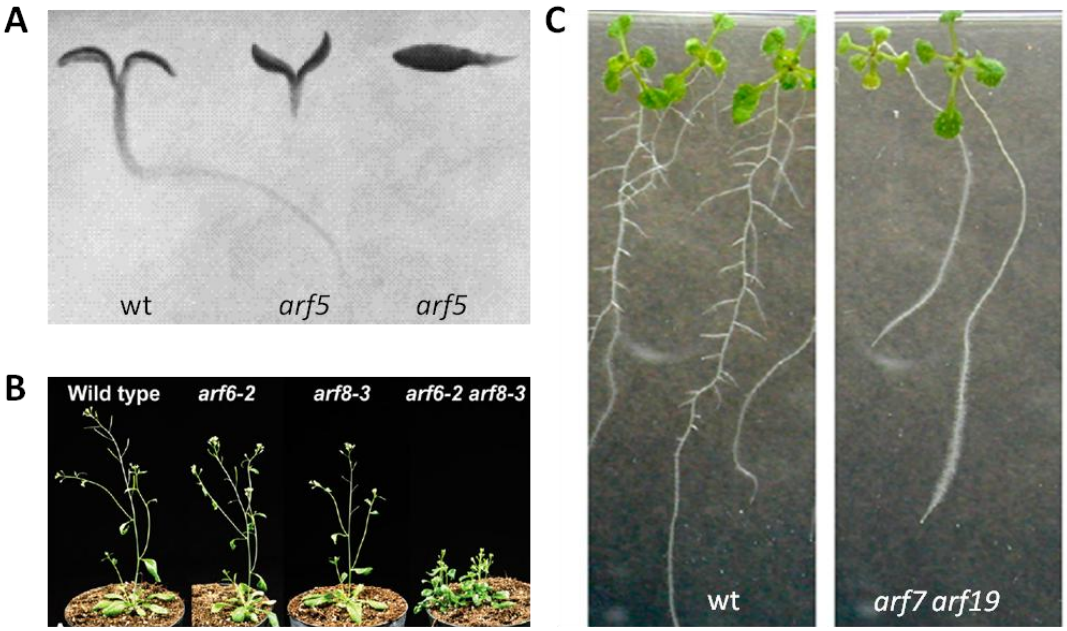

Fig. In-11. The phenotypes of the ARF activator mutants. **(A)** wild-type and *arf5* mutant seedlings (Berleth and Jurgens 1993). **(B)** wild-type, *arf6* mutant, *arf8* mutant and *arf6 arf8* mutant plants (Nagpal *et al.* 2005). **(C)** wild-type and the *arf7 arf19* double mutant seedlings (Okushima *et al.* 2007).

Nevertheless, the formation of adventitious roots can be induced in the *arf5* mutant under specific conditions. This enables the examination of the mutant phenotype in the older plant. The fully-grown plants are able to produce shoots which have defective “pin”-like inflorescences; this phenotype is similar to the *pin1* mutants

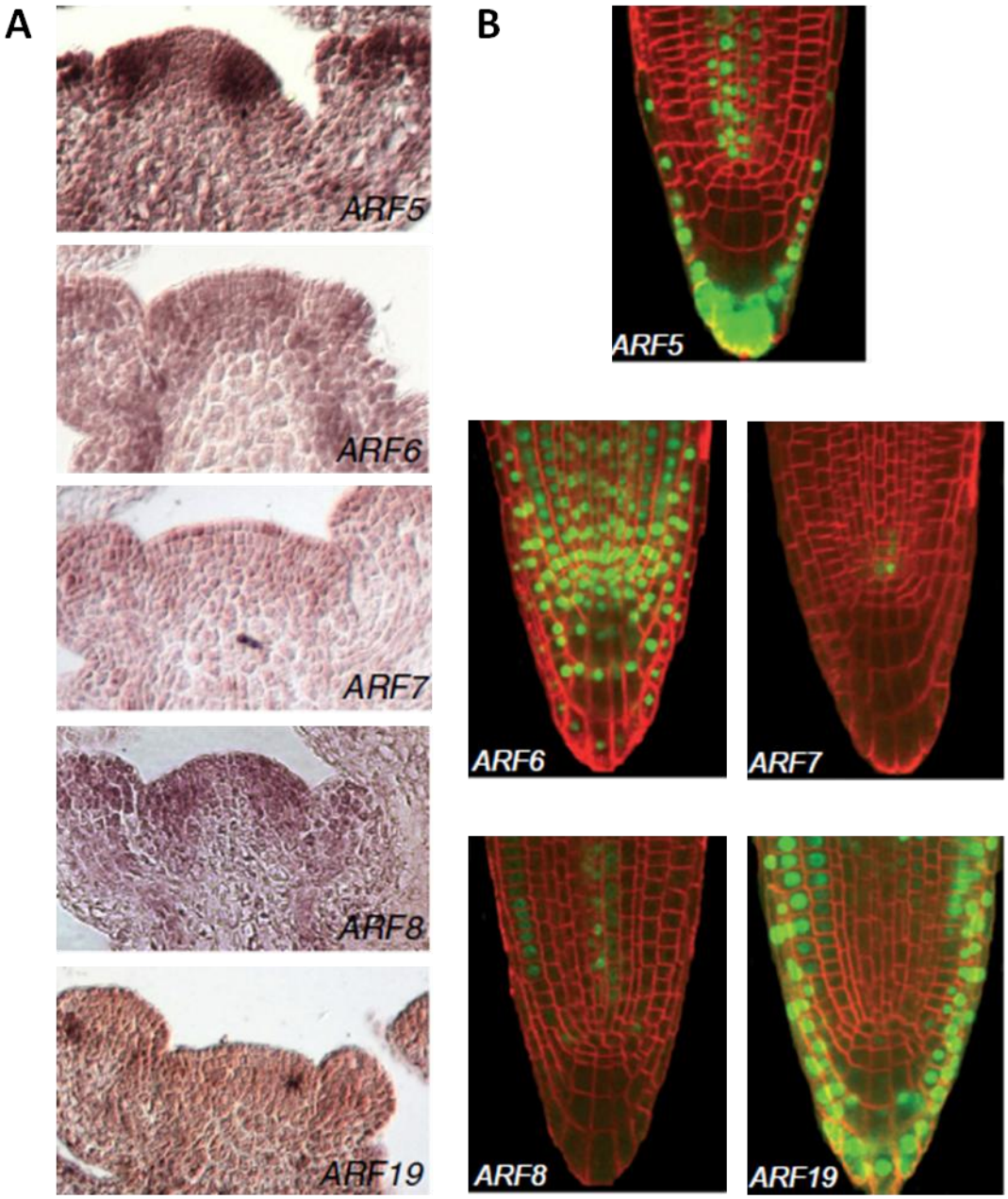

Fig. In-12. The expression of ARF activators in the shoot and root apical meristems. **(A)** Expression patterns of ARFs in the SAM shown by *in situ* hybridization (Vernoux *et al.* 2011) **(B)** Expression of ARFs in the RAM is depicted by transcriptional reporter lines consisting of a 2000 bp promoter fragment upstream of the ATG driving expression of GFP (Rademacher *et al.* 2011).

(Galweiler *et al.* 1998, Przemeck *et al.* 1996). The defects in the vascular development of the leaves include disrupted connection between individual xylem and phloem cells as well as the reduction of the vascular system to a single central strand (Berleth and Jurgens 1993, Przemeck *et al.* 1996).

ARF5 expression has been relatively well described. During embryogenesis this gene is expressed in the upper domain of the globular and the heart-stage embryos without any visible expression in the hypophysis and the underlying suspensor cells (Rademacher *et al.* 2011, Weijers *et al.* 2006). Later ARF5 is gradually confined to the vasculature of every plant organ with additional expression domains in the shoot and the root apices (Fig. In-12A and B) (Hardtke and Berleth 1998). In the shoot this gene is broadly expressed in the peripheral zone and the lateral organ primordia (Fig. In-12A) (Hardtke and Berleth 1998, Vernoux *et al.* 2011, Zhao *et al.* 2010). The root expression is confined to the vasculature and the columella region of the root tip (Fig. In-12B) (Hardtke and Berleth 1998, Rademacher *et al.* 2011, De Rybel *et al.* 2010).

ARF5 is required during embryogenesis where it mediates the establishment of the root pole through the specification of the hypophysis. ARF5 expression is limited to the cells adjacent to the hypophysis where it directly activates expression of a transcription factor TMO7 (Schlereth *et al.* 2010). Subsequently, TMO7 moves to the adjacent hypophysis precursor cell and mediates specification of the root pole (Schlereth *et al.* 2010, Weijers *et al.* 2006).

Due to the lethality of the *arf5* mutant the role of ARF5 in the mature plant is not so well characterized. ARF5 was shown to directly bind to promoters of several auxin-responsive genes and induce or repress expression of these genes. The direct regulation of Dof5.8 by ARF5 was shown to be important for vascular patterning during cotyledon development (Konishi *et al.* 2015). ARF5 induces DORNROSCHEN transcription during embryogenesis and this interaction regulates cotyledon development (Cole *et al.* 2009). Additionally, ARF5 directly induces expression of LEAFY, AINTEGUMENTA and AIL6 during initiation of flower primordium (Yamaguchi *et al.* 2013), ATHB8 during leaf vein formation (Donner *et al.* 2009), CUC1 and CUC2 during ovule development (Galbiati *et al.* 2013). ARF5 directly represses STOMAGEN which is important for the development of stomata (Zhang *et al.* 2014). The direct repression of ARR7 and ARR15 by ARF5 in shoot apical meristem is involved in regulation of the phyllotaxy (Zhao *et al.* 2010).

ARF5 appears to be the key mediator of auxin response in several developmental processes and because of this ARF5 is the most well-studied ARF. Nevertheless, many aspects of ARF5-mediated auxin response still require further investigations.

ARF6 and ARF8

ARF6 and ARF8 are closely related putative ARF activators with both independent and cooperative functions in plant development. ARF6 and ARF8 synergistically regulate flower development. Both *arf6* and *arf8* single mutant plants display a small delay in stamen development and produce fewer seeds than the wild-type, whereas in the *arf6 arf8* double mutant flower development is completely arrested and seeds are not produced (Fig. In-11B) (Nagpal *et al.* 2005). The *arf6 arf8* double mutant has significantly reduced levels of jasmonic acid (Nagpal *et al.* 2005). Both ARF6 and ARF8 were shown to be important for initiation of adventitious roots via the modulation of jasmonic acid homeostasis (Gutierrez *et al.* 2009, Gutierrez *et al.* 2012). A role for ARF8 independent from that of ARF6 was identified in light-dependant hypocotyl growth response (Tian *et al.* 2004); in this study ARF8 was shown to inhibit hypocotyl elongation in response to light. *arf8* mutants have parthenocarpic silique development indicating an additional role for ARF8 in fruit development (Goetz *et al.* 2006, Goetz *et al.* 2007). Finally, ARF8 was shown to be involved in lateral root emergence in response to nitrogen (Gifford *et al.* 2008).

ARF6 and ARF8 are expressed differentially throughout plant development. Whereas ARF6 is strongly expressed at all stages of embryonic development, ARF8 expression was not detected in embryos at all (Rademacher *et al.* 2011). Later ARF6 seems to be ubiquitously expressed in all cells of the RAM and shows a broad expression also in the SAM (Fig. In-12) (Rademacher *et al.* 2011, Vernoux *et al.* 2011). On the other hand ARF8 expression seems to be limited to specific tissues both in the root and the shoot (Fig. In-12) (Rademacher *et al.* 2011, Vernoux *et al.* 2011). Both ARF6 and ARF8 are expressed in multiple flower organs (Nagpal *et al.* 2005). The expression of ARF6 and ARF8 is controlled by microRNA167 and this regulation is important for flower development (Wu *et al.* 2006).

ARF7 and ARF19

ARF7 and ARF19 are closely related genes and, similarly to ARF6 and ARF8, they have both unique and overlapping functions.

a*rf7* mutant has impaired phototropic response towards blue light (Liscum and Briggs 1996; Harper *et al.* 2000) and impaired gravitropic response in hypocotyl (Watahiki and Yamamoto 1997). In addition, the mutant has epinastic rosette leaves (Watahiki and Yamamoto 1997) and slightly shorter length of the inflorescence stems (Okushima *et al.* 2005). The *arf7* mutant produces fewer lateral roots than the wild-type (Okushima *et al.* 2005).

arf19 single mutant is auxin-resistant and has ethylene-insensitive roots (Okushima *et al.* 2005; Li *et al.* 2006a). Unlike *arf7* mutant, *arf19* mutant shows normal phototropic and gravitropic responses of hypocotyl as well as normal growth of the leaves and the shoot (Okushima *et al.* 2005). The number of lateral roots is the same as in the wild-type (Okushima *et al.* 2005).

However, the double mutant *arf7 arf19* has drastic phenotype with severely defective gravitropic response and lateral root formation, thus suggesting an important redundancy between these two ARFs (Fig. In-11C) (Okushima *et al.* 2005, Li *et al.* 2006a). The individual phenotype of *arf7* mutant including impaired phototropic response and epinastic leaves are also found in the double mutant (Okushima *et al.* 2005). Additionally, the *arf7 arf19* mutant has a reduced number of inflorescence stems (Okushima *et al.* 2005). Nevertheless, the flowers of the double mutant appear normal (Okushima *et al.* 2005).

ARF7 expression was not detected at the earliest stages of the embryo but appeared later at the heart-stage embryo in the presumptive root meristem (Rademacher *et al.* 2011). Later ARF7 expression in the root tip is limited to the few cells above the quiescent center corresponding to the vasculature initials (Fig. In-12B) (Rademacher *et al.* 2011) and the vasculature in the older root (de Rybel *et al.* 2010). ARF7 is expressed throughout the shoot apex (Fig. In-12A) (Vernoux *et al.* 2011). ARF19 is not expressed during embryonic development. Later ARF19 expression is detected in the columella, epidermis and mature vasculature of the root (Fig. In-12B) (Rademacher *et al.* 2011). In the shoot ARF19 expression appears to be broad but with a higher expression in lateral organs (Fig. In-12A) (Vernoux *et al.* 2011).

It was established that both ARF7 and ARF19 play the key role in lateral root formation by direct activation of LBD (LATERAL ORGAN BOUNDARIES-DOMAIN) genes. LBD genes initiate asymmetric divisions in lateral root founder cells during

lateral root primordia initiation (Goh *et al.* 2012; Okushima *et al.* 2007). In the shoot the role of these ARFs remains to be fully established.

The plant hormone cytokinin

Cytokinin signalling pathway

Cytokinin is another plant hormone which together with auxin regulates plant development and acts notably in the regulation of meristem activity as seen before. Cytokinin is involved in growth at the shoot and the root apical meristems, formation of lateral roots, leaf senescence, apical dominance, biotic and abiotic stress, and other developmental processes (Argueso *et al.* 2009, Hwang *et al.* 2012).

Naturally occurring cytokinins are adenine derivates with a side chain attached at N6

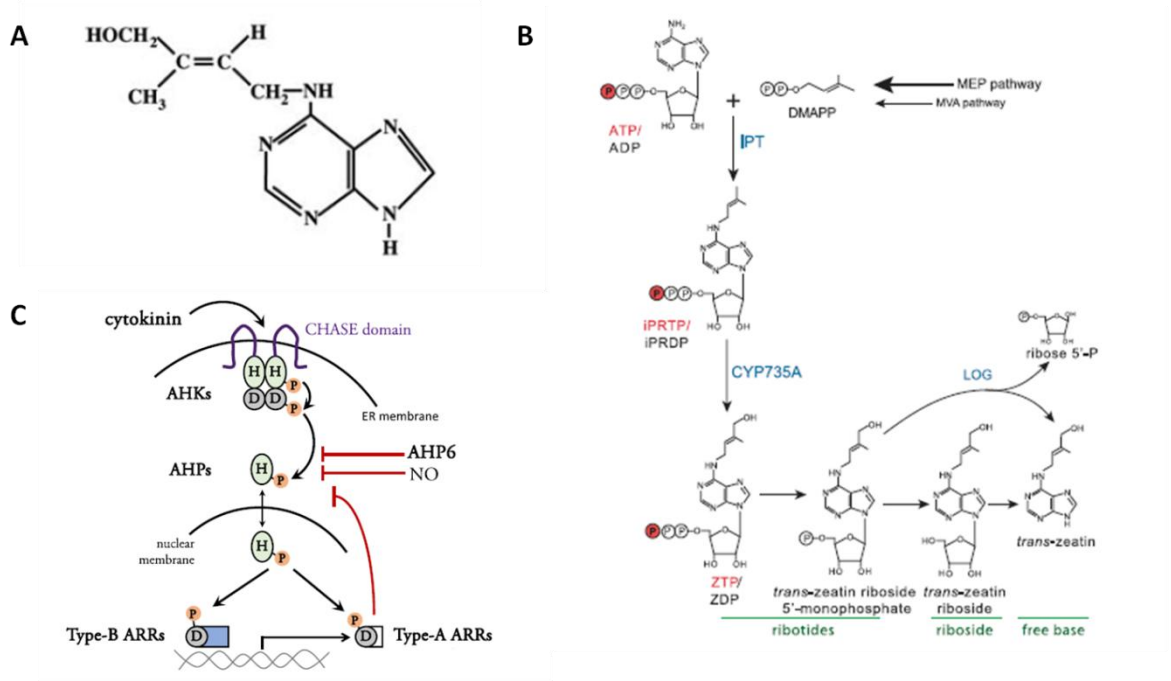

Fig. In-13. Structure of trans-zeatin, the most abundant natural cytokinin **(A).** Biosynthetic pathway of cytokinin **(B).** Current model for cytokinin phosphorelay signal transduction **(C).** (Kieber and Schaller 2014).

position which is either isoprene-derived or aromatic. The most abundant natural cytokinin is trans-zeatin (Fig. In-13A) (Kieber and Schaller 2014).

Cytokinin is thought to be biosynthesized from AMP and dimethylallyl pyrophosphate (DMAPP) (Kieber and Schaller 2014, Frebort *et al.* 2011). The first biosynthesis step is catalyzed by the enzyme isopentenyltransferase (IPT). The subsequent enzymatic reactions are catalyzed by a cytochrome P450 enzyme (CYP735A in *Arabidopsis thaliana*) and LONELY GUY (LOG) family of enzymes (Fig. In-13B). Cytokinins can be produced in various parts of the plant and then transported shootwards in xylem in form of tZ-riboside or rootwards in phloem as iP type cytokinins (Hirose *et al.* 2008, Kudo *et al.* 2010, Sakakibara 2006). The active cytokinins can be reduced to inactive forms by either irreversible cleavage by the cytokinin oxidase/dehydrogenase enzymes (CKX) or reversible conjugation to glucose by cytokinin glycosyltransferases (Fig. In-13B) (Kieber and Schaller 2014, Frebort *et al.* 2011).

Cytokinin signalling is similar to the bacterial two-component phosphorelay system (Kieber and Schaller 2014). Signalling is initiated by active cytokinins binding to histidine kinase receptors (AHKs) which then undergo autophosphorylation. In turn, the autophosphorylated AHKs can pass the phosphate group to the phosphotransfer proteins (AHPs) thus activating them. AHPs are mobile proteins that shuttle between the nucleus and the cytoplasm. Inside the nucleus, an activated AHP protein phosphorylates B-type response regulators (B-type ARRs). These B-type transcription factors propagate the cytokinin response by direct regulation of numerous cytokinin-responsive genes. This signalling cascade is negatively regulated by A-type ARRs and AHP6 (Fig. In-13C) (Kieber and Schaller 2014; Hwang *et al.* 2012, To and Kieber 2008). AHP6 is a non-functional phosphotransfer protein which lacks the phosphorylation site and acts as an inhibitor of cytokinin signalling in the root vasculature and in the SAM (Besnard *et al.* 2014, Bishopp *et al.* 2011, Mahonen *et al.* 2006).

Cytokinin signalling can be visualized *in planta* using a TCS synthetic reporter which consists of B-type ARR binding motif concatemers constitutively driving a reporter gene such as GFP (Muller and Sheen 2008, Zurcher *et al.* 2013) (Fig. In-3C, 7B).

Cytokinin Response Factors (CRFs)

The well-described cytokinin signalling pathway is based on a phosphorelay system which involves membrane-bound AHK cytokinin receptors, mobile AHP proteins and

the B-type ARR transcription factors. Together these three components mediate cytokinin response in various tissues. Nevertheless it was shown recently that the expression of a subset of cytokinin-induced genes is directly regulated by Cytokinin Response Factors (CRFs).

CRFs are a gene family of transcription factors belonging to a subset of AP2/ERF family of transcription factors and consisting of 12 members in *Arabidopsis thaliana* (Fig. In-14A). They are characterised by a presence of conserved CRF domain at the N-terminus and by a single AP2 domain in the middle region of the protein (Fig. In-14B). The AP2 domain is a well-studied DNA-binding domain; it is present not only in CRF genes but generally in members of the AP2/ERF superfamily of transcription factors (Licausi *et al.* 2013). The CRF domain is specific for the CRF gene family; it was shown to be involved in protein-protein interactions (Cutcliffe *et al.* 2011).

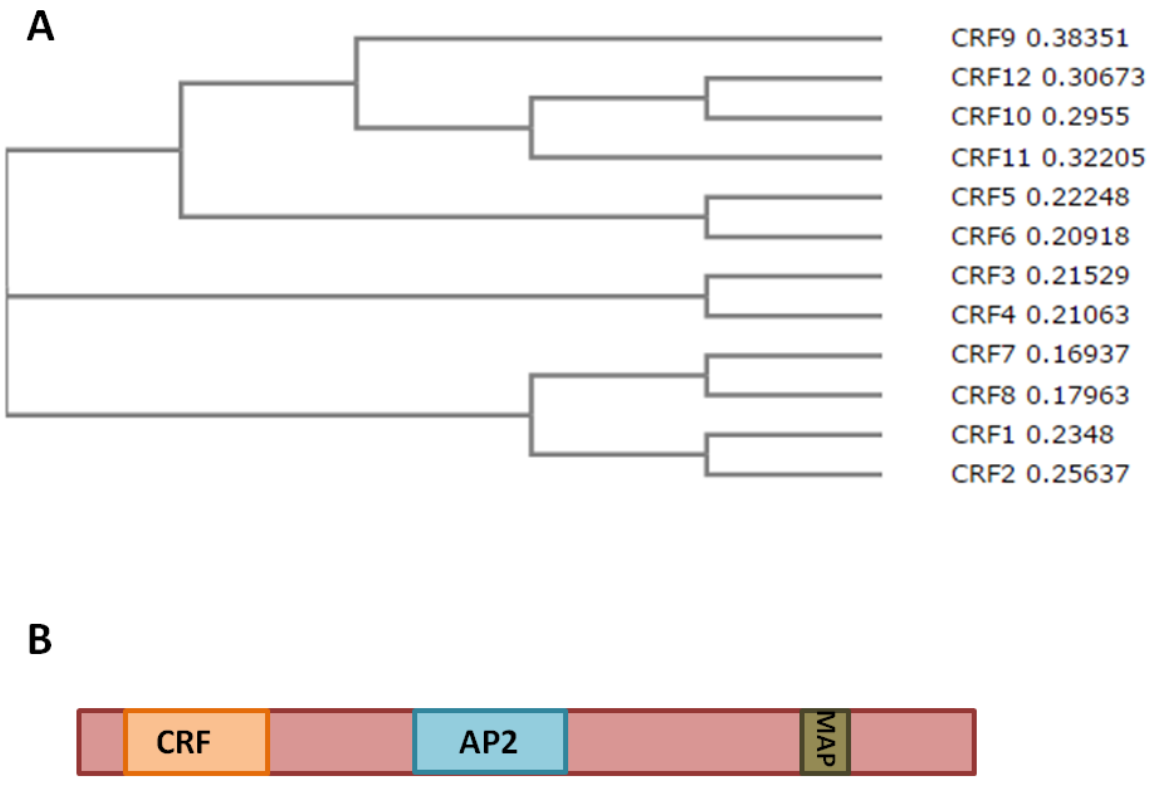

Fig. In-14. The CRF Gene Family of *Arabidopsis thaliana* **(A)**. Phylogenetic tree was constructed using CLUSTRAL multiple protein sequence alignment with MUSCLE (3.8). The structure of CRF proteins with CRF domain, AP2 domain and the putative MAP kinase phosphorylation site **(B)**.

Though their CRF domains CRF proteins are able to build homo- and heterodimers as well as directly interact with AHP proteins (Cutcliffe *et al.* 2011). In addition, many of the CRF genes contain a putative MAP kinase phosphorylation site in the C-terminus. CRF gene homologues are found in all groups of land plants (Rashotte and Goertzen 2010).

The name of this gene family, the Cytokinin Response Factors, implies that these genes show response to cytokinin treatment. Indeed, several members of the CRF family, including CRF2, CRF5 and CRF6, are upregulated by cytokinin and this cytokinin-induced upregulation is dependent on B-type ARRs (Rashotte *et al.* 2006). The CRF family members regulate a subset of genes that partially overlaps with B-type ARR targets (Raines *et al.* 2016; Rashotte *et al.* 2006). All this suggests the involvement of CRF genes in cytokinin signalling pathway. CRFs seem to act downstream of AHPs and possibly in parallel with B-type ARRs.

Earlier investigations implied that CRF proteins are localized in cytoplasm and are able to translocate to nucleus in response to cytokinin treatment (Rashotte *et al.* 2006). In contrast, this observation was not confirmed in alternative studies where CRF1 and CRF5 remained mostly nuclear-localized in both presence and absence of cytokinin (Raines *et al.* 2016).

CRFs were also shown to be involved in the regulation of auxin response. In particular, CRF2 and CRF6 directly control expression of PIN7 and PIN1 in the root (Simaskova *et al.* 2015).

The members of the family studied so far in detail are CRF1 to CRF6; their single and multiple mutants display a number of developmental phenotypes such as embryonic lethality in *crf5 crf6* double mutant, defects in cotyledon development caused by reduced cell expansion in *crf1 crf2 crf3 crf5 crf6* single and multiple mutants (Rashotte *et al.* 2006). The *crf2* and *crf3* show reduced root length, root meristem size and lateral root initiation whereas *crf6* mutant displays opposite effects (Jeon *et al.* 2016, Simaskova *et al.* 2015). Many CRFs including CRF1, CRF3 and CRF5 promote leaf senescence (Raines *et al.* 2016). On the other hand, CRF6 negatively regulates leaf senescence (Zwack *et al.* 2013).

Overall, the involvement of CRF genes in cytokinin signalling pathway is still incompletely understood.

Aims of the thesis

The goal of this thesis is to study transcriptional regulation of Auxin Response Factors (ARFs). The project focuses on the five Class II ARF activators from *Arabidopsis thaliana*: ARF5, 6, 7, 8 and 19. These five ARFs are thought to mediate auxin response through mostly transcriptional activation of auxin-responsive genes.

In the first chapter, the expression of ARF activators in the root and the shoot was studied using transcriptional reporter lines. These reporter lines contain long regions upstream of the start codon as well as downstream sequences including the first big introns which are argued to be potential binding sites for transcriptional regulators. Indeed, the study shows importance of the downstream sequences for the transcriptional regulation of ARFs. In addition, the post-transcriptional regulation of ARFs was accessed using translational reporter lines. These results indicate that some of the ARFs undergo protein movement or degradation that affects their spatio-temporal distribution.

In the second chapter, the transcriptional regulators of ARF activators were identified. This was done using a high-throughput yeast one-hybrid screen in collaboration with Siobhan Brady's lab, University of Davis (Gaudinier *et al.* 2011). The promoter sequences of the ARFs fused to reporter genes were screened against the root-specific library of transcription factor available at the University of Davis. In addition, during this project 87 additional mostly shoot-specific transcription factors were cloned and added to the collection. In this assay, regulators of ARF transcription acting both in the RAM and the SAM were identified. The resulting gene regulatory network was validated *in planta* and the nature of the interactions (repression or activation) was elucidated using a transient protoplast assay. The interactions were further confirmed by monitoring the expression of ARF activators in mutants of the regulatory transcription factors. Additionally, publically available information such as DAP-seq and microarray datasets provided information on the potential developmental significance of interactions *in planta*. Finally, the mutants of the regulatory transcription factors were investigated for developmental phenotypes in the root and the shoot.

In the third chapter, the biological significance of an interaction between the candidate ARF7 regulator, the CRF10 transcription factor, and ARF7 promoter was analyzed. Notably, this study attempted to understand if the interaction between CRF10 and the promoter of ARF7 could result in a number of developmental phenotypes observed in the *crf10* mutant such as early senescence of leaves, delayed hypocotyl response to blue light and disorganized RAM architecture.

Chapter I: The tissue-specific expression of ARF activators during growth and development in the RAM and the SAM

Introduction

The plant hormone auxin is an important intracellular signal which induces developmental changes enabling the plants to rapidly adapt their growth to varying environmental conditions. The auxin-induced growth and development is based on rapid reprogramming of cells and tissues which is mediated by the Auxin Response Factor transcription factors (ARFs). In *Arabidopsis thaliana*, the auxin-induced growth response is mostly mediated by the five ARF activators: ARF5, 6, 7, 8 and 19. These five ARFs activate expression of different target genes (Nagpal *et al.* 2005, Schlereth *et al.* 2010, Okushima *et al.* 2005) and this contributes to the diversity of auxin responses. The specificity of auxin responses comes in part from expressing ARF activators in precise tissues (Rademacher *et al.* 2011, Vernoux *et al.* 2011) or following a certain environmental stimulus such as transferring the plants from dark to light (Gutierrez *et al.* 2009). Thus the expression of ARF activators must undergo tight transcriptional regulation to ensure that the auxin response is triggered only when and where required.

In eukaryotes gene expression is controlled by transcription factors which bind regulatory DNA sequences and facilitate or hinder initiation of gene transcription. Transcription factors generally bind regulatory sites in the gene locus. Traditionally, promoter regions were considered to be enriched in these regulatory sites. Recent results indicate that in *Arabidopsis thaliana* the transcription factor binding sites are mostly localized between -1000 bp to +200 bp with a peak at 50 bp upstream of the transcription start site (Yu *et al.* 2016).

In addition to the promoter region, the introns and especially the first intron can contain transcription factor binding sites (Chorev and Carmel 2012). It was shown that introns can contain regulatory elements such as enhancers (Beaulieu *et al.* 2011; Bianchi *et al.* 2009; Scohy *et al.* 2000; Tourmente *et al.* 1993), silencers (Gaunitz *et al.* 2004; Gaunitz *et al.* 2005; Tourmente *et al.* 1993) or other regulators

(Bornstein *et al.* 1988; Zhang *et al.* 2011); these regulatory elements were found in most cases in the first big intron (the closest intron to the ATG initiation codon) (Beaulieu *et al.* 2011; Bornstein *et al.* 1988; Gaunitz *et al.* 2004; Rose *et al.* 2008; Scohy *et al.* 2000; Zhang *et al.* 2011). Bradnam and Korf 2008 identified that the first introns in most eukaryotes including *Arabidopsis thaliana*, *Caenorhabditis elegans*, and *Drosophila melanogaster* are significantly longer than all downstream introns within a gene and that they contain a higher number of intron mediated enhancement (IME) motifs within their sequence. IME is the name given to this observed intron-induced increase in mRNA accumulation (Laxa 2016). The first big intron was shown to be required for the correct expression or for enhancing expression in mice (Palmiter *et al.* 1991), human (Jonsson *et al.* 1992), *C. elegans* (Ho *et al.* 2001), *Arabidopsis thaliana* (Rose and Last 1997), maize (Vasil *et al.* 1989), rice (Jeon *et al.* 2000; Morello *et al.* 2002) and petunia (Jeong *et al.* 2007). The importance of the first big intron is further supported by the fact that this intron is more evolutionally conserved than other introns and enriched for regulatory epigenetic signals (Park *et al.* 2014). The mechanism by which introns control gene expression remains in most cases unknown but it was shown that introns can affect different steps in mRNA maturation such as transcription initiation, elongation, termination, nuclear export and mRNA stability (Chorev and Carmel 2012).

In this part of the thesis specificity of auxin response was analyzed by studying expression of ARF activators in various tissues. The expression patterns are remarkably different for each ARF activator both in the root and the shoot tissues. ARF expression was shown to be dependant not only on the regulation in the DNA region upstream of the start codon but also on the downstream region which includes the first intron. Furthermore, activity of some of the ARF activators is regulated post-transcriptionally through putative protein movement or degradation.

Results

ARF activators are differentially expressed in the root and the shoot

Both unique and partially overlapping functions of ARF activators in auxin-regulated developmental processes must correspond with tissue-specific expression patterns. Studying these patterns could potentially provide valuable information on the functionality and specificity of each ARF. The existing ARF transcriptional reporter lines created in Rademacher *et al.* 2011 consist of ca. 2000 bp promoter driving expression of the GFP fluorescent reporter; these promoters contain only sequences upstream of the transcription start site. The chosen promoter length and content in these lines might not be sufficient to correctly recapitulate the *in planta* expression of ARFs. For these reason I constructed my own transcriptional reporter lines containing longer promoter regions as described below.

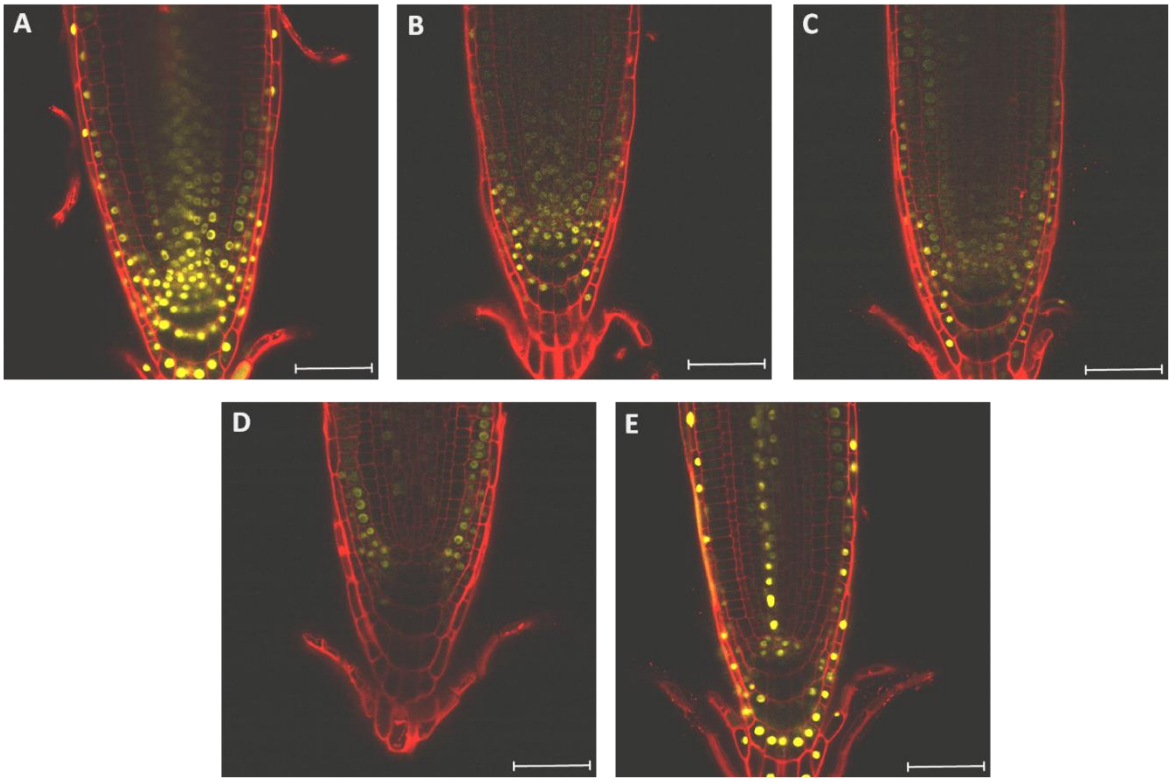

Fig. 1-1. Expression of ARF activators in the root tip of the primary root: **(A)** ARF5, **(B)** ARF6, **(C)** ARF7, **(D)** ARF8 and **(E)** ARF19. The plants were grown in 12h light/12h dark conditions for 6 days. Bar scale 50 µm.

ARF activators share a similar genomic structure: the gene coding sequence is interrupted by 11-14 introns (Suppl. Fig 1-1). In particular, in case of ARF5, 7 and 19 the first intron is 2-3 times bigger compared to the following smaller introns. The upstream intergenic regions between the ARF activator coding sequence and the preceding gene coding sequence vary in size between ca. 13 kb for ARF5 and ca. 3 kb for ARF7 (Suppl. Fig 1-1). For these reason I constructed transcriptional reporter lines which harbor long fragments of DNA upstream of the transcription start site (between 5,5 kb for ARF5 and 2,9 kb for ARF7) followed by the downstream sequences which include the first big intron (Suppl. Fig. 1-2A). The design was to include all potential sites of transcriptional regulation so that the reporter lines will accurately report *in planta* regulation. In case of ARF5, the length of the upstream sequences should be at least 4,1 kb because the genomic ARF5 DNA fragment driven by promoter of this size was able to complement *arf5* mutant phenotype

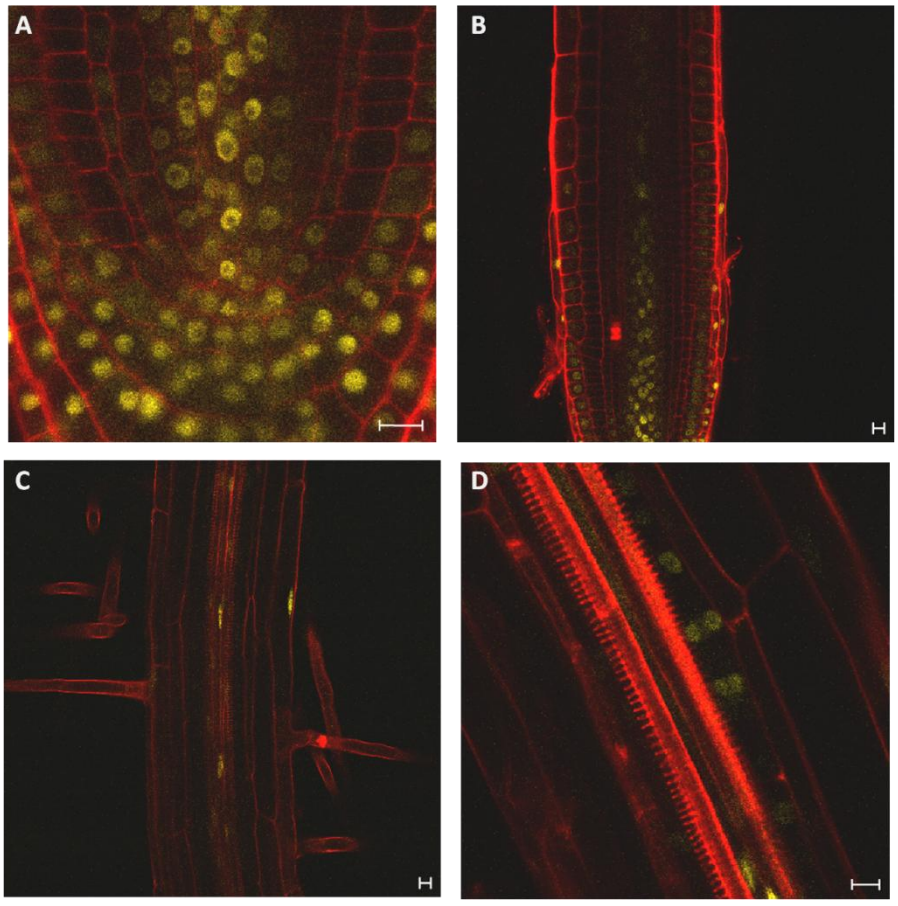

Fig. 1-2. Expression of ARF5 in the meristematic zone of the primary root **(A)**, in the meristematic and elongation zones **(B)**, in the older root **(C)** and in the lateral root primordia **(D)**. The plants were grown in 24h light conditions for 5 days. Bar scale 10 µm.

(Weijers *et al.* 2006). As for the other four ARF activators, the minimum required promoter length could only be speculated based on the length of the upstream region and the presence of the first big intron.

Each ARF activators displayed a unique expression pattern in the root tip (Fig. 1-1). The expression patterns showed robustness and didn't change when grown in different light regimes (12h light/12h dark, 16h light/8h dark or 24h light conditions).

In the root ARF5 is strongly expressed in most tissues of the meristematic zone except cortex and endodermis (Fig. 1-1A). Interestingly, ARF5 is expressed in the shared cortex/endodermis initial cell but absent in the subsequent cortex daughter

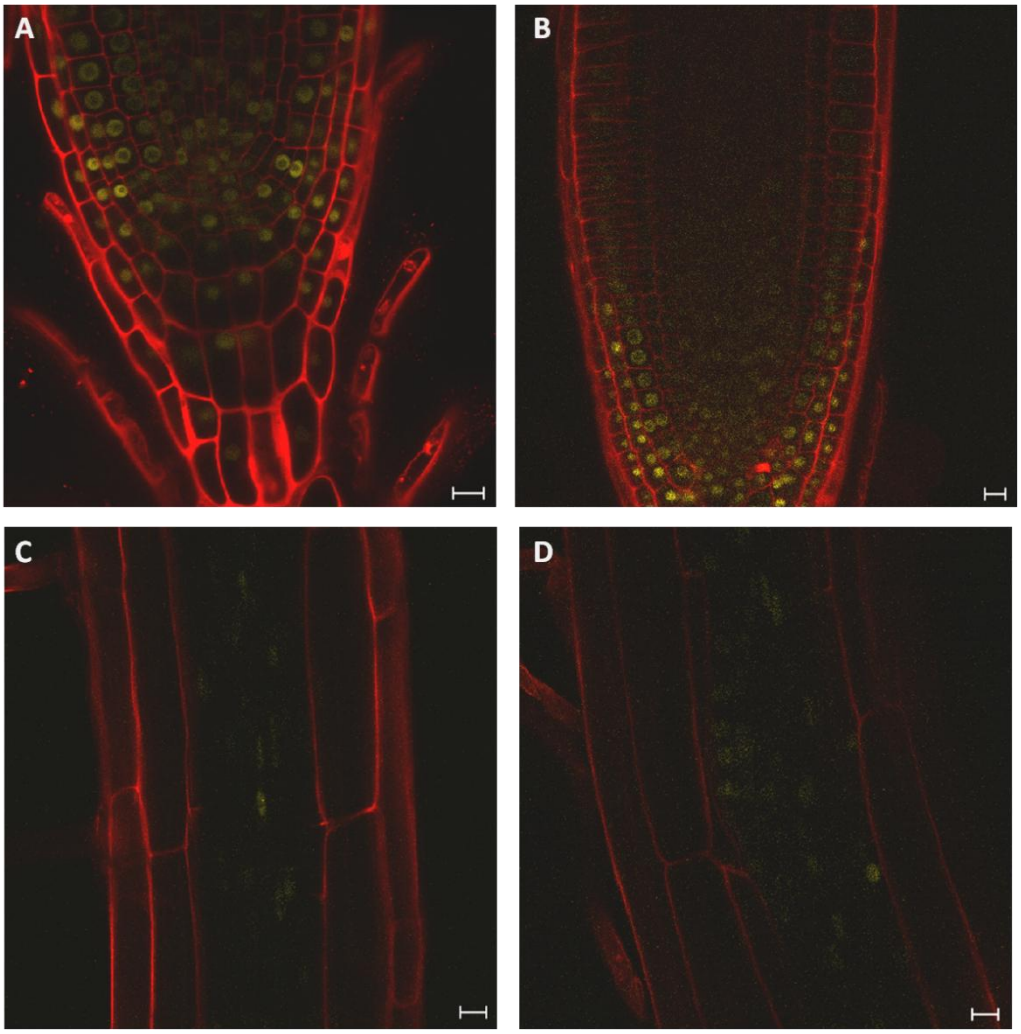

Fig. 1-3. Expression of ARF6 in the meristematic zone of the primary root **(A)**, in the meristematic zone **(B)**, in the older root **(C)** and in the lateral root primordia **(D)**. The plants were grown in 24h light conditions for 5 days. Bar scale 10 µm.

cells and present in only a few subsequent endodermis cells (Fig. 1-2A). Following the transition from maturation to the elongation zones the expression is rapidly restricted to the xylem pole of the vasculature and disappears from other tissues (Fig. 1-2B). In the older root the expression is found around the xylem cells with occasional strong expression in a few epidermal cells (Fig. 1-2C). ARF5 is also expressed in the lateral root primordia of all stages (Fig. 1-2D).

ARF6 is expressed throughout the root meristematic zone but it is absent or reduced in the lowest tier of columella (Fig. 1-1B, Fig 1-3A). At the end of the meristematic zone the expression is rapidly reduced and disappears completely in the elongation zone (Fig. 1-3B). In the older root the expression is either completely absent or a

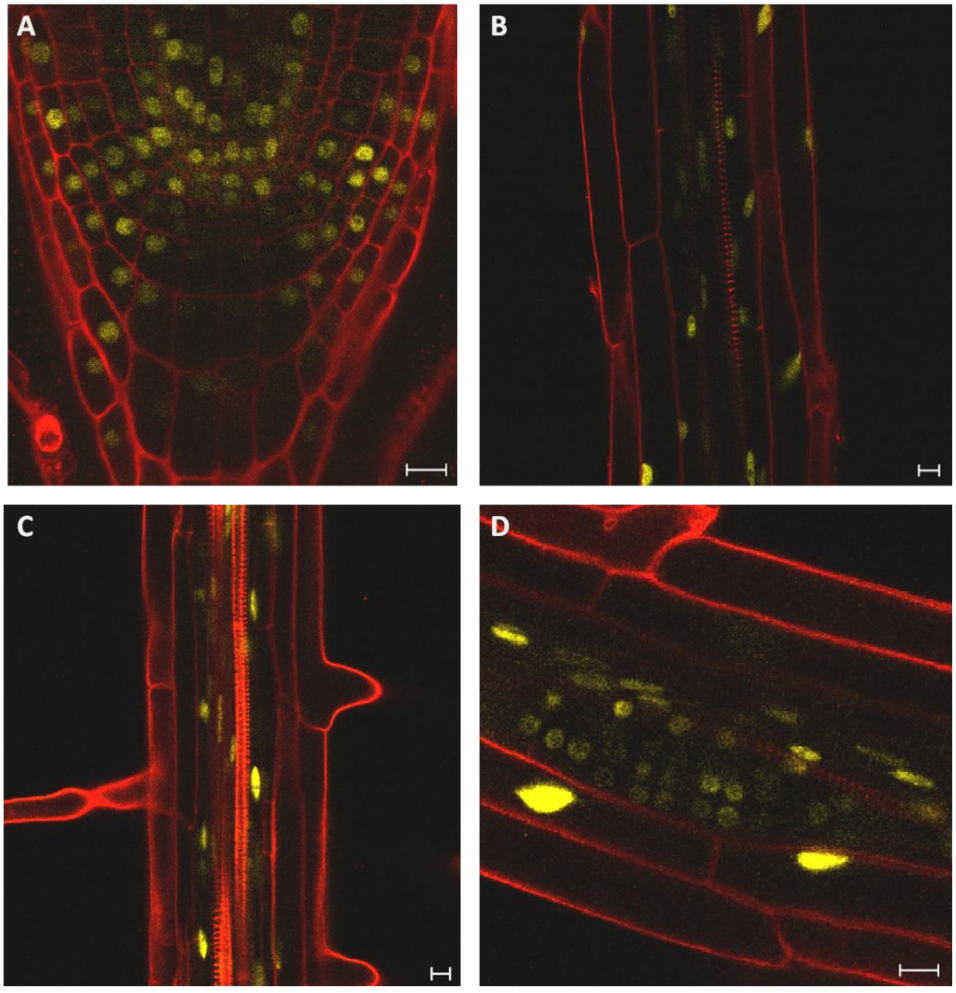

Fig. 1-4. Expression of ARF7 in the meristematic zone of the primary root **(A)**, in the lower older root **(B)**, in the upper older root **(C)** and in the lateral root primordia **(D)**. The plants were grown in 24h light conditions for 5 days. Bar scale 10 µm.

weak expression in the vasculature can be seen (Fig. 1-3C). ARF6 is also weakly expressed in the lateral root primordia detectable from stage III onwards (Fig. 1-3D).

In the root, ARF7 is expressed in multiple tissues but the expression is nevertheless not ubiquitous. ARF7 seems to be strongly expressed in and around the stem cell niche with highest expression levels are in the QC, vasculature initials and the cortex/endodermis initials (Fig. 1-1C and Fig. 1-4A). On the contrary, the expression is absent in the columella stem cells and columella proper (Fig. 1-4A). From the elongation zone upwards ARF7 expression is present in most of the cell (Fig. 1-4B)

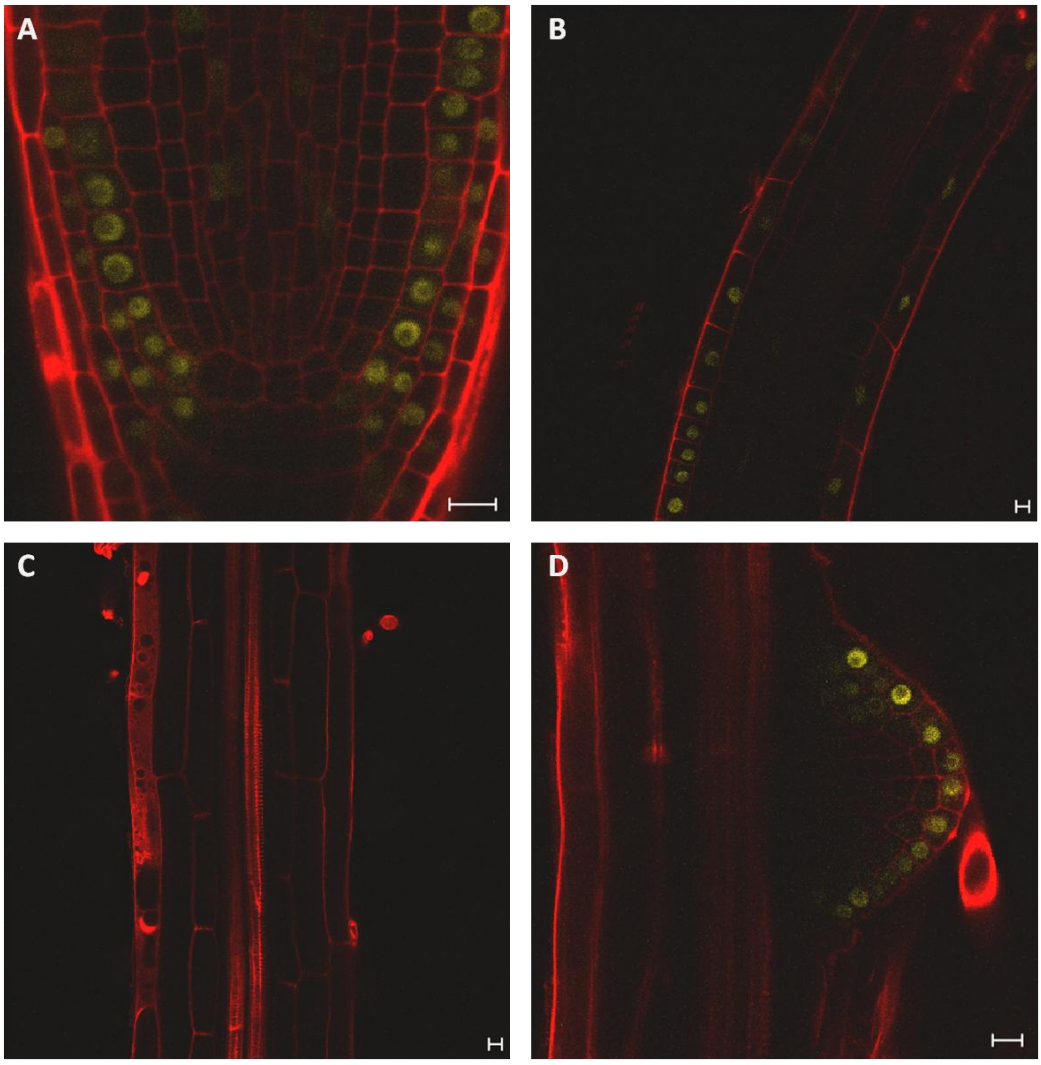

Fig. 1-5. Expression of ARF8 in the meristematic zone of the primary root **(A)**, in the elongation zone of the primary root **(B)**, in the older root **(C)** and in the lateral root primordia **(D)**. The plants were grown in 24h light conditions for 5 days. Bar scale 10 µm.

but becomes confined to the vasculature in the upper parts of the root (Fig. 1-4C). ARF7 is also expressed in the lateral root primordia at all stages (Fig. 1-4D).

The expression of ARF8 is very restricted. In the root tip ARF8 is expressed in the epidermis and lateral root cap cells of the maturation zone (Fig. 1-1D, Fig. 1-5A). ARF8 is also expressed in the shared epidermis/lateral rot cap initial cell (Fig. 1-5A). Occasionally a weak expression in early vasculature can be detected. At the start of the elongation zone the expression completely disappears (Fig. 1-5B). ARF8 is not expressed in the older root at all (Fig. 1-5C). In the lateral root primordia ARF8 is expressed only in the epidermal layer of the primordia from stage VI onwards (Fig. 1-5D).

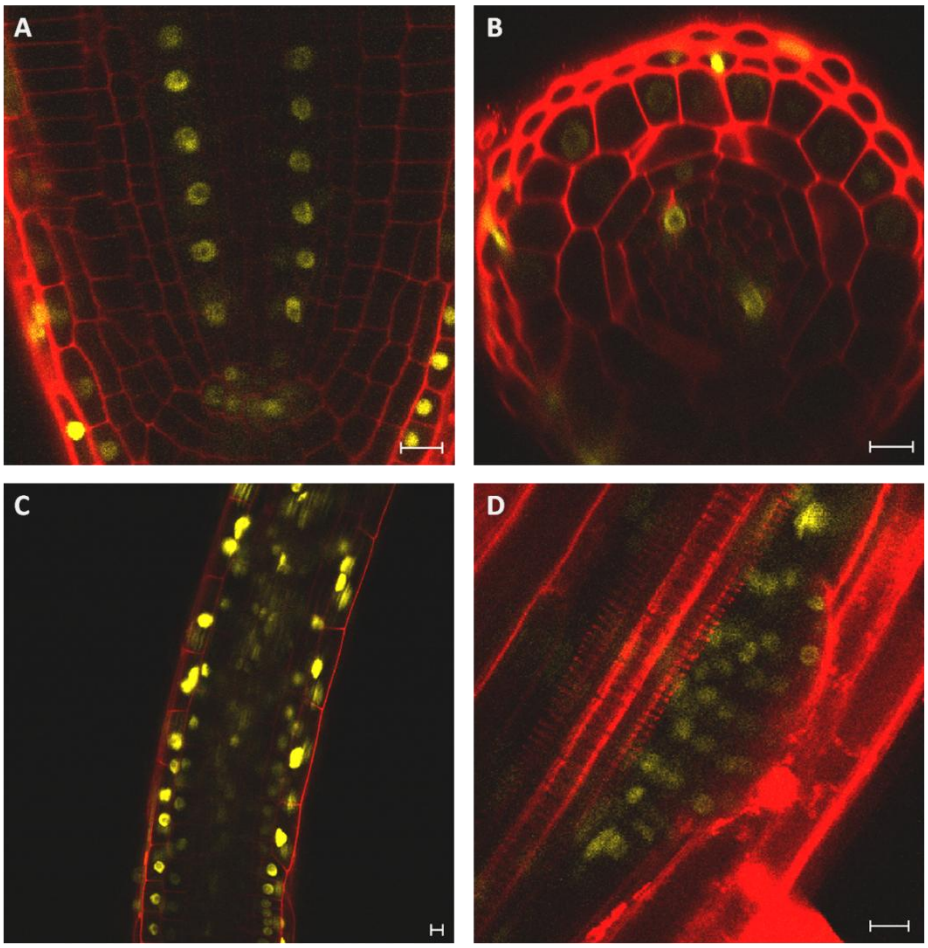

Fig. 1-6. Expression of ARF19 in the meristematic zone of the primary root **(A)** and **(B)**, in the elongation zone of the primary root **(C)** and in the lateral root primordia **(D)**. The plants were grown in 24h light conditions for 5 days. Bar scale 10 µm.

ARF19 shows a very interesting expression pattern in the primary root. It is expressed precisely in the QC and in two cell files of protoxylem (Fig. 1-1E, Fig. 1-6A, 1-6B). The protoxylem expression continues upwards along the lower part of the maturation zone and then disappears. In addition, ARF19 is also expressed in the epidermis, lateral root cap and the lower tier of columella of the primary root tip (Fig. 1-1E). Starting from the elongation zone upwards ARF19 seems to be expressed in every tissue (Fig. 1-6C). ARF19 is additionally expressed in the lateral root primordia of various stages (Fig. 1-6D).

The RAM expression patterns can be compared to the published data which were obtained using lines with ca. 2000 bp promoters driving a GFP reporter (Fig. In-12) (Rademacher *et al.* 2011). Thus the difference between these published lines and my constructs lies in the length of the promoter region (with my constructs having much longer promoters) and the presence of the first intron in my constructs. In case of ARF5 and 6 the patterns are similar. On the other hand, ARF8 vasculature expression is stronger in the GFP reporter line compared to my lines. ARF7 expression in the GFP lines is limited to a few cells above QC whereas my lines show a broad pattern. Finally, ARF19 published line doesn't appear to have the protoxylem expression domain which is present in my lines. Overall my longer promoter lines substantially differ in expression patterns compared to the Rademacher *et al.* lines with a shorter promoter.

All five ARF activators are expressed in the shoot apical meristem. In my transcriptional reporter lines ARF5 is found in the peripheral zone and the lateral organ primordia but completely absent from the central zone and the under-lying organizing center (Fig. 1-7A, F). ARF6 is specifically enrichment in the boundary domain which separate older primordia from the dome structure in the SAM (Fig. 1-7B, G). ARF7 expression is ubiquitous in all zones and all layers except L1 where it is reduced or absent (Fig. 1-7C, H). On the other hand, ARF8 is strictly expressed only in the L1 epidermal layer (Fig. 1-7D, I). ARF19 expression in the shoot apical meristem is enriched in the organ primordia but detected weakly also in most cells of L1 and L2 layers (Fig. 1-7E, J).

The expression patterns in the SAM can also be compared to the results obtained using pARF-GFP reporter lines which use 2000 bp shorter promoter (Rademacher *et al.* 2011) (Suppl. Fig. 1-4; this experiment was done by Géraldine Brunoud, ENS de

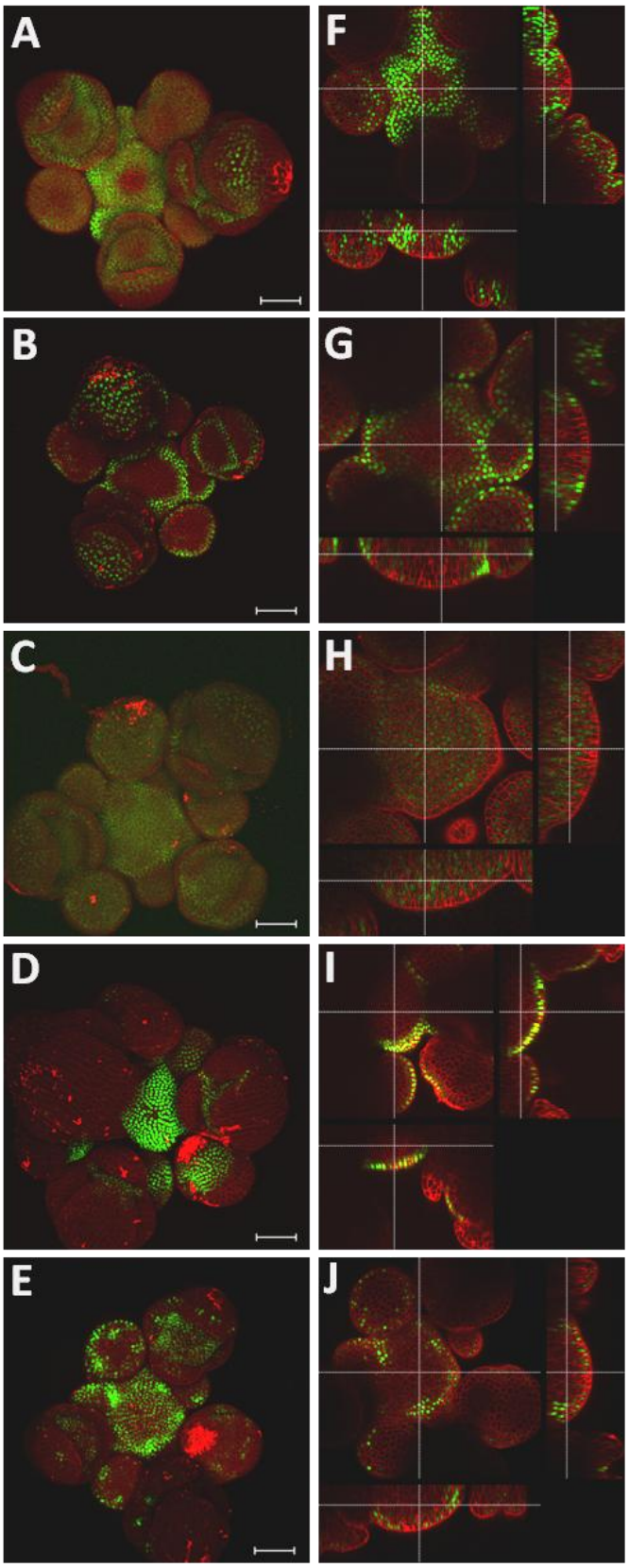

Fig. 1-7. Expression of ARF activators in the shoot apical meristem: **(A, F)** ARF5, **(B, G)** ARF6, **(C, H)** ARF7, **(D, I)** ARF8 and **(E, J)** ARF19. Bar scale 50 µm.

Lyon). In case of ARF5, 7, and 8 the patterns are similar. ARF6 is expressed ubiquitously and lacks the specific enrichment in the boundaries domain observed with my reporter lines. ARF19 expression appears broader as well.

The shoot expression patterns can be additionally compared to *in situ* hybridization results (Vernoux *et al.* 2011). In case of ARF5 and ARF7 the reporter line expression matches with the *in situ* patterns (Fig. In-12A). ARF6, ARF8 and ARF19 *in situ* images have lower expression and stronger background which hampers analysis. Nevertheless, ARF6 seems to have stronger staining around boundaries domain compared to the background which corresponds to my transcriptional reporter lines. ARF8 shows more an ARF5-type of expression pattern with stronger staining at the periphery and weaker in the center of the SAM; the L1-enrichment observed with the reporter lines is not detected here. ARF19 displays a higher staining in internal parts of organ primordia and flowers; this corresponds well to my transcriptional reporter lines. Overall, *in situ* hybridization can confirm the expression of ARF5, 6, 7 and ARF19 but not ARF8.

ARF7 expression in the RAM is regulated at the first intron

The transcriptional reporter lines described above contained both long upstream sequences and incorporated the downstream sequences including the first big intron which presence is characteristic for ARF activators. To investigate the importance of the first intron for the expression of ARFs, alternative transcriptional reporter lines were generated. These lines contained identical sequence upstream of the start codon as the lines described above but lacked any downstream sequences including the first introns. These promoter fragments were also fused to the nuclear-localized mVenus fluorescent reporter (Suppl. Fig. 1-2).

The expression of these shorter transcriptional reporter lines was visualized in the root and the shoot (Fig. 1-8 and Fig. 1-9). For ARF5, 6, 8 and 19 no difference was detected in expression patterns between the two different transcriptional reporter constructs both in the root (Fig. 1-1 and 1-8) and the shoot (Fig. 1-7 and 1-9).

On the other hand, a striking difference was obtained for ARF7 which showed no expression in the meristematic zone of the primary root (Fig. 1-1C and 1-8C) when using a shorter construct lacking the downstream sequences. Nevertheless the expression pattern in the older root was similar to the reporter lines with the full-

length promoter (Suppl. Fig. 1-3). This lack of expression in the RAM is very similar to the results obtained by Rademacher *et al.* 2011 using a short 2000 bp promoter. On the other hand, the SAM expression was not affected by the lack of the downstream sequences. This indicates that the sequences downstream of the ATG initiation codon are involved in the root-specific transcriptional regulation of ARF7.

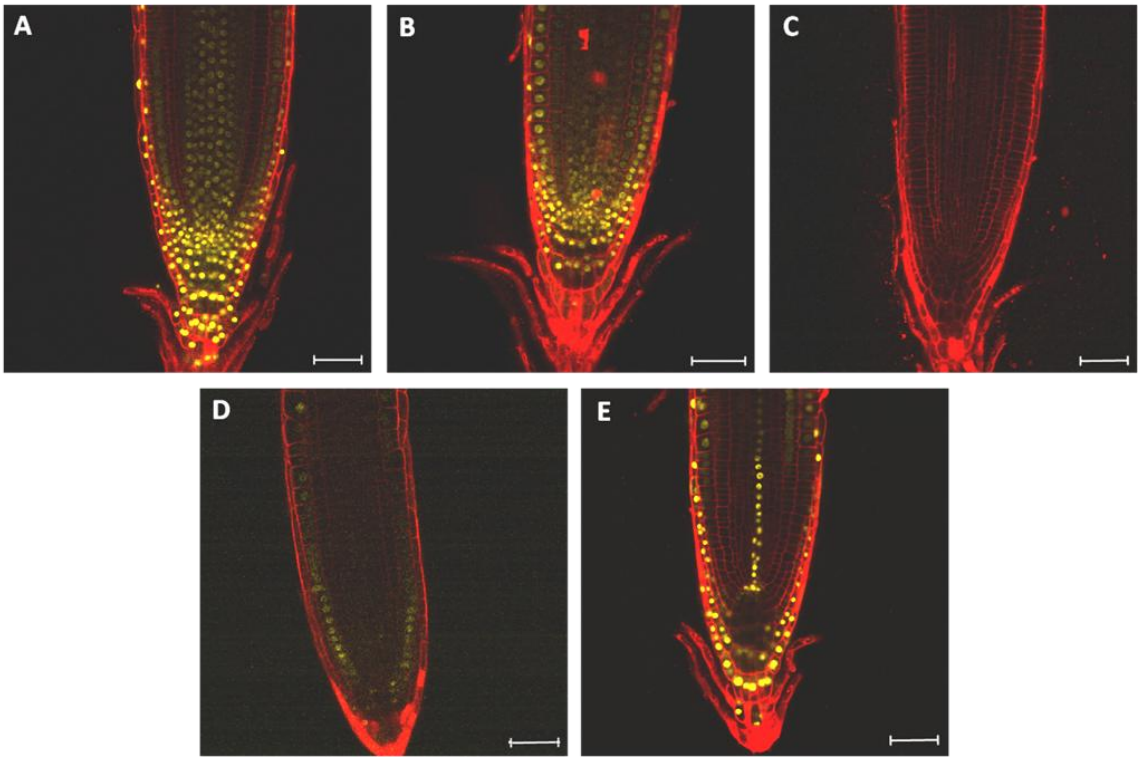

Fig. 1-8. Expression of ARF activators in the root tip of the primary root with alternative shorter promoter reporter lines. **(A)** ARF5, **(B)** ARF6, **(C)** ARF7, **(D)** ARF8 and **(E)** ARF19. Bar scale 50 µm.

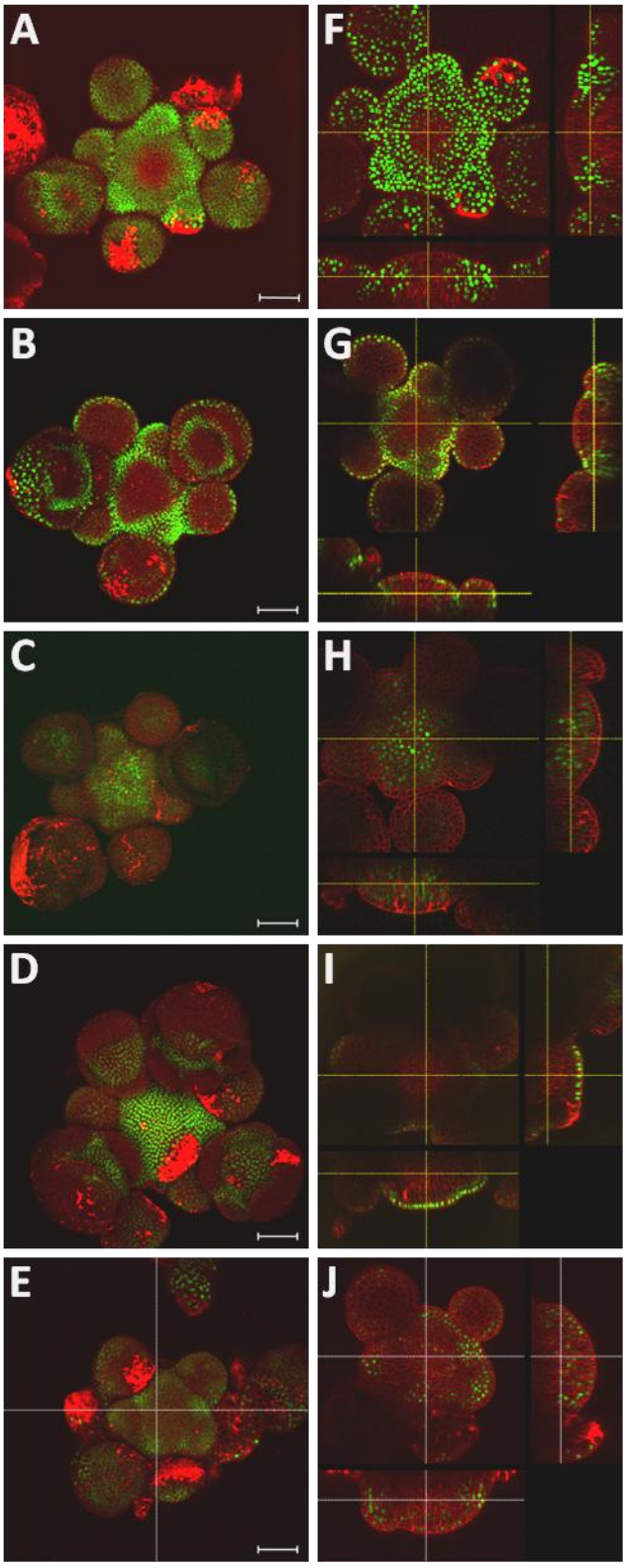

Fig. 1-9. Expression of ARF activators in the shoot apical meristem using shorter promoter constructs: **(A, F)** ARF5, **(B, G)** ARF6, **(C, H)** ARF7, **(D, I)** ARF8 and **(E, J)** ARF19. Bar scale 50 µm.

ARF activator distribution can be post-transcriptionally regulated

Studying expression patterns of ARFs provides information on where ARF mRNA is transcribed and, subsequently, where the ARF protein could be produced and function. Nevertheless, once expressed, a gene can undergo various post-transcriptional regulation steps which could render the resulting protein inactive or result in protein degradation. Oppositely, a protein might move to surrounding tissues mediating the auxin response non-cell-autonomously. To explore these possibilities, protein localization of the ARF activators was studied using reporter lines which incorporated simultaneously transcriptional and translational reporters (Suppl. Fig. 1-2C).

These constructs include a genomic sequence of the ARF activators starting from the promoter region and up to the stop codon at the end of ARF coding sequence. The genomic DNA is followed by the mVenus which doesn't contain any localization signal; this results in expression of the fused ARF-mVenus protein. mVenus is followed by a 2A peptide and a nuclear-localized mTurquoise2 (mTQ2) reporter gene. The 2A peptide is originated from the foot and mouth disease virus; it enables co-translational cleavage between the upstream and the downstream genes which

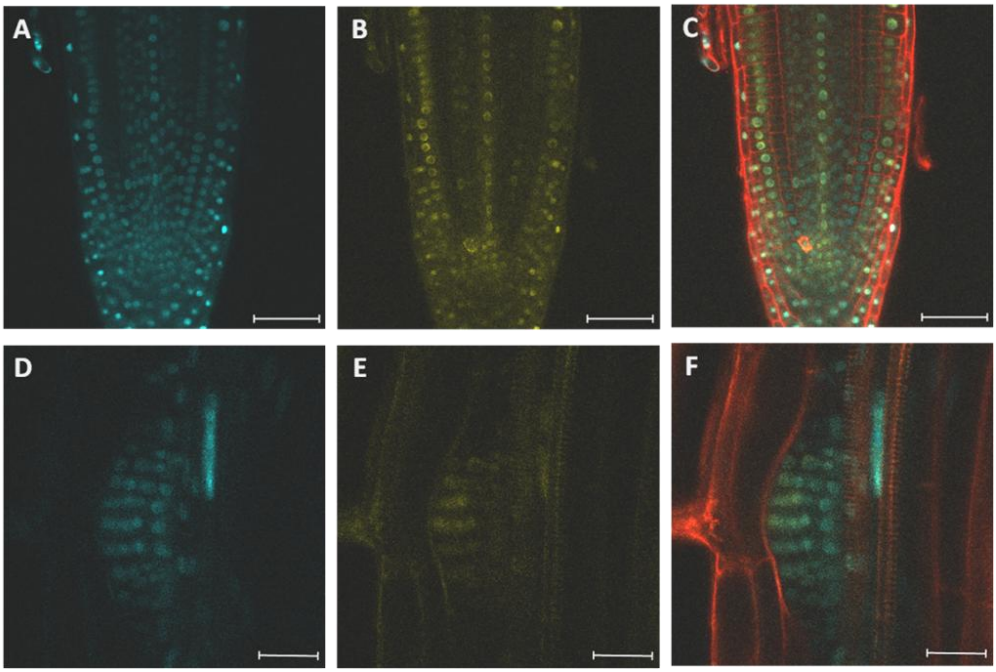

Fig. 1-10. ARF5 gene expression reported with mTurquoise2 **(A, D)** and protein localization reported with mVenus **(B, E)** in the RAM **(A-C)** and lateral root primordia **(D-F).** Overlay channels **(C, F)**. Bar scales 50 µm for A-C and 25 µm for D-F.

leads to expression of multiple none-fused genes from a single promoter (Kim *et al.* 2011a; Trichas *et al.* 2008). Thus the mTQ2 is cleaved off at the 2A peptide to render a separate nuclear-localized protein. Hence the native ARF promoter is driving a production of two independent proteins: ARF-mVenus fusions protein and mTQ2-NLS protein. In this construct, the ARF-mVenus protein recapitulates the distribution of the ARF protein in native conditions including such events as protein degradation or protein movement. On the other hand, mTQ2 is relocated to the nucleus in every cell where the promoter is active thus acting as a transcriptional reporter.

Among ARF activators, ARF5 showed particular striking difference between the gene expression and protein localization in the vasculature of the root tip. Here ARF5 gene is expressed in all tissues of the stele in the meristematic zone of the primary root (Fig.1-1A and 1-2A). On the other hand, the protein is concentrated in what appears to be xylem axis of the early vasculature and reduced or absent in the other tissues of the vasculature (Fig. 1-10 A to C). Similarly, the expression domain of ARF5 in the lateral root primordia include majority of the cells whereas the protein seems to be predominantly found at the tip of the primordia and it is absent or reduced in the basal cell layers (Fig. 1-10 D to F). Contrary to ARF5, ARF6 showed no difference in expression pattern between the transcriptional and the translational reporters in the RAM (Fig. 1-11).

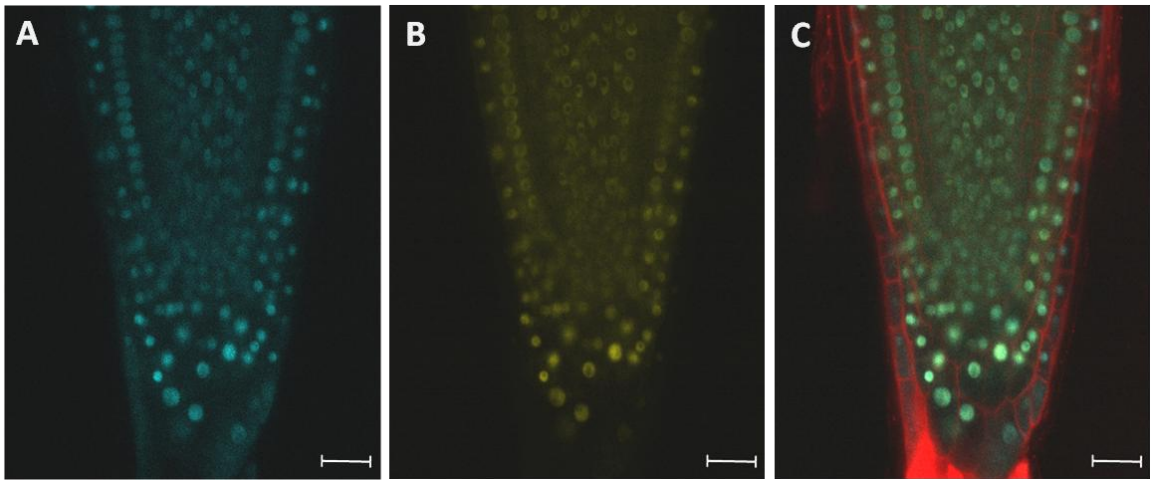

Fig. 1-11. ARF6 gene expression reported with mTurquoise2 **(A)** and protein localization reported with mVenus **(B)** in the root tip of the primary root**.** Overlay channels **(C)**. Bar scale 25 µm.

Interestingly, in the shoot apical meristem ARF5 protein occupies additional domain: it is found in the central zone despite not being expressed there (Fig. 1-7A, F and Fig. 1-12A, B). On the other hand, ARF6 protein localization mirrors its expression pattern with enrichment in the boundaries domain (Fig. 1-7B, G and Fig. 1-12C, D).

The results indicate that ARF5 protein moves to specific tissues whereas ARF6 protein is found in the same tissues where it is expressed. Thus it appears that different ARF activators can be both affected or unaffected by post-transcriptional protein movement.

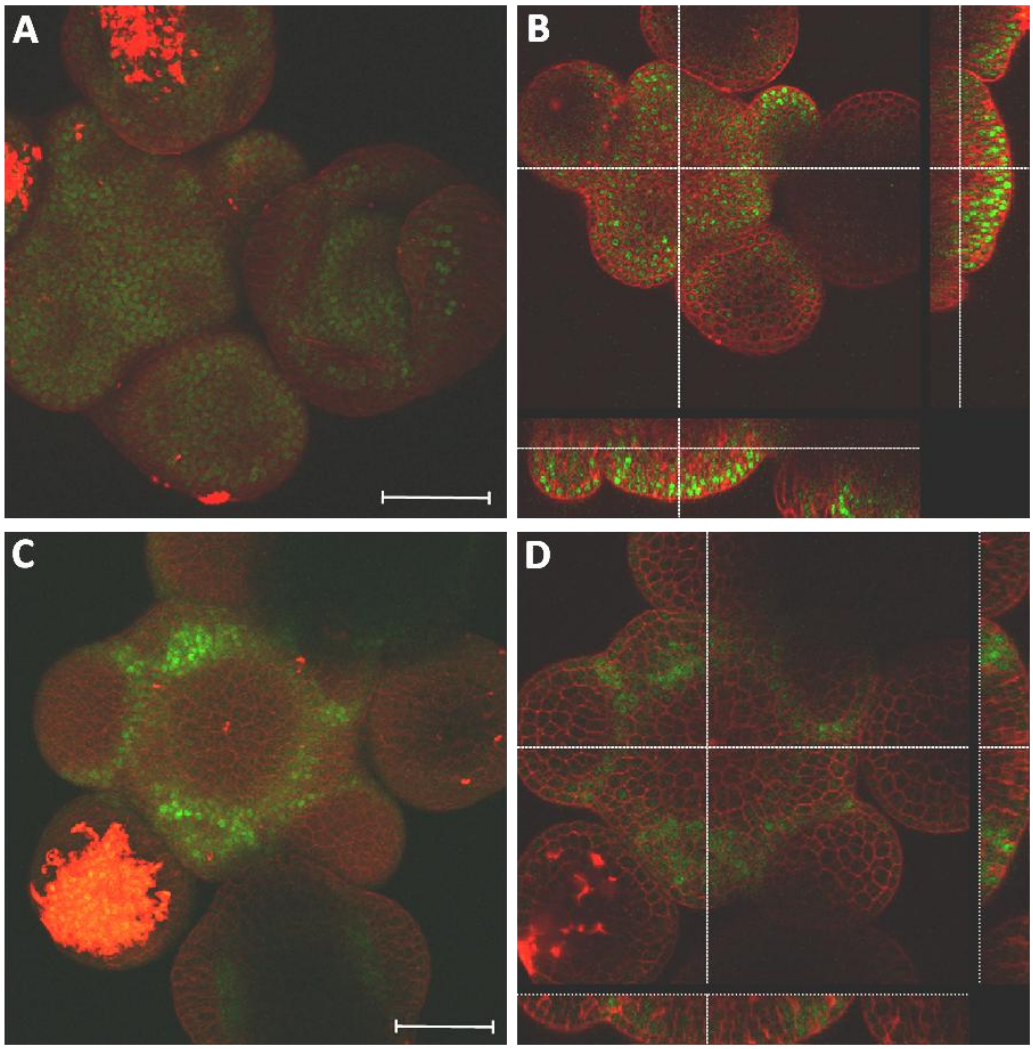

Fig. 1-12. ARF5 **(A, B)** and ARF6 **(C, D)** protein localization in the shoot apical meristem. Bar scale 50 µm.

ARF7 and ARF19 transcriptional reporter lines which have a C-terminal fusion of the ARF protein with the mVenus reporter lines were either silenced with a complete absence of fluorescence or showed a similar tendency: the expression pattern of mTQ2 recapitulates the expression previously observed in transcriptional reporter lines (Fig. 1-1) but the mVenus protein appears as speckles located in an unknown cellular compartment outside of the nucleus (Fig. 1-13). This result can be interpreted that a C-terminal fusion renders the ARF7 and ARF19 protein dysfunctional. To address this issue, the ARF7 and ARF19 N-terminal reporter fusions to mTQ2 reporter were created (Suppl. Fig. 1-2D). Surprisingly, for both ARF7 and ARF19 the N-terminal fusions also lead to speckles in non-nuclear compartments identically to the C-terminal fusions (Suppl. Fig. 1-5). Thus the localization of the fluorescent reporter tag does not affect the protein localization of ARF7 and ARF19.

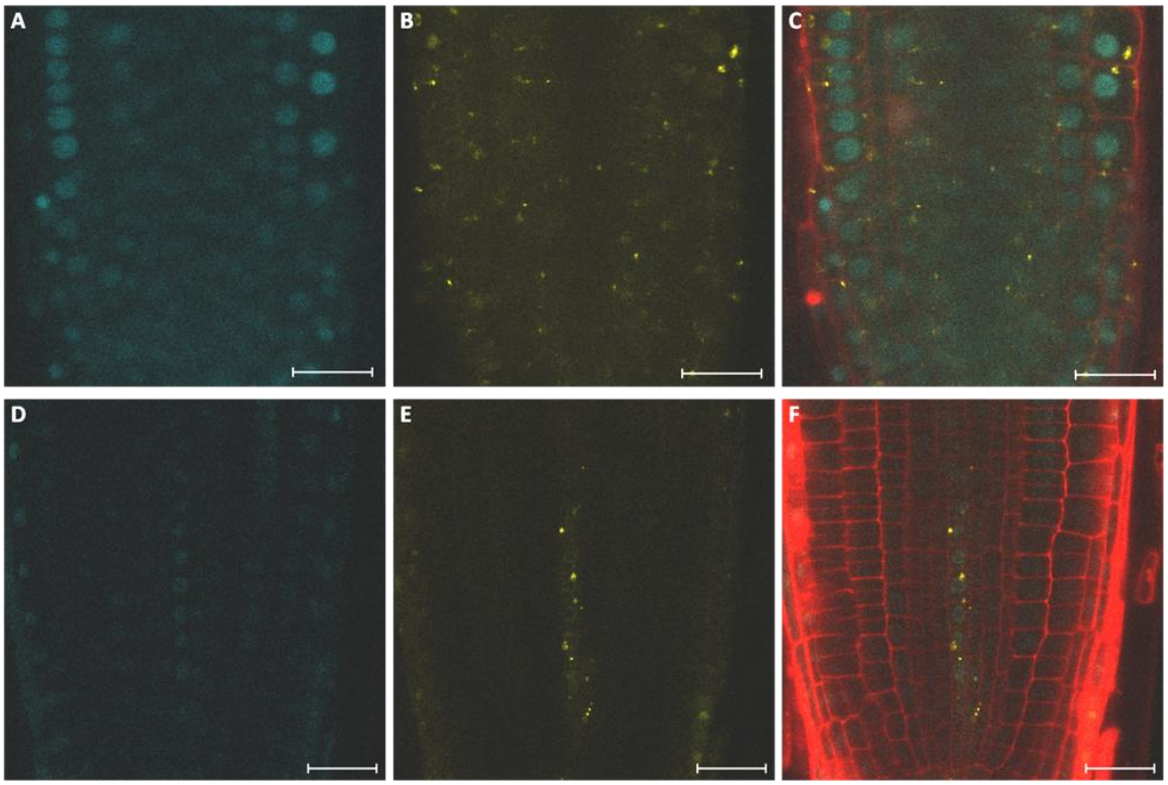

Fig. 1-13. ARF7 **(A-C)** and ARF19 **(D-F)** gene expression reported with mTurquoise2 **(A, D)** and protein localization reported with mVenus **(B, E)** in the root tip of the primary root**.** Overlay channels **(C, F)**. Bar scale 25 µm.

Discussion

In this chapter the expression and protein localization of ARF activators (ARF5, 6, 7, 8 and 19) in the root and the shoot was studied using transcriptional and translational reporter lines. The transcriptional reporter lines accurately and informatively reported ARF expression *in planta* due to longer ARF promoters in these lines which contain important regulatory elements both upstream and downstream of the initiation codon. In particular, the downstream sequence containing the first intron was shown to be important for expression of ARF7 in the RAM. In addition, translational reporter lines provided evidence for post-transcriptional protein movement in case of ARF5.

Tissue-specific expression of ARF activators provides insights into specificity and redundancy of their functions in plant development

Plant development relies heavily on hormonal signals. Among them auxin is particularly important because it is involved in a myriad of various developmental processes associated with cellular growth, organ initiation and development, responses to biotic and abiotic stresses. The auxin-induced changes in plant body structure are precise, timely and correspond well to plant's environment. It is astonishing that a great scope of different developmental changes can be regulated by a single basic molecule such as IAA. This raises the question of how the precision and specificity of auxin response is achieved.

The answer could be explained by considering the abundance and diversity of molecules which mediate auxin response. Alone, the presence of 23 ARFs in *Arabidopsis thaliana* can indicate that these ARFs could be involved in specific independent or redundant auxin responses. Indeed, from 5 ARF activators described in this study each of them shows involvement in both overlapping and independent auxin responses as indicated by single and double mutant phenotypes (Berleth and Jurgens 1993, Nagpal *et al.* 2005, Okushima *et al.* 2005, Przemek *et al.* 1996). Additionally, the ARF activators were shown to control different sets of downstream target genes (Nagpal *et al.* 2005, Okushima *et al.* 2005, Schlereth *et al.* 2010).

The functional diversity and specificity could be in part explained by tissue-specific expression of these ARFs. Accordingly, this study explored the diversity of ARF activator expression patterns in both the root and the shoot with a goal to draw new hints on the function of each ARF activator. In fact, each ARF activator shows distinct

expression patterns. In particular, when looking globally at the ARF activator expression in the RAM we see a clear specification in different domains where different combinations of ARFs are expressed. Here the expression patterns can be separated into blocks which can consist of a single tissue type or, alternatively, of multiple autonomous tissue types (Fig. 1-14). For example, columella initials and the mature columella cells are all enriched in ARF5 and ARF6 but deprived of other ARF activators. Similarly, endodermis and cortex both contain only ARF6 and ARF7 transcripts. This could indicate that the endodermis and cortex are able to react to auxin in the same manner even though they are functionally different tissues, thus forming a block of specific auxin response. On the contrary, we expect that cortex/endodermis on one side and columella on the other side would show a different reaction to auxin because of enrichment of different ARF activators in these two tissues.

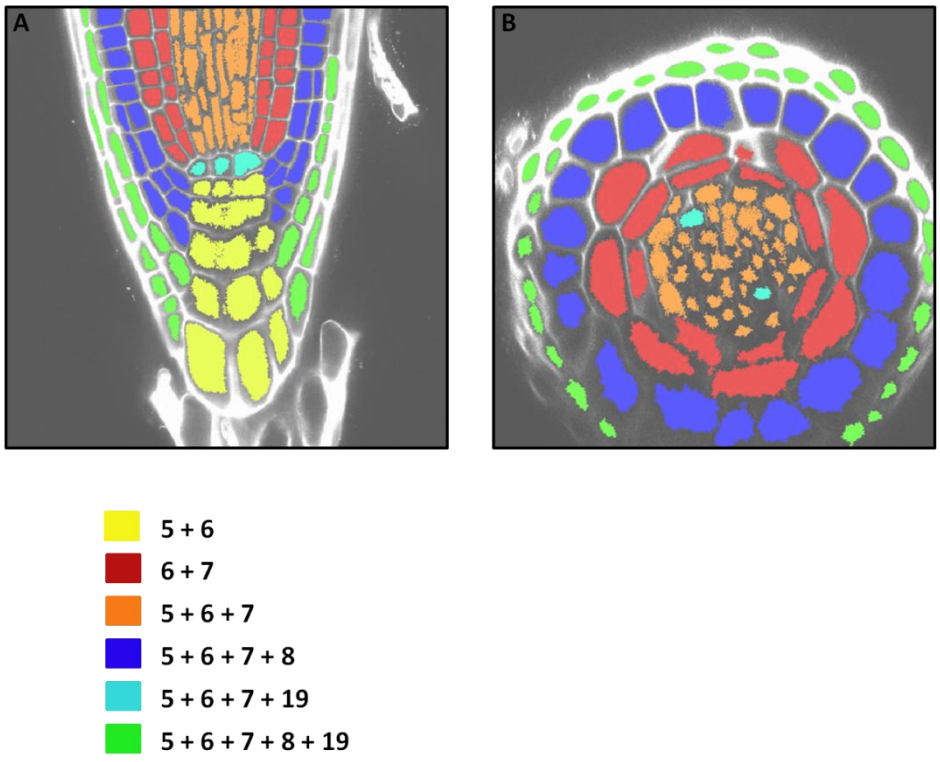

Fig. 1-14. Schematic of ARF activators expression in various tissues of the root apical meristem. Longitudinal **(A)** and radial **(B)** cross-section diagrams showing co-expression pattern of ARF5, 6, 7, 8 and 19. Colors indicate expression domains of indicated ARF activator.

Interestingly, this leads to the question how different ARFs co-expressed in the same tissue interact with each other. It is possible that each ARF activates its targets genes independently from the other ARFs expressed in the same tissue. The other possibility would be that together different ARFs can act as a team to co-activate a set of genes which they might not be able to activate individually. This potential cooperation could be achieved by building oligomer complexes consisting of different numbers and types of ARFs. The latter hypothesis is more supported by biological evidence because the ability of ARFs to oligomerize was recently shown (Korasick et al. 2014, Nanao *et al.* 2014).

The ability of ARF activators to cooperatively co-regulate specific subsets of target genes could be further investigated with additional experiments. One can imagine that, for example, by making double mutants between non-homologous ARFs (such as between ARF7 and ARF6) additional functions of these ARFs could be discovered. In part this was explored before with the *arf5 arf7* double mutant showing stronger defects in vasculature of cotyledons compared to the single *arf5* mutant (Hardtke *et al.* 2004). Similarly, expressing an ARF activator under a promoter of a different ARF activator (for example, expression of ARF5 under promoter of ARF6) could further lead to developmental phenotypes and this then could provide a clue on possible modular co-operation between individual ARFs.

Auxin response mediated by ARF activators can only be switched on in presence of auxin. Auxin is distributed unevenly in the RAM and the SAM (Fig. In-3 and In-7). In the RAM the auxin maxima includes QC, columella initials and columella stem cells as visualized by DR5 and DII reporters (Brunoud *et al.* 2012) (Fig. In-3). On the other hand, ARF activators can be found in all tissues of the RAM (Fig. 1-14). The question arises, how can the ARF activators propagate auxin response in the auxin-deprived tissues such as cortex and endodermis? Perhaps low levels of auxin could be sufficient to induce a subtle auxin response which would be different from the response induced in presence of high auxin? One can imagine a doze-dependant effect of auxin affecting differently gene regulation and, subsequently, the cellular responses. But if the auxin response is not switched on in the tissues with low auxin levels, then why some ARF activators are still expressed in these tissues? Perhaps constitutive expression in the normally auxin-deprived tissues can prime these

tissues for the rapid auxin response in case of a sudden increase in auxin content; such an increase in auxin could happen, for example, during a stress response.

Expression patterns of ARF activators fits their well-studied functions and suggests new potential functions

The tissue-specific expression patterns confirm already well-studied ARF-mediated auxin responses. One of these processes is the regulation of lateral root development which was argued to include all five ARF activators. In particular, all five ARF activators were speculated to be important for lateral root founder cell specification in the basal meristem, later on ARF7 and ARF19 control asymmetric cell divisions during lateral root initiation, and finally ARF5, 7, and 19 together were argued to regulate further development of the lateral root primordia (De Rybel *et al.* 2010, De Smet *et al.* 2010, Fukaki *et al.* 2005, Okushima *et al.* 2005). In this thesis ARF5, 7, and 19 were expressed at very early stages in lateral root primordia development. The role of ARF7 and ARF19 in lateral root initiation and formation is confirmed by mutant phenotypes with the single *arf7* mutant displaying reduced number of lateral roots while the double *arf7 arf19* mutant lacking lateral roots completely (Okushima *et al.* 2005). Similarly, the role of ARF5 in lateral root development is confirmed by the phenotype of a weak *arf5* mutant (mp^{S319}) which has increased pericycle cell divisions and the ARF5 overexpression line which shows abnormally positioned primordia (De Smet *et al.* 2010).

On the contrary, ARF8 first appears later at stage VI in the epidermal layer of an older primordia. ARF8 could be involved in lateral root development because the *arf8* mutant has a slight but significant increase in lateral roots whereas the ARF8 overexpression line produced slightly but significantly less lateral roots (Tian *et al.* 2004). A different study found no significant differences in lateral root number or length in ARF8 mutant and overexpression lines (Gutierrez *et al.* 2009). Nevertheless, the expression of ARF8 at the later stages of primordia development might indicate that ARF8 could be involved in development or emergence of the more mature primordia. The involvement of ARF8 in priming of lateral root founder cells appears quite speculative because ARF8 was not expressed in xylem pericycle cells. A more thorough analysis on ARF8 mutant and overexpression lines is needed to search for any defects in lateral root development.

Similarly to ARF8, ARF6 mutants and overexpression lines showed no significant lateral root development phenotypes (Gutierrez *et al.* 2009). Thus the significance of the ARF6 expression at later stages of primordia formation remains unclear. It would be interesting to see if the *arf6 arf8* double mutant has any defects in lateral root development at the later stages or during emergence.

The expression patterns can provide interesting clues to yet undiscovered functions of ARF activators in plant development. As such, ARF19 expression pattern in the RAM is particularly interesting. ARF19 is specifically expressed in QC and protoxylem but an ARF19-associated function in the control of the root stem cell niche or in xylem development has never been considered. In particular both QC and the xylem are domains of high auxin content. Interestingly, ARF19 expression can be induced by auxin (Wilmoth *et al.* 2005). Thus we could expect auxin to induce expression of ARF19 in QC and protoxylem which then should lead to activation of ARF19 target genes in these tissues and result in a certain cellular reprogramming. To investigate this hypothesis, an inducible overexpression of ARF19 in QC could lead to a transient increase in ARF19-mediated signaling in this tissue resulting in changes in gene expression which can be detected by RNA-seq or possibly resulting in a phenotype after a prolonged exposure to the inducer.

Further interesting new discoveries can be deduced from the expression patterns of ARFs. Thought-provoking is the expression of ARF8 specifically in meristematic tissues and only in the epidermal layers of both the RAM and the SAM. Could this mean that ARF8 is adapted to react to external clues which are perceived at the epidermis and mediate auxin response in accordance to the environmental conditions? The role of ARF8 in the response to environment has never been considered before.

ARF expression patterns in the SAM possibly illustrate their specific step-by-step involvement in lateral organ formation and development. ARF5, 7 and ARF19 might act the earliest during lateral organ initiation due to their enrichment in the forming primordia. ARF6 expression in the boundaries domain in the SAM stimulates to consider that this ARF might be important for organ separation at the later stages of lateral organ primordia development. Finally, ARF8 could serve as a mediator of environmental clue to coordinate organ development.

Which elements are important to correctly recapitulate expression patterns of genes?

Fluorescent and non-fluorescent reporter genes such as GFP or GUS have been used extensively to study expression of various genes *in planta*. The accuracy of the expression patterns reported by them depends on length and content of DNA sequences which drive these reporters. Numerous studies have included promoters as short as only 1000 bp in transcriptional reporter constructs. However it appears clearer and clearer that such short promoter fragments are often insufficient to recapitulate the correct expression pattern for many eukaryotic genes.

Indeed, when I compare the expression patterns of my ARF transcriptional reporter lines containing between 3 kb and 5,5 kb promoters to the expression reporter lines created by Rademacher *et al.* which include 2 kb promoter, I tend to see a different and often more restricted pattern. For example, ARF6 is expressed in the SAM only at the boundaries domain in my reporter lines whereas in Rademacher *et al.* lines the expression is ubiquitous throughout the SAM. This restriction might be due to transcriptional repressors which downregulate expression of ARF6 in specific tissues and which could be binding ARF6 promoter in the region between -3000 and -2000 bp not included in the shorter reporter construct. On the other hand, the 5 kb and 2 kb ARF5 promoters used in my and the Rademacher *et al.* constructs respectively both recapitulated successfully *in situ* hybridization pattern in the SAM. The expression patterns with longer promoter constructs correspond more to ARF functions as indicated by ARF mutant phenotypes. For example, ARF7 is not expressed in the meristematic zone of the RAM in the shorter promoter constructs but present in my longer promoter construct; this corresponds to the well-described function of ARF7 in root gravitropism (Okushima *et al.* 2005, Sato *et al.* 2015). Thus choosing a longer promoter generally leads to more accurate representation of the transcriptional regulation and allows more accurate predictions of gene function.

Often, DNA regions upstream of the gene start codon are considered to be sufficient to recapitulate the actual expression patterns of genes. This view has been challenged extensively in the recent years and the importance of the downstream sequences as sites of transcriptional regulation is becoming more evident. Multiple genes were shown to contain enhancer elements within the gene itself particularly in the introns. For example, the expression of the floral homeotic gene AGAMOUS (AG)

is regulated in the second intron where it's transcriptional regulators WUS and LEAFY bind (Busch *et al.* 1999, Lohmann *et al.* 2001). The expression of PAT1 gene which encodes a tryptophan biosynthesis enzyme is regulated at the first and the second introns (Rose and Last 1997). The first intron in the maize gene Sh1 gene enhances gene expression levels (Vasil *et al.* 1989) while the first intron of the petunia ADF1 gene controls pattern of expression (Jeon *et al.* 2007).

Indeed, in this study ARF7 expression in the root is dependent on the presence of an upstream sequence including the first intron. This might indicate that there is a root-specific transcriptional regulator that binds specifically in the first intron or, less likely, in the first exon. Thus the first explanation would be that the downstream sequences within ARF7 genomic DNA act as a part of the promoter. A few experiments could be proposed to confirm this hypothesis. One can try to drive the expression of a reporter gene using only the first intron as a promoter *in planta* to see if this region is sufficient to enable expression in the RAM. Another way is to make a construct with first intron inserted in a reverse orientation and to see if the reversed intron could still act as an enhancer of ARF7 expression in the RAM.

Alternatively, a different mechanism could be proposed: introns can increase mRNA levels without containing enhancers or promoters. This mechanism termed intron-mediated enhancement is proposed to be based on the intron affecting processivity of the transcriptional machinery which leads to more stable mRNA being produced (Rose 2008). For the intron-mediated enhancement, the introns must be arranged in a proper orientation; therefore a construct with first intron inserted in a reverse orientation would not enhance the gene expression anymore. Thus a few experiments could enable to distinguish a mechanism by which the first intron of ARF7 could be controlling gene expression.

Besides the introns, the downstream sequences located in the 3-prime region or the terminator could also be important for transcriptional regulation of the relevant gene. For example, WUS regulates the expression of CLV3 by binding regulatory elements both in the upstream and the downstream regions, the latter are located in the 3' region of CLV3 (Perales *et al.* 2016). Consequently, including these regions in the transcriptional reporter constructs might be required to recapitulate the correct expression patterns in certain situations.

Overall, it seems that multiple components are required to accurately recapitulate the expression patterns with reporter gene constructs. The accuracy of the pattern has to be verified in each individual case with alternative methods that shows mRNA accumulation *in planta* such as *in situ* hybridization. Nevertheless, *in situ* hybridization method has its limitations; in particularly the genes with low expression levels are difficult to visualize owning to the high background staining, and the cellular resolution can be insufficient to attribute expression to specific tissues (Rozier *et al.* 2014, Vernoux *et al.* 2011).

Post-transcriptional movement or degradation of ARF proteins provides another level of control in the auxin signaling pathway

Often it is presumed that the tissues where the gene is expressed and the tissues where the gene acts are identical. In many papers the expression of a gene is sufficient to justify the tissue-specific function of this gene. Post-transcriptional modifications are often neglected. Similarly, for the majority of the ARFs post-transcriptional regulation has not been studied in details.

In embryos, ARF5 protein does not move but remains in the same tissues where it is expressed and acting non-cell-autonomously through a secondary signal, the mobile transcription factor TMO7 (Schlereth *et al.* 2010; Weijers *et al.* 2006). On the contrary, the presence of ARF5 protein in the central zone of the SAM where its not expressed is published in Zhao *et al.* 2010; nevertheless the potential protein movement is not considered in this paper. In this thesis the cell movement of ARF5 protein in the SAM is confirmed. Further, in the RAM, ARF5 protein is shown to either move towards the xylem or to be degraded in the surrounding vasculature tissues. Thus the function of ARF5 in the xylem development might be reinforced by the accumulation of its protein specifically in this tissue.

ARF6 and ARF8 were never been shown to be involved in non-cell-autonomous cell signaling which could require a protein movement. Indeed, in my study I could not detect any protein movement or degradation for ARF6 in the RAM or the SAM. It was shown that ARF6 and ARF8 undergo a different type of post-transcriptional regulation: their mRNA can be degraded by microRNA167 affecting expression pattern specifically in flowers (Wu *et al.* 2006). This type of regulation would also be reflected in the differences between the transcriptional and the translational reporters. Since I see no difference in case of ARF6, I conclude that in the RAM and the SAM

microRNA-mediated degradation of ARF6 mRNA cannot be detected under my growth conditions.

ARF7 and ARF19 proteins provide puzzling results: both N-terminal and C-terminal protein fusions result in relocation of their proteins in non-nuclear compartments. It appears that the proteins aggregate. Could this aggregation be due to addition of a fluorescent protein tag and the subsequent misfolding of the proteins? Although this explanation cannot be formally discarded, the fact that aggregation persists despite changing the terminus of the fusion speaks against it. Is it possible that ARF7 and ARF19 proteins are intrinsically unstable and undergo constant degradation unless stabilized by an unknown factor? Interestingly, both ARF7 and ARF19 show broad expression patterns in many tissues such as in the older root upwards from the meristematic zone (Fig. 1-4 and 1-6) and to some extend in the SAM (Fig. 1-7). Could their excessive expression be compensated by constant protein degradation rendering ARF7- and ARF19- mediated auxin response inactive by default? In that case which triggers could lead to stabilization and activate normal function of these proteins? Currently no answers can be provided to these questions.

Material and methods

Cloning and generation of ARF reporter lines

The various transcriptional and translational reporter lines generated in this study are schematically illustrated in Suppl. Fig. 1-2. The constructs were transformed into *Agrobacterium tumefaciens* C58pMP90 strain by electroporation and then transformed into Col-0 plants by floral dip method (Clough and Bent 1998). As exception, the ARF7 and ARF19 N-terminal fusion translational reporter lines were transformed into qDII CLV3 background (created by Carlos Galvan Ampudia, ENS de Lyon and containing ratiometric qDII auxin reporter and pCLV3-mCherry marker).

Multisite Gateway cloning technology was used for the generation of ARF transcriptional reporter lines harboring DNA sequences both upstream and downstream from the start codon. The long promoter fragments were amplified by PCR; they included both sequences upstream of the start codon and small downstream sequences as indicated: pARF5 -5418 bp to + 134 bp, pARF6 -3255 to +197 bp, pARF7 -2973 bp to + 374 bp, pARF8 -5091 to + 42 bp, -4906 to + 452 bp. For ARF5, 6, 8, and 19 the fragments were inserted into pDONR P4-P1R and recombined with 3x mVenus-N7 pDONR211 (containing triple mVenus coding sequences and N7 nuclear localization signal), OCS terminator pDONR P2R-P3 (containing the stop codon followed by a octopine synthase (OCS) terminator) and pK7m34GW (the destination vector containing kanamycin resistance gene for *in planta* selection) to produce pARF-3xmVenusN7 constructs. For ARF7, the fragment was cloned into a pCR8/GW/TOPO and recombined with a nuclear-localized mVenusN7, 35S terminator and pK7m34GW to produce pARF7-mVenusN7 construct (Suppl. Fig. 1-2A).

Similarly, the shorter transcriptional reporter lines were amplified by PCR with sequences as indicated: : pARF5 -5418 bp to -1 bp, pARF6 -3255 to -1 bp, pARF7 -2973 bp to -1 bp, pARF8 -5091 to -1 bp, -4906 to -1 bp. Identical to the reporter constructs described above, the fragments were inserted into pDONR P4-P1R and recombined with 3x mVenus-N7 pDONR211, OCS terminator pDONR P2R-P3 and pK7m34GW destination vector to yield pARF-3xmVenusN7 shorter transcriptional reporter lines (Suppl. Fig. 1-2B).

The translational reporter lines were generated by amplifying genomic DNA fragments containing long upstream regions and downstream regions up to but not including the stop codon. The sizes of the upstream regions were identical to the once used for the transcriptional reporter lines (for example, for ARF5 the amplified fragment started from -5418 bp and ended at the stop codon). The resulting genomic DNA fragments were inserted into pDONR P4-P1R and recombined with mVenus pDONR211 (none-nuclear localized), 2A-mTQ2 pDONR P2R-P3 (2A peptide followed by a nuclear-localized mTurquoise2) and pK7m34GW destination vector to yield pARF:ARF-mVenus-2A-mTQ2-NLS reporter lines. This reporter lines combined both translational reporter (ARF-mVenus fusion protein) and a transcriptional reporter (mTQ2-NLS) expressed under endogenous ARF promoter (Suppl. Fig. 1-2C).

The additional translational reporter lines for ARF7 and ARF19 consisting of the N-terminal fusion between ARF7 or ARF19 protein and the mTQ2 were constructed. To achieve that ARF7 and ARF19 coding sequence was amplified from genomic DNA which included the complete sequence starting after (but not including) the start codon and finishing with the stop codon. The ARF7 and ARF19 genomic coding sequence was then inserted into the pDONR P2R-P3 plasmid. Separately, mTQ2 coding sequence containing the start codon but not including the stop codon was amplified by PCR and inserted into pDONR211 plasmid. Finally, the promoter of ARF7 and ARF19 (upstream region up to but not including the start codon) cloned previously into pDONR P4-P1R during the construction of the transcriptional reporter lines was recombined together with mTQ2 pDONR211, ARF7 or ARF19 pDONR P4-P1R and the destination vector pK7m34GW to yield pARF7-mTQ2-ARF7 and pARF19-mTQ2-ARF19 constructs (Suppl. Fig. 1-2D).

Root microscopy

For root microscopy plants were grown on half-strength Murashige and Skoog (MS) medium supplemented with 1% sucrose and 1% agar. The seedlings were grown in either 24h light, 12h light/12h dark or 16h light/8h dark conditions and imaged at 5 or 6 days in light. Plant cell membranes were visualized by staining with 15 µg/ml propidium iodide solution. The roots were examined in the TCS-SP5 confocal microscope (Leica) with excitation at 514 nm and emission at 526-560 nm for mVenus and 605-745 nm for propidium iodide.

Shoot microscopy

For the shoot microscopy plants were grown in 8h light/16h dark conditions for 6 weeks and then transformed to 16h light/8h dark conditions for 2 weeks to induce bolting. The bolted shoots were dissected under a stereomicroscope and planted into an Apex Culture Medium (half-strength MS medium supplemented with 1% sucrose, 0.8% agarose, 1x vitamin solution (myo-Inositol 100 mg/L, nicotinic acid 1 mg/L, pyridoxine hydrochloride 1 mg/L, thiamine hydrochloride 10 mg/L, glycine 2 mg/L)), for overnight incubation at 16h light/8h dark conditions. Before microscopy cell membranes were visualized by staining the shoot apexes with 100 µg/ml propidium iodide solution. The shoot apexes were examined in the TCS-SP5 confocal microscope (Leica) with excitation at 514 nm and emission at 526-560 nm for mVenus and 605-745 nm for propidium iodide.

The shoot microscopy of the pARF-GFP lines from Rademacher *et al.* 2011 was performed by Geraldine Brunoud, ENS de Lyon (Suppl. Fig. 1-4).

Supplementary information

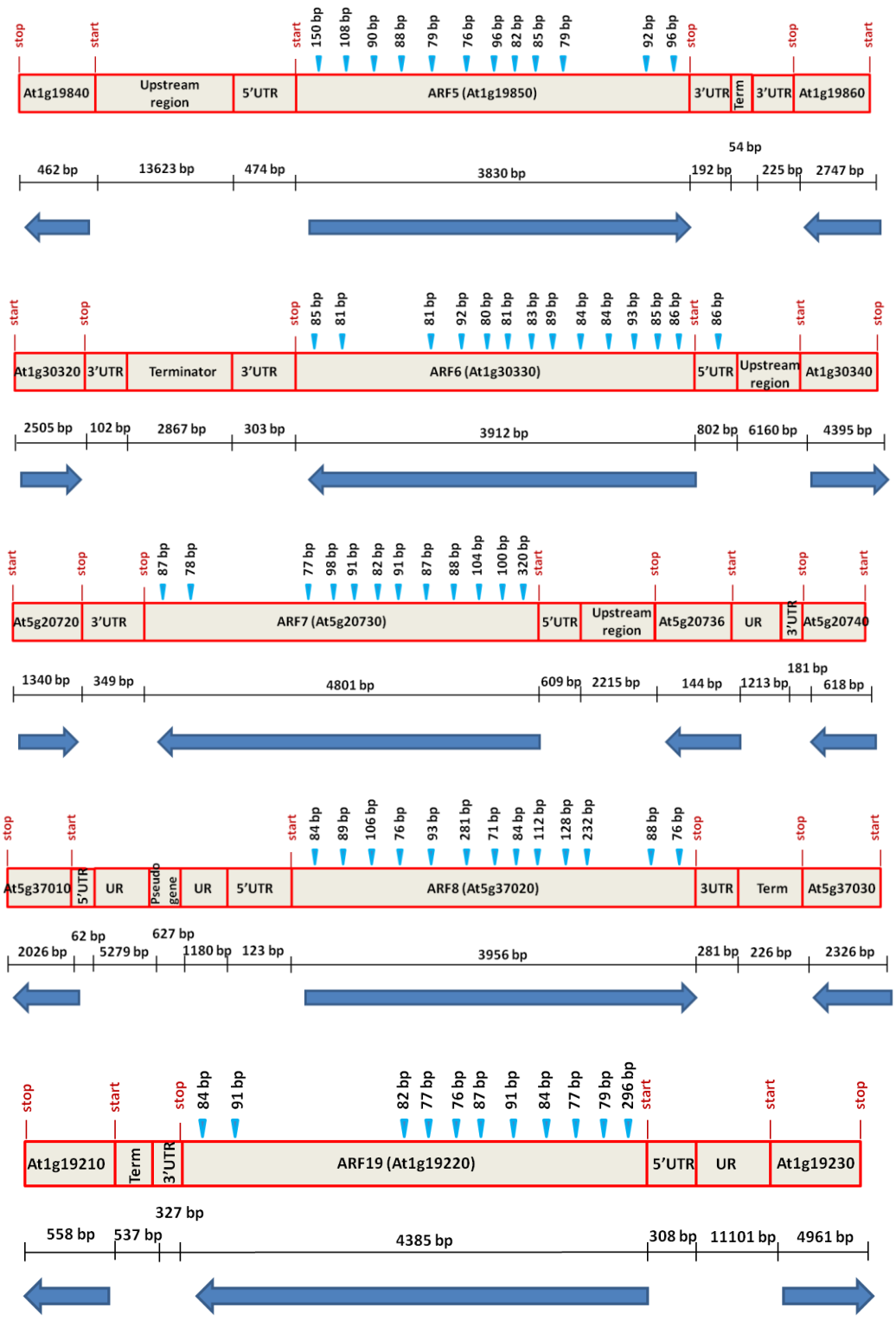

Supplementary Fig. 1-1. Schematic representation of the ARF5 (upper row), ARF6 (upper middle row), ARF7 (middle row), ARF8 (lower middle row) and ARF19 (lower row) locus. Small blue triangles indicate introns with size specified. Big blue arrows show direction of the transcription. UR = upstream region; term = terminator.

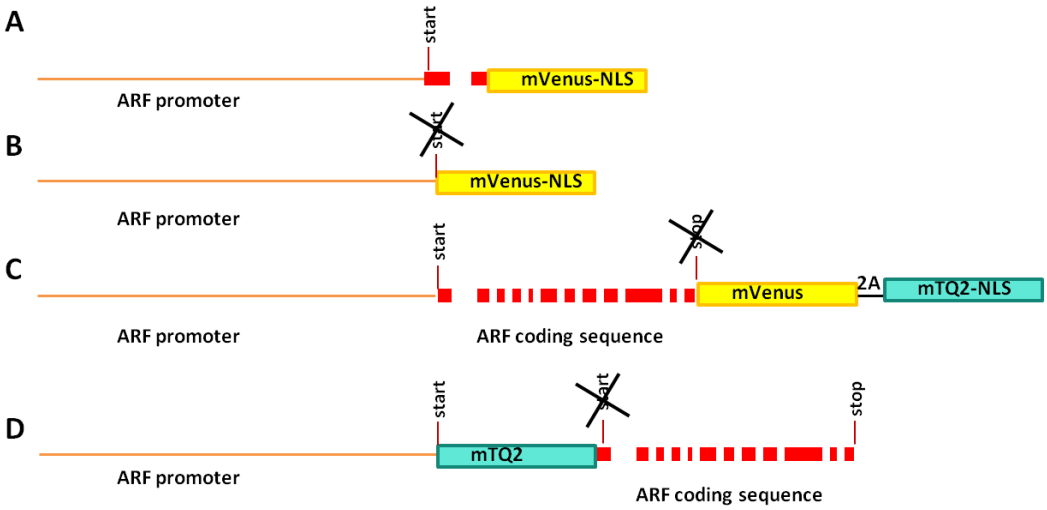

Supplementary Fig. 1-2. Overview of transcriptional and translational reporter lines constructed in this study. In the transcriptional reporter lines upstream sequences and downstream sequences including the first intron **(A)** or only upstream sequences **(B)** of ARFs are driving expression of the nuclear-localized mVenus reporter. In the translational reporter lines the genomic DNA fragments including upstream and downstream region of ARFs were fused C-terminally to the mVenus reporter lacking localization signals. This is followed by the 2A peptide and the nuclear-localized mTQ2; the 2A peptide allows post-translational cleavage of the mTQ2-NLS which then serves as a transcriptional reporter in this construct **(C)**. Additionally, for ARF7 and ARF19 translational reporter lines containing N-terminal fusions between the mTQ2 reporter (without localization signal) and the ARF7 or ARF19 genomic coding sequence were constructed. **(D)**. Red boxes represent exons, spaces between them represent introns.

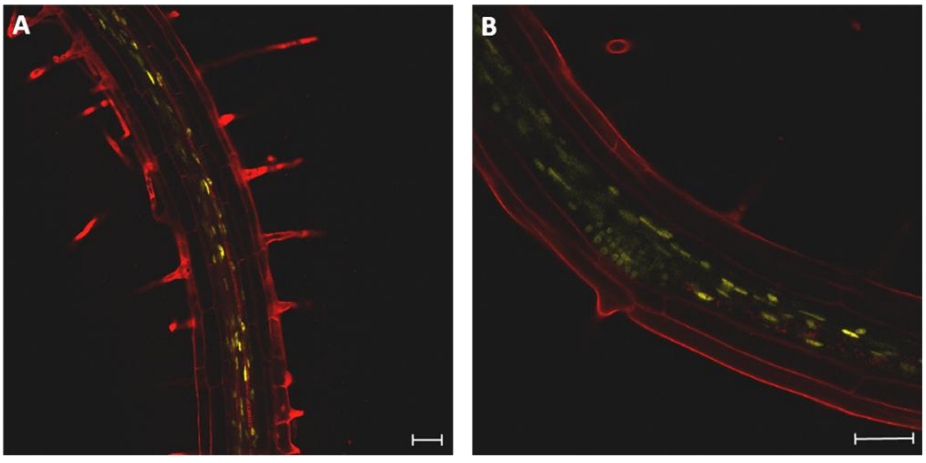

Supplementary Fig. 1-3. Expression of ARF7 in the older root **(A)** and the lateral root primordial **(B)** using the alternative transcriptional reporter line with shorter promoter. Bar scale 50 µm.

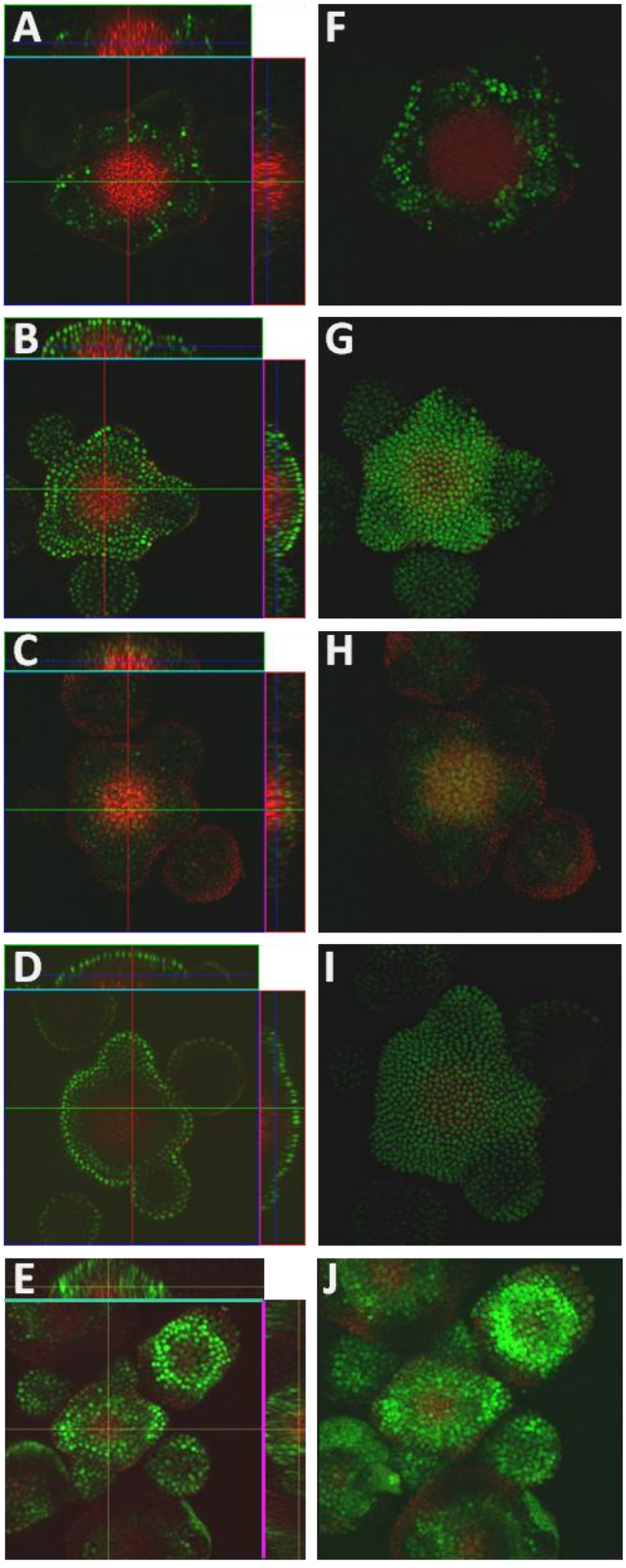

Supplementary Fig. 1-4. Expression of ARF activators in the shoot apical meristem: **(A, F)** ARF5, **(B, G)** ARF6, **(C, H)** ARF7, **(D, I)** ARF8 and **(E, J)** ARF19. The pARF-GFP lines from Rademacher *et al.* 2011. The imaging was done by Geraldine Brunoud, ENS de Lyon.

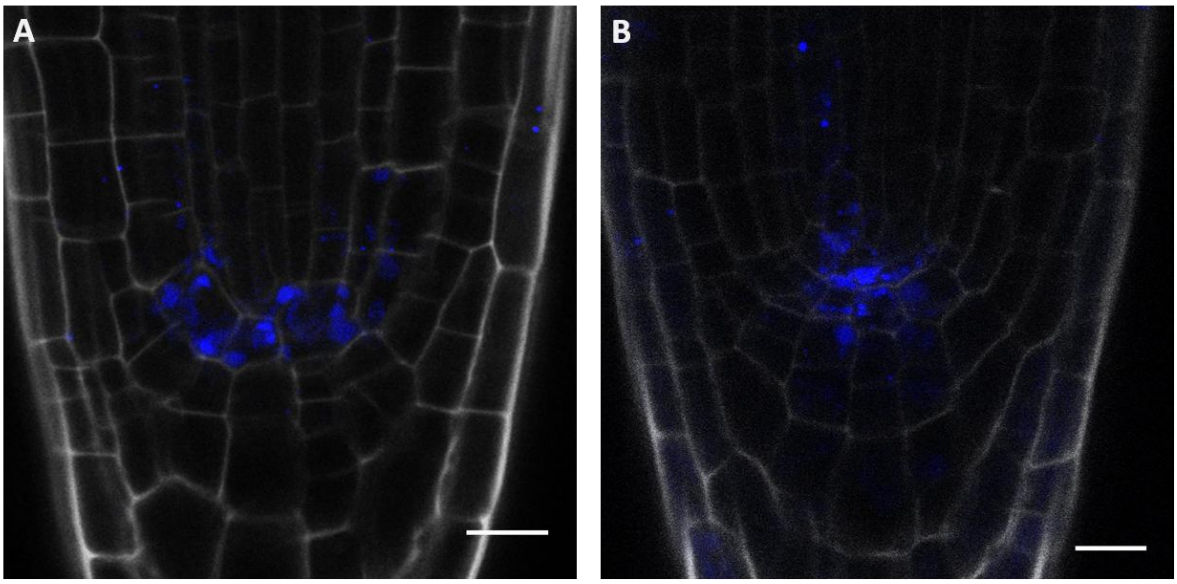

Supplementary Fig. 1-5. Protein localization of ARF7 **(A)** and ARF19 **(B)** with N-terminal translational fusions. Scale bar 10 µm.

Chapter II: Auxin Response Factor (ARF) activators are transcriptionally regulated by gene-specific repressor network

Introduction

The plant hormone auxin is known for its involvement in a myriad of developmental processes including the control of root and shoot growth, development of flowers and seeds, responses to biotic and abiotic stresses. Such diversity of auxin responses is possible due to specialization and divergent functions of each of the five ARF activators: ARF5, 6, 7, 8 and 19. As shown in the previous chapter, these ARF activators are expressed in specific tissues in the RAM and the SAM where they mediate auxin signaling through direct activation of auxin target genes. But how are these specific expression domains of each ARF activator established?

One possible explanation would be that the expression of ARF activators is regulated during transcription by specific transcriptional regulators which either activate or repress the expression of each ARF in precise tissues. In this study, the potential regulators of ARF transcription were identified using a yeast one-hybrid method.

The yeast one-hybrid (Y1H) assay enables detection of sequence-specific physical interactions between a promoter and a transcription factor (TF). The yeast one-hybrid assay consists of two components. The first component is the screened promoter of interest which is fused to a reporter gene; this construct is called the “bait”. On the other hand, the coding sequence of the transcription factor of interest is fused to a yeast transcription activation domain (AD); this construct is termed the “prey”. Both constructs are introduced into a yeast strain. If the prey transcription factor binds to the bait promoter, the physical interaction leads to transcriptional activation though AD domain. As a result, the reporter gene fused to the bait is expressed and the interaction can be easily detected (Reece-Hoyes and Walhout 2012) (Fig. 2-1A). In this thesis, the yeast one-hybrid method from Siobhan Brady lab is applied which yields reliable results with a low number of false positive interactions (Gaudinier *et al.* 2011). The prey collection originally consisted of the transcription factors enriched in the root stele but I expanded this library with shoot-specific transcription factors

during this thesis and it now contains approximately half of all existing transcription factors in *A. thaliana.* Thus although the number of identified interactions will be limited by the incomplete prey collection, this method can still be used to identify a substantial number of interactions which may play important role in the root and the shoot development.

The main advantage of the yeast one-hybrid method is the ability to find potential regulators of the promoter of interest. It is possible to do a high-throughput screen of multiple promoters against a library of transcription factors which leads to the construction of gene regulatory networks. Gene regulatory networks are a type of graphical models that describe interactions and regulations between individual components of this network taking place in a given biological system. Such networks can include protein-protein or transcription factor-promoter interactions. Several transcription factor-promoter gene regulatory network generated with yeast one-hybrid method have been described before in *Arabidopsis thaliana* (Brady *et al.*

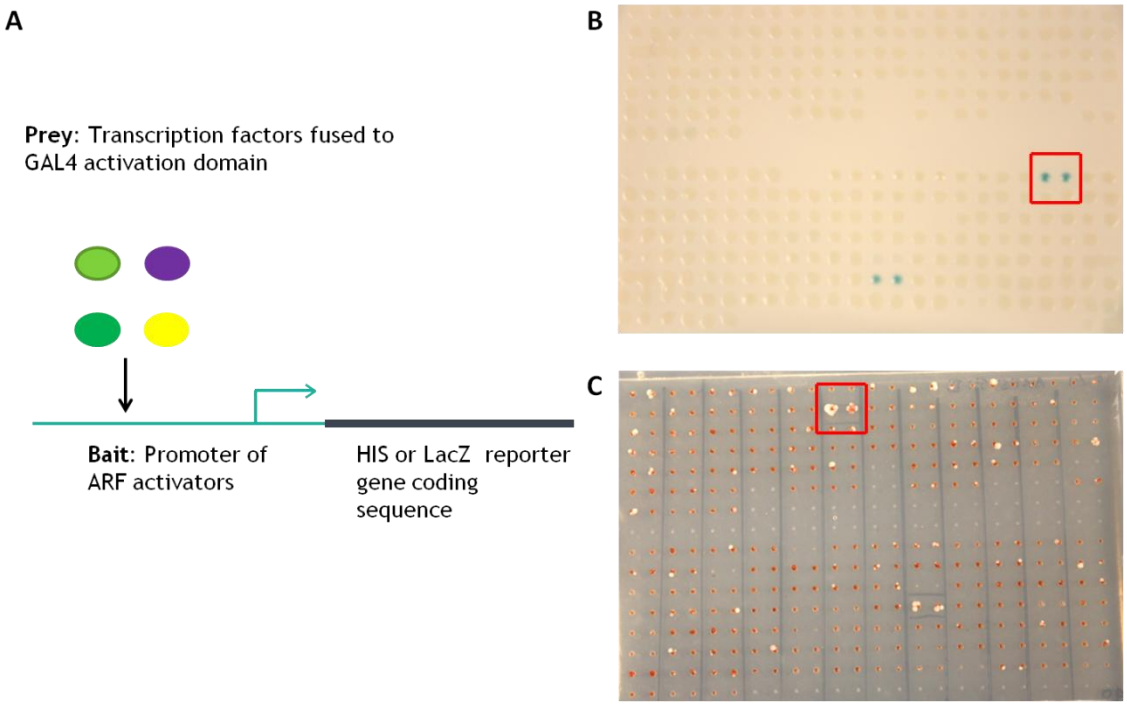

Fig. 2-1. Schematic diagram of the yeast one-hybrid assay **(A)**. Promoter-transcription factor interaction detected by X-gal assay **(B)** and 3-AT assay **(C)**. Examples of positive interactions are highlighted in red.

2011, Gaudinier *et al.* 2011), human (Reece-Hoyes *et al.* 2011) and *C. elegans* (Deplancke *et al.* 2006, Vermeirssen *et al.* 2007). The networks represent theoretical interactions because it is not known in which tissues of the organism and at what stages of development this interaction could be important *in vivo*. Nevertheless, the data from the gene regulatory networks provides insight into the complexity of gene interactions and serves as a base to find new biologically significant regulations.

The elementary brick of a gene regulatory network is the simple interaction between the transcription factor and the promoter of the target gene (Fig. 2-2A). Furthermore, transcriptional regulation networks often contain additional elements that add complexity to the apparently straightforward transcription factor – target gene promoter interactions. These elements can include feedback loops, feed-forward loops, negative or positive autoregulation (Alon 2007*,* Lee *et al.* 2002, Shen-Orr *et al.* 2002, Yeger-Lotem *et al.* 2004). Each of these network motifs has specific properties that affect dynamics of the network. For example, during auto-regulation, the transcription factor can influence its own expression by binding its own promoter and repressing (negative autoregulation) or activating (positive autoregulation) its own transcription (Fig. 2-2B and C). Negative autoregulation is often associated with genes that are able to produce rapidly large amounts of protein due to strong expression of their promoters (Fig. 2-2I); the negative autoregulation allow a rapid decrease in the production of its own protein when the protein concentration reaches a particular threshold. Thus this control mechanism is often associated with a need for a rapid response that has to be just as rapidly attenuated. In addition, negative autoregulation can reduce fluctuations in production of the gene: when amounts of protein produced are too high, the excess proteins bind and repress their own expression which then leads to a reduction of protein levels; but when the protein production is low, the repression doesn't occur and the protein levels can freely increase. An example of such system is the bacterial master regulator LexA which controls expression of genes involved in response to DNA damage; LexA negatively autoregulates its own transcription. It was experimentally shown that the autoregulatory ability of LexA increases stability of the response system allowing the bacteria to adapt their cellular response in proportion to DNA damage and prevents false activation of the response caused by transient fluctuations in the triggering signal (Alon 2007, Camas *et al.* 2006).

The positive autoregulation means that the gene is able to increase production of its own protein (Fig. 2-2C). This type of control is associated with systems that respond slowly to the stimulus; this could be due to low activity of the promoter and thus low levels of protein are produced. The response of such system to the stimulus is slower than in a simple system lacking autoregulation (Fig. 2-2I) (Maeda and Sano 2006). The positive autoregulation increases variations in protein concentration between different cells: some cells will accumulate more protein because the gene will amplify its own production whereas other cells will end up with less protein. Such variable distribution of a single protein within the tissue appears to have advantages in specific situations such as helping cell populations to adapt better to stochastic environments (Alon 2007).

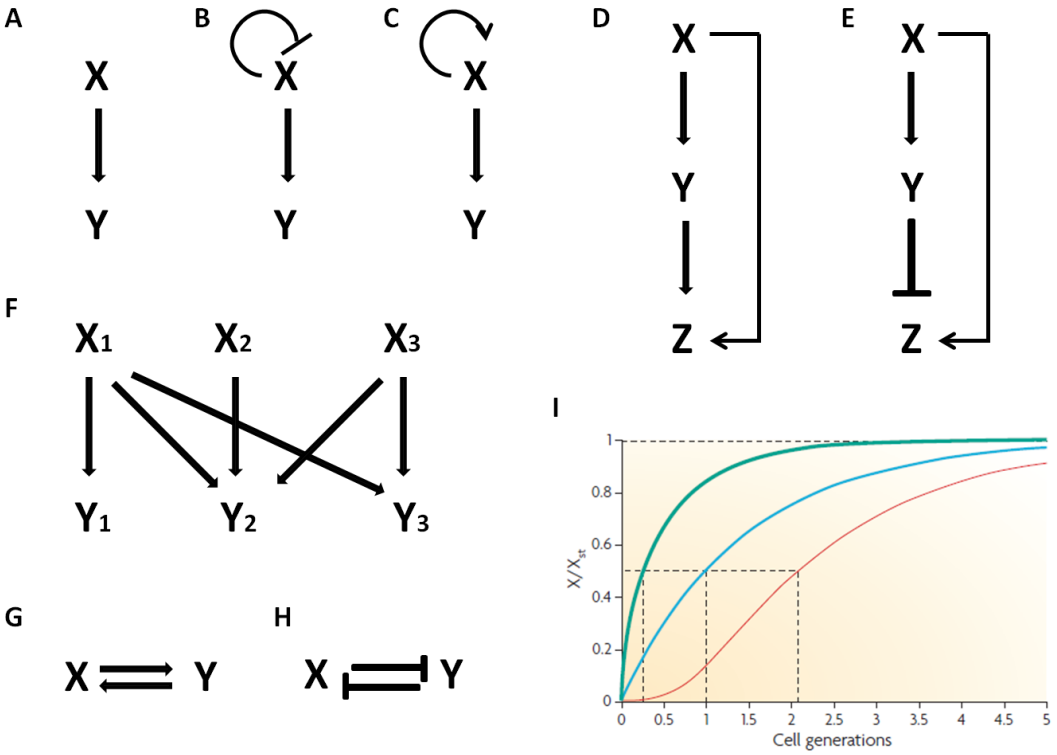

Fig. 2-2. Network motifs found in gene regulatory networks: **(A)** Simple regulation, **(B)** negative autoregulation, **(C)** positive autoregulation, **(D)** coherent feed-forward loop, **(E)** incoherent feed-forward loop, **(F)** the dense overlapping regulon, **(G)** double-positive feedback loop and **(H)** double-negative feedback loop. **(I)** The response time of the system is faster in the negative autoregulation (green line) and slower in positive auto-regulation (red line) compared to a simple regulation (blue line). X/Xst, X concentration relative to steady state Xst (Alon 2007).

In the feed-forward loop, the transcription factor regulates expression of a second transcription factor which then alone or together with the first transcription factor regulates the target gene expression. There are multiple variations of this motif because each step in this network can be either an activation or a repression (Fig. 2-2D and E). The most frequently occurring types of the feed-forward loop are the coherent type 1 (Fig. 2-2D) and incoherent type 1 (Fig. 2-2E) (Ma *et al.* 2004, Mangan and Alon 2003). The coherent type1 loop allows delay of the system reaction after stimulus because the final activation of the cellular response only occur when both first and second transcription factors accumulate in large enough amounts to affect in tandem the expression of their final common target. Such system would only activate after a long-term induction because a short-term signal would soon terminate, and so the production of the second transcription factor would never reach required concentrations to affect the final target. Such a sophisticated system is adapted to mediate only persistent stimuli and to be stitched off rapidly when needed (Mangan *et al.* 2003). On the other hand, the incoherent type 1 loop (Fig. 2-2E) has two transcription factors that act oppositely on the same promoter: one represses and another activates it. Because the production of the second transcription factor is delayed, the first TF is able induce expression of the final target both transiently and rapidly before the second transcription factor is produced in sufficient amount to attenuate expression of the final target. This results in a transient pulse-like activation of gene expression (Basu *et al.* 2004).

Often a group of several genes can be co-regulated together in a synchronized manner. This network motif called the regulon often consists of genes involved in the same pathway. For example, the bacteria Pho regulon consists of at least 47 genes involved in phosphate homeostasis (Lamarche *et al.* 2008). In yeast the expression of genes encoding the subunits of the 26S proteasome are co-regulated by the transcription factor Rpn4 (Mannhaupt *et al*. 1999, Shirozu *et al.* 2015, Xie and Varshavsky 2001). The dense overlapping regulon is one variation of this gene network motif (Fig. 2-2F). In this motif a number of transcription factors control in combination expression of multiple genes (Lee *et al.* 2002, Shen-Orr *et al.* 2002).

The negative and positive autoregulation, feed-forward loops and dense overlapping regulons are examples of network motifs included in sensory responses: such networks are designed to respond rapidly to stimulus and also make reversible decisions. In a developmental context, the signal often requires to trigger an

irreversible cell-fate decision. Developmental networks include all the above mentioned motifs but also a few other motifs such as double-positive and double-negative feedback loops. These loops are made of two transcription factors that regulate each other (Fig. 2-2G, H). In the double-positive feedback loop two transcriptional activators activate each other (Fig. 2-2G). Such as arrangements means that following the initial stimulus, both transcription factors remain active irreversibly and activate each other even after the stimulus is gone. In the double-negative loop two repressors repress each other (Fig. 2-2H). Following the stimulus, one transcription factor irreversibly switches off expression of the other. In both double-positive and the double-negative feedback loops a transient signal acts as a switch and locks the system into the permanent steady-state. In addition to transcription factors, these loops were also observed for miRNA regulation and post-transcriptional interactions such as phosphorylation (Cai *et al.* 2013, Johnston *et al.* 2005, Xiong and Ferrell 2003). In summary, gene regulatory networks include multiple motifs that add complexity and specificity for each interaction in the network.

The gene regulatory networks are based on the ability of transcription factors to regulate expression of specific genes. The transcriptional regulators are identified due to their ability to bind regulatory *cis*-elements within the gene locus which can be located in the region upstream from the initiation codon, within the downstream region including the introns and sometimes even in the terminator regions. Transcription factors are recruited to specific short DNA sequences called binding sites which are on average 10 nucleotides in length but can range between 5 and 30 nucleotides in both eukaryotes and prokaryotes (Stewart *et al.* 2012). Several potential binding sites can be identified in the gene locus but only a small portion of them might be associated with the potential regulator *in vivo* in a given condition. For example, in human cells the number of unbound motif sites is on average 430 times higher than the number of transcription factor-bound sites as determined by ChIP-seq (Wang *et al.* 2012), suggesting that the mechanism of TF binding is more complex than a simple recognition of the relevant sequence.

Often the binding sites for different transcription factors are located together in clusters. This can allow for combinatorial binding between variable transcription factors if they are co-expressed in the tissue of interest. An example is the MAD transcription factor from *D. melanogaster* which co-binds with tissue-specific transcription factors such as Tinman in the dorsal mesoderm or Scalloped in the wing

imaginal disc. Thus MAD interacts with a different partner in each specific tissue and this cell-specific cooperation results in specification of particular cell fates (Guss *et al.* 2001, Lee and Frasch 2005). The combinatorial binding between transcription factors allows thus specificity of developmental responses.

Transcription factors occupy their regulatory binding sites either continuously or only at specific stages of development and under certain conditions even though they may be expressed and available in the relevant tissues (Jakobsen *et al.* 2007, Sandmann *et al.* 2007). Non-occupation of binding site can be explained by a lack of specific interacting partners; this again reinforces the importance of combinatorial binding in regulation of gene expression. Overall, it is clear that the timing and spatial distribution of the transcription factor expression does not fully determine its transcriptional activity and that the occupancy of the binding sites must be considered when predicting how individual transcription factors might influence expression of target genes.

The combinatorial binding described above appears to often require direct protein-protein interactions between transcription factors bound to closely located sites. Such clusters of transcriptional regulators can act together as a genetic switch that induces specific developmental response only when all components are present in the required concentrations. For example, the *D. melanogaster* Twist and Dorsal transcription factors cooperate to regulate target genes in specific parts of the embryo when present at low concentrations (Szymanski and Levine 1995, Zinzen *et al.* 2006). Similarly, in *A. thaliana* ARF6, the brassinosteroid-signaling TF BZR1 and the light-response TF PIF4 interact with each other and cooperatively regulate expression of common targets genes involved in hypocotyl development (Oh *et al.* 2014a).

An alternative mechanism of transcription factor cooperativity is based on indirect interactions between individual TFs which could be facilitated through binding a common co-activator or a co-repressor. An example of a common co-repressor is the *A. thaliana* transcription factor TOPLESS (TPL) which can interact with different transcription factors. The partners of TPL are often identified as transcriptional repressors and contain repressor domains such as EAR domain (Causier *et al.* 2012, Oh *et al.* 2014b, Pauwels *et al.* 2010, Wang *et al.* 2013, Zhu *et al.* 2010). Overall, TPL was shown to interact with transcription factors from at least 17 different gene

families through their repressor domains (Causier *et al.* 2012). The number and diversity of interactions would allow construction of variable repressor complexes consisting of tissue-specific partners of TPL.

The relative positioning of the TF binding sites including their orientation, the spacing relative to each other and order has a profound influence on the ability of the transcription factors to interact and to cooperatively regulate gene expression. For example, the 55 base pair enhancer motif of the human interferon gene is occupied by 8 proteins with overlapping binding sites. Small changes in the enhancer motif affected function of all eight proteins indicating the importance of the co-operative binding (Panne *et al.* 2007, Thanos and Maniatis 1995).

In this chapter part of the gene regulatory network that controls expression of ARF activators was identified. *In planta* confirmation experiments led to the surprising discovery that the majority of the transcriptional regulators repress expression of ARFs. Analysis of the publically available DAP-seq and microarray gene expression datasets further validated these interactions and allowed to identify additional regulatory motifs within the network. Mutants of the transcriptional regulators were used to determine biological processes in which these regulations are important and provided clues on how specificity of ARF expression patterns is achieved.

Results

Yeast one-hybrid assay revealed an elaborate network of transcription factors controlling expression of ARF activators

The transcriptional regulators of ARF activator expression were identified using a yeast one-hybrid assay (Fig. 2-1A). The ARF promoter fragments (bait) were fused to the lacZ or HIS3 reporter genes and screened against a library of transcription factors fused to a Gal4 activation domain (preys) in yeast. The physical interaction between the bait and the prey resulted in expression of these reporter genes which then enabled the selection of successful interactions through an X-gal assay (in case of lacZ) or by growing the yeast on a medium deficient in histidine amino acid (in case of HIS reporter gene) (Fig. 2-1B and C). An interaction was considered as positive when either one of the assays (or both) showed positive result.

An important point was to decide on the size of the DNA fragments from the ARF locus to use as a bait in this approach. Ideally these fragments should contain all binding sites for the regulatory transcription factors. The ARF activators all share a similar structure: within their coding sequence they contain 11-14 introns (Suppl. Fig. 1-1). In particular, for ARF5, 7 and 19 the first intron is 2-3 times larger than the other introns. Because this first intron was suspected to be important for the transcriptional

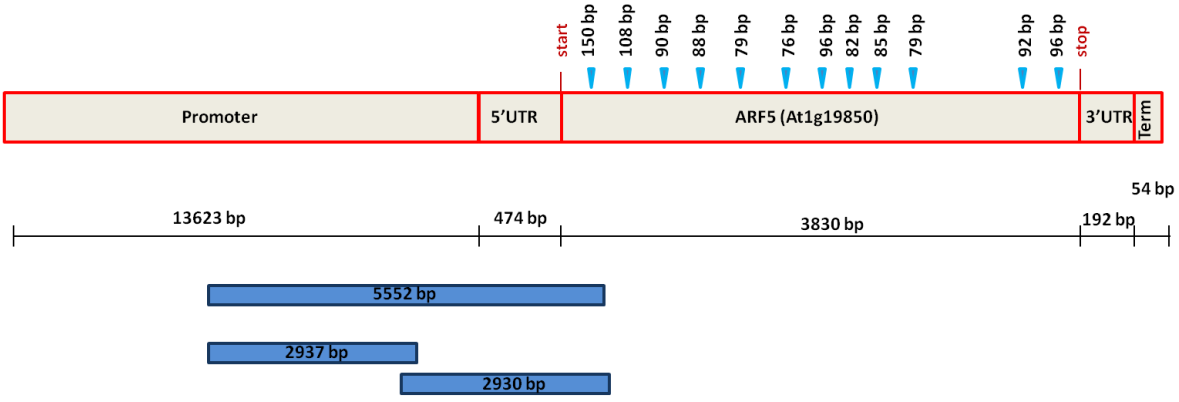

Fig. 2-3. Schematic of yeast one-hybrid bait design with ARF5 as example. Top row: schematic representation of ARF5 locus; small blue triangles indicate introns. Blue boxes indicate sequences screened in Y1H assay: total sequence screened (top blue box) and the two fragments screened separately (middle and lower blue boxes).

regulation, the sequences screened in the yeast one-hybrid included both upstream promoter region and a small part of the downstream region containing this first intron. Overall, large promoter regions were screened with ca. 5000 bp promoters for ARF5, 8 and 19 and ca. 3000 bp promoters for ARF6 and ARF7. The length and the content of the bait fragments gives confidence that a majority of the regulatory interactions would be identified even though there is a chance that some interactions might still be missed. Due to the limitations of the assay, the larger promoters of ARF5, 8 and 19 were screened in two separate fragments (Fig. 2-3). The promoter size and

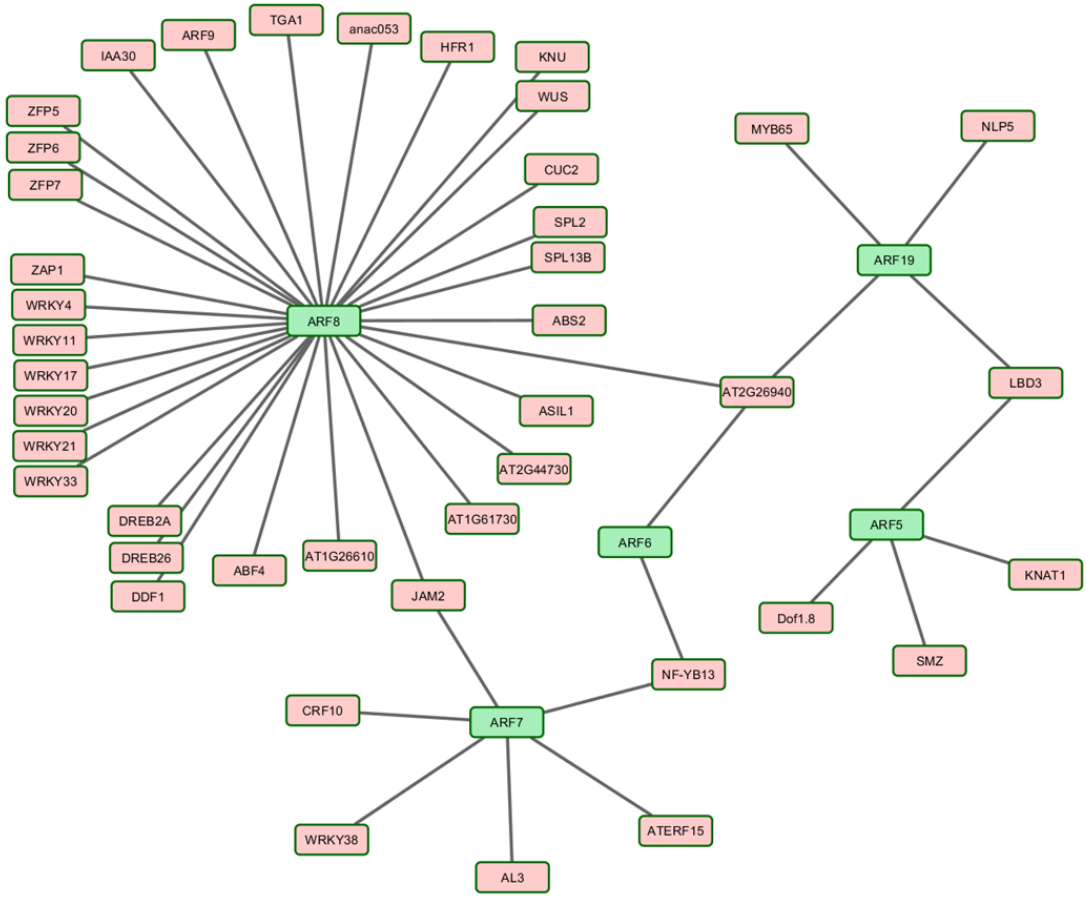

Fig. 2-4. Yeast one-hybrid promoter- transcription factor interaction network for ARF activators. Green boxes are five ARF activators; pink boxes are transcription factors binding to the ARFs.

sequence corresponds precisely to the promoters used in the construction of the transcriptional reporter lines described in chapter I. In this regard, the transcriptional reporter lines reveal the expression patterns generated, in part, by the transcriptional regulators identified in this study. In the chapter the reporter lines were shown to have a generally good consistency between the observed expression pattern in the SAM and the published *in situ* hybridization results; this shows that the fragments used for the bait constructs contain most of the regulatory sequences required to recapitulate *in planta* expression patterns.

The yeast one-hybrid screen for promoters of ARF5, 6, 7, 8, and 19 was conducted in collaboration with Siobhan Brady's lab at the UC Davis. The Siobhan Brady's lab possesses a library of ca. 800 root-specific stele enriched transcription factors used in the yeast one-hybrid screen. In addition to that, I cloned 87 more transcription factors that I added to this collection in this study (see Suppl. Table 2-3). The additional genes include shoot-specific transcription factors which were shown to play important roles in the shoot development. Additionally, a number of genes from signalling pathways of various hormones were added. The goal was to find regulators of ARFs involved in both root and shoot development and to find any potential cross talk between auxin and other hormones. At the time of conducting this experiment, the final prey library represented approximately half of all predicted *A. thaliana* transcription factors.

A summary of results of the yeast one-hybrid screen are displayed in Figure 2-4. Overall 42 transcription factors bound to the promoters of ARF activators in my assay. The network includes 47 interactions because a few of the transcription factors regulate multiple ARFs. The ARF activators were not uniform in the amount and type of interaction partners. Numerous interactions were identified for ARF8. On the other hand, ARF5 had 4, ARF6 had 2, ARF7 had 6 and ARF19 only 4 interaction partners.

Most of the transcription factors originated from the root-specific library. Only four transcription factors come from the 87 shoot-specific transcription factors that I added to the collection: WUS and KNU which bind to ARF8, KNAT1 binding to ARF5 and CRF10 binding to ARF7.

As described previously, ARF5, 8, and 19 promoters were screened in two separate fragments. Interestingly, almost all of the transcription factors were found in the screen with the promoter fragments closest to the transcription. The only exception is HFR1 which bound to the second promoter fragment of ARF8; its binding site is therefore localized between -5091 and -2900 bp upstream of the gene start codon.

The results show that a few transcription factors bind to the promoters of multiple ARF activators. None of the transcription factors identified bound to the promoters of all five ARF activators in this screen. Interestingly, At2g26940 controls ARF6, 8 and 19. This gene, which belongs to the C2H2-type zinc finger protein family is a putative repressor due to the presence of a putative EAR domain at the C-terminus (Ciftci-Yilmaz and Mittler 2008).

Another common regulator is the bHLH-type transcription factor JAM2 which acts redundantly with JAM1 and JAM3 as negative regulators of jasmonate signaling (Sasaki-Sekimoto *et al.* 2013). JAM2 interacts with various JAZ proteins and was shown to act as a repressor (Nakata and Ohme-Takagi 2013; Sasaki-Sekimoto *et al.* 2014; Song *et al.* 2013). This particular regulation indicates a cross-talk between the jasmonate and the auxin signaling. A link between ARF7 and the JA signaling is a new surprising result. On the other hand, ARF8 regulates jasmonic acid homeostasis and this regulation plays a distinct role during flower maturation (Nagpal *et al.* 2005) and adventitious root development (Gutierrez *et al.* 2012); thus the ARF8 expression appears to be subjected to the feedback control through JAM2.

LBD3, a LOB domain transcription factors, simultaneously regulates ARF19 and ARF5 transcription. Interestingly, LBD3 was shown to be the only member of the LOB gene family which is upregulated by cytokinin in leaves and together with its close homologue LBD4 in the root (Naito *et al.* 2007). This result indicates a new link between the cytokinin and the auxin pathways. The role of LBD3 in plant development hasn’t been studied yet, but other members of the LBD family were shown to play important roles in lateral organ development. For example, LBD16 and LBD29 are involved in lateral root development (Feng *et al.* 2012, Goh *et al.* 2012) whereas LOB and LBD6 play a role in shot apical meristem maintenance and lateral organ specification (Byrne *et al.* 2002).

The final common transcription factor is NFYB13 (NUCLEAR FACTOR Y, SUBUNIT B13) which hasn't been studied yet. Kang *et al.* 2004 identified this gene as a homolog of human TATA-BP-associated phosphoprotein Dr1. The human Dr1 protein is known to repress RNA polymerase II transcription by precluding the entry of TFIIA and TFIIB into the pre-initiation complex to prevent the formation of an active transcription complex (Inostroza *et al.* 1992).

The majority of transcription factors which regulate ARFs are not common to multiple ARFs and could specifically control a single ARF activator. The regulator of ARF5, SMZ was shown to be a repressor of flowering by direct repression of the gene FT. SMZ also directly represses other flowering regulators including itself, its paralog SNZ, AP2 and TOE3 (Mathieu *et al.* 2009). Another regulator of ARF5, At1g64620 (Dof1.8) is a Dof-type zinc finger DNA-binding protein. Although not much information is available on this particular gene, interestingly, the Dof1.8 is specifically expressed in the central and the rib zones of the shoot apical meristem, in shoot phloem and shoot xylem (Yadav *et al.* 2009, Yadav *et al.* 2014). Thus Dof1.8 could be involved in regulation of ARF5 at the shoot apical meristem.

ARF19 promoter is regulated by NLP5, an NLP family protein which binds to the nitrate-responsive cis-element in promoters and activate nitrate-responsive transcription (Konishi and Yanagisawa 2013). Therefore ARF19 could be involved in the auxin-mediated nitrate signaling. Another regulator of ARF19, MYB65, controls anther development (Millar and Gubler 2005).

Among the ARF7 regulators WRKY38 acts as negative regulator of plant basal defense against plant pathogens (Kim *et al.* 2008). This prominent link between auxin signaling and the biotic stress is also characteristic for ARF8 which is regulated by several WRKY transcription factors. One of them is WRKY4 which is induced by SA and has a positive role in plant resistance to necrotrophic *Botrytis* infection and a negative effect on plant resistance to biotrophic *Pseudomonas syringae* (Lai *et al.* 2008). WRKY11 and WRKY17 are negative regulators of basal defense against *Pseudomonas syringae* (Journot-Catalino *et al.* 2006). WRKY33 was shown to negatively regulate SA pathway and positively JA pathway; it was shown to be required for resistance against the necrotrophs *A. brassicicola* and *B. cinerea* (Birkenbihl *et al.* 2012; Zheng *et al.* 2006). Altogether, it appears that ARF7 and

ARF8 could be involved in the JA and SA hormone pathway homeostasis in response to biotic stress.

One of the interesting regulators of ARF8 promoter is HFR1. HFR1 is a positive regulator of photoreceptor phytochrome B dependent seed germination. HFR1 forms a heterodimer with PIF1, the negative regulator of seed germination, and this prevents PIF1 from binding its target DNA. The HFR1-PIF1 module regulates the expression of various genes involved in cell division, cell wall modification and hormone pathways to promote seed germination (Shi *et al.* 2013). Interestingly, *hfr* mutants show longer hypocotyls under continuous far-red light which is similar to the phenotype of *arf8* mutant (Tian *et al.* 2004).

ARF8 promoter also interacts with WUS and KNU. WUS is a well-studied protein which plays a central role in maintenance of the shoot apical meristem (Brand *et al.* 2000, Lenhard and Laux 2003, Mayer et al. 1998, Schoof *et al.* 2000; Yadav *et al.* 2011). KNU was shown to be a repressor of WUS (Sun *et al.* 2009). KNU represses WUS only at the flower stage 6 when the stem cell maintenance is no longer required and the shoot apex undergoes the final transformation into a flower (Sun *et al.* 2009). The control of ARF8 expression by WUS and KNU might be linked to the role of ARF8 in flower development or indicate a role of ARF8 in shoot apical meristem maintenance.

A number of ARF8 regulators play a prominent role in abiotic stress. One of them is NTL4 (Anac053), a membrane bound transcription factor. Under drought-stress conditions it is protealytically cleaved off from the membrane, translocates to the nucleus, binds to the promoter of *Atrboh* gene which encodes an NADPH oxidase involved in ROS production, and this leads to ROS accumulation and triggers leaf senescence (Lee *et al.* 2012). NTL4 is also involved in other stresses including cold, H_2O_2 treatment, MMS treatment, ABA treatments (Kim *et al.* 2007), heat, air-drying and salt stresses (Lee *et al.* 2012). Another transcriptional regulator of ARF8, DREB2A is also involved in drought-stress response; it specifically interacts with cis-acting dehydration-responsive element/C-repeat (DRE/CRT) and regulates genes involved in drought stress such as RD29A (Sakuma *et al.* 2006). On the other hand, DREB26 is involved in heat and cold stresses (Krishnaswamy *et al.* 2011). The transcriptional regulator DDF1 was shown to be involved in cold, salt, drought and heat stresses in a GA-dependant manner (Kang *et al.* 2011). Finally, ABF4 is

involved in ABA signaling in response to water stress and is induced by ABA, high salinity or water stress (Yoshida *et al.* 2010). Overall, the involvement of ARF8 in abiotic stress responses is a new unexpected result.

Several additional ARF8 transcriptional regulators are involved in developmental processes. For instance, SPL2 plays a role in lateral organ formation in the shoot during the reproductive phase (Shikata *et al.* 2009). SPL13 controls the switch from the cotyledon stage to the vegetative-leaf stage (Martin *et al.* 2010). ZFP5 is a key regulator of root hair initiation and development (An *et al.* 2012). ZFP6 controls trichome initiation through GA and cytokinin signaling and by regulating the expression of ZFP5 (Zhou *et al.* 2013). ZFP6 and ZFP7 are involved in light and ABA responses during germination and early seedling development (Joseph *et al.* 2014).

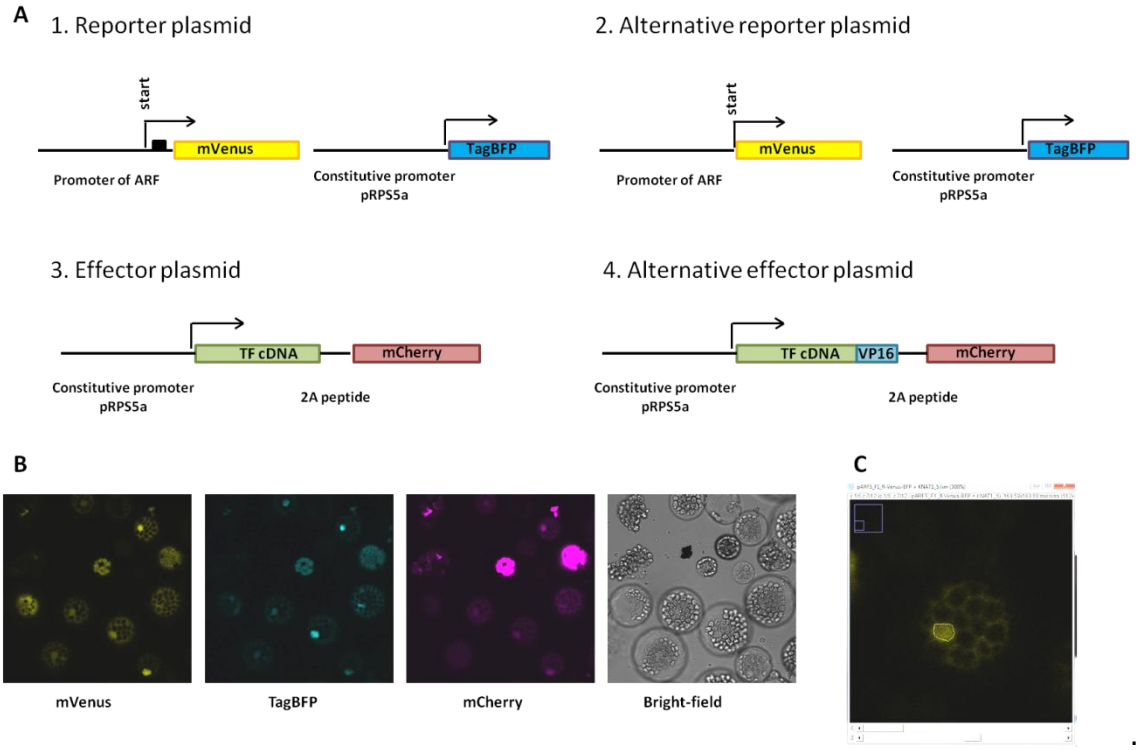

Fig. 2-5. Design and imaging of the transient protoplast assay. **(A)** Design of the standard reporter plasmid containing upstream and downstream sequences of the ARF promoter including the first intron (1), the alternative reporter plasmid containing only upstream sequences of the ARF promoter (2), the standard effector plasmid (3), and an alternative effector plasmid containing VP16 domain fused to the TF coding sequence (4). **(B)** Images obtained during confocal microscopy with channels for mVenus, TagBFP, mCherry and the bright-field. **(C)** ImageJ software was used for the measurement of the fluorescence. The nucleus of each protoplast was selected and the mean fluorescence was measured.

The majority of the ARF activator transcriptional regulators act as repressors

The promoter-TF interaction network discovered in the yeast one-hybrid screen provides information on factors binding to ARFs in a heterologous organism. Nevertheless, it's important to consider that these interactions might function in yeast but not in *Arabidopsis thaliana*. Additionally, it remains unclear if the discovered TFs are repressors or activators of ARF transcription *in planta*. These questions were addressed in a transient expression analysis using *Arabidopsis thaliana* leaf protoplasts.

Leaf mesophyll cells were co-transformed with a reporter plasmid and an effector plasmids (Fig. 2-5A). The reporter plasmid contained the promoter of the respective ARF driving expression of the nuclear-localized mVenus reporter gene. The promoter length was the same as used in yeast one-hybrid screen. The same reporter plasmid contained a constitutively expressed nuclear-localized TagBFP which was used as the marker to confirm successful transformation. In the effector plasmid the constitutive promoter pRPS5a drove expression of the relevant TF and simultaneously the nuclear-localized mCherry which served as the marker for the successful transformation of the protoplasts with this plasmid. The transcription factor coding sequence and the mCherry were separated by the 2A peptide which enables co-translational cleavage; thus the TF protein and the mCherry were produced as separate proteins despite being driven by a shared promoter (Kim *et al.* 2011a, Trichas *et al.* 2008). Following plasmid transformation into protoplasts, the fluorescence levels of the mVenus reporter gene were measured using a confocal microscope. This was done by taking z-stack images of protoplasts; for each individual protoplast an image corresponding to the center of the nucleus was selected from the z-stack and the fluorescence intensity in the nucleus was measured (Fig. 2-5B and C).

It is expected that in some cases this experiment would be unable to confirm interactions as the mVenus levels might remain unchanged. In this case a TF may bind, but be insufficient to regulate expression, for example, it may be missing an essential co-factor. To address this I also developed a second alternative effector plasmid containing the herpes simplex virus protein VP16-domain fused to the C-terminus of a TF coding sequence (Fig. 2-5A). This alternative TF-VP16 fusion

protein could potentially acts as an activator of ARF transcription because the VP16-domain acts as a transactivation domain (Hirai *et al.* 2010).

In addition, an alternative reporter plasmid was also constructed. The only difference to the standard reporter is the sequence of the ARF promoter: whereas the standard ARF promoter contained both upstream sequences and small downstream sequences including the first intron, the alternative promoter contained only upstream sequences up to the start codon (Fig. 2-5A). This shorter promoter lacking downstream elements could be used to identify which of the regulatory transcription factors are binding the ARF promoters in the downstream region.

For ARF5, 6 and 7 five independent experiments whereas for ARF8 and ARF19 four independent experiments were conducted. The first type of experiment included the reporter plasmid against the effector plasmid (Fig. 2-5A); this experiment was repeated two times for ARF5, 6, 7 and 8, and one time for ARF19. Second type of experiment included an alternative reporter plasmid containing a shorter promoter (lacking downstream regions) against the effector plasmid; it was done once for

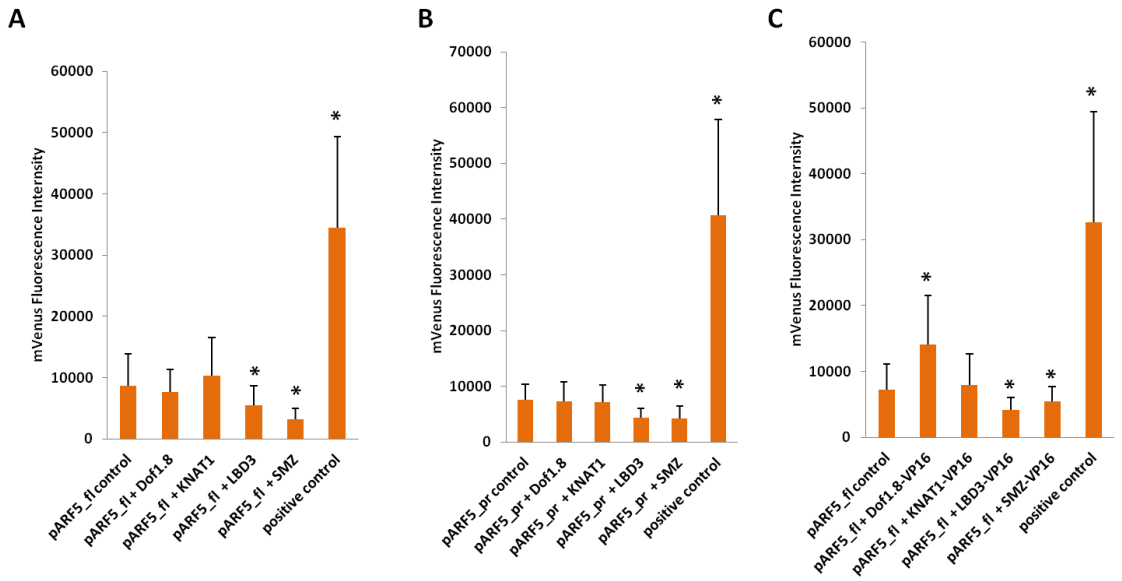

Fig. 2-6. Control of the ARF5 expression by the regulatory transcription factors in *Arabidopsis thaliana* mesophyll protoplasts. Interactions were conducted using either the standard full-length ARF5 promoter (pARF5_fl) **(A)** or alternative shorter ARF5 promoter (pARF5_pr) **(B)** against the appropriate TFs. Additionally a VP16 activation domain was fused to the TFs and the interactions were examined with the standard ARF5 promoter **(C)**. Error bars represent standard deviation of the mean value (n= 40 protoplasts). An unpaired t-test was used to calculate significance with *p < 0.1.

ARF5, 6, 7 and 19. Third type of experiment included the reporter plasmid against an alternative effector plasmid containing TF-VP16 domain fusion; this was done two times for all ARFs.

Interestingly, in the case of ARF5, 6, 7 and 19 the reporter plasmid alone was able to produce a basal level of mVenus fluorescence in protoplasts, possibly due to presence of TFs in the leaf mesophyll cells that activate the promoter. This allowed detection of both activation and repression. On the contrary, ARF8 promoter was not producing any basal level of mVenus fluorescence. To overcome this problem, a small part of the 35S promoter was inserted into the ARF8 promoter before the transcription start site which boosted the basal expression level.

The results are shown using ARF5 as an example because ARF5 is regulated only by four different transcription factors in yeast: At1g64620 (Dof 1.8), KNAT1, LBD3 and SMZ. The protoplast assay using full-length ARF5 promoter showed that LBD3 and SMZ act as repressors (Fig. 2-6A). The same results were obtained using alternative shorter promoter (Fig. 2-6B) indicating that the binding sites of these transcription factors lie upstream of the start codon. When an alternative effector plasmid with VP16 domain fusion was utilized LBD3 still acted as a strong repressor of ARF5 whereas SMZ-induced repression was almost completely lifted (Fig. 2-6C). This result suggests that the LBD3 is a stronger repressor of ARF5 transcription compared to SMZ. Interestingly, Dof1.8 had no effect on the ARF5 expression

	1 (normal)	2 (normal)	3 (normal)	4 (VP16)	5 (VP16)	Final score
Dof1.8	0	0	0	+	+	**2**
KNAT1	0	0	0	0	-	**1**
LBD3	-	-	-	-	-	**4**
SMZ	no data	-	-	-	0	**3**

Table 2-1. Scoring interactions between the promoter ARF5 and the regulatory transcription factors based on protoplast assay results. “+” indicated increase, “-“ reduction and “0” no change of mVenus reporter gene levels compared to control ($p \leq 0.1$). The score was given between 0 and 4: 4 when the interaction was confirmed in at least 4 independent experiments and 0 when the interaction wasn’t confirmed even in a single experiment. “normal” indicates using standard effector plasmid; “VP16” indicated using an alternative effector plasmid with TF-VP16 domain fusion.

levels by itself (Fig. 2-6A and B) but when fused to the VP16 domain it was acting as a strong activator of ARF5 expression (Fig. 2-6C). This suggests that there is an interaction between the ARF5 promoter DNA and the Dof1.8 protein. Finally, KNAT1 could not change the expression level of ARF5 promoter in any of the experiments (Fig. 2-6 A, B and C).

The interactions were given scores between 0 and 4: if they were confirmed in at least 4 independent experiments, they received score 4; if they were confirmed in 3 independent experiments, they received score 3 etc. The resulting score for ARF5 interactions is presented in Table 2-1. The complete table with scores for all

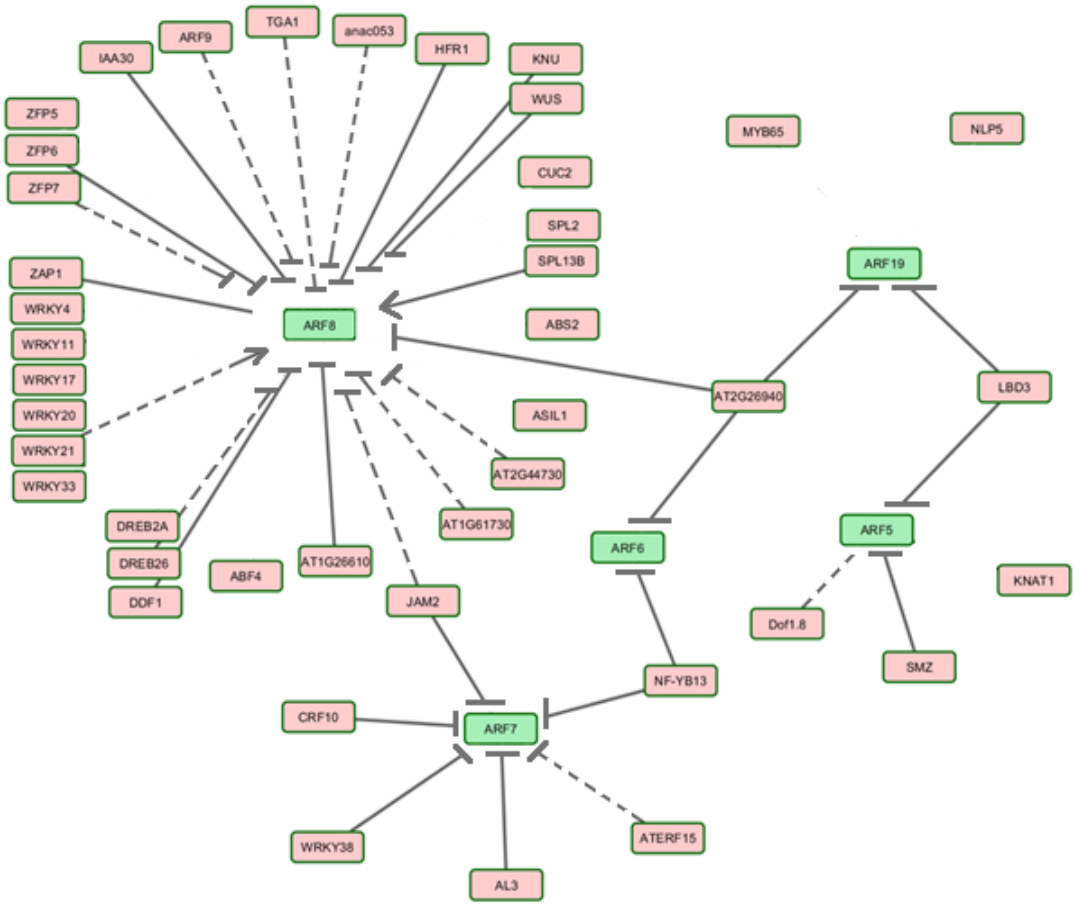

Fig. 2-7. Yeast one-hybrid promoter-transcription factor interaction network for ARF activators after transient protoplast assay. Green boxes are five ARF activators; pink boxes are transcription factors binding to the ARFs. The solid line indicates interactions with score 4 or 3, dash lines with score 2, and no line with score 1 or 0.

interactions is listed in Supplementary Table 2-1. The interactions with score 3 or 4 were considered as confirmed regulations, score 2 as possible regulations, score 1 or 0 as not confirmed regulations. The resulting promoter-TF interaction network is illustrated in Fig. 2-7. Here the solid lines represent confirmed regulations and the dashed lines possible regulations; the absence of a line indicates that the regulation could not be confirmed in the protoplast assay.

Overall, there are 47 interactions in this network from which 15 could not be confirmed as regulations in protoplasts. Thus 68.1% of the regulations were confirmed and 31.9% were not confirmed in the protoplasts.

Most strikingly, the results demonstrate that the majority of the transcription factors are repressors of ARFs *in planta*. The only two activators identified are the regulators of ARF8 transcription WRKY21 and SPL13b.

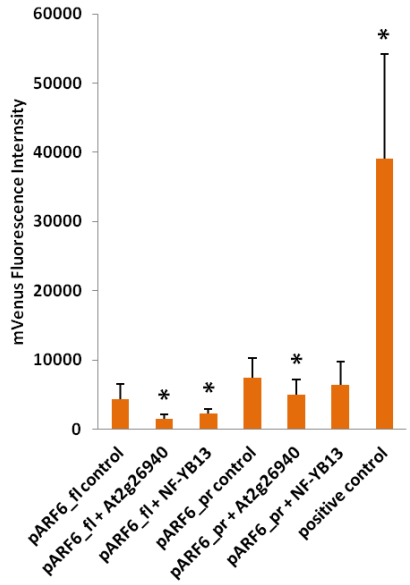

Fig. 2-8. Control of the ARF6 expression by the regulatory transcription factors in *Arabidopsis thaliana* mesophyll protoplasts. Interactions were conducted using either the standard full-length ARF6 promoter (pARF6_fl) or alternative shorter ARF6 promoter (pARF6_pr) against the appropriate TFs. Error bars represent standard deviation of the mean value (n= 40 protoplasts). An unpaired t-test was used to calculate significance with *p < 0.1.

As described above, two different reporter plasmids were used in the protoplast assay: the plasmid containing a longer promoter that included also downstream sequences such as the first intron and an alternative promoter which lacked downstream sequences. This method allowed me to differentiate transcription factors that bind downstream sequences in the ARF promoters. Indeed, in case of ARF6 the transcription factor NFYB13 induced expression of the mVenus reporter only in the longer promoter but not in the shorter promoter which lacked downstream sequences (Fig. 2-8). This shows that NFYB13 is likely to bind the ARF6 promoter in the downstream region. This example illustrates the importance of using both upstream and downstream sequences in the bait construct to optimize the amount of detected interactions.

Publically available databases can be used to further validate and explore the interactions

The transient protoplast assay utilizes cells extracted from a specific tissue (leaves) which are not pluripotent cells but instead retain the intrinsic programming of the leaf mesophyll cells (Faraco *et al.* 2011). It is conceivable that some interactions might require specific cellular components not present in the leaf tissue and this could result in false negative results. Therefore, the capacity to confirm interactions is limited by the chosen system and other methods should be applied as well. One of them is to use the available literature to search for the transcription factor binding sites in the promoters of ARFs. In addition, the publically available database with results for the DNA affinity purification sequencing (DAP-seq) provides information on the binding sites of multiple transcription factors in *Arabidopsis thaliana* at the genomic scale (O'Malley *et al.* 2016). In DAP-seq ca. 200 bp fragments of the *A. thaliana* genomic DNA are incubated with an affinity-tagged *in vitro* expressed TF; the unbound DNA is removed while the DNA bound by the TF is sequenced; the sequenced reads are mapped to the reference genome.

For example, the regulator of ARF5 transcription Dof1.8 (At1g64620) belongs to the Dof gene family protein, members of this family have been shown to bind target DNA at the consensus sequence T/AAAAG (Yanagisawa and Schmidt 1999). Indeed, the DAP-seq identified AAAG (or CTTT on the opposite strand) as the binding site of Dof1.8 (Fig. 2-9C). Promoter analysis of ARF5 confirms the presence of CTTT site at

-981 bp and AAAG site at +203 which corresponds to the summit of the two peaks detected in DAP-seq (Fig. 2-9A).

Similarly, the WRKY33, a regulator of ARF8 expression, belongs to the family of WRKY transcription factors that bind a W-box with a consensus sequence (C/T)TGAC(T/C) (Pandey and Somssich 2009, Zheng *et al.* 2006). This is identical to the sequence identified in the DAP-seq (TTGACT) (Fig. 2-9D). The ARF8 promoter contains two W-boxes at positions -799 bp and -786 bp which correspond to the peak in the DAP-seq analysis (Fig. 2-9B). Interestingly, the interaction between WRKY33 and the promoter ARF8 could not be confirmed in protoplasts but was supported with the *in silico* analysis.

On the other hand, WUS displays no peak in the promoter of ARF8 in DAP-seq analysis but acts as a strong repressor of ARF8 transcription in the protoplast assay.

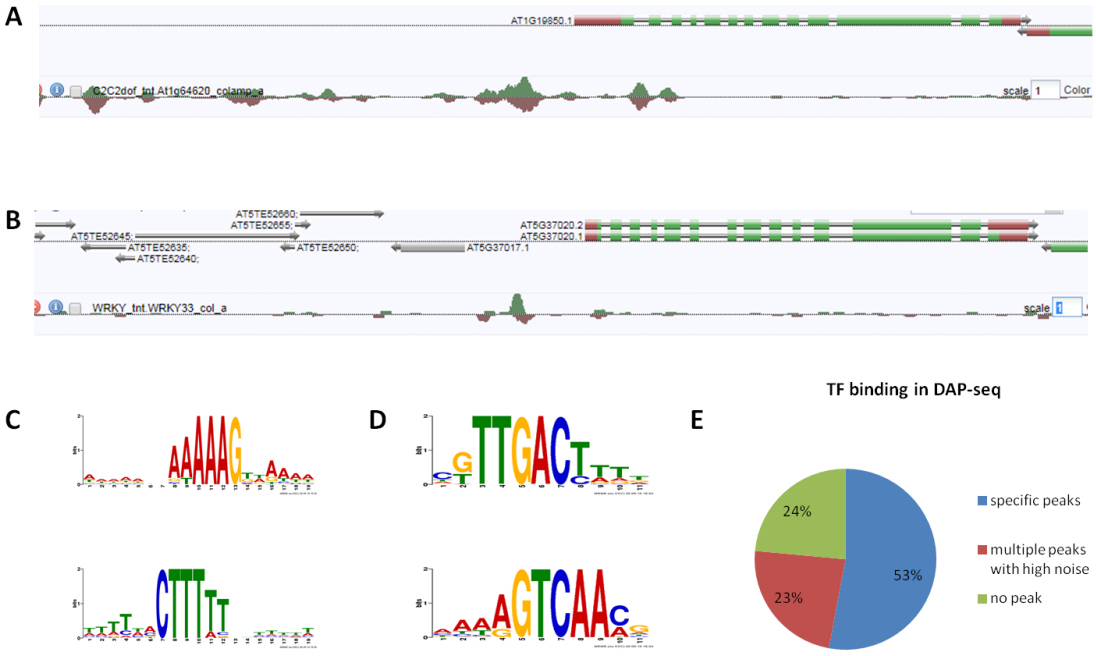

Fig. 2-9. *In silico* analysis of the transcription factor binding sites using DAP-seq database. DAP-seq peaks of Dof1.8 in the promoter of ARF5 **(A)** and WRKY33 in the promoter of ARF8 **(B)**. Consensus binding sequences identified for Dof1.8 **(C)** and WRKY33 **(D)** with DAP-seq analysis. **(E)** Summary of the DAP-seq analysis for the 17 TFs available in DAP-seq. **(**O'Malley *et al.* 2016).

WUS was shown to bind a sequence TCATA**TAAT**CCATT of the CLV3 promoter in Yadav *et al.* 2011 with the middle four nucleotides TAAT being essential for the binding ability. The promoter ARF8 has two similar sequences in the promoter region: TACATTAATTCATT and TACTATAATTCATT sites located at -4820 bp and -870 bp upstream of the transcription start site. Thus even through this interaction could not be supported by the DAP-seq analysis the putative binding sites can be predicted using the available published information.

Complete results for the binding site analysis is presented in Supplementary Table 2-2. Overall, the DAP-seq database contains information on only 17 out of 42 of the regulatory transcription factors identified in this study. From the 17 transcription factors available, 53% show very specific peaks with distinguishable putative binding sites, 23% display multiple peaks with high noise background which hinders analysis and 24% shows no peak in the promoter region (but specific peaks elsewhere in the genome) (Fig. 2-9E, Suppl. Table 2-2). Among TFs with specific binding in the DAP-seq are MYB65, WRKY17, WRKY20 and WRKY33; these four interactions were not confirmed previously using the transient protoplast assay but could be confirmed with this method. Thus the binding specificity of the transcription factors to the ARF promoters was additionally validated in many cases.

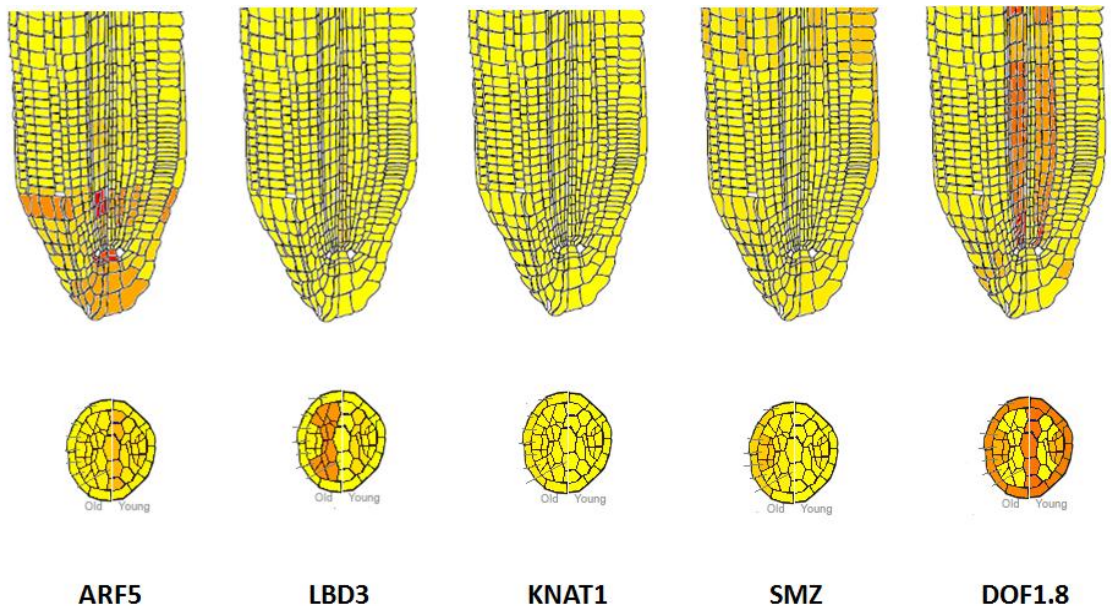

Fig. 2-10. Expression profiles of ARF5 and its regulatory transcription factors in the root (Brady *et al.* 2007*)*

The repression of ARF expression by the regulatory transcription factors suggests that these transcription factors should be expressed in tissues opposite to where their target ARF activators are found. The expression pattern of ARF activators has been described in the root and the shoot apical meristem in chapter I. On the other hand, the information on the expression of the regulatory transcription factors can be found using root and shoot gene expression maps (Brady *et al.* 2007; Yadav *et al.* 2009, Yadav *et al.* 2014). In these works the fluorescence-activated cell sorting of protoplasts coupled with microarray was used to generate expression profiles in the root and the shoot apical meristems with a tissue-specific resolution.

As an example, the ARF5 expression map recapitulates the expression pattern provided by the transcriptional reporter line well (Fig. 1-1A and 1-2). The ARF5 regulators LBD3, SMZ and Dof1.8 are also expressed in specific tissues of the RAM whereas KNAT1 is not expressed in the root at all (Fig. 2-10). Interestingly, the expression of ARF5 is predominantly limited to the xylem in the root above the early meristematic zone (Fig. 1-1A and 1-2). LBD3, a strong repressor of ARF5, is expressed in procambium cells of the root but absent from the xylem. Another repressor of ARF5, SMZ, is enriched in phloem and phloem-pole pericycle. Thus the repressors of ARF5 show a complementary expression pattern in the root. This could indicate that LBD3 and SMZ are repressors which block ARF5 expression from the high cytokinin signaling domains (procambium and phloem) and limit its expression to the high auxin signaling domain (xylem).

On the other hand, Dof1.8 is strongly expressed in xylem, pericycle and weaker in phloem. Nevertheless, Dof1.8 was not shown to be a repressor of ARF5 but in fact only acted as a transcriptional activator when fused to a VP16 domain in the protoplast assay (Fig. 2-6). Therefore Dof1.8 might represent an activator of ARF5 transcription acting in xylem cells of the root.

Similarly, the shoot gene expression map can be used to localize expression of ARFs and their regulators. Unfortunately, among ARF activators only ARF19 shows a tissue-specific expression profile whereas ARF5, 6, 7, and 8 are expressed almost ubiquitously in the SAM (Suppl. Fig. 2-1). This doesn't correspond to the transcriptional reporter expression patterns (Fig. 1-7) or the published *in situ* hybridization results (Vernoux *et al.* 2011). The authors of the shoot gene expression map used *apetala1-1;cauliflower1-1* double mutant shoot apexes which has a highly

disorganized inflorescence to generate their data (Han *et al.* 2014). Therefore it appears that the shoot expression map data cannot be applied with the confidence required for this study.

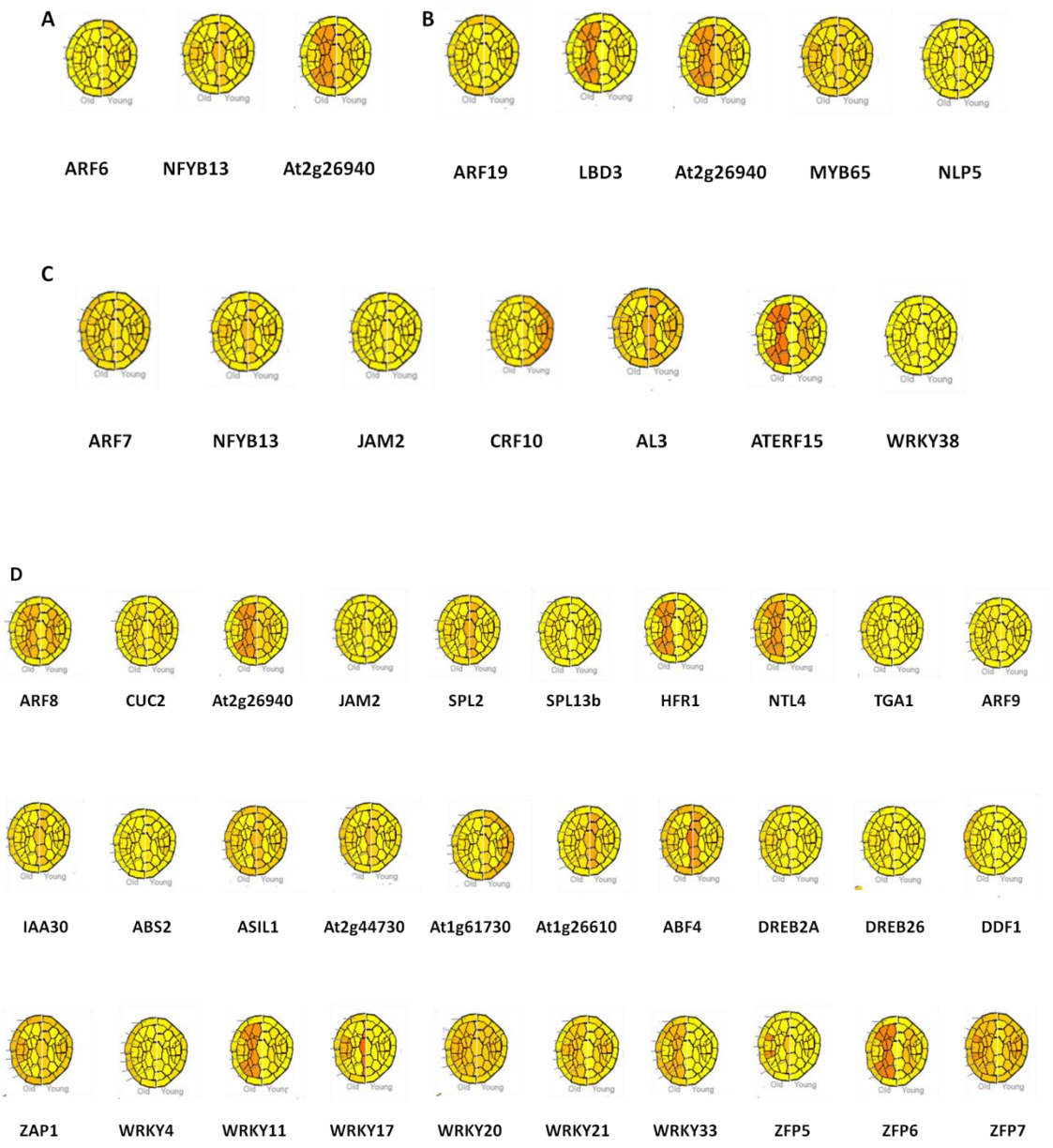

Fig. 2-11. Expression profiles of ARF6 **(A)**, ARF19 **(B)**, ARF7 **(C)**, ARF8 **(D)** and their regulatory transcription factors in the root (Brady *et al.* 2007*)*.

Overall, the root expression maps support the antagonistic expression patterns of repressors in case of ARF6 and ARF19 (Fig. 1-1, Fig. 2-11A and B). ARF7 shows a wide expression pattern in multiple tissue types of the RAM which contradicts with the specific expression patterns for some of the repressor (Fig. 1-1, Fig. 2-11C). This could mean that repressors act in a highly specific way to reduce ARF7 expression at certain times or only act to tune the level of expression. ARF8 expression is very limited in the RAM and this corresponds well with the expression of repressors in various tissues (Fig. 1-1, Fig. 2-11D).

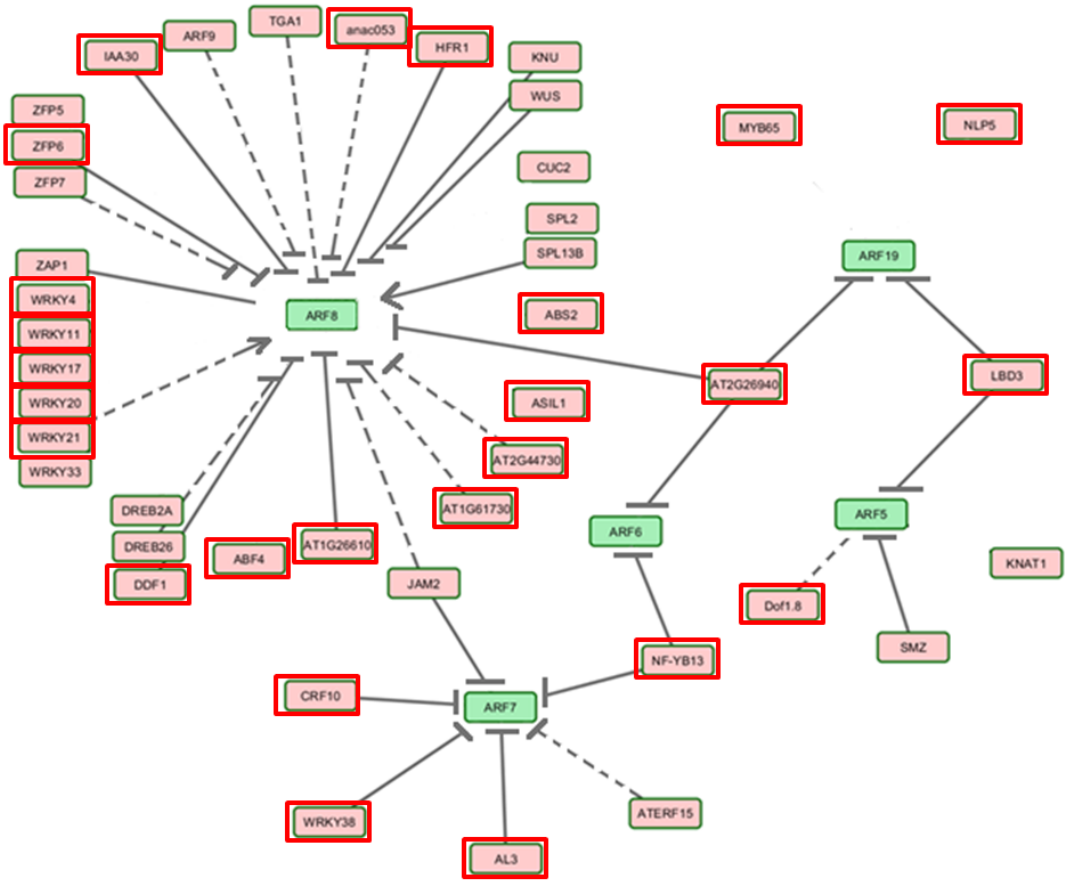

Fig. 2-12. T-DNA insertion mutants of the ARF regulatory transcription factors used in this study (red squares).

Mutants of the regulatory transcription factors indicate co-regulation of multiple ARF activators

The regulation of ARFs by the identified transcription factors might play a role directing the specificity of auxin response in one of the multitude of developmental processes regulated by auxin. A more detailed in-depth analysis is required to narrow down in which processes these interactions could be important. For this purpose T-DNA insertion mutants of 25 regulatory transcription factors were utilized (Fig. 2-12) (Suppl. Table 2-4). I first verified that these mutants are homozygous using PCR. Then I measured the quantity of mRNA compared with the wild-type to determine whether these represented knock-outs. The majority of the mutants are knock-down or knock-out lines (Suppl. Fig. 2-2). However, a small number of the T-DNA insertions (*wrky38*, *abs2* and *at1g26610*) cause overexpression of the mRNA. In this case the T-DNA insertion is predicted to result in a large hybrid mRNA containing a fusion of the gene RNA and the T-DNA sequence which is unlikely to be successfully transcribed into a functional protein. Overall, this collection of mutants represents regulators of all five ARF activators (Fig. 2-12).

A number of experiments can be conducted using this collection of mutant. Mutating the regulatory transcription factors is expected to induce changes in expression of their target ARFs; this could lead to defects in growth and development caused by destabilized levels of auxin signaling. The resulting growth-related phenotypes of the mutants might provide clues to the processes regulated through each particular TF-ARF interaction.

To start with, the expression levels of ARF activators in the mutant background can be quantified using qRT-PCR method. One can measure not only the expression of the ARF activator which is regulated by the particular transcription factor, but also other ARF activators. This would allow detection of co-regulation of multiple ARF activators by a single regulatory transcription factor. Alternatively, if the target ARF regulates expression of other ARF activators, such cross-regulation could also result in changes of expression level in non-target ARFs.

The expression of ARF activators in mutants of the 25 transcription factors was first investigated both in the root and the shoot of 7-days old seedlings. As an example, the *lbd3* mutant contains a T-DNA insertion in the intron region which results in a complete knock-out of the gene expression (Fig. 2-13A and B). In the protoplast

assay LBD3 was shown to be a strong repressor of ARF5 and ARF19 transcription. Indeed, ARF5 expression in upregulated significantly in the shoot but not in the root of the *lbd3* mutant (Fig. 2-13C). Similarly, ARF19 expression is increased in the root but not the shoot of the *lbd3* mutant (Fig. 2-13C). This could indicate that the LBD3-pARF5 interaction is more important in the shoot development whereas the LBD3-pARF19 interaction is more essential for the root development. Additionally, ARF6 is also upregulated in the *lbd3* mutant which could mean that LBD3 directly or indirectly affects expression of other ARFs.

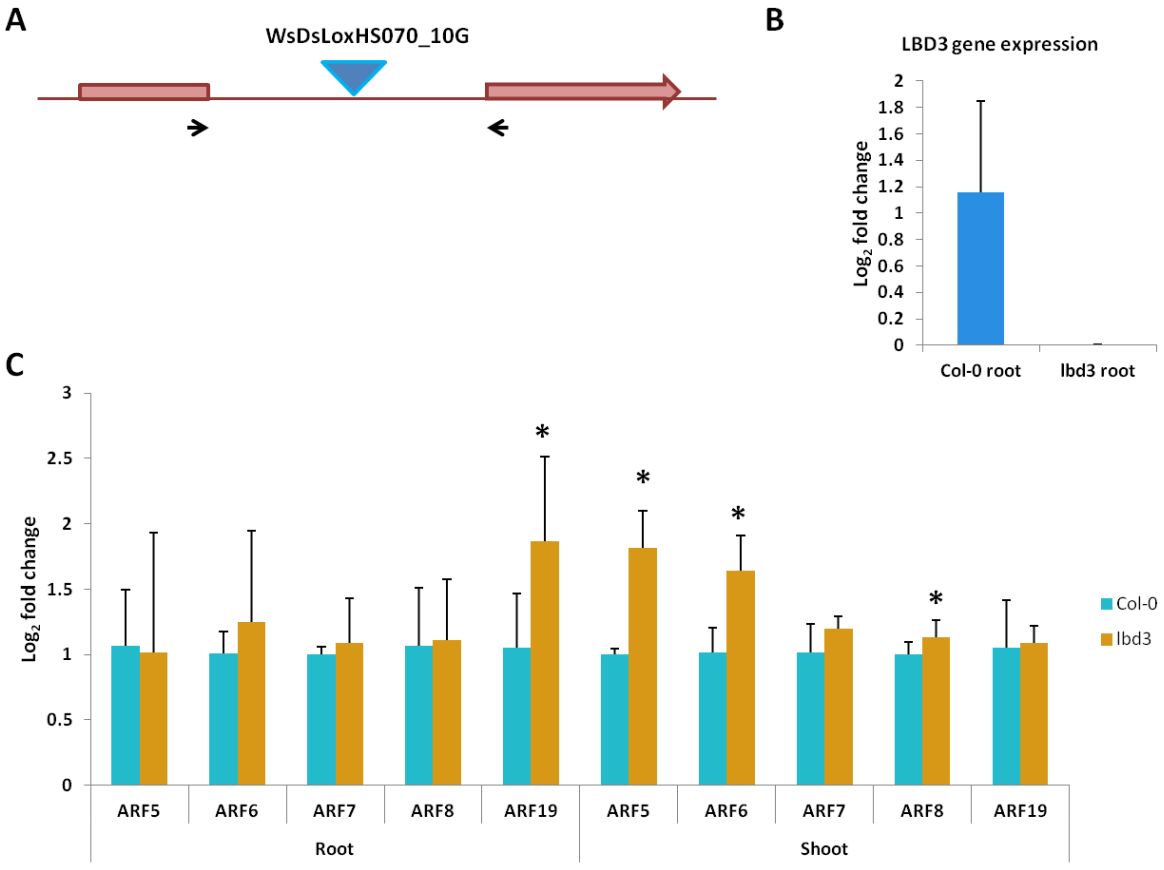

Fig. 2-13. Expression of ARF activators in *lbd3* mutant. **(A)** Schematic representation of the LBD3 locus with T-DNA insertion site marked as a blue triangle. Large boxes indicate exons, lines indicate non-coding sections of the mRNA; black arrows indicate qRT-PCR primer binding sites. **(B)** Expression of LBD3 in the wild-type and the *lbd3* mutant background. **(C)** Expression of ARF activators in the root and the shoot of 7-days old seedlings in the wild-type and *lbd3* mutant plants. Mann-Whitney U test was used to calculate significance with *p < 0.1.

Overall, out of the 25 mutants examined, 10 mutants (40% of the mutants) showed significant changes in the expression of the target ARF activators. In all cases, the changes in the target ARF expression were accompanied by significant changes in expression of at least one or multiple non-target ARF activators. This shows that the changes in expression levels of one ARF activator affects expression levels of other ARF activators hinting at a cross-regulation of ARF expression. This may not be direct as few TFs were shown to bind multiple ARFs but could represent modulation in auxin response feeding back on ARF expression. In the remaining 15 mutants (60% of the mutants) the target ARF expression didn't change significantly but expression of other non-target ARFs was significantly affected. It should be noticed that it is possible these 60% maybe be bona fide interactions, but the interaction only

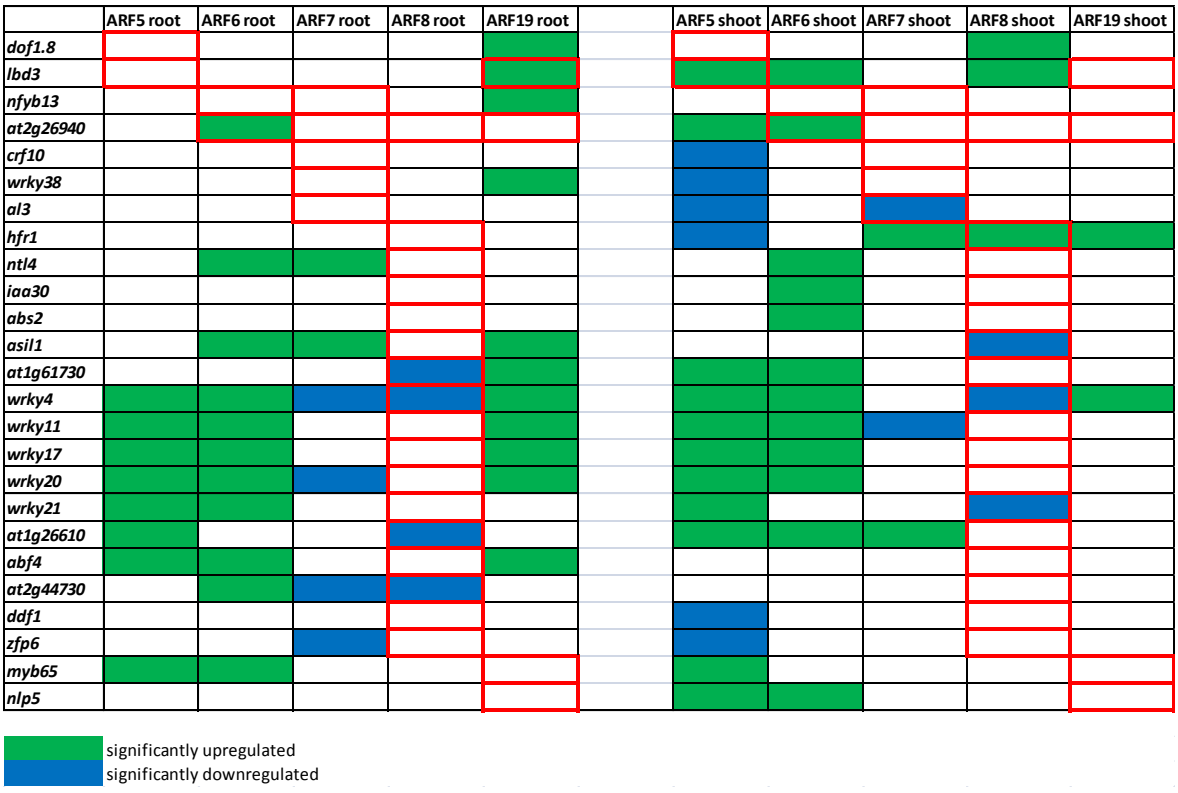

Table. 2-2. Expression of ARF activators in mutants of the regulatory transcription factors. Expression was measured in the roots and the shoots of 7-days seedlings with qRT-PCR. Mann-Whitney U test was used to calculate significance with *p < 0.1. Green boxes indicate statistically significant upregulation, blue boxes indicate statistically significant downregulation of the corresponding ARF in the mutant background compared to wild-type control. The red border indicates the target ARF regulated by the given TF in the Y1H assay.

occurs under specific conditions or in specific tissues. To be successfully detected some interactions might require sampling of more specific tissues, for example only lateral root primordia, instead of whole root and whole shoot tissues examined here. The overall results of this experiment are summarized in Table 2-2. This experiment was done with the help of Stéphanie Lainé, ENS de Lyon.

There are a few common trends which point at co-regulation of multiple ARF activators. In the mutants of several ARF7 transcriptional regulators (*crf10*, *wrky38*, *al7*) the expression of ARF5 in the shoot is downregulated. On the contrary, the expression of ARF5 in the shoot is upregulated in the mutants that target ARF19 in Y1H assay (*myb65*, *nlp5*, *lbd3*).

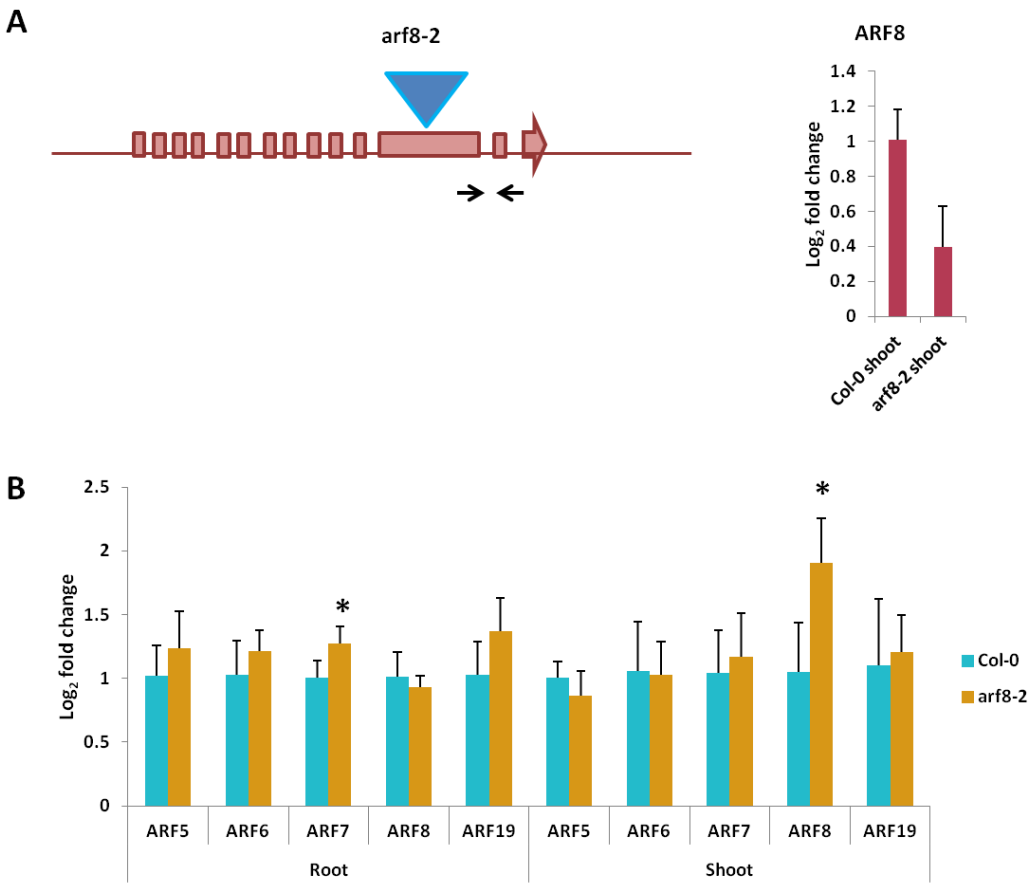

Fig. 2-14. Expression of ARF activators in *arf8-2* mutant. **(A)** Schematic representation of the ARF8 locus with T-DNA insertion site marked as a blue triangle. Large boxes indicate exons, lines indicate non-coding sections of the mRNA; black arrows indicate qRT-PCR primer binding sites. Expression of ARF8 in the wild-type and the *arf8-2* mutant background using primers after T-DNA insertion. **(B)** Expression of ARF activators in the root and the shoot of 7-days old seedlings in the wild-type and *arf8-2* mutant plants. ARF8 primers used here bind to the site before T-DNA insertion. Mann-Whitney U test was used to calculate significance with *p < 0.1.

Interestingly, in mutants of the TFs which target ARF8 in Y1H the expression of ARF8 is either downregulated or, more often, not significantly affected (*wrky4*, *wrky11*, *wrky17*, *wrky20*, *wrky21*, a*t1g26610*, *abf4*) whereas ARF5, 6, and 19 expression is frequently upregulated. One can question why the expression of their target ARF8 is often not significantly affected. This could be explained by the ability of ARF8 to regulate its own expression levels. Indeed, in the *arf8-2* mutant ARF8 expression is upregulated in the shoot indicating that ARF8 is able to negatively regulate its own expression (Fig. 2-14).

To analyze further how mutation of a regulatory transcription factor can affect the expression of its target ARF, several crosses between the full length pARF-mVenus transcriptional reporter lines (described in chapter I) and the TF mutants were generated. A few of these crosses were analyzed in the root. One of the interactions

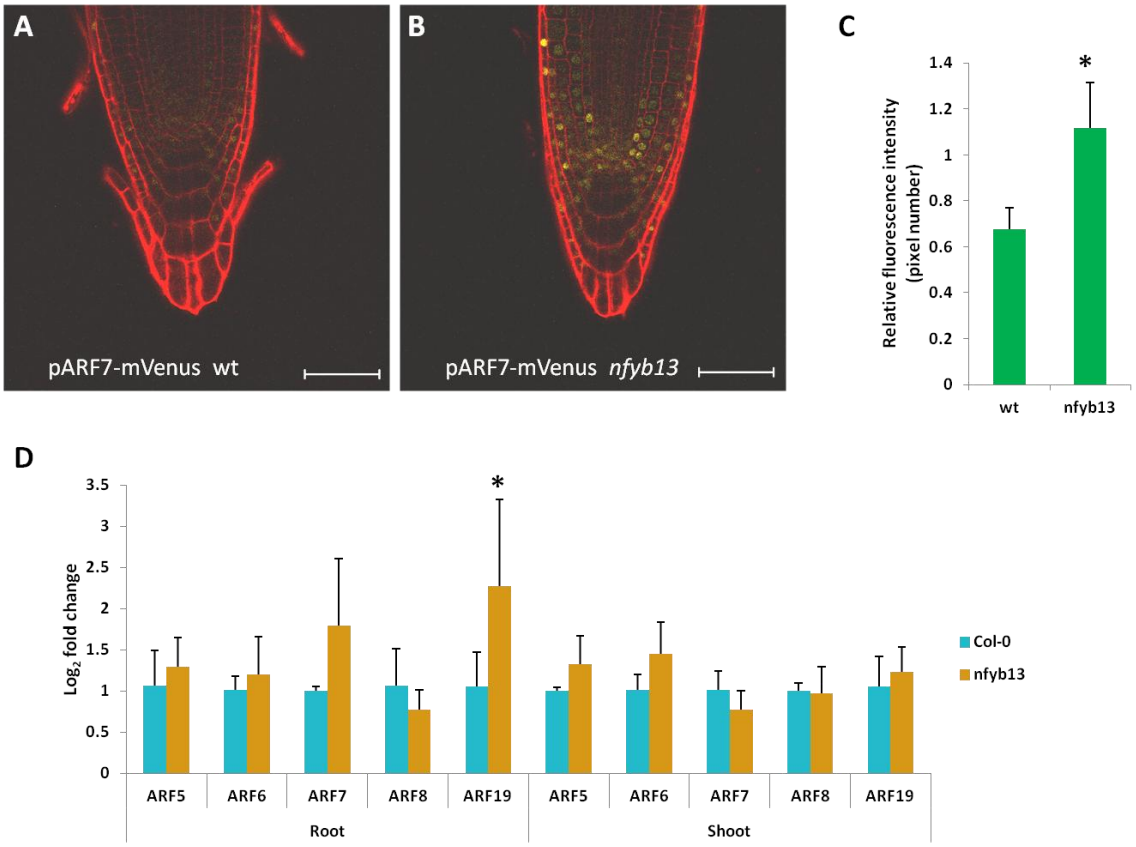

Fig. 2-15. Expression of ARF7 in the roots of wild-type **(A)** and *nfyb13* **(B)** mutant seedlings. mVenus fluorescence was measured in the roots of 6 days old seedlings grown in 16h light/8h dark condition **(C)**. Number of replicates: 23 mutant plants, 25 wild-type plants. An unpaired t-test was used to calculate significance with *p ≤ 0.0001. Bar scale 50 µm. Expression of ARF activators in the *nyyb13* mutant in the root and the shoot tissues of 7-days old seedlings **(D)**.

confirmed in the protoplast assay is repression of ARF6 and ARF7 expression by NFYB13 transcription factor. Indeed, ARF7 expression was significantly increased in the *nfyb13* background compared to the control in the root apical meristem when looking at the crosses between the mutant and the pARF7-mVenus transcriptional reporter (Fig. 2-15 A-C). The analysis of the ARF activator expression with qRT-PCR showed that ARF7 expression is higher in the root of the mutant seedling even through this upregulation was not statistically significant due to large variability between replicates (Fig. 2-15D). The qRT-PCR analysis shows results for the whole root whereas the confocal microscopy on the pARF7-mVenus cross reports upregulation in the root apical meristem. Thus the reporter line analysis can confirm interactions on more tissue-specific level.

Expression of the several transcription factors is regulated by auxin

The transcriptional regulators identified in this study were shown to influence expression levels of multiple ARFs thus partially affecting auxin signaling output. An ability to influence the auxin signaling pathway so strongly means that the expression of the transcriptional regulators themselves are likely to be precisely controlled. One possible mechanism could be direct activation or repression of the transcription factor

	IAA 30 min	IAA 1h	IAA 3h
LBD3			
KNAT1			
AT2G26940			
SPL13b			
TGA1			
IAA30			
WRKY33			
ZFP6			

increased expression
reduced expression

Table. 2-3. Expression of transcription factors after treatment with 1 µM IAA for 30 min, 1h or 3h. Expression values results were obtained from Arabidopsis eFP browser were deposited by Shimada lab (Winter *et al.* 2007, Goda *et al.* 2008). Green boxes indicate significant upregulation, blue boxes indicate significant downregulation of gene expression compared to mock treatment.

by auxin which would provide an efficient feedback control. This possibility was investigated using publically available microarray datasets that provide information on auxin inducibility of genes.

One such dataset was obtained by Shimada lab and published in the *Arabidopsis* eFP Browser (Winter *et al.* 2007, Goda *et al.* 2008). In this dataset 7 days old seedlings were treated with 1 µM IAA for 30 min, 1h and 3h. Rapid change in gene expression in response to auxin can be observed in 3 transcription factors with upregulation after 30 min treatment for WRKY33 and IAA30 and downregulation for ZFP6. In addition to that, 3 more transcription factors were downregulated after 1h treatment: At2g26940, LBD3 and TGA1 whereas SPL13b was upregulated after 1h treatment. Finally, KNAT1 was downregulated after 3h treatment (Table 2-3, Suppl. Fig. 2-3).

Thus overall, 8 transcription factors change expression in response to auxin. The upregulated genes are a mix of the activators (SPL13b) and repressors (IAA30), whereas the downregulated genes appear to be repressors (LBD3, ZFP6, At2g26940, TGA1). From my early protoplast assay it is not clear if KNAT1 and WRKY33 are repressors of activators of ARFs. The identified feedback regulations are represented in Fig. 2-16. For simplicity, in this figure the auxin feedback on the transcription factor expression is represented as coming from the relevant target ARF even though it might be coming from regulation by different ARF activators.

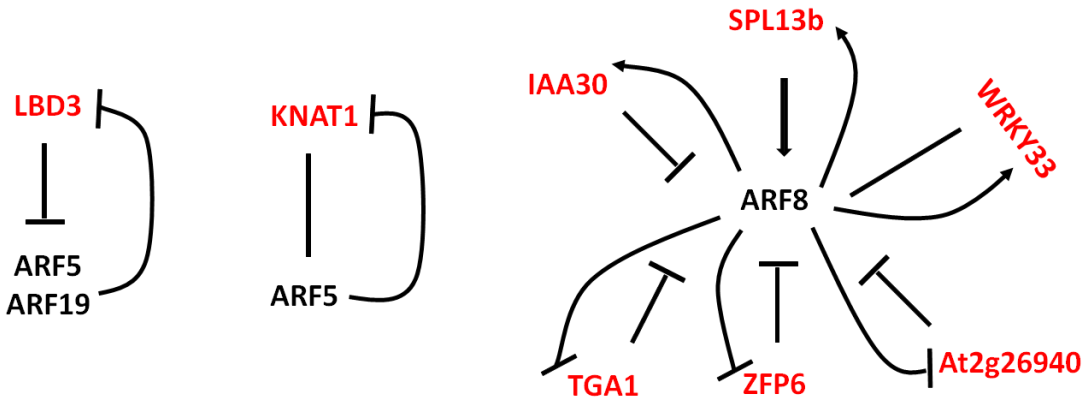

Fig. 2-16. Feedback regulations between the transcription factors and the auxin signaling output.

Mutants of the regulatory transcription factors show auxin-related defects in root and shoot development

The previous results confirmed that the ARF activators often show abnormal expression in the mutants of their transcriptional regulators. This disrupted expression is likely to lead to changes in expression of auxin-inducible genes which are directly regulated by ARF activators and this, in turn, could interfere with normal growth and development. To test this possibility, the mutant plants were analyzed for defects in the root and the shoot development which have been previously shown to be regulated by auxin signaling.

For the shoot phenotype analysis, the plants were grown in short day conditions (8h light/16h dark) for 43 days during which period the number of leaves and the rosette diameter was measured. After 43 days, the plants were transferred to the long-day conditions (16h light/8h dark) to induce bolting and after 3 and 4 weeks of further growth the following parameters were measured: the length of the main stem, number of cauline branches (growing from the main stem) and number of axillary branches (growing from the rosette).

Overall, 64% of the mutants (16 out of 25 mutants) showed defects in shoot development whereas 36% of the mutants were unaffected (9 out of 25 mutants).

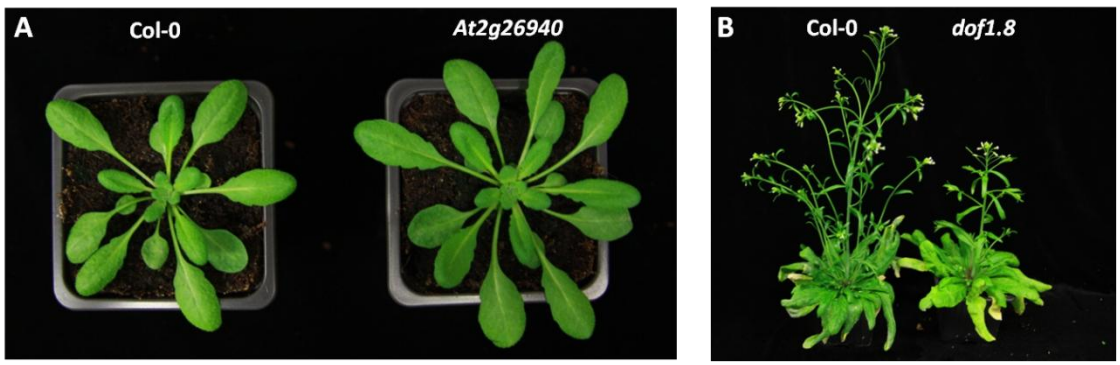

Fig. 2-17. Examples of shoot growth phenotypes in the mutants of regulatory transcription factors. *At2g26940* mutant has bigger rosette diameter and increased number of leaves **(A)**. *dof1.8* mutant has reduced main shoot length, reduced number of axillary branches **(B)**.

The results are summarized in Table 2-4. Several of the mutants have increased number of leaves and increased rosette size during the vegetative phase; these include mostly the regulators of ARF8 *wrky4*, *wrky11*, *wrky17*, *wrky20*, *abf4*, *zfp6*, the regulator of ARF19 *nlp5* and the regulators of multiple ARFs *nfyb13* and *at2g26940* (Fig. 2-17A, Table 2-4). On the contrary, only two mutants have reduced number of leaves during the vegetative phase including *crf10* (regulator of ARF7) and *dof1.8* (regulator of ARF5). Thus the majority of the mutants show faster development during the vegetative phase.

dof1.8 mutant is additionally affected in shoot development in reproductive phase with reduced shoot length and reduced number of axillary branches (Fig. 2-17, Table 2-4). Two other mutants, *al3* (regulator of ARF7) and *asil1* (regulator of ARF8), also have reduced shoot length in the reproductive phase indicating stunted development.

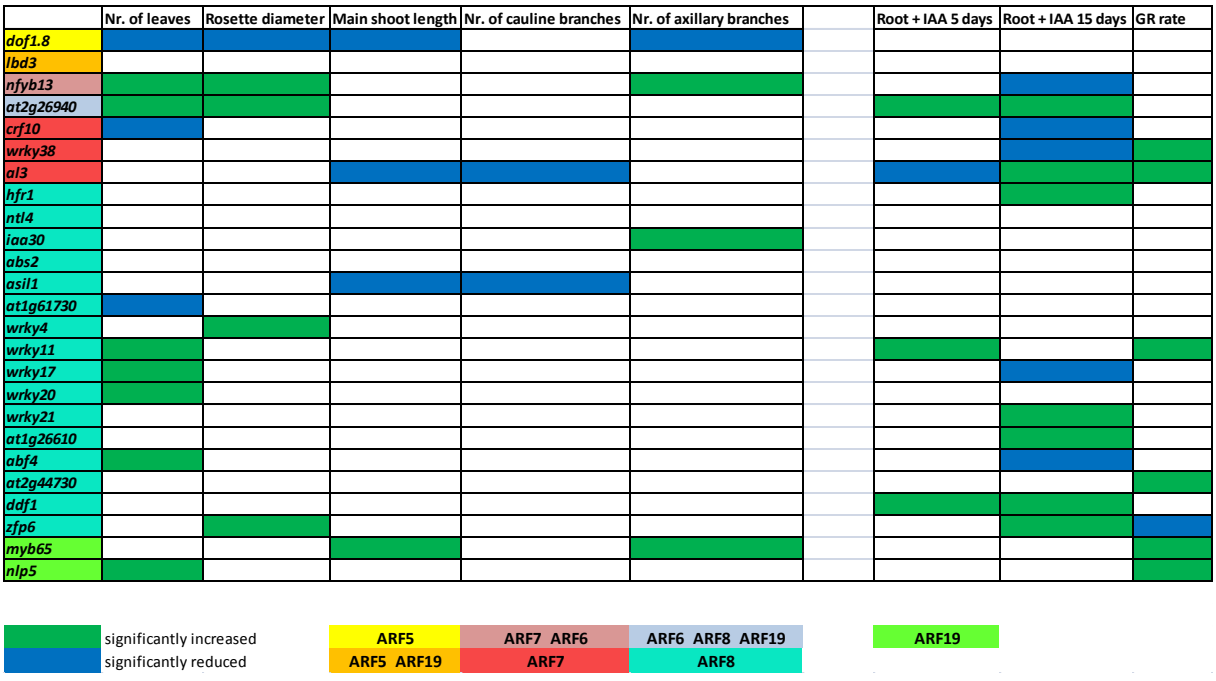

Table. 2-4. Phenotypic analysis of the shoot and the root growth defects in 25 mutants of the regulatory transcription factors. For the shoot phenotype, the number of leaves, rosette diameter, main shoot length, number of cauline branches and number of axillary branches was measured. For the root analysis, the main root length was measured when grown on media with IAA. Green boxes indicate statistically significant increase, blue boxes indicate statistically significant reduction compared to the wild-type. Colored boxes around mutant's names indicate which ARFs these TFs regulate in the Y1H assay. GR rate = rate of gravitropic response. For the shoot phenotype, unpaired t-test test was used to calculate significance with *p ≤ 0.05. For the root phenotype, one-way analysis of variance (ANOVA) test was used to calculate significance with *p ≤ 0.05.

Myb65, iaa30 and *nfyb13* mutants have increased number of axillary shoots which might indicate a reduced apical dominance (Table 2-4).

Auxin transport or signaling perturbations in *pin1* and *arf5* mutants lead to production of defective “pin”-like inflorescences (Galweiler *et al.* 1998, Przemeck *et al.* 1996). The growth of the “pin”-like inflorescences can be induced even in the wild-type plants if they grow on the medium containing the auxin transport inhibitor NPA (Reinhardt *et al.* 2000). One can speculate that this growth reaction to NPA can be altered in the mutants of the regulatory transcription factors which control expression of ARF5 (Przemeck *et al.* 1996). For these reason, the two mutants, *lbd3* and *dof1.8*, were grown on medium supplemented with NPA for 25 days until they produced inflorescences. Each plant produced a defective inflorescence but the severity of the phenotype could vary. The strongest phenotype was a single pin inflorescence lacking any organs, followed by a pin with 1-3 poorly developed flowers and, rarely, relatively normal shoot lacking pin (Fig. 2-18). The percentage of plants with these phenotypes was counted in the mutants and the wild-type plants. Neither mutant showed any difference compared to the wild-type (Fig. 2-18) indicating that both mutants are unable to overcome this NPA-induced defect in shoot development.

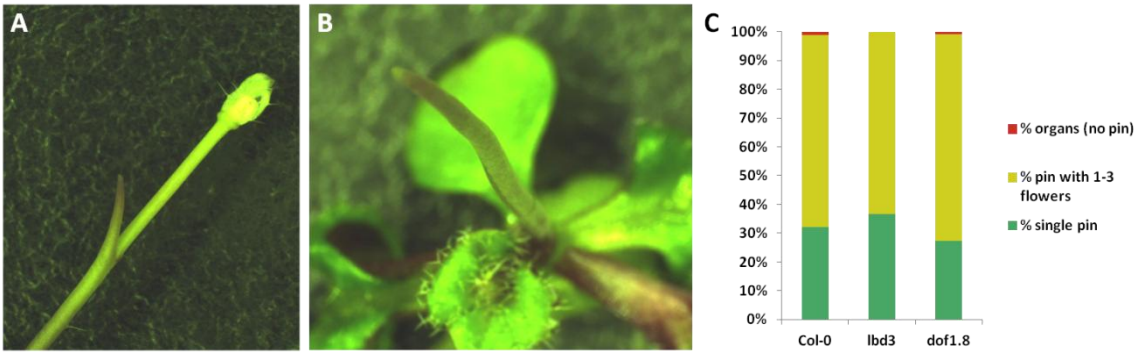

Fig. 2-18. Plants grown on NPA supplemented medium develop pin-line inflorescences with a few underdeveloped flowers **(A)** or as a single pin without any organs **(B)**. Percentage of plants with inflorescences containing a single pin without any organs (green), pin with a few underdeveloped organs (yellow) or organs without pin (red) in the wild-type Col-0 and mutant *lbd3* and *dof1.8* plants. The result is representative from three independent experiments (n > 70 plants per genotype).

The root phenotype analysis was done by Jingyi Han using a robot (University of Nottingham, Anthony Bishopp's group). She measured the length of the main root when grown on medium with or without IAA. Results for the root growth on medium without IAA are not completed by the time of writing this thesis. Results for the root growth on medium with IAA indicate that 13 out of 25 mutants are significantly affected (Table 2-4, Suppl. Fig. 2-4). The root growth is increased in the presence of auxin in 7 mutants and reduced in 5 mutants compared to the wild-type. The *al3* mutant shows reduced growth at 5 days but increased growth at 15 days.

In addition, Jingyi Han measured auxin-dependant gravitropic response in the roots of the mutants. In this assay, the 5 days old seedlings were turned at a 90° angle to induce downwards growth of the root and the root growth kinetics were analyzed every hour for the subsequent 12h. Among the mutants, *wrky38* and *nlp5* showed faster gravitropic response at most of the time points measured whereas *zfp6* showed slower gravitropic response (Table 2-4, Suppl. Fig. 2-5). *Myb65*, *wrky11*, *at2g44730* and *al3* have significantly faster gravitropic response at the later time points (Suppl. Fig. 2-5). Interestingly, WRKY38 and AL3 regulate expression of ARF7 whereas NLP5 and MYB65 regulate expression of ARF19 in my yeast one-hybrid screen. Both ARF7 and ARF19 were shown to be the main ARFs involved in root gravitropic response (Li *et al.* 2006a, Okushima *et al.* 2005).

Taking the shoot and the root phenotyping data together, 22 out of 25 mutants have significant deviation in growth (Table 2-4). Only *lbd3, ntl4* and *abs2* showed normal root and shoot growth in all experiments. Interestingly, 8 mutants have growth phenotypes in both the root and the shoot whereas the other 14 mutants are affected only in either root or the shoot development. In summary, the mutant phenotyping experiments showed that mutation of ARF transcriptional regulators can substantially affect development leading to growth defects.

Discussion

In this chapter I identified transcriptional regulators that control expression of ARF activators in *Arabidopsis thaliana*. The protoplast assay, DAP-seq screen and the analysis of the molecular and physiological mutant phenotypes confirmed that the majority of the interactions are functional *in planta* and that the majority of the TFs are repressors of ARFs. DAP-seq and the literature review allowed me to identify promoter binding sites for several interactions. The differential expression of ARFs and the mutant phenotypes illustrate that these interactions might be important for the auxin signaling output and are involved in regulation of plant development.

Does the yeast one-hybrid gene regulatory network reflect *in planta* gene interactions?

Nevertheless, there are a few questions which arise from the yeast one-hybrid screen. One question would be, how representative are the interactions obtained from Y1H assay? Does the screen succeeded in capturing all potential interactions? Are some of the identified interactions false positive?

It is obvious that not all interactions can be detected even using high-throughput screen as the one used in this thesis. The first limitation is the size of the prey collection: only about half of the predicted transcription factors are present which means that there is a possibility to detect only half of the potential interactions. Another reason lies within the chosen system: using yeast as a heterologous organism might perturb some of the interactions leading to false negative results. One can imagine that if a particular interaction needs a plant-specific co-repressor or a co-activator not present in the yeast, such an interaction will not work in the assay. One can conclude that the present network represents a smaller part of the complex gene network in *Arabidopsis thaliana*. This network would therefore be a result of a random sampling of a larger and more complex pool.

Additionally, other biases could have been introduced by the chosen method and could have influenced the outcome of the assay. Besides the reduced TF pool size and potential inability to detect some interactions in yeast, the importance of choosing sufficient promoter construct must be evaluated. Did the chosen promoter fragments allowed to catch all potential interactions? In the literature it was shown that 86% of the transcription factor binding sites in *Arabidopsis thaliana* are localized

between -1000 bp and +200 bp with a peak at 50 bp upstream of the transcription start site (Yu *et al.* 2016). They demonstrate that the probability of having a transcription factor binding site upstream of -2000 bp is only 0.0004 (Yu *et al.* 2016). Indeed, in the yeast one-hybrid screen, longer promoters of ARF5, 8 and 19 were assayed in two separate fragments which together spanned approximately 5,5 kb sequence (Fig. 2-3). Interestingly, all detected interactions with one exception were detected in the 3 kb fragment closest to the transcription start site. This means that in general, using approximately 3 kb upstream region would be sufficient to catch all the potential interactions. Including downstream regions in the bait fragment appears to be important as well. Among the interesting results, NFYB13 was shown to bind promoter of ARF6 in the downstream region because this transcription factor was unable to interact with the promoter construct lacking downstream regions (Fig. 2-8). Indeed, the importance of introns in transcriptional regulation has been discussed in Chapter I. But should the yeast one-hybrid construct have included more downstream regions such as the 3-prime and the terminator regions? To answer this question, downstream regions of ARF promoters need to be screened in the yeast one-hybrid assay for comparison. Such an experiment would also shed light on the importance of 3-prime and terminator regions for the transcriptional regulation of ARFs. However, as the transcriptional reporter lines constructed in this study also lacked 3-prime and terminator regions, the promoters screened in the yeast on-hybrid assay should be sufficient to identify the transcription factors that can produce patterns of gene expression observed in the transcriptional reporter lines. As discussed in chapter I, my transcriptional reporter lines were in most cases able to recapitulate the correct *in planta* ARF expression patterns and this increased my confidence that the Y1H promoters contain regulatory binding sites for the majority of important regulators.

Another bias might come from the nature of the prey collection. The original transcription factors in the collection were mostly selected based on their expression in the root stele (Brady *et al.* 2011). Many of the root stele TFs are also expressed in other tissues and might play a role in development of other organs. In addition, multiple shoot-specific transcription factors were added to the collection. Nevertheless, the resulting gene regulatory network might be biased to more accurately represent regulations specific for the root tissues and even for the root vascular tissue. This conclusion is not supported by my data because 64% of the mutants of regulatory transcription factors (16 out of 25) were shown to have defects

in shoot development indicating that both root and shoot regulators were identified in my screen.

ARF activator expression is predominantly regulated by transcriptional repressors

Auxin controls growth either during development or in response to environmental stimuli. In order for the correct auxin response to be established, whole tissues have to be reprogrammed in a relatively rapid manner. For example, the root architecture can adapt relatively fast to phosphorus availability by arresting primary root growth and initiating lateral root development (Niu *et al.* 2013, Svistoonoff *et al.* 2007). Such a fast response would require extensive alterations in gene expression at the cellular and tissue levels. Recent studies indicate that the tissue-specific reprogramming is co-regulated by a core set of transcription factors acting together as a module (D'Alessio *et al.* 2015, Germanguz *et al.* 2016, Rackham *et al.* 2016). Indeed, it was shown that an induction of a few specific transcription factors can lead to complete reprogramming of already differentiated cells into a different type of cells (Takahashi and Yamanaka 2006, Vierbuchen *et al.* 2010). A question arises if in plants ARF activators constitute these core transcription factors which could reprogram cell- and tissue fates in response to auxin. The key roles contributed to the individual ARFs in plant development speak in favor of this (Berleth and Jurgens 1993, Nagpal *et al.* 2005, Okushima *et al.* 2005). Each ARF activator controls auxin-induced responses which appear to be specific for the particular ARF.

One of the reasons that each ARF is able to induce individual specific responses is the fact that ARFs are not found ubiquitously in the plant; instead they are expressed in specific tissues as shown in Chapter I. These expression patterns are likely to be produced due to transcriptional regulators that bind regulatory regions within ARF gene locus and switch on expression of ARFs only in specific tissues or under specific conditions. In this chapter, the transcription factors which regulate expression of ARF activators were identified. Most strikingly, the subsequent experiments led to discovery that the ARF activators are mostly regulated by transcriptional repressors *in planta*. Why is this need to repress expression of ARF activators by a large number of different regulators? Generally, auxin induces changes in plant growth and development. Some of these changes could be irreversible such as an initiation of organ development. The initiation and growth of a new organ must cost the plant a

large amount of resources and therefore, it should only be done when necessary. In addition, the timing of organ initiation is tightly regulated both in the root and the shoot. An untimely auxin response could cause co-initiation of multiple organs and result in developmental perturbations. Thus it is highly important to have timely and regulated developmental events which would require a precise control of auxin signaling. One can imagine a system in which ARF activators are expressed from a strong promoter that guarantees swift production of ARFs and fast auxin response. On the other hand, this system would be kept in an OFF state by transcriptional repressors; such repression could be then removed when needed to render the system in the ON state. A large number of repressors might be required so that removing one repressor will switch on the auxin signaling only in very specific tissue. The gene regulation by repression could be a sophisticated regulatory mechanism to enable swift auxin response limited to a specific time frame and a specific location.

Repression of gene expression is a mechanism utilized frequently in developmental context. This mechanism limits expression of key regulatory proteins to specific tissues or specific time point and prevents inappropriate responses. For example, the transcription factor AGAMOUS is an important regulator of flower development in *A. thaliana*; its expression is regulated by the repressor complex consisting of two proteins, LUG and SEU, and this prevents ectopic and untimely expression of AG (Franks *et al.* 2002, Liu and Meyerowitz 1995, Sridhar *et al.* 2004). A few small gene regulatory networks that include gene repression have been described before. As such, the specification of cortical neurons in mammals during embryonic development is established by a gene network based on gene repression and derepression interactions (Srinivasan *et al.* 2012). In *Drosophila melanogaster* the key transcription factor Bicoid establishes the body plant along the anterior posterior axis during embryonic development by activating expression of different target genes and this leads to positioning of boundaries between individual body segments. However, the Bicoid-dependant activation is limited by a set of repressors that suppress expression of the Bicoid-target genes and this repression sets correctly the body structure of the embryo (Chen *et al.* 2012). It appears that gene repression can play an important role in developmental processes both in plants and in animals.

Regulation of ARF8 by multiple transcription factors might indicate its special significance in auxin signaling

In the yeast one-hybrid screen ARF8 had significantly more interactions than other ARFs (31 interactions for ARF8 compared to 2-6 interactions for other ARFs). The average number of transcriptional regulators identified in Y1H assay using S. Brady protocol is 3.36 transcription factors pro promoter (Gaudinier *et al.* 2011). A completely different study came to a surprisingly similar result: the amount of transcription factor binding sites was calculated as 5.4 on average per gene in *Arabidopsis thaliana* (Yu *et al.* 2016). S. Brady reports a few promoters that had a large amount of interactions in yeast on-hybrid assay such as PHB promoter with 30 TFs and REV promoter with 37 TFs. They found a significant correlation between the genes regulated by a large number of TFs and their developmental importance (Brady *et al.* 2011, Gaudinier *et al.* 2011). This developmental importance was calculated as a positive correlation between having a morphological root phenotype and a number of TF regulators identified (Brady *et al.* 2011). This leads to speculation that ARF8 must have an important function in development. Nevertheless, other ARF activators such as ARF5 control key developmental processes and their significance in plant development is undisputed. But then why ARF8 is different from other ARF activators in the number of transcriptional regulators? Could it be an artifact of using heterologous organism, the yeast? The fact that many of the ARF8 regulations identified in the yeast one-hybrid were confirmed *in planta* indicates that the interactions are not artifacts. It appears that the majority of the interactions are in fact biologically significant interactions. Another possible artifact could be caused by random insertion of the promoter in the yeast genome which is the case for T-DNA insertions during plant transformation; the function of T-DNA might be affected by the surrounding endogenous DNA sequences. The yeast one-hybrid experimental design is based on the bait construct being integrated into the yeast genome by site-specific homologous recombination. The insertion site is therefore identical for all promoters and the positioning of the bait construct in the genome could not explain differences in the screen efficiency. Then could an intrinsic property of ARF8 promoter sequence allow more efficient interactions in yeast whereas promoters of other ARFs somehow prevent many interactions from working in yeast? The promoter of ARF6 screened in yeast one-hybrid has 38,4% similarity in sequence to promoter ARF8 (aligned using EMBOSS

Needle pairwise sequence alignment tool). Similarly, alignment of ARF7 and ARF19 promoters used in yeast one-hybrid assay yielded 37,4% similarity. On the other hand, aligning promoters of non-homologous genes ARF5 and ARF8 shows that there is 43,2% similarity. Therefore the individual differences between promoter sequences are equally significant between homologous and non-homologous genes. It remains unclear if individual sequence specificity of ARF promoters can affect transcription of LacZ and HIS reporter genes in yeast and lead to biased results in the number of regulators identified. In conclusion, it is more probably that the number of interactions reflects different regulation *in planta*.

The number of interactions identified in ARF8 could be justified by the need for multiple regulators *in planta.* In fact, the expression of ARF8 in the root and the shoot is the most restricted of all ARFs; it is found only in the L1 layer of the SAM and the epidermis layer of the RAM (Fig. 1-1 and Fig. 1-7). For example, ARF8 expression is completely absent from the root above the elongation zone (Fig. 1-5) whereas other ARFs are expressed at least to some extend in the older root tissues. The protoplast assay also showed that ARF8, unlike other ARF activators, is not expressed in the leaf tissue. Such a restricted expression pattern could indeed require a combined action of multiple transcriptional repressors.

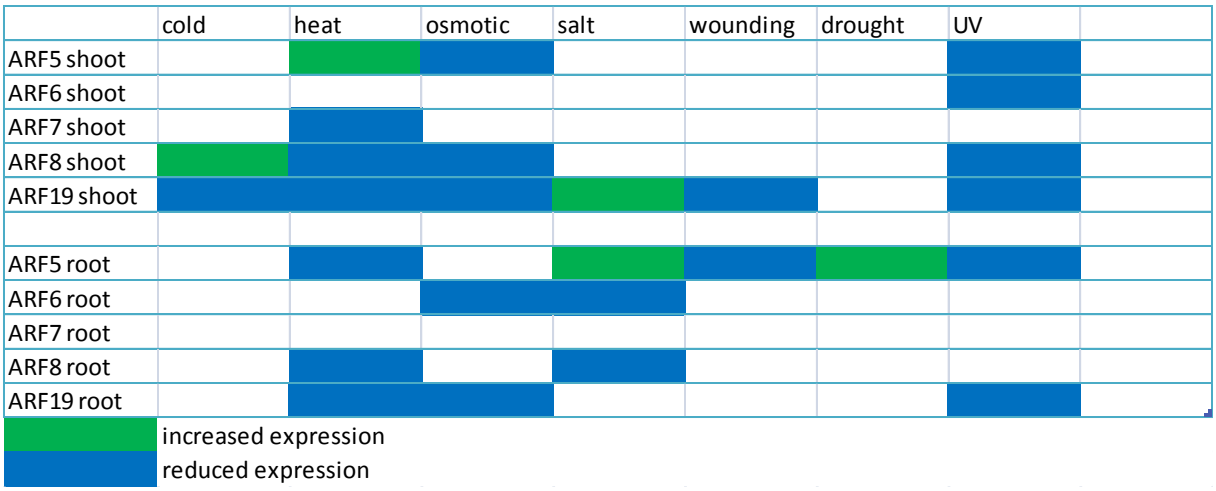

Table 2-5. Expression of ARF activators in the root and the shoot after abiotic stimuli. 18 days old Col-0 plants were treated with various abiotic stresses (cold, heat, osmotic, salt, wounding, drought and UV). Increased (green box) or reduced (blue box) expression at least higher than 1.5 fold in the period up to 3h after treatment are considered relevant (Kilian *et al.* 2007).

As described previously, multiple ARF8 regulators are involved in responses to the environment including biotic and abiotic stress. Strikingly, ARF8 expression in the RAM and the SAM is limited to the surface epidermal layer which mediates communication between the plant's inner tissues and the environment. Could ARF8 function as a hub that conveys environmental information and integrates it into auxin signaling output? To investigate this hypothesis, publically available microarray datasets can be used to evaluate response of ARFs to abiotic stresses. In fact, looking at the expression changes of ARFs after various abiotic stresses (cold, drought, heat, wounding, osmotic, UV and salt stresses) (Kilian *et al.* 2007) (Table 2-5) it appears that ARF19 and ARF5 react more broadly to different abiotic stressed than ARF8, even through ARF8 shows responses to broader range of abiotic stresses than ARF7 and ARF6. In accordance with this data, the specific role of ARF8 in abiotic stress response is not particularly evident. Nevertheless, perhaps ARF8 has a different role in the response to environmental stimuli than ARF5 or ARF19; ARF8 could detect changes in the epidermis and then propagate the signal in the other tissues acting as a mediator whereas ARF5 and ARF19 could follow up and switch on the auxin response.

In this study ARF8 is also shown to be able to negatively autoregulate its own expression (Fig. 2-14). Indeed, negative autoregulation is a mechanism which allows a rapid decrease in production of the protein when the protein levels reach a particular threshold (Fig. 2-2B, I). This mechanism is often associated with strong promoters (Alon 2007, Camas *et al.* 2006, Rosenfeld *et al.* 2002). Thus such mechanism could allow for a rapid response due to the strong promoter and rapid attenuation of this response in dependence on the protein concentration. In addition, negative autoregulation reduces variations in protein concentrations: by high protein concentrations ARF8 would reduce protein production by repressing its own expression whereas at low protein concentrations the protein production rate will be increased (Becskei and Serrano 2000). The need for a rapid response is consistent with the putative role of ARF8 as a mediator of environmental responses because the ever-changing environmental conditions might require rapid growth and developmental adaptations. In this case, ARF8 must remain at constant low expression levels under normal conditions so that the rapid and strong increase in its

protein would work as a sensor switch. In addition, such an environmental sensor must be returned to low protein levels just as rapidly to be ready for the next stimulus. Interestingly, the expression levels of ARF8 in the mutants of its regulatory TFs are in most of the cases either normal or reduced compared to wild-type (Table 2-2). This is an unexpected result because an upregulation of ARF8 would be more logical particularly because most of these TFs are repressors of ARFs. Could it be that due to negative autoregulation ARF8 normalizes or even reduces its own expression? Does this mean that high levels of ARF8 are disadvantageous and damaging for the plant? The results of this study suggest that keeping ARF8 at constant low protein levels is necessary for the plant to respond effectively to the environment. Further experiments are required to shed more light on this regulation. These experiments could include, for example, misexpression of ARF8 in specific tissues using an inducible system; contrary to the described constitutive overexpression of ARF8 (Tian *et al.* 2004) an inducible system would allow to overcome the decrease in ARF8 expression caused by the negative autoregulation.

Gene regulatory network motifs describe regulations that could be important during development

The gene regulatory network identified in this study contains not only simple regulations between the transcription factor and its target promoter but also more complicated motifs. The negative autoregulation was identified for ARF8 as discussed before; in addition, studying expression of the relative regulatory transcription factor in the mutant background of this TF with primers binding before the insertion site provided evidence for additional autoregulatory loops (Suppl. Fig. 2-2). In addition, several double-negative and double-positive feedback loops were identified based on the auxin signaling output controlling expression of the TFs (Fig. 2-16). The complex set of regulations identified in this study is illustrated in Fig. 2-19.

Fig. 2-19. Gene regulatory network controlling expression of ARF activators in *Arabidopsis thaliana.* Small red arrow under the TF name plate indicates gene expression activation of the target ARFs by the relative TF, small red perpendicular line indicates gene repression of the target ARFs by the TF.

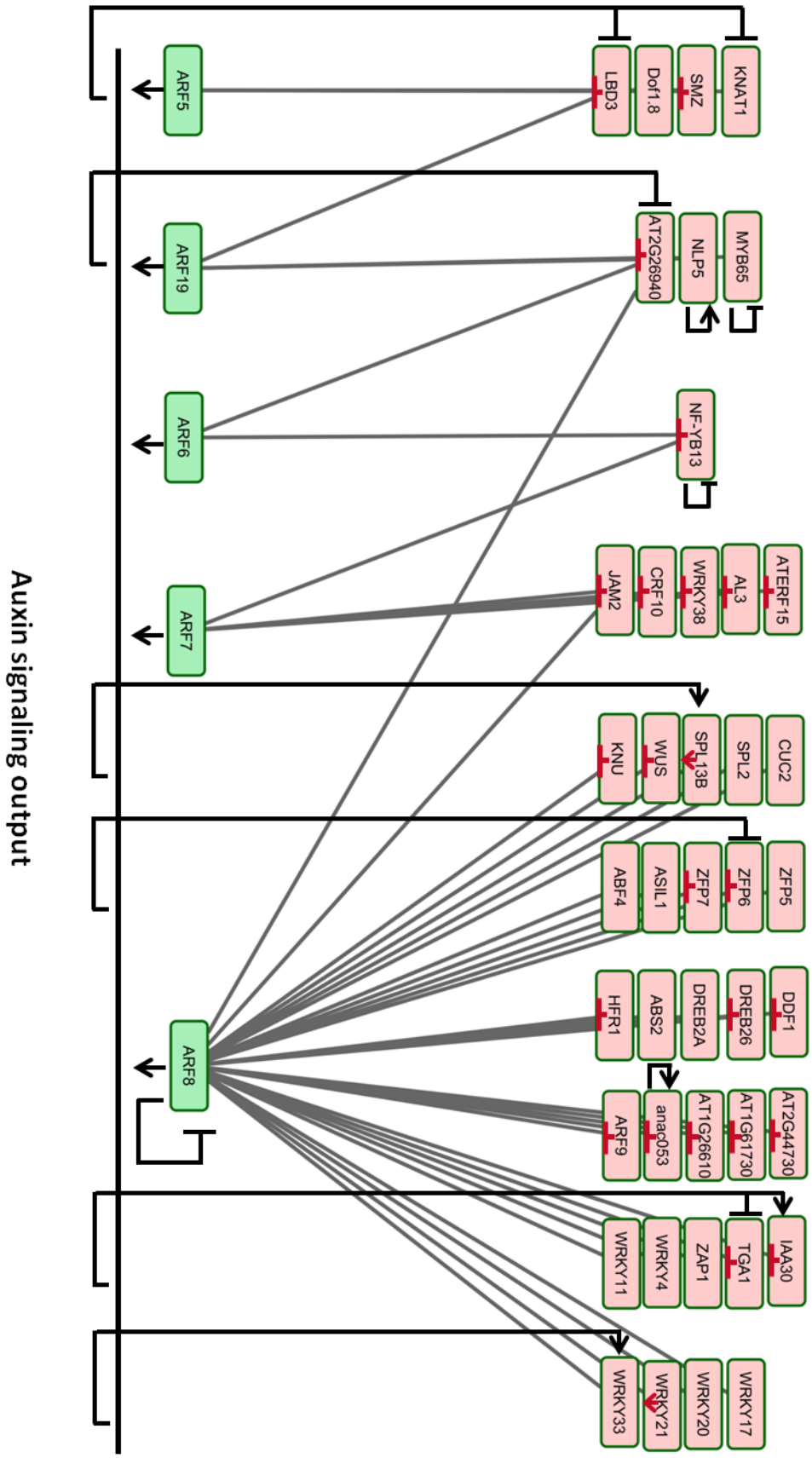
Auxin signaling output
ARF5
ARF19
ARF6
ARF7
ARF8
LBD3
Dof1.8
SMZ
KNAT1
AT2G26940
NLP5
MYB65
NF-YB13
JAM2
CRF10
WRKY38
AL3
ATERF15
KNU
WUS
SPL13B
SPL2
CUC2
ABF4
ASIL1
ZFP7
ZFP6
ZFP5
HFR1
ABS2
DREB2A
DREB26
DDF1
ARF9
anac053
AT1G26610
AT1G61730
AT2G44730
WRKY11
WRKY4
ZAP1
TGA1
IAA30
WRKY33
WRKY21
WRKY20
WRKY17

The genes LBD3, ZFP6, At2g26940 and TGA1 identified as repressors of ARFs are negatively regulated by auxin. This means that ARFs mediate auxin response by directly or indirectly repressing expression of their own repressors. Such system is an example of a double-negative feedback loop which consists of two mutually repressing components. In addition to transcriptional gene regulatory networks, such loops were identified between miRNA and its target TFs and in post-transcriptional interactions such as phosphorylation (Cai *et al.* 2013, Johnston *et al.* 2005, Xiong and Ferrell 2003). This type of loop is usually associated with developmental networks and it is used to initiate irreversible cell fate decisions (Alon 2007). Cell fate decisions separated by a double-negative feedback loop have been described before. For example, such loops are responsible for the transition from epithelial to mesenchymal cell types during cancer formation (Diepenbruck *et al.* 2017, Siemens *et al.* 2011, Yang *et al.* 2013).

Interestingly, double-negative feedback regulation between LBD3 and its target ARF5 could be responsible for the pattern formation in the root vasculature. This hypothesis is based on the mutually exclusive expression patterns in the root stele: LBD3 is expressed in the procambium domain (Fig. 2-10) whereas ARF5 is confined

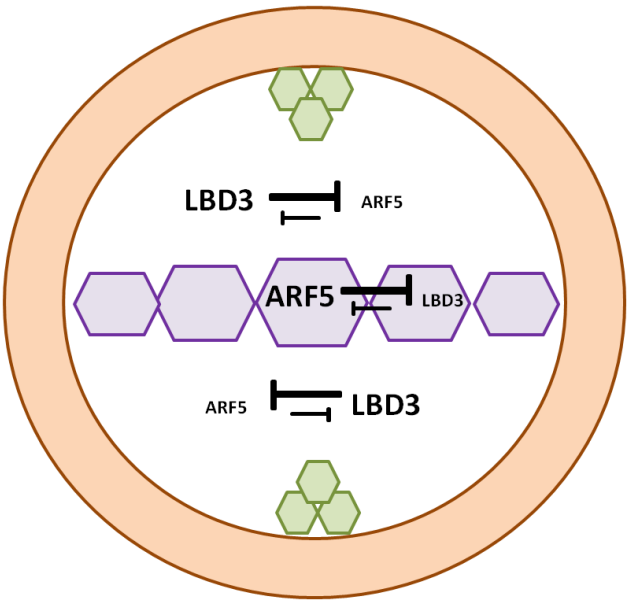

Fig. 2-20. Schematic of double-negative feedback loop between LBD3 and ARF5 and their possible interaction in root stele. Violet cells are xylem, green cells are phloem, brown circle represent pericycle.

predominantly to the xylem starting from the upper meristematic zone (Fig. 2-10, Fig. 1-2). Similarly, the other target of LBD3, ARF19, is expressed in protoxylem only in the meristematic zone (Fig. 1-6). Could it be that LBD3 restricts ARF5 and ARF19 expression in procambium through direct repression and, at the same time, ARF5 and ARF19 repress expression of LBD3 in the xylem (Fig. 2-20)? If this is the case, the double-negative feedback loop would create two zones of separate cell fates: xylem and procambium. It seems that this feedback loop might be driving pattern formation in the root vasculature. Nevertheless, so far no root-related phenotype was detected for the *lbd3* mutant (Table 2-4); further examinations are required to detect any alternations in vasculature development in this mutant.

On the other hand, the ARF activator SPL13b is positively regulated by auxin and provides an example of a double-positive feedback loop. This element is also specific for developmental gene networks and functions to amplify an initial transient activating signal (Alon 2007). In this loop, a signal would initiate a permanent activation loop where two genes would simultaneously activate each other expression. SPL13 controls the switch in leaf development from cotyledons to vegetative leaves (Martin *et al.* 2010). SPL13 is also expressed in developing anthers and could therefore be involved in flower development (Xing *et al.* 2010). The role of ARF8, the target of SPL13, in flower development is well-described (Nagpal *et al.* 2006). It is feasible that the positive interaction between these genes could regulate a

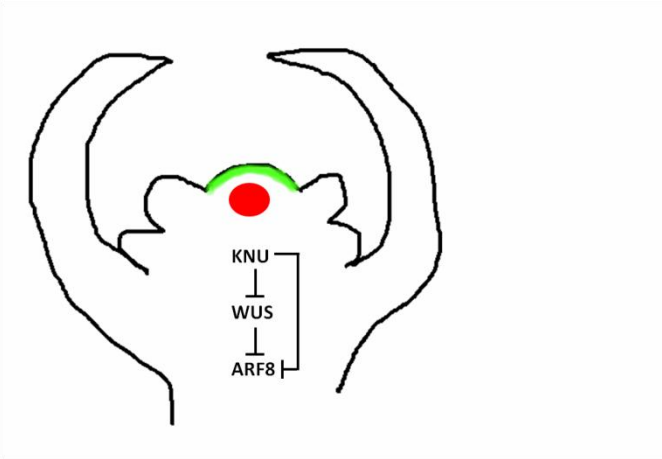

Fig. 2-21. Schematic of the feed-forward loop between WUS, KNU and ARF8 during flower development. Expression domain of ARF8 is marked in green, expression domains of WUS and KNU overlap and are marked in red.

developmental switch during flower maturation. Because I didn't have the *spl13* mutant during my thesis, I could not examine it to see any phenotypes that would confirm this hypothesis.

Two other regulations identified in this study are the repression of ARF8 by WUS and KNU. Interestingly, KNU was shown to repress expression of WUS at the later stages of flower development and this leads to termination of the stem cell niche in the flower (Sun *et al.* 2009). In my thesis these repressive interactions between KNU, WUS and ARF8 produce a feed-forward loop motif (Fig. 2-21). KNU and WUS are both expressed in the organizing center (Payne *et al.* 2004, Sun *et al.* 2009) whereas ARF8 is expressed in L1 layer of the dome structure (Fig. 1-7). Thus one can imagine that ARF8 expression is excluded from the organizing center by the action of WUS in the younger flower primordia and later by KNU in the developing flowers (Fig. 2-21).

Expression of ARF activators is co-regulated *in planta*

Studying changes in expression levels of ARF activators in the mutants of the regulatory transcription factors provided additional level of confirmation for the interactions and allowed to speculate in which tissue (root or shoot) the interaction could have a biologically important role. Surprisingly, in most cases the levels of ARFs other than those identified as targets in Y1H assay were also affected and often, ARFs appear to be co-regulated in modules. Indeed, ARF5, 6 and 19 are often upregulated together whereas ARF7 and ARF8 could be downregulated together.

A few questions arise when looking at these results. Could it be that this modular co-expression is a mechanism to generate equilibrium and achieve homeostasis of auxin signaling output because in the mutants a part of the auxin signaling pathway is compromised? If so then one can assume that differentially regulated ARF modules act antagonistically to each other in certain processes. This would mean that misexpression of one ARF activator can be compensated by an antagonistic misexpression of another ARF activator. A similar situation is observed for PIN auxin efflux carriers with an auxin-dependant cross-regulation of *pin* expression; if one PIN protein is lost, the other PIN proteins compensate by ectopic expression (Vieten *et al.* 2005).

Material and methods

Plant material

25 mutants of transcription factors and the *arf8-1* mutant were obtained from NASC. T-DNA accession numbers are listed in Supplementary Table 2-4. T-DNA insertions were analyzed by genotyping using primers listed in Appendix.

Y1H assay

The yeast on-hybrid assay was conducted according to Gaudinier *et al.* 2011 (Fig. 2-1). The ARF5 promoter sequences screened in the Y1H assay were amplified by PCR. For ARF5, 8 and 19 two fragments with partially overlapping sequences were screened separately. The overall ARF promoters screened correspond to the promoters used in the construction of the transcriptional reporter lines (pARF5 -5418 bp to + 134 bp, pARF6 -3255 to +197 bp, pARF7 -2973 bp to + 374 bp, pARF8 -5091 to + 42 bp, -4906 to + 452 bp). The amplified fragments were cloned either into pDONR P4P1R or into pEntry 5' TOPO plasmids by the Gateway BP-reaction or using the pENTR 5'-TOPO kit respectively. The resulting plasmids were recombined by the Gateway LR-reaction into both pMW2 and pMW3 Gateway destination vectors designed for yeast expression and containing respectively HIS3 or LacZ reporter genes (Gaudinier *et al.* 2011). The resulting vectors were transformed into YM4271 yeast strain. The transgenic yeast was checked for the ability of the promoter to induce the expression of the reporter gene in the absence of an interacting transcription factor (auto-activation). The HIS3 reporter gene auto-activation was checked by growing the yeast on the selection medium lacking histidine and supplied with 3-AT (3-Amino-1,2,4-triazole) concentrations of from 10 mM up to 100 mM. The LacZ reporter gene auto-activation was checked by conducting an X-gal assay with exposure for ≤ 30 min.

87 transcription factors were cloned and added to the existing root-specific transcription factor library (Suppl. Table 2-3). The transcription factors were amplified by a PCR from the cDNA collections which were obtained by isolating total RNA from various tissues. The full-length transcription factor cDNA PCR product (without a stop codon) was inserted into a pEntry-Zeo plasmid by the Gateway BP reaction and then recombined into pDest-AD-2µ destination vector designed for yeast expression and

containing a GAL4 activation domain (Gaudinier *et al.* 2011). The vectors were transformed into the yeast strain YΛ1867.

The yeast one-hybrid screen was conducted as described in detail in Gaudinier *et al.* 2011 using a BioRad VersArray robot to replicate the yeast. Briefly, yeast plates containing transcription factor libraries (the prey) were propagated from glycerol stocks on the tryptophan dropout selective medium. The yeast strains containing the promoters of ARFs (the bait) were propagated on the histidine and uracil dropout medium. The prey and the bait plates were mated on yeast peptone dextrose (YPD) medium plates for 2 days at 30°C. To select for diploids which contain both the bait and the prey constructs, the yeast was transformed from YPD plates into a histidine, uracil and tryptophan dropout selective medium for 2 days at 30°C. The yeast interaction was checked by growing diploid yeast on 3-AT plates and on YPD plates containing nitrocellulose filter (for X-gal assay). 3-AT plates were left growing by RT in the dark for 10 days and then photographs were taken. X-gal plates were left growing for 2 days at RT and then X-gal staining was performed at 37°C with photographs taken at 30 min, 1h, 2, 3, 4, 8h and 24h. Positives were scored from both assays separately and considered positive interactions if they were scored in at least one of the assays (Fig. 2-1B and C).

Transient expression in *Arabidopsis thaliana* protoplasts

For the transient protoplast assay the reporter and the effector plasmids were constructed as shown in Fig. 2-5A.

For the reporter plasmid, the promoter fragment of the respective ARF was amplified by PCR and cloned into pDONR P4-P1R plasmid; the promoter sequence is the same as used in Y1H assay. Note that just like in the Y1H assay the standard promoter constructs contained both upstream sequence and also included short sequences downstream of ATG including the first big intron. In addition, for ARF5, 6, 7 and 19 shorter promoters was also made which, in difference to the standard promoter, only included upstream sequences up to ATG. For the ARF8 promoter a short part of the 35S promoter (-107 to +1) was inserted into the construct. The 35S promoter was amplified by PCR with AccIII restriction enzyme sites, linearized with AccII and ligated at position -115 of the ARF8 promoter. Separately, a construct containing NLS followed by mVenus coding sequence and an octopine synthase (OCS) terminator was cloned into pDONR 211 plasmid. Thirdly, a construct

containing promoter of RPS5a (promoter of the ribosomal protein S5A) driving TagBFP followed by a NLS signal and finally a nosT terminator was cloned into pDONR P2R-P3 plasmid. The pARF pDONR P4-P1R, the NLS-Venus-term pDONR 211 and the pRPS5a-TagBFP-NLS-term were recombined with a multisite Gateway reaction into pDEST R4-R3. As a positive control the following reporter construct was created: promoter RPS5a driving the expression of nuclear-localized mVenus plus the RPS5a promoter driving expression of TagBFP.

For the effector plasmids, the promoter of RPS5a (ribosomal protein S5A) cloned into pDONR P4-P1R plasmid was directly received from Carlos Galvan-Ampudia. The cDNA of the respective transcription factor without the stop codon was cloned into pDONR 211 plasmid. The construct containing a self-cleaving 2A peptide (Kim *et al.* 2011a; Trichas *et al.* 2008) followed by mCherry coding sequence, an NLS and a nosT terminator was cloned into pDONR P2R-P3 plasmid. Finally, these three plasmids were recombined with a multisite Gateway reaction into pDEST R4-R3. An alternative effector plasmid included an activator VP16 domain from the herpes simplex virus fused to the TF cDNA.

For the protoplast assay Col-0 seedlings were grown in shortday conditions (8h light/16h dark) for 37-45 days. Leaves of similar size from the second or third pair were collected and digested in an enzyme solution (1% cellulose R10, 0.25% macerozyme R10, 0.4M mannitol, 10 mM $CaCl_2$, 20 mM KCl, 0.1% BSA, 20 mM MES at pH 5.7) overnight at room temperature. Protoplasts were collected through a 70 micron mesh and centrifuged for 2 min at 100 x g. The protoplasts were washed twice with an ice-cold W5 solution (154 mM NaCl, 125 mM $CaCl_2$, 5 mM KCl, 5 mM glucose, 2 mM MES at pH 5.7) and incubated on ice for 30 min. The protoplasts were then resuspended in the MMG solution (0.4 M mannitol, 15 mM $MgCl_2$, 4 mM MES at pH 5.7) with final concentration 150 000 cells/ml. 10 µl of each the effector and the reporter plasmid DNA (concentration 3 mg/µl) were mixed with 200 µl of the protoplasts. Immediately, 220 µl of the PEG solution (40 % PEG 4000, 0.2 M mannitol, 0.1 M $CaCl_2$) was added, incubated for 5 min at RT and then washed twice in W5 solution. The protoplasts were resuspended in 800 µl of the W5 solution and incubated for 24 hours in 16h light/8h dark growth chamber. Before imaging, the protoplasts were resuspended in 400 µl W5 solution and subsequently transformed into an 8-well imaging chamber.

A Zeiss 710 LSM confocal microscope was used for imaging the protoplasts (Fig. 2-5B). The sequential scanning was performed with mVenus (excitation at 514, emission at 520-559), TagBFP (excitation at 405 and emission at 423-491), mCherry (excitation at 561, emission at 598-636) and bright-field channels. Z-stacks of several protoplasts were taken. The data was analyzed using ImageJ software. The image with the best focus for each protoplast was selected from the z-stack. The nucleus was selected and the mean fluorescence was measured as illustrated in Fig. 2-5. For the statistical analysis an unpaired t-test was conducted with $p < 0.1$ considered as statistically significant. The number of replicates was 40 protoplasts.

For each ARF-TF interaction 4 or 5 independent experiments were performed. The first type of experiment included the reporter plasmid against the effector plasmid (Fig. 2-5A) (repeated two times for ARF5, 6, 7 and 8, and one time for ARF19). Second type of experiment included an alternative reporter plasmid containing a shorter promoter (lacking downstream regions) against the effector plasmid (repeated once for ARF5, 6, 7 and 19). Third type of experiment included the reporter plasmid against an alternative effector plasmid containing TF-VP16 domain fusion (repeated two times for all ARFs) (Suppl. Table. 2-1).

Expression analysis with qRT-PCR

Wild-type and mutant seedlings were grown in 24h light conditions on 1/2 MS plates containing 1% sucrose and 1% agar for 7 days. The whole root and the whole shoot parts of the seedlings were collected separately. For one root sample, roots from 30 seedlings grown on the same plate were pooled together. For one shoot sample, 8 shoots from seedlings grown on the same plate were pooled together. Per genotype 3 independent replicates were collected.

RNA was extracted using Spectrum Plant Total RNA kit (Sigma-Aldrich). The DNA was removed using TURBO DNA-free kit (Invitrogen). The cDNA was produced using SuperScript VILO cDNA Synthesis kit (Thermo Fischer) with 500 ng RNA. The cDNA was diluted 1:100 before use. The qRT-PCR was performed using Applied Biosystems Fast SYBR Green Master Mix. Expression of TUB4 gene was used as standard. All primers are listed in Appendix. The statistical analysis was performed with Mann-Whitney test using R.

This experiment was done with the help of Stéphanie Lainé, ENS de Lyon.

Expression analysis of crosses between ARF transcriptional reporter lines and T-DNA mutants

Several mutants of the regulatory transcription factors were crossed with pARF-mVenus transcriptional reporter lines described in Chapter I. The crosses were genotyped and selected for the presence of homozygous pARF-mVenus reporter construct. For the microscopy, the following plants from F3 generation were compared: wild-type for the mutant gene containing homozygous pARF-mVenus construct versus homozygous for the mutant gene containing homozygous pARF-mVenus construct.

For the root microscopy, plants were grown for 6 days at 16h light/8h dark conditions on 1/2 MS medium supplemented with 1% sucrose and 1% agar. Plant cell membranes were visualized by staining with 15 µg/ml propidium iodide solution. The roots were examined in the TCS-SP5 confocal microscope (Leica) with excitation at 514 nm and emission at 526-560 nm for mVenus and 605-745 nm for propidium iodide. Images were taken with identical settings for the control and the mutant plants. The mVenus fluorescence intensity was measured using ImageJ software.

Shoot phenotype analysis of the TF mutants

25 T-DNA insertion mutants and the wild-type Col-0 were grown in 8h light/16h dark conditions on soil for 43 days. Leaf number was counted every 3 days starting from day 24. Rosette diameter was measured at 43 days. After 43 days of growth in the above conditions, the plants were transferred to 16h light/8h dark conditions to induce bolting. The following parameters were measured at 21 and 27 days in the 16h light/8h dark conditions: length of the main stem, number of cauline branches growing from the main stem, number of axillary branches growing from rosette (the main stem not included).

The number of replicates per genotype was 12 plants. For the statistical analysis an unpaired t-test was conducted with $p \leq 0.05$ considered as statistically significant.

Root phenotype analysis of the TF mutants

Root phenotype analysis was done by Jingyi Han (University of Nottingham, Anthony Bishopp's group). For root length measurement and for gravitropic analysis plants were grown on ½ MS medium in 12h light/12h dark conditions. For root length analysis, plants were grown either on medium lacking IAA or supplemented with 10

µM IAA. Images were taken at 5 and 15 days in light and the root length was measured. For the gravitropic response, plants were grown for 5 days, then turned at a 90°C angle and the images of the root gravitropic growth were taken every 1 hour for the next 12h hours in the dark with the infrared camera. Statistical analysis was done with one-way analysis of variance (ANOVA) test with $p \leq 0.05$ considered as statistically significant.

Growth on NPA for shoot phenotype analysis

Plants were grown on plates laid horizontally with medium containing 11.82g/l Arabidopsis medium (Duchefa), 2 mM $Ca(NO_3)_2$ x $4H_2O$ and 0.7% Agar, pH 5.8 and supplemented with 10µM NPA. The plants were grown at 16h light/8h dark conditions until analyzed at 25 days old. The plants were examined under a stereo microscope and classified in one of the three categories: plants with a single pin inflorescence, plants with pin and 1-3 flowers, plants with flowers only (no pin). At least 70 plants were counted per genotype. Three independent experiments were performed.

Supplementary information

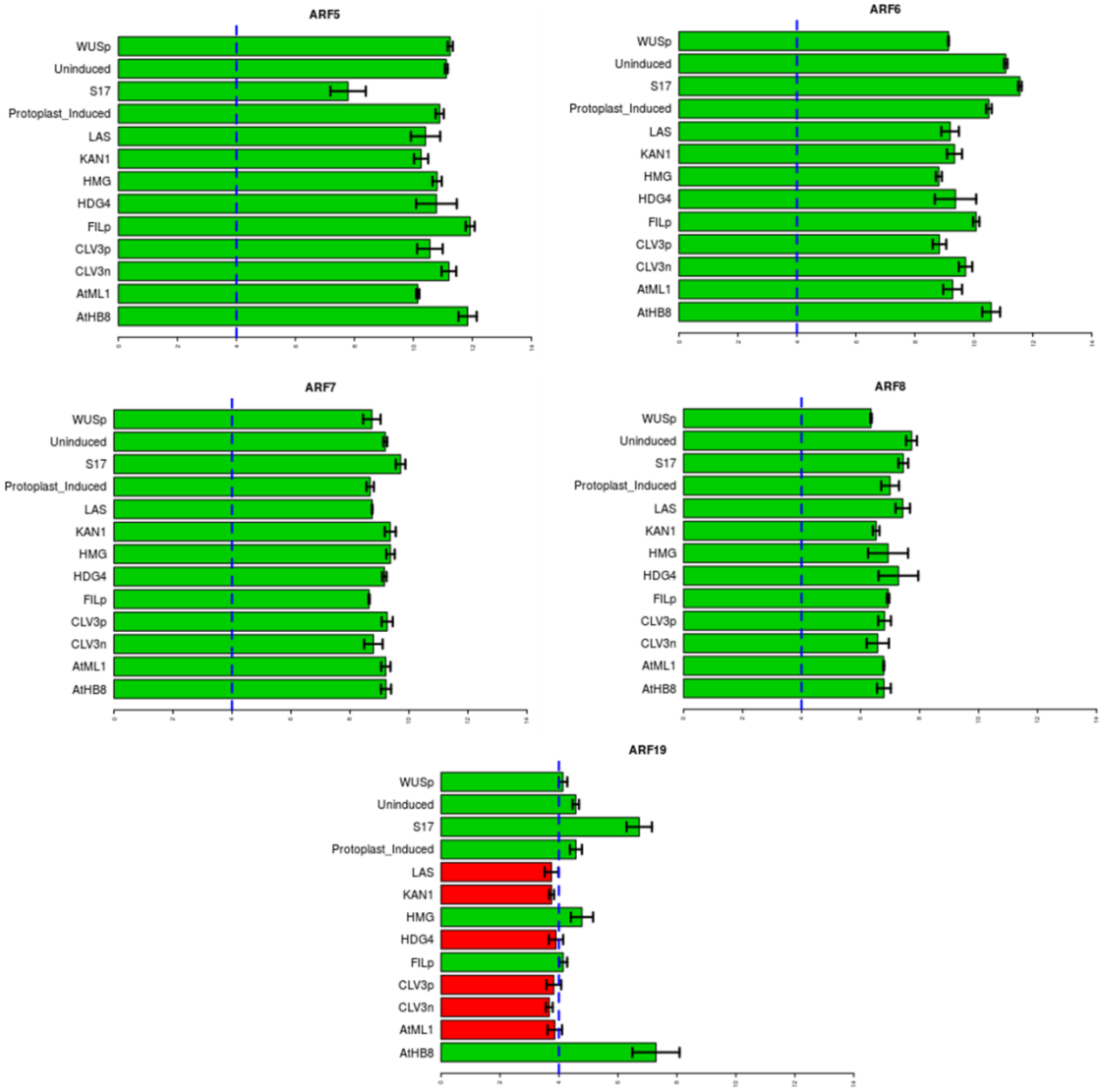

Supplementary Fig. 2-1. Expression profile of ARF5, 6, 7, 8 and 19 in the shoot apex of the *apetala1-1;cauliflower1-1* double mutant (Yadav *et al.* 2009; Yadav *et al.* 2014). The expression domains are the following: WUSp = rib zone, Uninduced = control for induction by protoplasting, S17 = shoot phloem, Protoplast_Induced = control for induction by protoplasting, LAS = adaxial organ boundaries, KAN1 = abaxial organ boundaries, HMG = meristematic L1 layer, HDG4 = L2 layer, FILp = organ primordia, CLVp = central zone, CLV3n = control with GFP negative protoplasts, AtMIL1 = ubiquitous L1 layer, AtHB8 = shoot xylem.

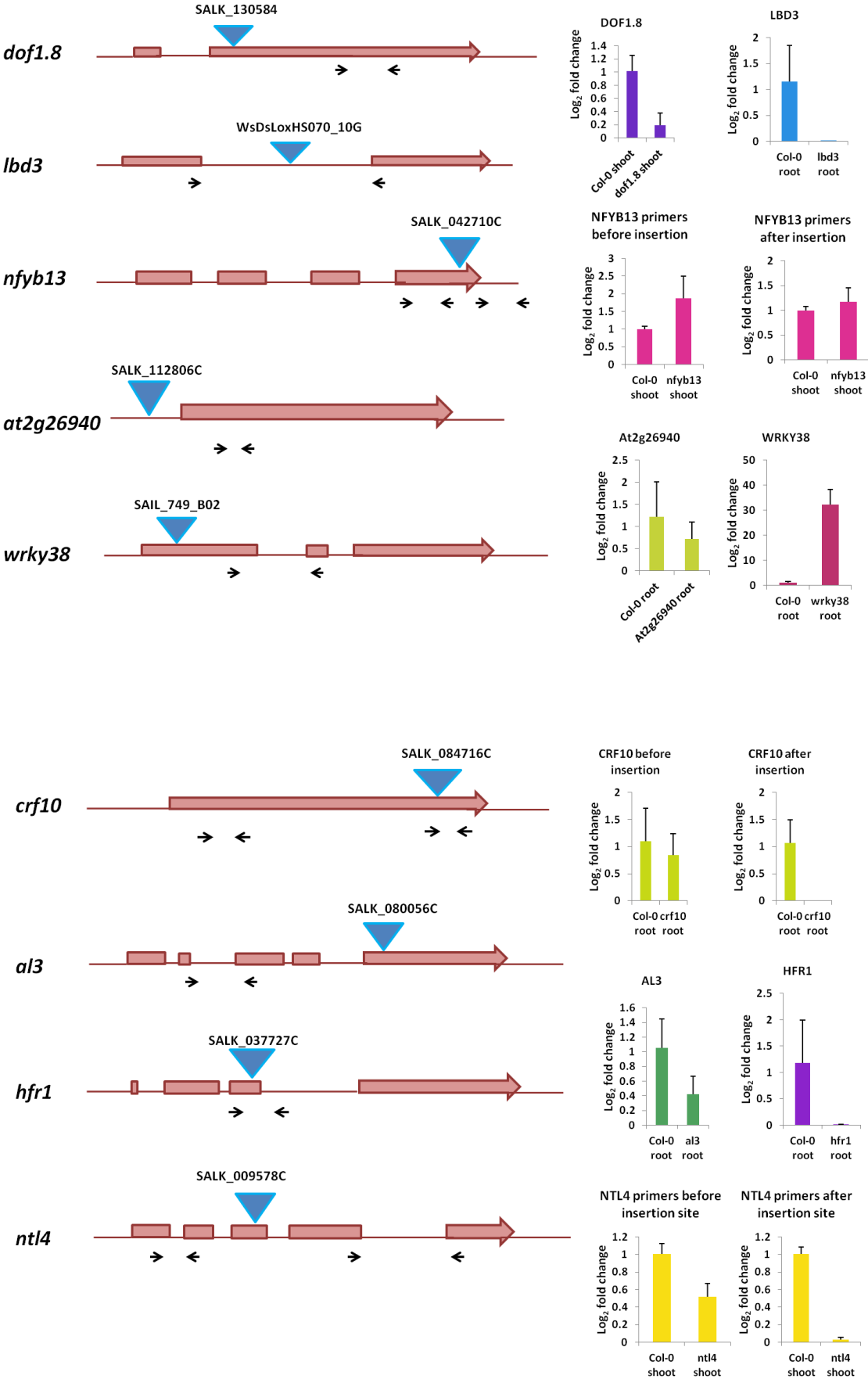
SALK_130584
dof1.8
WsDsLoxHS070_10G
lbd3
SALK_042710C
nfyb13
SALK_112806C
at2g26940
SAIL_749_B02
wrky38
DOF1.8
Log2 fold change
Col-0 shoot
dof1.8 shoot
LBD3
Col-0 root
lbd3 root
NFYB13 primers before insertion
Col-0 shoot
nfyb13 shoot
NFYB13 primers after insertion
At2g26940
Col-0 root
At2g26940 root
WRKY38
Col-0 root
wrky38 root
SALK_084716C
crf10
SALK_080056C
al3
SALK_037727C
hfr1
SALK_009578C
ntl4
CRF10 before insertion
Col-0 root
crf10 root
CRF10 after insertion
AL3
Col-0 root
al3 root
HFR1
Col-0 root
hfr1 root
NTL4 primers before insertion site
Col-0 shoot
ntl4 shoot
NTL4 primers after insertion site

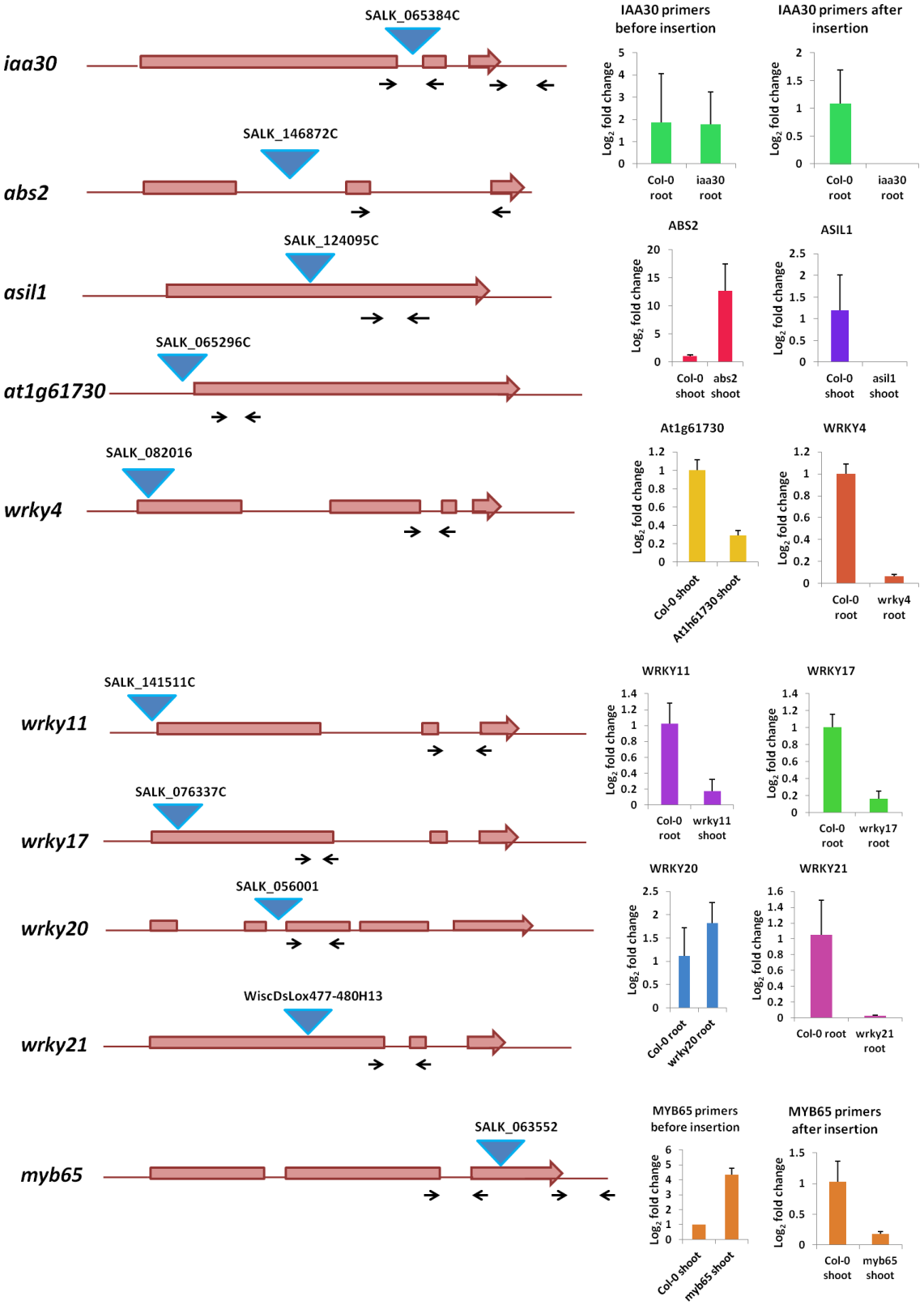
iaa30
SALK_065384C
abs2
SALK_146872C
asil1
SALK_124095C
at1g61730
SALK_065296C
wrky4
SALK_082016
wrky11
SALK_141511C
wrky17
SALK_076337C
wrky20
SALK_056001
wrky21
WiscDsLox477-480H13
myb65
SALK_063552
IAA30 primers before insertion
IAA30 primers after insertion
ABS2
ASIL1
At1g61730
WRKY4
WRKY11
WRKY17
WRKY20
WRKY21
MYB65 primers before insertion
MYB65 primers after insertion
Log2 fold change
Col-0 root
iaa30 root
Col-0 shoot
abs2 shoot
asil1 shoot
Col-0 shoot
At1h61730 shoot
wrky4 root
wrky11 shoot
wrky17 root
Col-0 root
wrky20 root
wrky21 root
myb65 shoot

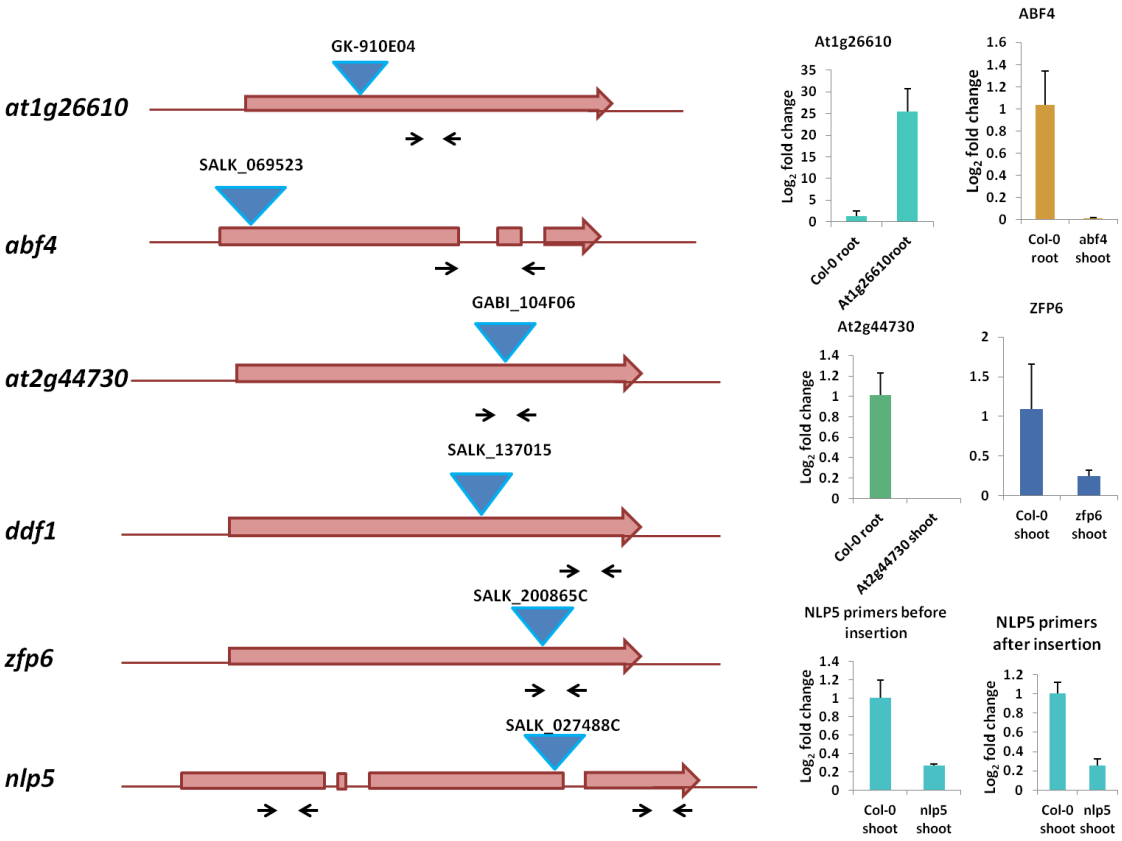

Supplementary Fig. 2-2. Schematic representations of the transcription factors locus indicating T-DNA insertion site (blue triangle), the coding sequences (thick brown arrow) interrupted by non-coding sequences (thin brown arrow). On the right: expression of the mutant genes in the mutant backgrounds was measured with qRT-PCR using primers located at positions indicated by black arrows in the schematic. For *ddf1* expression could not be measured due to low abundance of this gene.

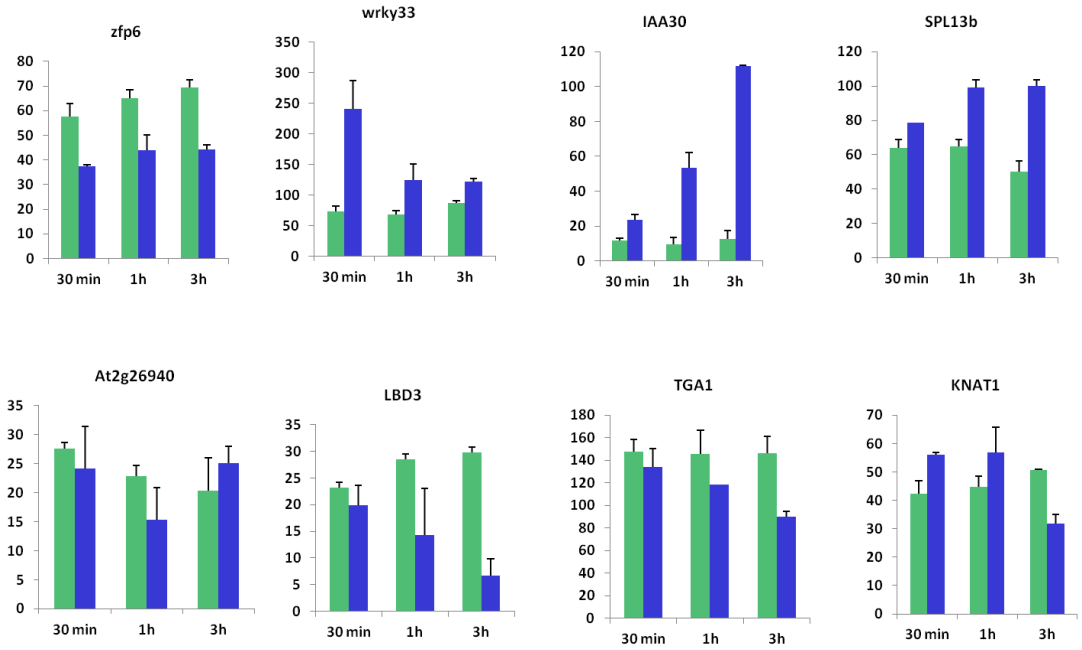

Supplementary Fig. 2-3. Expression of transcription factors which are differentially expressed after treatment with 1 µM IAA for 30 min, 1h or 3h. Expression values results were obtained from Arabidopsis eFP browser were deposited by Shimada lab (Winter *et al.* 2007, Goda *et al.* 2008).

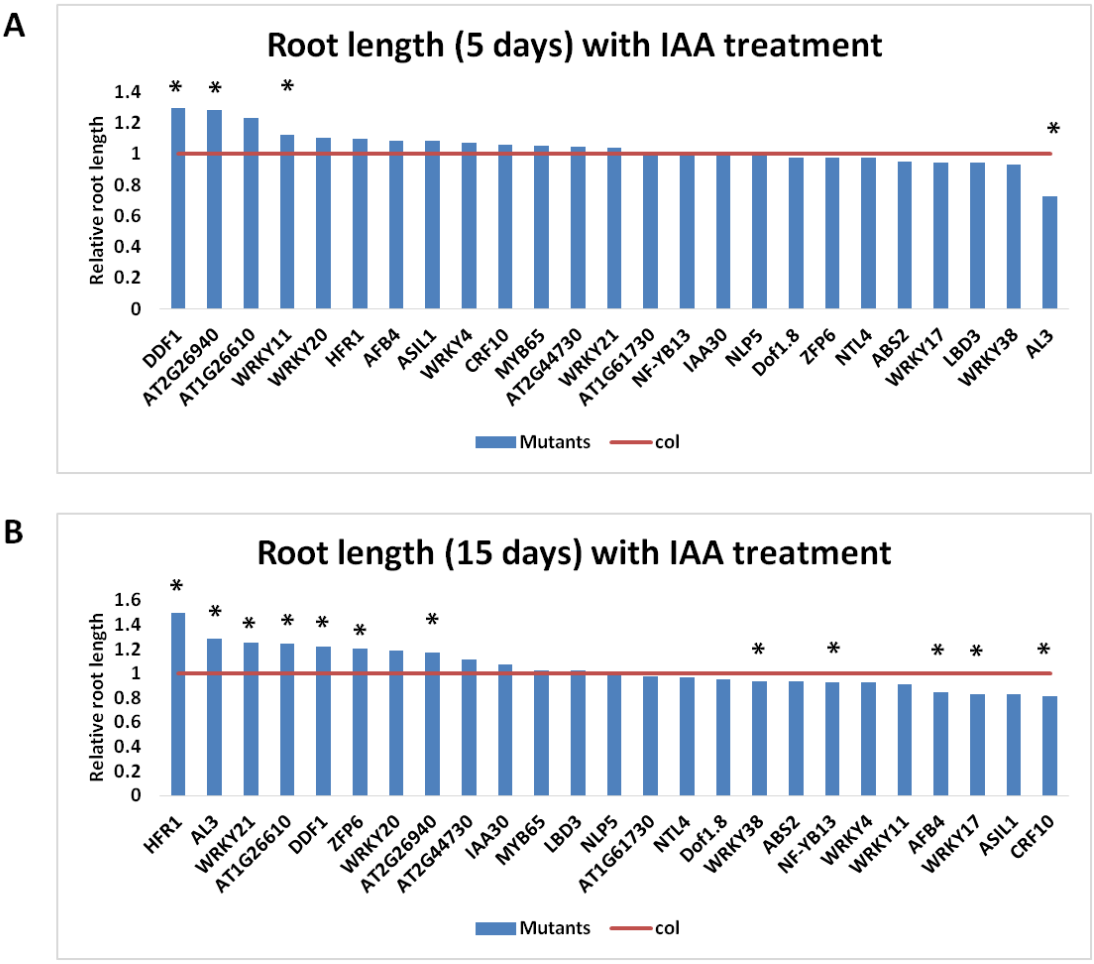

Supplementary Fig. 2-4. Root length of the TF mutants grown on the medium supplemented with10 µM IAA for 5 days **(A)** and 15 days **(B)**. Experiment done was by Jingyi Han (University of Nottingham, Anthony Bishopp's group). One-way analysis of variance (ANOVA) test was used to calculate significance with *p ≤ 0.05.

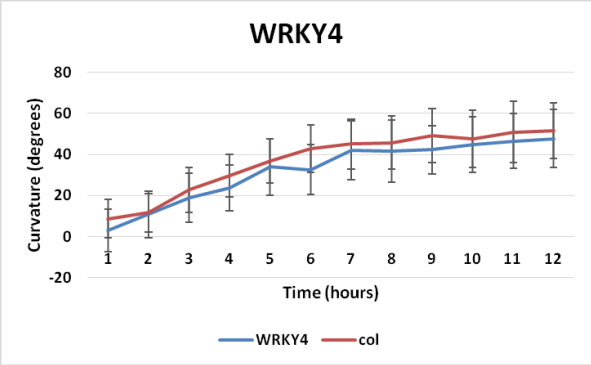
WRKY4
Curvature (degrees)
Time (hours)
WRKY4
col

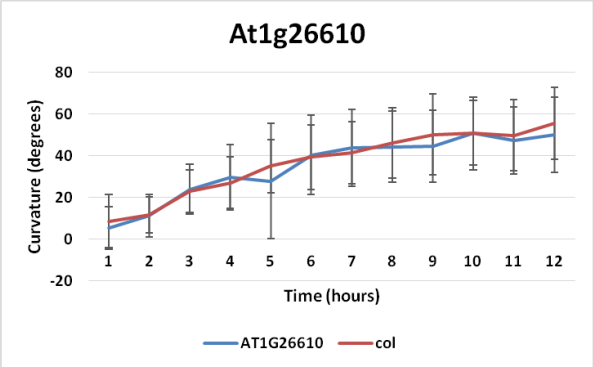
At1g26610
Curvature (degrees)
Time (hours)
AT1G26610
col

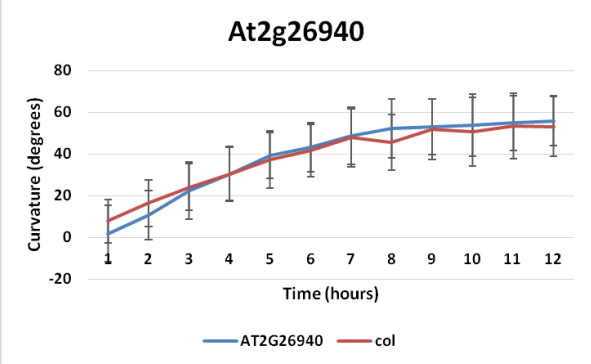
At2g26940
Curvature (degrees)
Time (hours)
AT2G26940
col

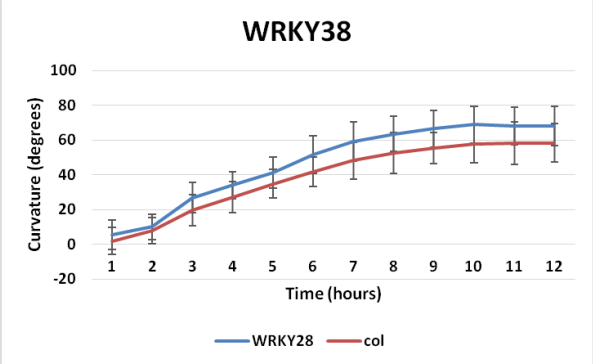
WRKY38
Curvature (degrees)
Time (hours)
WRKY28
col

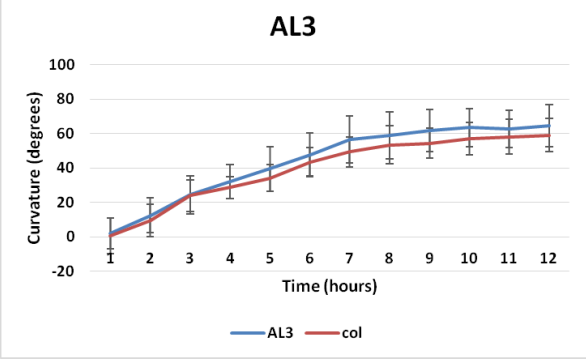
AL3
Curvature (degrees)
Time (hours)
AL3
col

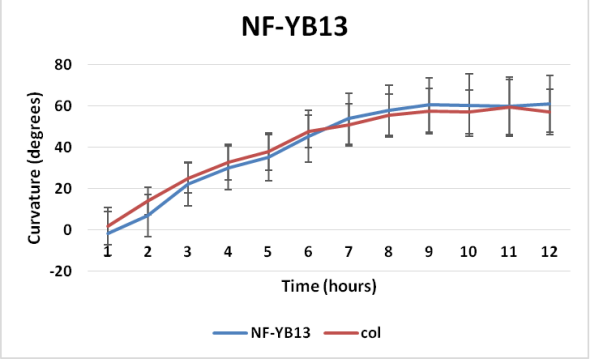
NF-YB13
Curvature (degrees)
Time (hours)
NF-YB13
col

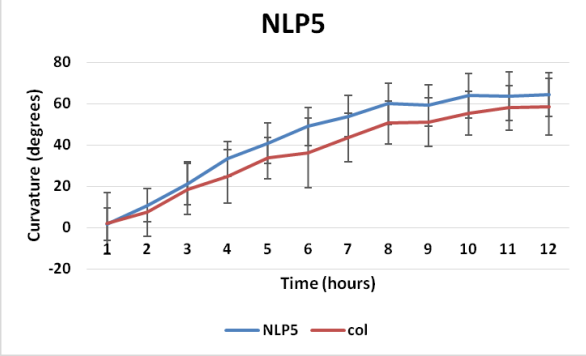
NLP5
Curvature (degrees)
Time (hours)
NLP5
col

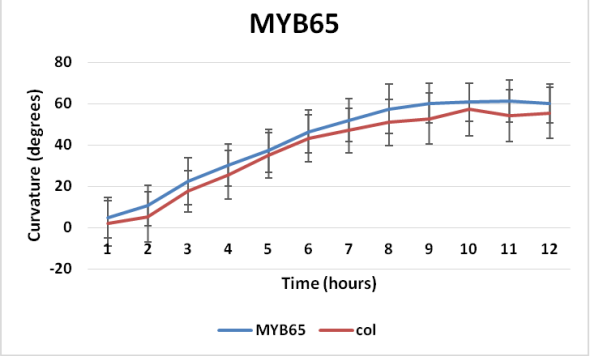
MYB65
Curvature (degrees)
Time (hours)
MYB65
col

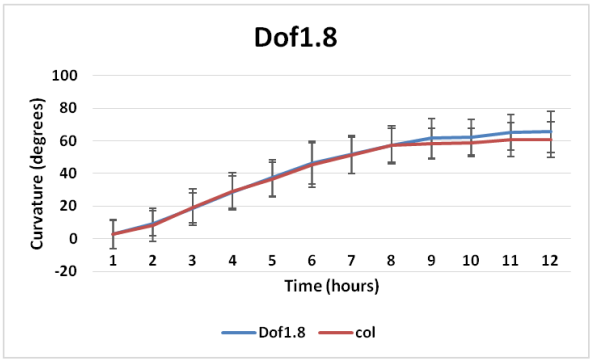
Dof1.8
Curvature (degrees)
Time (hours)
Dof1.8
col

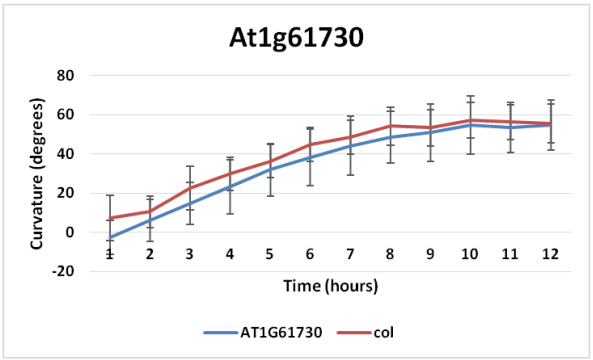
At1g61730
Curvature (degrees)
Time (hours)
AT1G61730
col

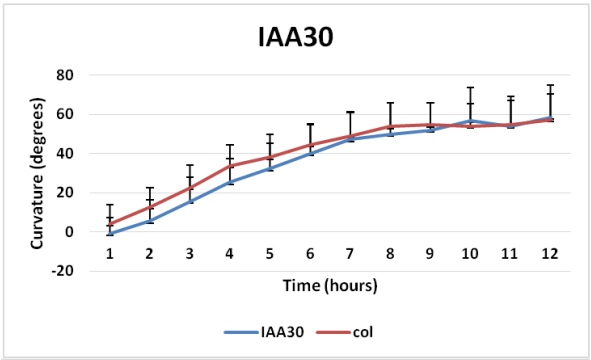
IAA30
Curvature (degrees)
Time (hours)
IAA30
col

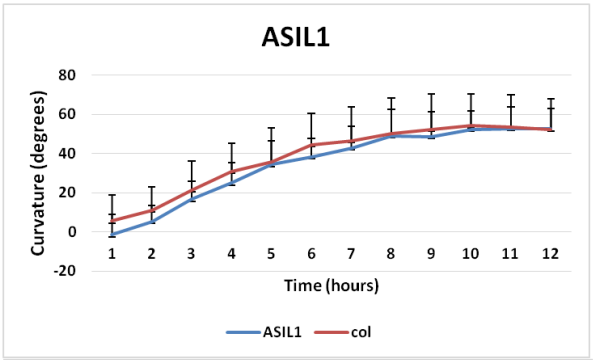
ASIL1
Curvature (degrees)
Time (hours)
ASIL1
col

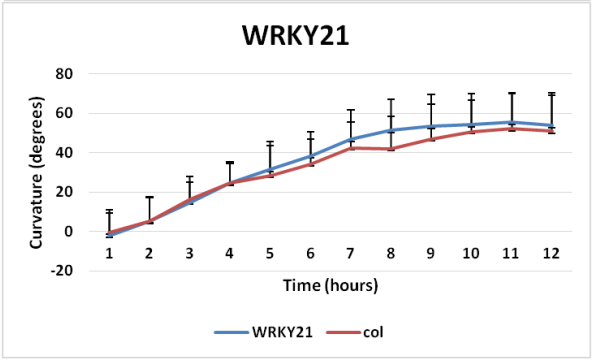
WRKY21
Curvature (degrees)
Time (hours)
WRKY21
col

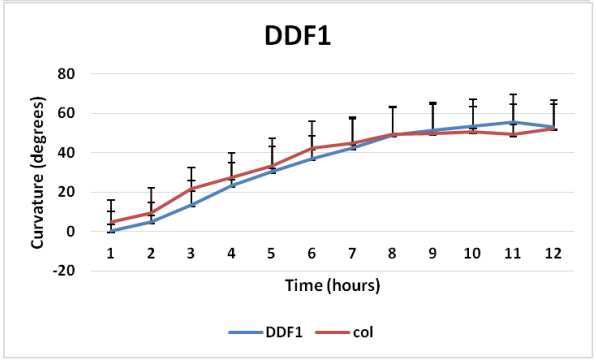
DDF1
Curvature (degrees)
Time (hours)
DDF1
col

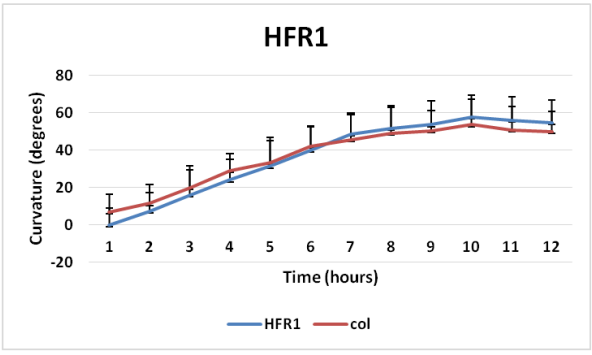
HFR1
Curvature (degrees)
Time (hours)
HFR1
col

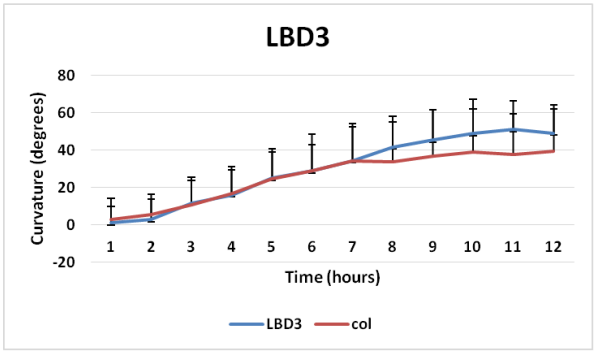
LBD3
Curvature (degrees)
Time (hours)
LBD3
col

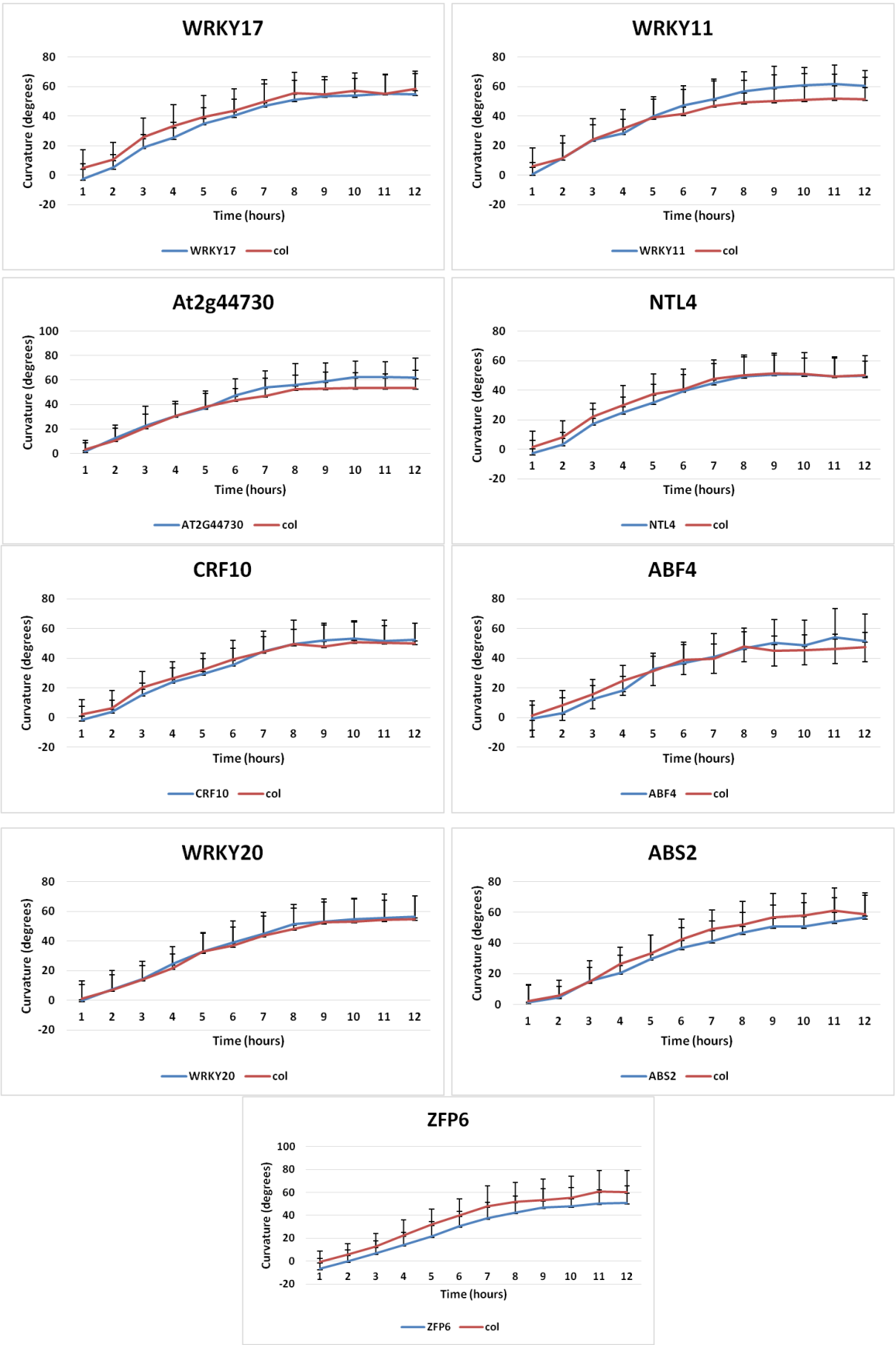

Supplementary Fig. 2-5. Kinetic analysis of root growth gravitropism in mutants of regulatory transcription factors. Seedlings were grown for 5 days in 12h light/12h dark conditions and turned at a 90° angle. Images were taken every 1h for 12h duration. Experiment was done by Jingyi Han (University of Nottingham, Anthony Bishopp's group).

Promoter	Transcription factor	normal 1	normal 2	normal 3	VP16 1	VP16 2	Final score	Description
ARF5	Dof1.8	0	0	0	+	+	2	confirmed, activation when fused to VP16
	KNAT1	0	0	0	0	-	1	not confirmed
	LBD3	-	-	-	-	-	4	confirmed repression
	SMZ	no data	-	-	-	0	3	confirmed repression
ARF6	At2g26940	-	-	-	-	-	4	confirmed repression
	NF-YB13	-	-	0	-	-	4	confirmed repression
ARF7	CRF10	-	-	-	-	-	4	confirmed repression
	JAM2	0	-	0	-	-	3	confirmed repression
	NF-YB13	-	-	-	-	-	4	confirmed repression
	ATERF15	no data	0	0	-	-	2	possible repression
	AL3	-	-	0	-	-	4	confirmed repression
	WRKY38	-	-	-	-	-	4	confirmed repression
ARF19	At2g26940	-		-	-	-	4	confirmed repression
	LBD3	0		-	-	-	3	confirmed repression
	MYB65	no data		no data	0	0	0	not enough data
	NLP5	0		-	0	0	1	not confirmed
ARF8	HFR1	-	0	-	-	-	4	confirmed repression
	CUC2	0	0	-	0	0	1	not confirmed
	KNU	-	-	-	-	-	4	confirmed repression
	SPL2	+	0		0	0	1	not confirmed
	WUS	-	-	-	-	0	4	confirmed repression
	ZAP1	+	0	0	-	-	3	possible repression or activation
	At2g26940	-	-		-	-	4	confirmed repression
	JAM2	0	0		-	-	2	possible repression
	WRKY4	0	0		0	0	0	not confirmed
	WRKY11	-	0		0	0	1	not confirmed
	WRKY17	-	0		no data	no data	1	not confirmed
	WRKY20	-	0		0	0	1	not confirmed
	WRKY21	+	0		0	+	2	possible activation
	WRKY33	0	0		-	0	1	not confirmed
	SPL13b	0	0	-	+	+	3	confirmed activation
	ARF9	0	-		-	0	2	possible repression
	IAA30	0	-		-	-	3	confirmed repression
	TGA1	0	-		0	-	2	possible repression
	ZFP5	0	-		0	0	1	not confirmed
	ZFP6	-	-		-	0	3	confirmed repression
	ZFP7	0	-		0	-	2	possible repression
	ABF4	-	0		0	no data	1	not confirmed
	ABS2	0	0		0	0	0	not confirmed
	ASIL1	0	0		0	-	1	not confirmed
	At1g26610	-	-		-	-	4	confirmed repression
	At1g61730	0	0		-	-	2	possible repression
	At2g44730	0	-		0	-	2	possible repression
	NTL4	no data	-		0	-	2	possible repression
	DDF1	-	-		-	0	3	confirmed repression
	DREB2A	0	0		0	0	0	not confirmed
	DREB26	0	-		0	-	2	possible repression

Supplementary Table 2-1. Scoring interactions between the promoters of ARF activators and the regulatory transcription factors based on protoplast assay results. "+" indicated increase, "-" reduction and "0" no change of mVenus reporter expression levels compared to control. The score was given between 0 and 4: 4 when the interaction was confirmed in at least 4 independent experiments and 0 when the interaction wasn't confirmed in any experiment. "normal" indicates using standard effector plasmid; "VP16" indicated using an alternative effector plasmid with TF-VP16 domain fusion. An unpaired t-test was used to calculate significance with *p < 0.1.

TF ATG	Gene	BS from literature	BS from DAP-seq	Peak in DAP-seq	Reference
AT2G17950	WUS	TAAT	TCANTCA / TGANTGA	no peak	Yadav *et al.* 2011
AT5G14010	KNU	no data	no data	no data	
AT1G16530	LBD3	(G)CGGC(G)	no data	no data	Husbands *et al.* 2007
AT4G08150	KNAT1	no data	no data	no data	
At5g53950	CUC2	CGT(G/A).	C(G/T)T(A/G)N_6A(A/C)GN_2A	multiple peaks	Lindemose *et al.* 2014
AT2G26940		no data	no data	no data	
AT1G01260	JAM2	no data	no data	no data	
AT5G23090	NF-YB13	no data	no data	no data	
AT3G54990	SMZ	no data	no data	no data	
AT1G64620	Dof1.8	no data	AAAG / CTTT	specific peaks	
AT5G43270	SPL2	GTAC	no data	no data	Liang *et al.* 2008
AT5G50670	SPL13b	GTAC	GTAC	specific peak	Liang *et al.* 2008
AT1G02340	HFR1	no data	no data	no data	
AT3G10500	NTL4	CGT(G/A).	CTTN_6CAAGN_2A	specific peak	Lindemose *et al.* 2014
AT5G65210	TGA1	TGACG	TGACGTCA	specific peaks	Katagiri *et al.* 1989
AT4G23980	ARF9	TGTCTC / TGTCGG	no data	no data	Boer *et al.* 2014, Ulmasov *et al.* 1995
AT3G62100	IAA30	no data	no data	no data	
AT2G36080	ABS2	no data	no data	no data	
AT1G54060	ASIL1	GTGATT	no data	no data	Gao *et al.* 2009
AT2G44730		no data	no data	no data	
AT1G61730		no data	no data	no data	
AT1G26610		no data	no data	no data	
AT3G19290	ABF4	ACGTG(G/T)C	no data	no data	Hattori *et al.* 2002
AT5G05410	DREB2A	G/ACCGAC	G(T/G)CGGT / ACCG(A/C)C	multiple peaks	Sakuma *et al.* 2002
AT1G21910	DREB26	G/ACCGAC	CACCGNC / GNCGGTG	no peak	Sakuma *et al.* 2002
AT1G12610	DDF1	G/ACCGAC	GTCG / CGAC	no peak	Sakuma *et al.* 2002
At1g68550	CRF10	no data	CCGCCGC / GCGGCGG	multiple peaks	
AT3G42790	AL3	no data	no data	no data	
AT2G31230	ATERF15	(TG)CCACC(GG)	GCCGCC / GGCGGC	no peak	Lee *et al.* 2010
At3g11440	MYB65	no data	AACNG / CNGTT	specific peak	
At1g76350	NLP5	tGACcCTTN_{10}AAGagtcc	no data	no data	Konishi and Yanagisawa 2010
AT5G22570	WRKY38	(C/T)TGAC(T/C)	no data	no data	Pandey and Somssich 2009
AT2G04880	ZAP1	(C/T)TGAC(T/C)	no data	no data	Pandey and Somssich 2009
AT1G13960	WRKY4	(C/T)TGAC(T/C)	no data	no data	Pandey and Somssich 2009
AT4G31550	WRKY11	(C/T)TGAC(T/C)	TTGAC / GTCAA	multiple peaks	Pandey and Somssich 2009
AT2G24570	WRKY17	(C/T)TGAC(T/C)	TTGACT / AGTCAA	specific peaks	Pandey and Somssich 2009
AT4G26640	WRKY20	(C/T)TGAC(T/C)	TTGAC / GTCAA	specific peak	Pandey and Somssich 2009
AT2G30590	WRKY21	(C/T)TGAC(T/C)	TTGAC / GTCAA	specific peaks	Pandey and Somssich 2009
AT2G38470	WRKY33	(C/T)TGAC(T/C)	TTGAC / GTCAA	specific peak	Pandey and Somssich 2009
AT1G10480	ZFP5	no data	no data	no data	
AT1G67030	ZFP6	no data	no data	no data	
AT1G24625	ZFP7	no data	no data	no data	

Supplementary Table 2-2. Analysis of the transcription factor binding sites in the ARF promoters using DAP-seq database (O'Malley *et al.* 2016) and the available literature. The TF binding sites (BS) identified in the literature or in the DAP-seq are shown in 3rd and 4th columns respectfully. The presence or absence of the DAP-seq binding peak in the promoter of the ARF which they regulate in Y1H assay is indicated in the 5th column.

Nr	AGI	Splice variant	Name
	Shoot-specific TFs:		
1	At5g61850	At5g61850.1	LFY,LEAFY
2	At1g69120	At1g69120.1	AP1, APETALA 1
3	At3g54340	At3g54340.1	AP3, APETALA 3
4	At1g26310	At1g26310.1	CAL, CAULIFLOWER
5	At5g20240	At5g20240.1	PI, PISTILLATA
6	At2g45190	At2g45190.1	YAB1, FIL, YABBY 1
7	At1g08465	At1g08465.1	YAB2
8	At4g00180	Unknown	YAB3
9	At2g26580	At2g26580.1	YAB5
10	At1g69180	At1g69180.1	CRC, CRABS CLAW
11	At1g62360	At1g62360.1	STM
12	At2g17950	At2g17950.1	WUS, WUSCHEL
13	At2g28610	At2g28610.1	PRS, WOX3
14	At5g16560	At5g16560.1	KAN1, KANADI 1
15	At4g17695	At4g17695.1	KAN3, KANADI 3
16	At5g42630	At5g42630.1	ATS, KAN4
17	AT5G15840	AT5G15840.1	CONSTANS
18	At2g32700	At2g32700.6	LUH
19	At1g24590	At1g24590.1	DRNL, DORNROSCHEN-LIKE
20	At1g12980	At1g12980.1	DRN, DORNROSCHEN
21	At5g60910	At5g60910.1	FUL, FRUITFULL
22	At2g45660	At2g45660.1	SOC1, AGL20
23	At4g24540	Unknown	AGL24
24	At2g22540	At2g22540.1	SVP, AGL22
25	At5g03790	At5g03790.1	LMI1
26	At3g61250	At3g61250.1	LMI2
27	At1g68640	At1g68640.1	PAN, PERIANTHIA
28	At1g68480	At1g68480.1	JAG, JAGGED
29	At1g76420	At1g76420.1	CUC3
30	At3g15170	At3g15170.1	CUC1
31	At5g53950	At5g53950.1	CUC2
32	At4g18960	At4g18960.1	AG, AGAMOUS
33	At5g15800	At5g15800.1	SEP1, SEPALLATA
34	At4g08150	At4g08150.1	BP, KNAT1
35	At1g70510	AT1G70510.1	KNAT2
36	At5g25220	AT5G25220.1	KNAT3
37	At5g11060	Unknown	KNAT4
38	At4g00220	AT4G00220.1	JLO
39	At5g63090	AT5G63090.2	LOB
40	At4g28190	AT4G28190.1	ULT, ULTRAPETALA
41	At4g35900	AT4G35900.1	FD
42	At3g23130	AT3G23130.1	FLO10, SUP

43	At5g57390	AT5G57390.1	PLT5
44	At5g65510	AT5G65510.1	PLT7
45	At1g51190	AT1G51190.1	PLT2
46	At2g31070	AT2G31070.1	TCP10
47	At5g14010	AT5G14010.1	KNU
48	At1g55580	AT1G55580.1	LAS
49	AT1G53160	AT1G53160.2	SPL4
50	AT1G24260	AT1G24260.1	SEP3
	TFs important in auxin signaling:		
51	At5g60450	AT5G60450.1	ARF4
52	At2g46530	AT2G46530.3	ARF11
53	At1g34170	Unknown	ARF13
54	At1g35540	AT1G35540.1	ARF14
55	At1g77850	AT1G77850.1	ARF17
56	At1g35240	AT1G35240.1	ARF20
57	At1g34390	AT1G34390.1	ARF22
58	At1g43950	AT1G43950.1	ARF23
	TFs important in cytokinin signaling:		
59	At3g16857	AT3G16857.2	ARR1
60	At4g31920	AT4G31920.1	ARR10
61	At1g67710	AT1G67710.1	ARR11
62	At2g25180	Unknown	ARR12
63	At2g01760	AT2G01760.1	ARR14
64	At5g58080	AT5G58080.1	ARR18
65	At3g62670	AT3G62670.1	ARR20
66	At5g61380	AT5G61380.1	TOC1
67	At4g18020	AT4G18020.1	PRR2
68	At4g00760	Unknown	PRR8
69	At4g27950	AT4G27950.1	CRF4
70	At1g68550	AT1G68550.1	CRF10
71	At3g25890	AT3G25890.1	CRF11
72	At1g25470	Unknown	CRF12
	TFs important in GA signaling:		
73	At1g66350	AT1G66350.1	RGL1
74	At5g66350	AT5G66350.1	SHI
75	At2g33810	AT2G33810.1	SPL3
76	At5g67110	AT5G67110.1	ALC, ALCATRAZ
77	At5g06100	AT5G06100.2	MYB33
78	At2g20180	Unknown	PIF1

79	At2g43010	AT2G43010.1	PIF4
80	At3g59060	AT3G59060.4	PIF5
	TFs important in ethylene signaling:		
81	At5g21120	AT5G21120.1	EIL2
	TFs important in ABA signaling:		
82	At2g36270	AT2G36270.1	ABI5
83	At1g45249	AT1G45249.1	ABF2
	TFs important in brassinosteroid signaling:		
84	At1g75080	AT1G75080.1	BZR1
85	At1g19350	AT1G19350.3	BZR2, BES1
86	At3g28910	AT3G28910.1	MYB30
87	At1g32130	AT1G32130.1	IWS1

Supplementary Table 2-3. List of transcription factors cloned for the yeast one-hybrid prey collection during this thesis

	Name	Line	Nasc order nr.	Insertion site
1	LBD3	WiscDsLoxHs070_10G	N906703	Intron
2	NF-YB13	SALK_042710C	N656418	exon close to end
3	MYB65	SALK_063552	N563552	last exon
4	NLP5	SALK_027488c	N685529	third exon
5	NTL4	SALK_009578C	N654990	third exon
6	IAA30	SALK_065384C	N668427	first intron
7	ABS2	SALK_146872C	N677334	first intron
8	ASIL1	SALK_124095C	N654384	exon
9	At1g61730	SALK_065296C	N666282	5'-UTR
10	WRKY4	SALK_082016	N582016	first exon
11	WRKY17	SALK_076337C	N655632	first exon
12	WRKY20	SALK_056001	N556001	intron
13	WRKY21	WiscDsLox477-480H13	N857761	first exon
14	AT1G26610	GK-910E04	N487316	exon
15	At2g26940	SALK_112806C	N670045	5'-UTR
16	WRKY11	SALK_141511C	N686899	5-UTR
17	ABF4	SALK_069523	N569523	first exon
18	At2g44730	GABI_104F06	N409954	exon
19	Dof1.8	SALK_130584	N630584	second exon
20	CRF10	SALK_084716C	N654285	exon
21	AL3	SALK_080056C	N681366	last exon
22	WRKY38	SAIL_749_B02	N876493	first exon
23	DDF1	SALK_137015	N637015	exon
24	ZFP6	SALK_200865C	N688121	exon
25	HFR1	SALK_037727C	N655442	third exon

Supplementary Table 2-4. List of transcription factors mutants used in this thesis.

Chapter III: Cytokinin Response Factor 10 regulates ARF7 expression to control plant development

Introduction

In the previous chapter I identified transcription factors that regulate expression of ARF activators. Mutants of these TFs were shown to have auxin-related phenotypes with defects in various aspects of growth and development. In this chapter I focus on one particular transcriptional regulator CRF10 which is a member of the Cytokinin Response Factor gene family acting in cytokinin signaling pathway. In my screen CRF10 was identified as a repressor of ARF7 transcription. In this chapter I will examine phenotypes of the *crf10* mutant and attempt to link them with the regulation of ARF7 expression.

The CRF10-ARF7 interaction is particularly interesting because it represents a potential case of cross-talk between auxin and cytokinin signaling pathways. The plant hormones auxin and cytokinin regulate various aspects of plant development in sometimes synergetic but more often in an antagonistic way. For some developmental processes the precise involvement of each hormone is not well understood which prevents correct interpretation of the cytokinin-auxin interaction. One of such poorly described processes is senescence of leaves. Leaf senescence is a deterioration process which is tightly regulated and involves multiple changes on the molecular, cellular and tissue levels (Lim *et al.* 2007). Leaf senescence can be triggered by the leaf developmental age or induced by external clues including environmental stress such as drought, nutrient or light deprivation, or pathogen attack (Gan and Amasino 1997, Hensel *et al.* 1993, Jiang *et al.* 1993, Rousseaux *et al.* 1996). The process of senescence is accompanied by extensive changes in metabolism; the first visible signs of senescence are the changes in the leaf color caused by the breakdown of the chlorophyll (Woolhouse 1984). The leaves cease active anabolism and start catabolic activity; the cellular macromolecules including proteins, lipids and RNA are broken down into smaller components and transported to the growing parts of the plant such as the young leaves (Bate *et al.* 1991, Gan and

Amasino 1997, Li *et al.* 2017, Woolhouse 1984). At the end of the process, the senescent leaves undergo programmed cell death; this process is different in many aspects from other programmed cell death responses of plants such as the pathogen-induced hypersensitive response (Cao *et al.* 2003, Doorn and Woltering 2004, Lim *et al.* 2007). The molecular and genetic features of the leaf senescence have been studied in detail using global transcriptomics and metabolics approaches (Breeze *et al.* 2011, Buchanan-Wollaston *et al.* 2005, De Michele *et al.* 2009, Desclos *et al.* 2009, Gepstein *et al.* 2003, Guo *et al.* 2004, Li *et al.* 2017, Lin *et al.* 2015) and examining the mutants with early or delayed leaf senescence phenotypes (Besseau *et al.* 2012, Woo *et al.* 2001, Xie *et al.* 2014, Xiong *et al.* 2005, Yoshida *et al.* 2002). Nevertheless, many questions regarding this process remain opened. As such, it is unclear how the leaf age is recognized to induce the senescence program at the correct time.

There are clear data demonstrating involvement of plant hormones in the regulation of leaf senescence at all stages (Lim *et al.* 2007). Cytokinin was identified as one of the key hormones involved in this process. The cytokinin levels are reduced in the senescing leaves (Gan and Amasino 1996, Singh *et al.* 1992), and the cytokinin biosynthesis genes are downregulated whereas the genes involved in cytokinin degradation, the cytokinin oxydases, are upregulated in senescing leaves (Buchanan-Wollaston *et al.* 2005). The exogenous application of cytokinin (Dyer and Osborne 1971, Gan and Amasino 1996*,* Nooden *et al.* 1979, Richmond and Lang 1957) or an endogenous increase in cytokinin through genetical manipulations leads to the delayed leaf senescence (Gan and Amasino 1995, McCabe *et al.* 2001, Ori *et al.* 1999). Cytokinin signaling during leaf senescence is transmitted through the cytokinin receptor AHK3 (Kim *et al.* 2006), the type-B response regulator ARR2 (Kim *et al.* 2006, Kim *et al.* 2012) and the members of the Cytokinin Response Factors gene family (Raines *et al.* 2016, Zwack *et al.* 2013). Among them, CRF1, CRF3 and CRF5 promote leaf senescence whereas CRF6 negatively regulates leaf senescence. Overall it is clear that cytokinin negatively regulates leaf senescence. The precise details behind the involvement of cytokinin in this process remain incompletely understood through it is speculated that the cytokinin is associated with the control of the sink/source regulation (Zwack and Rashotte 2013).

The role of auxin in leaf senescence is less well characterized. Auxin levels are reduced in the older leaves, and the leaf senescence is induced when the auxin levels in the leaf decline sufficiently to match the auxin levels in the stalk (Shoji *et al.* 1951). The evolvement of auxin in this process can be traced through the phenotypes of some of the auxin biosynthesis and signalling pathway components. The YUCCA proteins catalyze important step in IAA biosynthesis; an overexpression of YUCCA6 results in increased levels of IAA and causes delay of senescence (Cha *et al.* 2015, Kim *et al.* 2011b). Auxin response Factor 2 (ARF2) is a repressor of auxin signalling and the loss-of-function mutants of *arf2* show delay in leaf senescence (Ellis *et al.* 2005, Lim *et al.* 2010), indicating that ARF2 is a positive regulator of leaf senescence. The activators of auxin signalling ARF7 and ARF19 are induced in senescing leaves and the triple mutant *arf2 arf7 arf19* showed an enhanced delay of the senescence compared to *arf2* single mutant (Ellis *et al.* 2005). Based on the delay-of-senescence effect of auxin, it could be speculated that auxin, similarly to cytokinin, is a negative regulator of leaf senescence.

Another aspect of plant development controlled by auxin is the phototropic response. Plants are able to sense and differentiate between different light conditions and orient their growth accordingly. In particular, seedlings are able to display positive phototropism towards blue light in hypocotyl (Sakai and Haga 2012). This reaction is mediated by the blue light photoreceptors phototropins. Phototropins are serine/threonine kinases which bind a blue-light absorbing chromophore; they undergo autophosphorylation in response to blue light and initiate a signal transduction cascade that results in a phototropic response (Christie *et al.* 2015). Ultimately, this signalling pathway causes auxin redistribution in hypocotyl leading to increased auxin accumulation on the shaded side (Esmon *et al.* 2006, Hohm *et al.* 2014). The accumulated auxin stimulates increased hypocotyl elongation on the shaded side compared to the lighted side and induces directional hypocotyl bending response. This auxin-induced reorganisation of the hypocotyl growth is thought to be mediated by ARF7 because of the disrupted phototropic response in the *arf7* mutant (Harper *et al.* 2000, Liscum and Briggs 1996). ARF7 is able to differentially induce a small subset of target genes at opposing hypocotyl flanks including the members of expansin family (EXPA1 and EXPA8) which regulate cell wall extension (Esmon *et al.* 2006). The involvement of auxin in phototropic response towards blue light is well-

studied. Contrary to auxin, cytokinin has not been described as an important hormone in phototropic responses.

In this chapter, the potential antagonistic or synergetic interactions between auxin and cytokinin signalling pathways are investigated in various aspects of plant development including leaf senescence, phototropic response of hypocotyl and the maintenance of the root apical meristem, and the role of the transcriptional regulation of ARF7 by CRF10 in these processes is evaluated. The investigation is based on the developmental phenotypes of the *crf10* mutant which include early senescence of leaves, reduced response to blue light in hypocotyl and disorganized structure of the RAM.

Results

Genetic characterization of the *crf10* mutant

The second chapter of this thesis described identification of transcription factors which control expression of ARF activators. One of the regulatory transcription factors, the Cytokinin Response Factor 10 (CRF10), was identified as a transcriptional regulator of ARF7. The subsequent protoplast assay showed that CRF10 acts as a repressor of ARF7 transcription in the leaf mesophyll protoplasts (Fig. 2-4 and 2-7). CRF10 is a member of the Cytokinin Response Factors gene family which act in the cytokinin signaling pathway. Several members of the CRF gene family have been analyzed in details (see Introduction) but CRF10 is not amongst them. The closest homologues of CRF10 are CRF11 and CRF12 which have not been analyzed either (Fig. In-14A).

The CRF10 protein contains 324 amino acids. It consists of the structural domains characteristic for the members of the CRF gene family: the N-terminal CRF domain responsible for protein-protein interactions (ca. amino acids 40-74), followed by the AP2 DNA-binding domain (ca. amino acids 111-170) (Fig. 3-1A). Several members of the CRF gene family were shown to contain a conserved MAP kinase phosphorylation site (SP(T/V)SVL) (Rashotte and Goertzen 2010), but CRF10 contains only a truncated version of this site (SPV followed by VPV) suggesting that this site is not functional. In addition, a comparison of CRF10 protein structures across multiple *Arabidopsis thaliana* ecotypes was conducted in this thesis. This comparison helped to identify strongly conserved amino acids. An additional conserved region was found in the CRF10 gene: the C-terminal conserved region (defined as CCR in this thesis) between amino acids 285 and 324 (Fig. 3-1A).

A T-DNA insertion mutant for CRF10 was isolated from public mutant libraries (SALK_084716C) and confirmed to contain a homozygous insertion inside the CRF10 gene. It was designated as *crf10-1* mutant in this thesis. The T-DNA insertion site was predicted to be at the C-terminus of the CRF10 gene. The precise T-DNA insertion location was identified by amplifying and sequencing the genomic DNA at the CRF10 locus in the *crf10-1* mutant background. This analysis indicated that T-DNA has two left borders which suggest that it is an inverted tandem repeat of the T-DNA (Wei *et al.* 2015). The insertion site was after the amino acid 296 inside the

conserved C-terminal domain with unknown function (Fig. 3-1A). qRT-PCR was used to confirm the mutation: the primer pair binding before the T-DNA insertion site showed normal levels of CRF10 mRNA whereas the primer pair spanning the insertion site showed absence of CRF10 mRNA (Fig. 3-1A). Overall this genetic analysis showed that a truncated CRF10 mRNA is still produced. This may include the 5-prime region of the CRF10 mRNA, the coding sequence of CRF10 up to the T-DNA insertion site and some the T-DNA sequences. From the sequences it can be predicted that the resulting mRNA could be transcribed into a chimeric protein

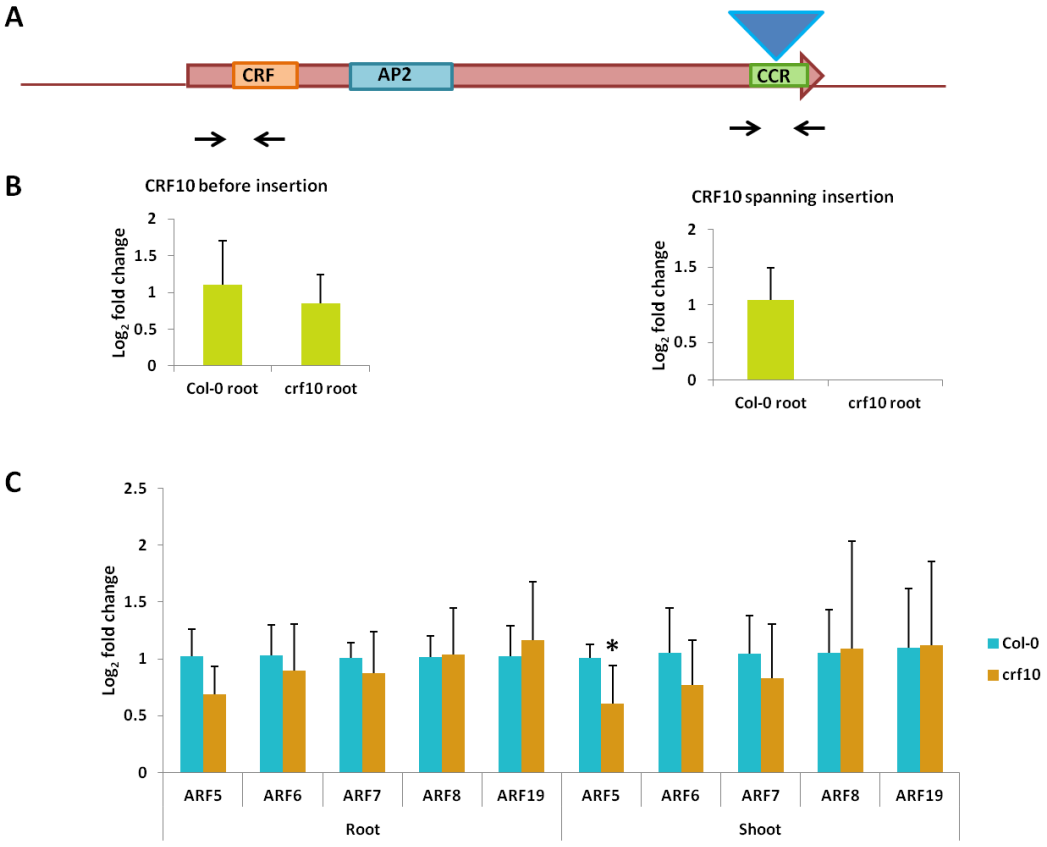

Fig. 3-1. Characterization of the *crf10-1* mutant. **(A)** Schematic representation of the CRF10 locus with T-DNA insertion site marked as a blue triangle. The conserved domains are marked: AP2, CRF and the C-terminal conserved region (CCR). Black arrows indicate qRT-PCR primer binding sites. **(B)** Expression of CRF10 in the wild-type and the *crf10-1* mutant background. Two primers pairs were tested binding before and spanning the T-DNA insertion. **(C)** Expression of ARF activators in the root and the shoot of 7-days old seedlings in the wild-type and *crf10-1* mutant plants. Mann-Whitney U test was used to calculate significance with *p < 0.1.

containing an incomplete CRF10 coding sequence up to and including the amino acid 296 fused to 39 additional amino acids from the T-DNA. It remains unclear if such a chimeric protein could be functional.

Alternative mutants with a T-DNA insertion in the CRF10 gene are not available from the public T-DNA collections. I thus generated CRISPR mutants using RNA guides designed to introduce a mutation close to the 5' of the CRF10 coding sequence. By the time of writing this thesis, homozygous mutants were being selected but were still growing and not available for analysis. In this work I focus on the *crf10-1* mutant.

Arabidopsis thaliana T-DNA insertion mutant can contain multiple T-DNA insertions scattered around the genome (Krysan *et al.* 1999, Wei *et al.* 2015). Often the additional T-DNA insertions remain undetected because the genotyping efforts only follow the segregation of the known T-DNA. The undetected additional T-DNA insertions could affect gene expression in the mutant line and cause a phenotype which could be falsely contributed to the known T-DNA insertion. For this reason it is important to try to identify additional T-DNA insertions in each mutant line. For several SALK lines public information is available on potential off-target T-DNA insertions. The SALK_084716 line was indeed reported to contain 3 different T-DNA insertions: in the CRF10 gene (AT1G68550), in the non-coding intergenic region between AT1G55950 and AT1G55960, and in the coding sequence of AT1G26190 (Table 3-1). Genotyping confirmed homozygous insertions for two of these T-DNA: in the CRF10 and the intergenetic region between At1g55950 and At1g55960. The third T-DNA insertion in the coding region of At1g26190 was not detected at all. These results don't exclude the possibility that there could be other as yet undetected T-DNA insertions within the genome. In summary, the phenotypic results for the *crf10-1* mutant are still preliminary and should be taken with caution. The phenotypes

	Insertion site	In my mutant	Description
1	AT1G68550 coding sequence	homozygous	CRF10 gene
2	Intergenic region between AT1G55950 and AT1G55960	homozygous	AT1G55950 is a DNA-binding storekeeper protein-related transcriptional regulator. At1g55960 is a polyketide cyclase/dehydrase and lipid transport superfamily protein.
3	AT1G26190 coding sequence	absent	triphosphate tunnel metalloenzyme

Table 3-1. Potential T-DNA insertions inside the *crf10-1* mutant.

should be confirmed in the future experiments using alternative CRISPR mutants as well as back-crossed *crf10-1* mutants.

The regulatory potential by CRF10 of ARF7 transcription was confirmed using transient protoplast assay (Fig. 2-4 and 2-7). Further confirmation could be obtained using the DNA affinity purification sequencing (DAP-seq) database which provides information on binding sites of multiple transcription factors in *Arabidopsis thaliana* genome (O'Malley *et al.* 2016); this method is briefly described in chapter II. In the DAP-seq data CRF10 shows strong background peaks in ARF7 promoter but no

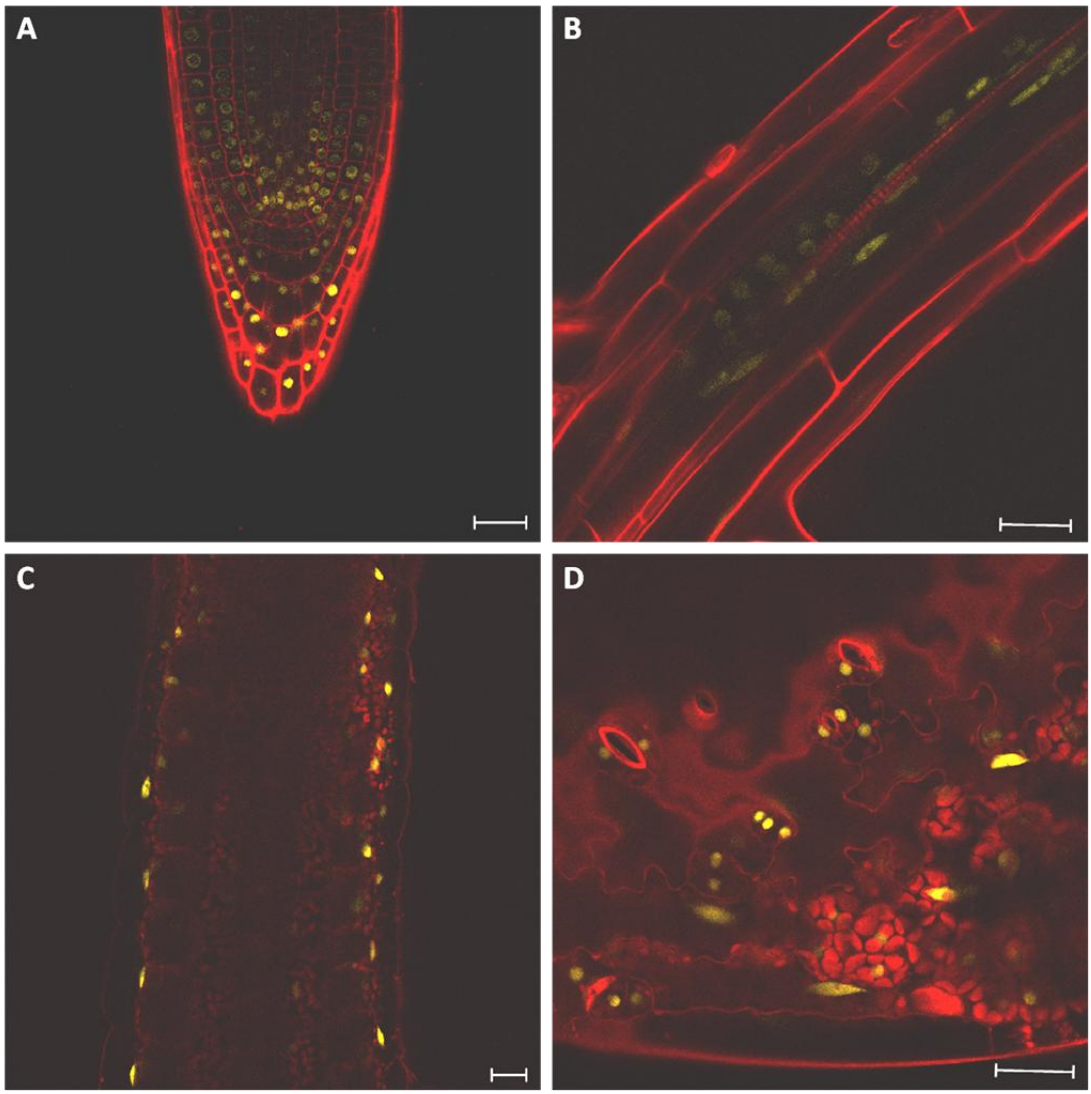

Fig. 3-2. Expression of CRF10 in the meristematic zone of the primary root **(A)**, in the lateral root primordia **(B)**, in the hypocotyl **(C)** and in the leaves **(D)**. The plants were grown in 16h light/8h dark conditions for 5 days. Bar scale 25 µm.

clear single peak is visible (Suppl. Fig. 3-1A); thus this interaction cannot be confirmed using DAP-seq. The consensus binding site suggested by the DAP-seq for CRF10 is GGCGG (Suppl. Fig. 3-1B). Such a sequence is found in ARF7 promoter at position -217 bp before the start codon. One can conclude that the direct binding of CRF10 to ARF7 promoter should be confirmed in future experiments for example by using ChiP assay.

The expression of ARF activators in the *crf10-1* mutant background was studied using qRT-PCR in the whole root and the whole shoot tissues of 7 days old seedling (Fig. 3-1C). The expression of ARF7 was not significantly affected under these growth conditions at this whole-tissue level. However, ARF5 expression was reduced in the mutant background (Fig. 3-1C).

CRF10 is expressed in various tissues

CRF10 gene is strongly expressed in multiple tissues (Suppl. Fig. 3-2). In the root the expression is limited mostly to the meristematic zone as indicated with the publically available microarray datasets (Suppl. Fig. 3-2).

In order to access CRF10 expression on a more cell-specific level, transcriptional reporter line was generated harboring 4000 bp promoter regions fused to the

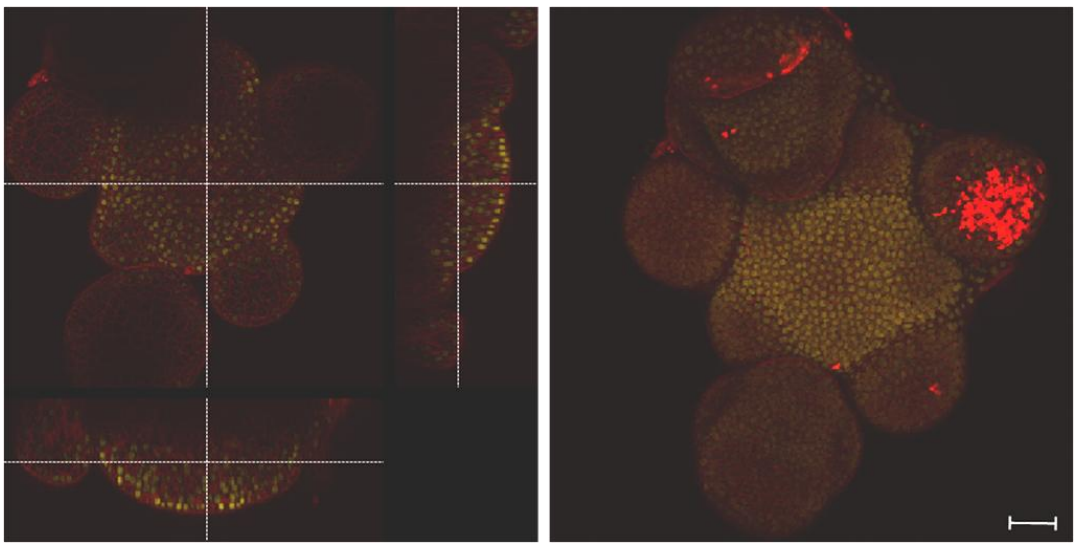

Fig. 3-3. Expression of CRF10 in the shoot apical meristem. Bar scale 25 µm.

nuclear-localized mVenus fluorescent reporter. CRF10 was found to be strongly expressed only in the meristematic zone of the root; here it was enriched in all cells except the QC and columella initial layers (Fig. 3-2A). In the older part of the root, CRF10 was barely expressed in the vasculature but strongly in lateral root primordia (Fig. 3-2B). In addition to the root, CRF10 showed strong expression in the epidermal layer of the hypocotyl (Fig. 3-2C) and in the stomata guard cells of the leaves (Fig. 3-2D). CRF10 was also broadly expressed in the dome structure of the shoot apical meristem encompassing the central and peripheral zones (Fig. 3-3). The expression was strongest in the L1 layers and declining progressively in the deeper layers (Fig. 3-3).

The gene expression studies do not provide information on post-transcriptional protein localization of the gene. To study the CRF10 protein localization, a translational reporter line was generated harboring 4000 bp CRF10 promoter driving the CRF10 protein fused to the mVenus fluorescent reporter at the C-terminus (pCRF10:CRF10-mVenus). The translational reporter was transformed into both the Col-0 and the *crf10-1* mutant backgrounds. The CRF10 protein was barely detected in the root tip even at the highest laser intercity (Fig. 3-4). This result was identical for the reporter line inserted in Col-0 and *crf10-1* mutant backgrounds. Nevertheless,

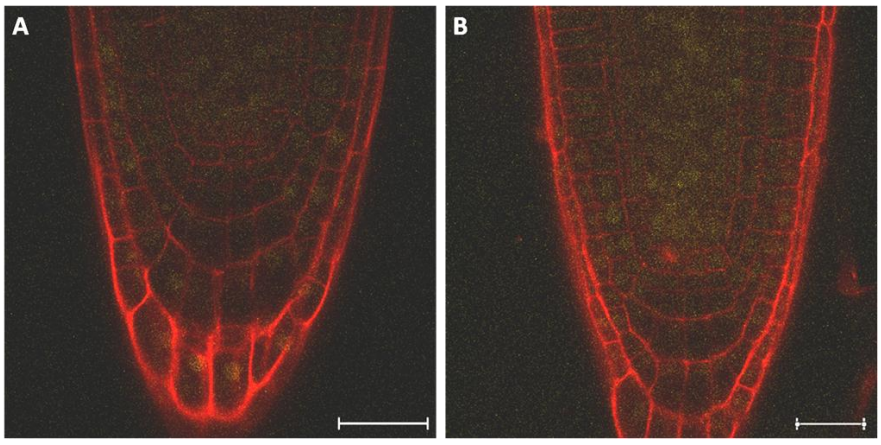

Fig. 3-4. CRF10 protein localization reporter with the pCRF10:CRF10-mVenus translational reporter line. The construct was inserted in Col-0 background **(A)** and *crf10-1* background **(B)**. Bar scale 25 µm.

the actual protein localization pattern appeared to be similar to the expression pattern in the root tip (Fig. 3-2A and Fig. 3-4). The difficulty to visualize the protein localization could be explained by a possible natural low abundance of the CRF10 protein. On the other hand, the C-terminal fusion between the CRF10 and the mVenus could interfere with the protein folding rendering it dysfunctional and more prone to degradation. The functionality of this line could be verified by looking if this line complements *crf10-1* mutant phenotypes.

Expression of the several members of the CRF gene family is upregulated after cytokinin treatment (Rashotte *et al.* 2006); this property prompted researches to name the whole gene family the Cytokinin Response Factors. The publically available microarray datasets showed that the expression of CRF10 is not changing in response to cytokinin treatment in the root tissue (Yokoyama *et al.* 2007), or the whole seedlings (Lee *et al.* 2007, AtGenExpress hormone treatment data from

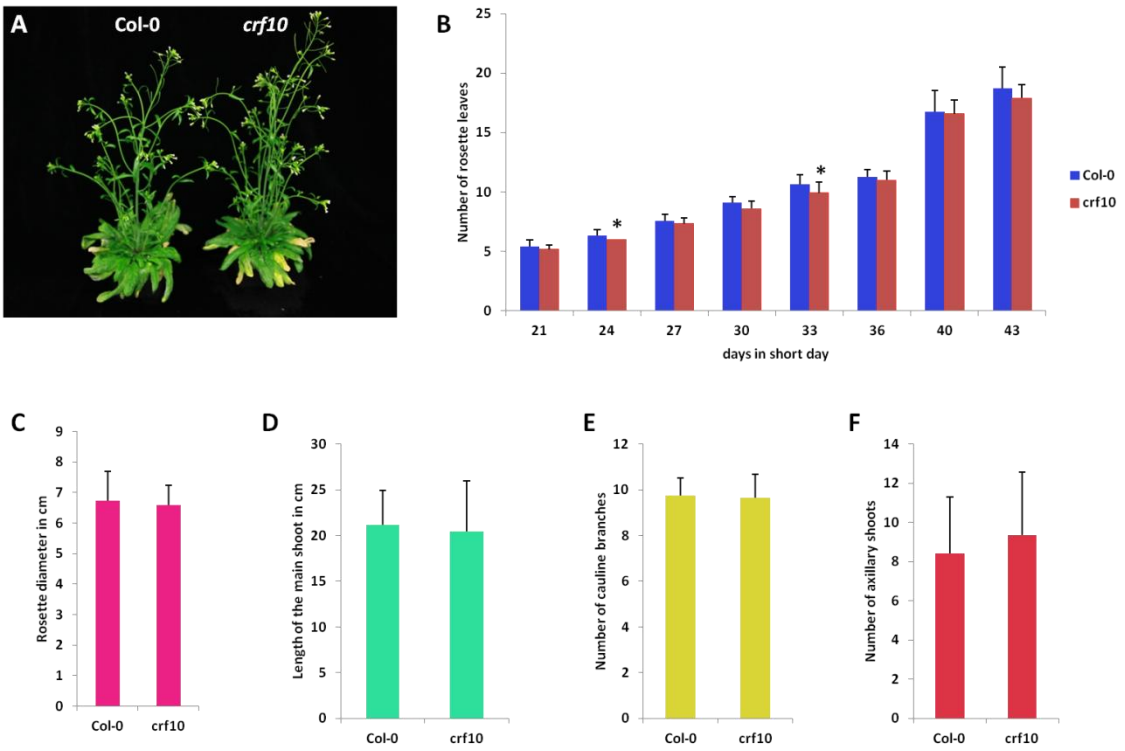

Fig. 3-5. Shoot growth analysis of the *crf10-1* mutant. The number of rosette leaves at 21-43 days growing in 8h light/16h dark conditions **(B)**. The rosette diameter at 43 days in 8h light/16h dark conditions **(C)**. Plants grown in the 8h light/16h dark for 43 days and then further at 16h light/8h dark for 21 days: images of the plants **(A)**, length of the main stem **(D)**, number of cauline branches growing from the main stem **(E)** and the number of axillary branches growing from the rosette **(F)**. n = 12 plants. The unpaired t-test test was used to calculate significance with *p ≤ 0.05.

Shimada lab). To confirm these results roots of 5 days old seedlings harboring pCRF10-mVenus transcriptional reporter were treated with 5 µM BAP for 30 min or 2h. Neither the expression intensity nor the expression pattern changed in response to the treatment (Suppl. Fig. 3-3). These results confirm that CRF10 expression is not induced by cytokinin in the RAM.

crf10 mutant has an ARF7-dependant early senescence phenotype

The *crf10-1* mutant was analyzed for defects in shoot growth and development. The mutant displayed small but statistically significant reduction in the number of rosette leaves produced when growing in short-day conditions (8h light/16h dark) (Fig. 3-5). Other growth parameters were not significantly different from wild-type including length of the main stem, number of cauline branches, number of axillary branches

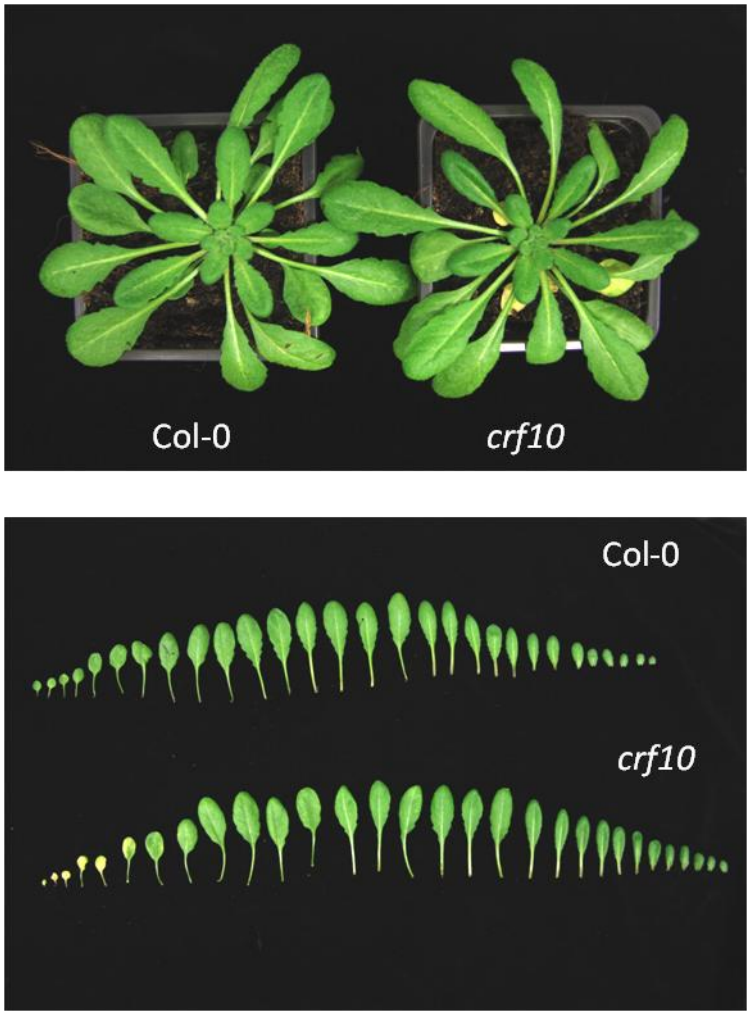

Fig. 3-6. Early leaf senescence phenotype of the *crf10-1* mutant. Images of the Col-0 and *crf10-1* plants grown at 8h light/16h dark conditions for 45 days.

(Fig. 3-5). The most prominent phenotype displayed by the mutant was early senescence of leaves; by 45 days in the short-day growth conditions the mutant contained numerous yellow leaves whereas the wild-type plants had no senescing leaves (Fig. 3-6).

As the CRF10 transcription factor was identified as a regulator of ARF7 expression in the yeast one-hybrid and the protoplast assays, I also investigated the role for ARF7 in this process. The *arf7-1* mutant displays a leaf-related phenotype: the mutant plants have epinastic leaves with elongated petioles and smaller rosette size (Fig. 3-7A and C). The mutant of ARF19, an ARF activator closely related to ARF7, displays no obvious leaf-related phenotype (Fig. 3-7A and C). The double mutant *arf7-1 arf19-*

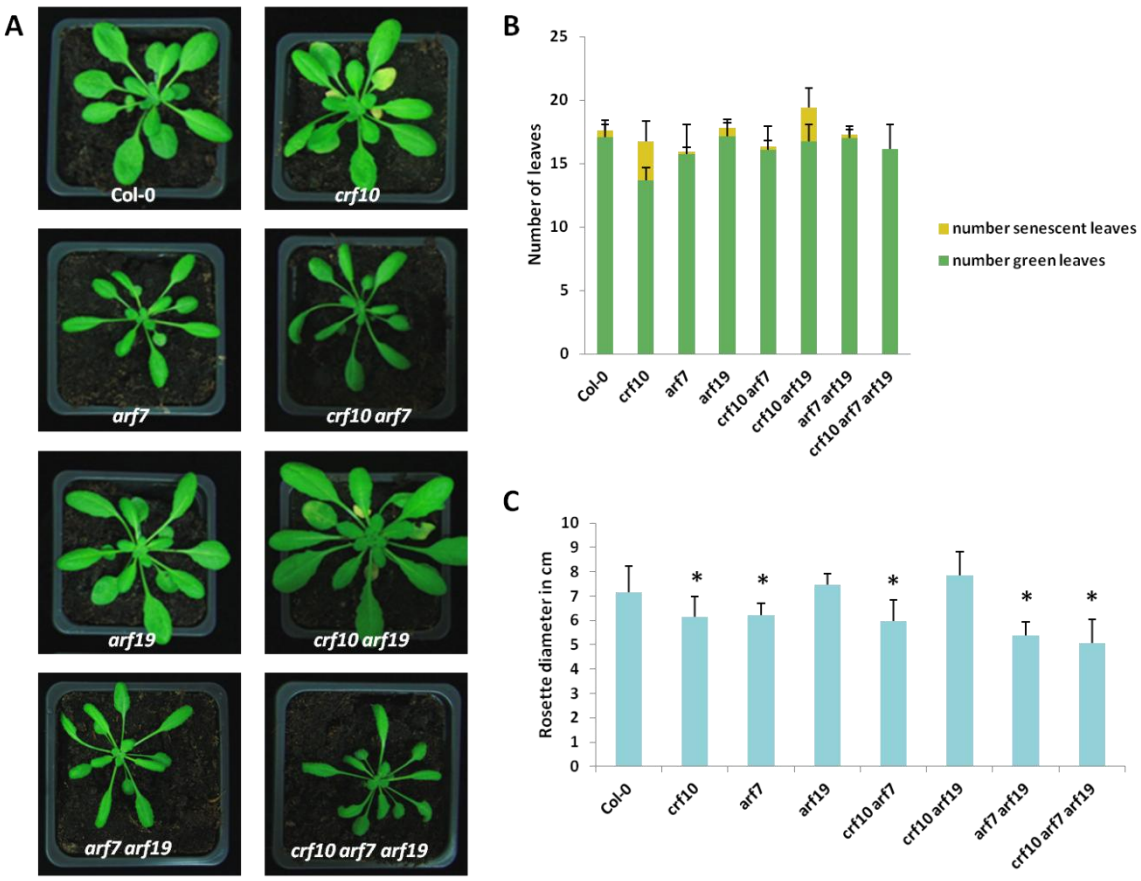

Fig. 3-7. The phenotypes of the *crf10, arf7*, *arf19* single, double and triple mutants grown for 45 days in 8h light/16h dark conditions. Images of the rosette **(A)**, the number of green and senescent leaves **(B)** and the rosette size **(C)**. n = 12 plants. The unpaired t-test test was used to calculate significance with *p ≤ 0.05.

1 shows phenotype similar to the *arf7-1* single mutant but with a stronger reduction of the rosette size (Fig. 3-7A and C).

To identify the potential cross-talk between CRF10 and ARF7 during leaf development, double mutants *crf10-1 arf7-1, crf10-1 arf19-1*, and the triple mutant *crf10-1 arf7-1 arf19-1* were created (Fig. 3-7). The early senescence phenotype of the *crf10* single mutant was retained in the *crf10 arf19* double mutant (Fig. 3-7B). On the contrary, the double mutant *crf10 arf7* lacked early senescence phenotype and displayed the epinastic leaf phenotype of the *arf7* single mutant (Fig. 3-7A and B). The triple mutant *crf10 arf7 arf19* showed phenotype similar to *arf7 arf19* double mutant with epinastic leaves, reduced rosette size and lack of early senescence (Fig. 3-7). These results imply that the *crf10* early senescence phenotype is dependent on the presence of a functional ARF7 gene but independent from ARF19 gene.

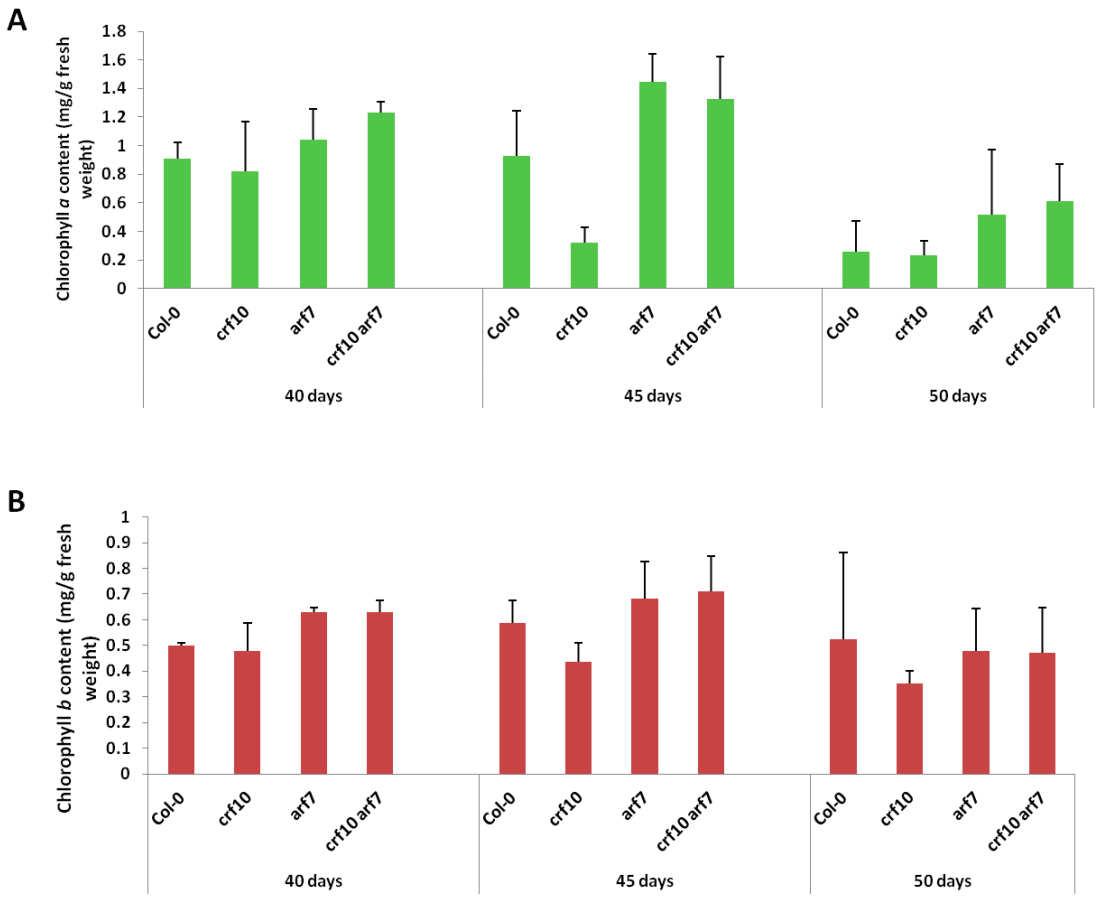

Fig. 3-8. Chlorophyll content in the leaf 3 of the wild-type, *crf10*, *arf7* and *crf10 arf7* plants grown for 40, 45 or 50 days in 8h light/16h dark conditions. **(A)** Amount of chlorophyll *a* in mg per g fresh weight. **(B)** Amount of chlorophyll *b* in mg per g fresh weight. n = 3 plants.

To confirm that the observed yellowing of the leaves corresponds to senescence, the chlorophyll content was measured in the leaf 3 (counting from the oldest) of the wild-type, *crf10, arf7* and the *crf10 arf7* mutants at 40, 45 and 50 days of growth. The chosen time points correspond to the time before (40 days) and after (45 and 50 days) the leaf 3 is displaying visible yellowing in the *crf10* mutant background. On the other hand, the wild-type plants display yellowing of the leaf 3 only at 50 days. The *arf7* and *crf10 arf7* mutants retained green color in leaf 3 even at 50 days old. In accordance with the observations, the yellowing was accompanied by decrease in chlorophyll *a* and chlorophyll *b* content in the *crf10* mutant at 45 days whereas in the wild-type plants the chlorophyll *a* content was reduced later at 50 days (Fig. 3-8), thus confirming a difference in senescence timing. The *arf7* and *crf10 arf7* mutants displayed delay in chlorophyll *a* degradation compared to wild-type (Fig. 3-8).

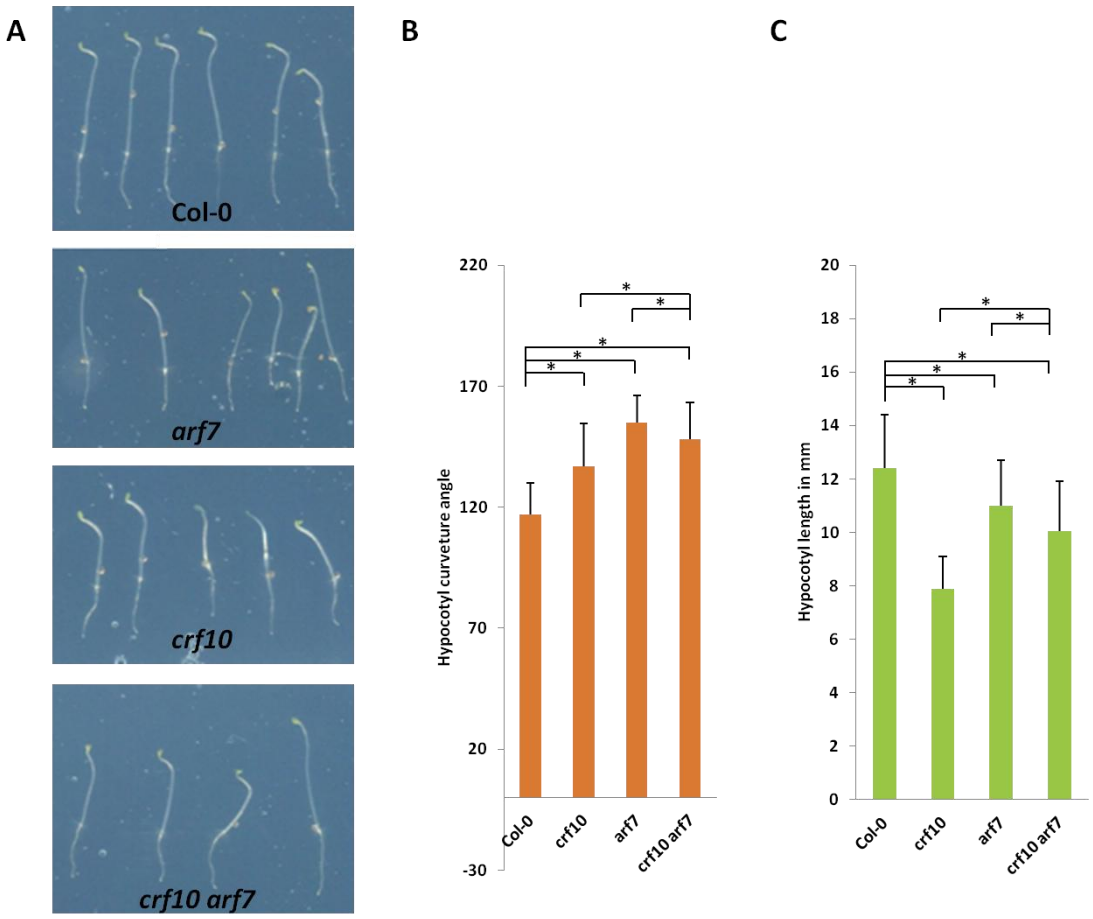

Fig. 3-9. Hypocotyl growth orientation in response to blue light in the wild-type, *arf7-1*, *crf10-1* and *arf7-1 crf10-1* plants. Seedlings were grown for 4 days in the dark and then exposed to blue light for 7h **(A)**. Hypocotyl bending angle **(B)** and the hypocotyl length **(C)** were measured. N ≥ 40. The unpaired t-test test was used to calculate significance with *p ≤ 0.05.

In summary, the *crf10-1* mutant shows early senescence of leaves accompanied by chlorophyll degradation; this phenotype is dependent on the presence of a functional ARF7 gene but independent from ARF19.

The closest homologues of CRF10 gene are CRF11 and CRF12. *crf11* and *crf12* mutants were analyzed for early senescence phenotypes. Neither *crf11* nor *crf12* single mutants displayed early senescence of leaves (Suppl. Fig. 3-4). Nevertheless, the *crf12* mutant showed other leaf-related phenotype: the leaves are flatter, even slightly curling upwards and the rosette size is reduced (Suppl. Fig. 3-4A). The double mutants *crf10 crf11* and *crf10 crf12* were made but were not yet analyzed at the time of writing this thesis.

crf10 mutant shows perturbation in hypocotyl response to blue light

The ARF7 gene was originally identified as a regulator of plant growth due to its disrupted phototropic response (Liscum and Briggs 1996). Dark-grown *arf7* mutants are unable to bend their hypocotyls towards the blue light (Harper *et al.* 2000) (Fig. 3-9A and B).

In order to analyze genetic interaction between ARF7 and CRF10 in this process, the *crf10-1* mutant was examined for defects in hypocotyl response towards the blue light. The *crf10-1* mutant showed a reduced response compared to the wild-type even through it was not as strong as in the *arf7-1* mutant (Fig. 3-9A and B). The double mutant *crf10-1 arf7-1* showed slightly weaker defects in hypocotyl orientation compared to the *arf7-1* single mutant (Fig. 3-9A and B).

In addition, *crf10* has a significantly shorter hypocotyl length (Fig. 3-9C). The hypocotyl length of the *arf7-1* mutant was reduced compared to the wild-type but longer than in the *crf10* mutant. The double mutant had an intermediate phenotype between the two single mutants (Fig. 3-9C).

To investigate if CRF10 could influence expression of ARF7 in this response, the expression of ARF7 was investigated using pARF7-mVenus transcriptional reporter line. The seedlings were grown for 4 days in the dark before being induced by the blue light for 7h. Images were taken at the site of the hypocotyl bending (Fig. 3-10). The results are preliminary because this experiment was done only once. ARF7 was expressed only in a few epidermal cells both at the lighted and the shaded side

showing no apparent preferential expression for either side (Fig. 3-10A). In the *crf10-1* mutant this expression pattern was unchanged (Fig. 3-10B).

In summary, both ARF7 and CRF10 appear to be involved in the hypocotyl reorientation response towards blue light. How CRF10 and ARF7 interact in this response remains incompletely understood and requires further experiments.

crf10 mutant has a defect in root apical meristem morphology

Several members of the Cytokinin Response Factor gene family including CRF2, CRF3 and CRF6 show root-related developmental phenotypes in the mutants (Jeon *et al.* 2016, Simaskova *et al.* 2015). In order to unravel a potential role of CRF10 in the root development, the *crf10-1* mutant was examined for root growth and development defects (Fig. 3-11). The primary root length was only slightly different to the wild-type (Fig. 3-11B). The length of the meristematic zone of the root (Fig. 3-11D) containing actively dividing cells was measured and the number of the cortex cells in this zone was counted (Fig. 3-11E and F); *crf10-1* mutant appears to have a slightly more cortex cells in the meristematic zone even through the length of the zone was similar to the wild-type. Overall, these results indicate that the growth of the primary root is not strongly affected in the *crf10-1* mutant under normal growth conditions. Surprisingly, when grown on medium supplemented with auxin, *crf10-1*

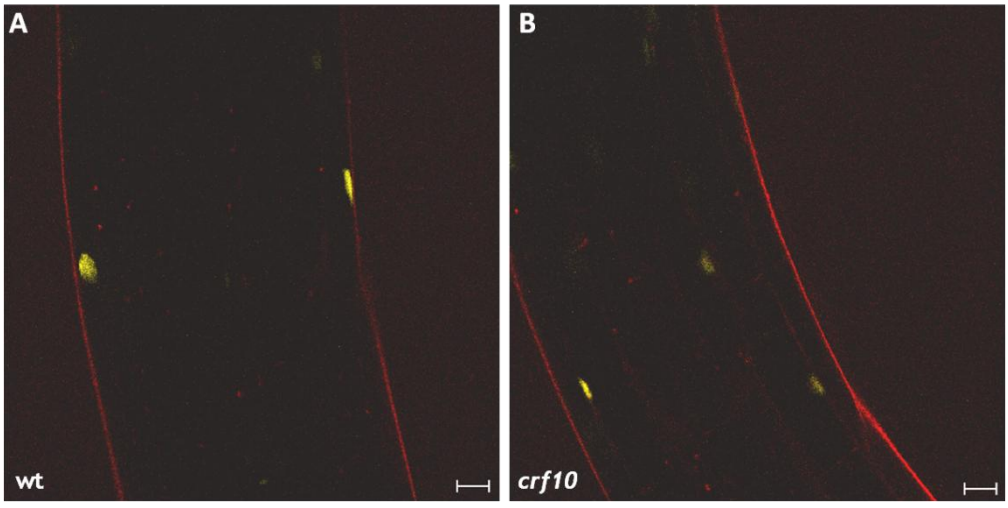

Fig. 3-10. Expression of ARF7 visualized with pARF7-mVenus transcriptional reporter line in wild-type **(A)** and *crf10-1* **(B)** plants. Images showing hypocotyl of the plants grown for 4 days in the dark and exposed to blue light for 7h. Images were taken at the bend of the hypocotyl.

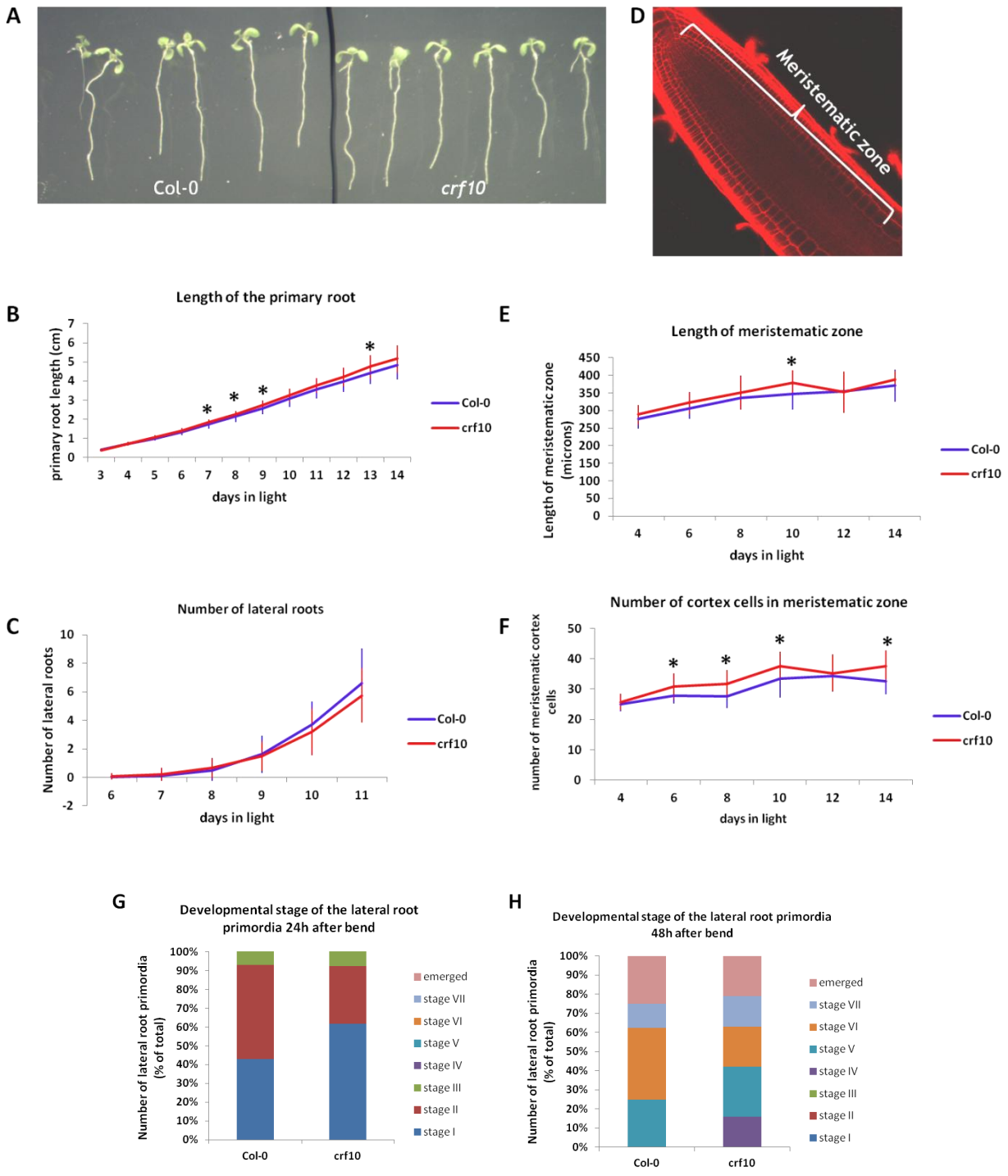

Fig. 3-11. Root growth analysis of the *crf10-1* mutant. Images of the 8 days old plants **(A)**. Length of the primary root **(B)** and the number of lateral roots **(C)**, n = 34**.** Root meristematic zone was measured using confocal images **(D, E)** and the number of the cortex cells in the meristematic zone was counted **(F),** n≥ 14 (except day 14, n≥ 8). Bending assay showing developmental stages of the lateral root primordia 24h and 48h after the bend **(G** and **H)**; n≥ 13**.** Plants were grown in 16h light/8h dark conditions except for the bending assay, which was performed at 24h light conditions. The unpaired t-test test was used to calculate significance with *p ≤ 0.05.

mutant has significantly reduced length of the primary root after 15 days of growth (Table 2-4 and Suppl. Fig. 2-4) indicating increased sensitivity to auxin. The mutant showed normal gravitropic response (Suppl. Fig. 2-5).

Lateral root emergence was also analyzed by counting the number of lateral roots (Fig. 3-11C), and I did not find statistically significant differences. The timing of lateral root development was then studied with a bending assay. In this assay, 3-days old plants grown on a solid medium are rotated at 90°; this rotation induces initiation of a lateral root at the bend (Peret *et al.* 2012a). For each seedling, the developmental stage of the lateral roots was identified at 24h and 48h after the stimulus according to Peret *et al.* 2009. At 24h and 48h after the bend, lateral roots in the *crf10-1* mutant

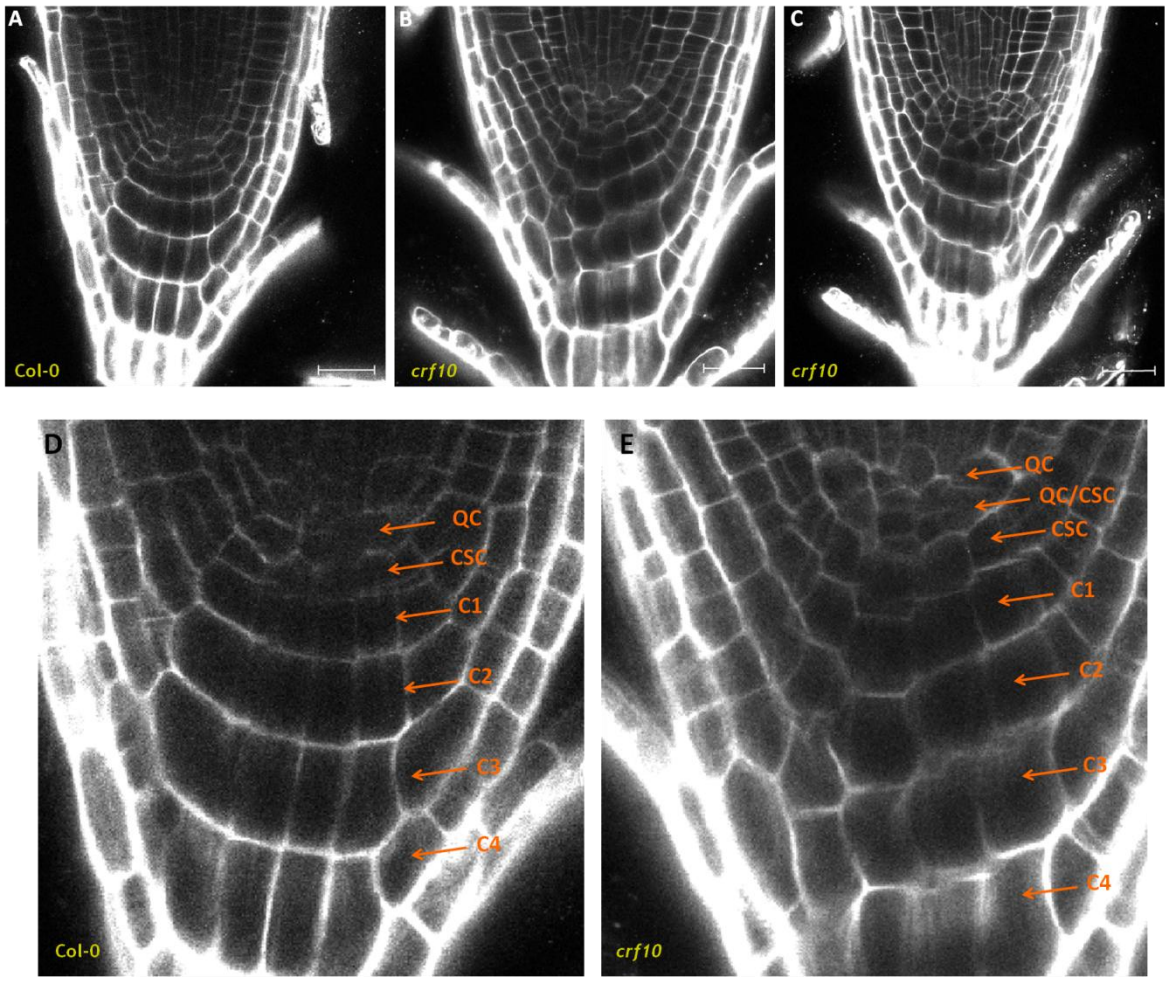

Fig. 3-12. Root apical meristem of the wild-type **(A, D)** and the *crf10* mutant **(B-C, E)**. Arrows indicate layers of the proximal meristem: QC = quiescent center, CSC = columella stem cell layer, C1-4 = columella layers 1 to 4. Plants were grown for 8 days in 24h light conditions in Nottingham. Bar scale 25 µm.

were often at the younger stage of development compared to the wild-type (Fig. 3-11G and H). These results indicate that lateral root emergence or development is slower in the mutant compared to the wild-type.

Interestingly, the *crf10-1* plants had defects in the root apical meristem morphology. It appeared that cells at the QC and columella stem cell (CSC) positions were more disorganized compared to normally well-organized rows of cells in the wild-type (Fig. 13-2 A-C). The cells of the QC, columella stem cell layer, upper columella layers and sometimes the lateral root cap/epidermis initials often had abnormal shape in the mutant. On closer examination, a difference was detected in the number of layers at the QC and CSC positions: if normally the wild-type plants contain a single QC and a single CSC layer (Fig. 3-12D), the *crf10-1* mutants often contained three cell layers at this position (Fig. 3-12E). Morphologically, it looked like the *crf10-1* mutant might contain a double QC layer and a single CSC layer, or, alternatively, a single QC layers followed by a double CSC layer (Fig. 3-12E). This phenotype was visible after 6 days growth in 24h light or after 7 days in 16h light/8h dark growth conditions.

The above-described phenotype of disorganization in the QC and CSC layers was strong in Nottingham in 24h light or 16h light/8h dark growth conditions. On the other hand, when grown in the laboratory in Lyon under 16h light/8h dark conditions the phenotype was much weaker with some *crf10-1* mutant plants showing normal RAM architecture. This raised questions about reproducibility of the phenotype. It is important to note that the experiment presented in Fig. 3-12 was conducted in Nottingham at 24h light conditions; all the other experiments in Fig. 3-13 to 3-17 were conducted in Lyon at 16h light/8h dark conditions. Currently, double mutants *crf10 crf11* and *crf10 crf12* were made but not analyzed yet; potentially these mutants might increase the strength of the *crf10* single mutant phenotype.

The disorganized proximal meristem observed in the *crf10-1* mutant raised a question if this growth defect could affect the function of the columella cells. The mature columella cells contain starch granules which can be detected with a Lugol's staining. The presence of the starch granules was analyzed in the c*rf10-1* mutant (Suppl. Fig. 3-5). In the mutant as well as in the wild-type mature columella cell layers contain starch granules indicating completed differentiation and normal functionality. No apparent agravitropic response associated with the lack of starch granules was

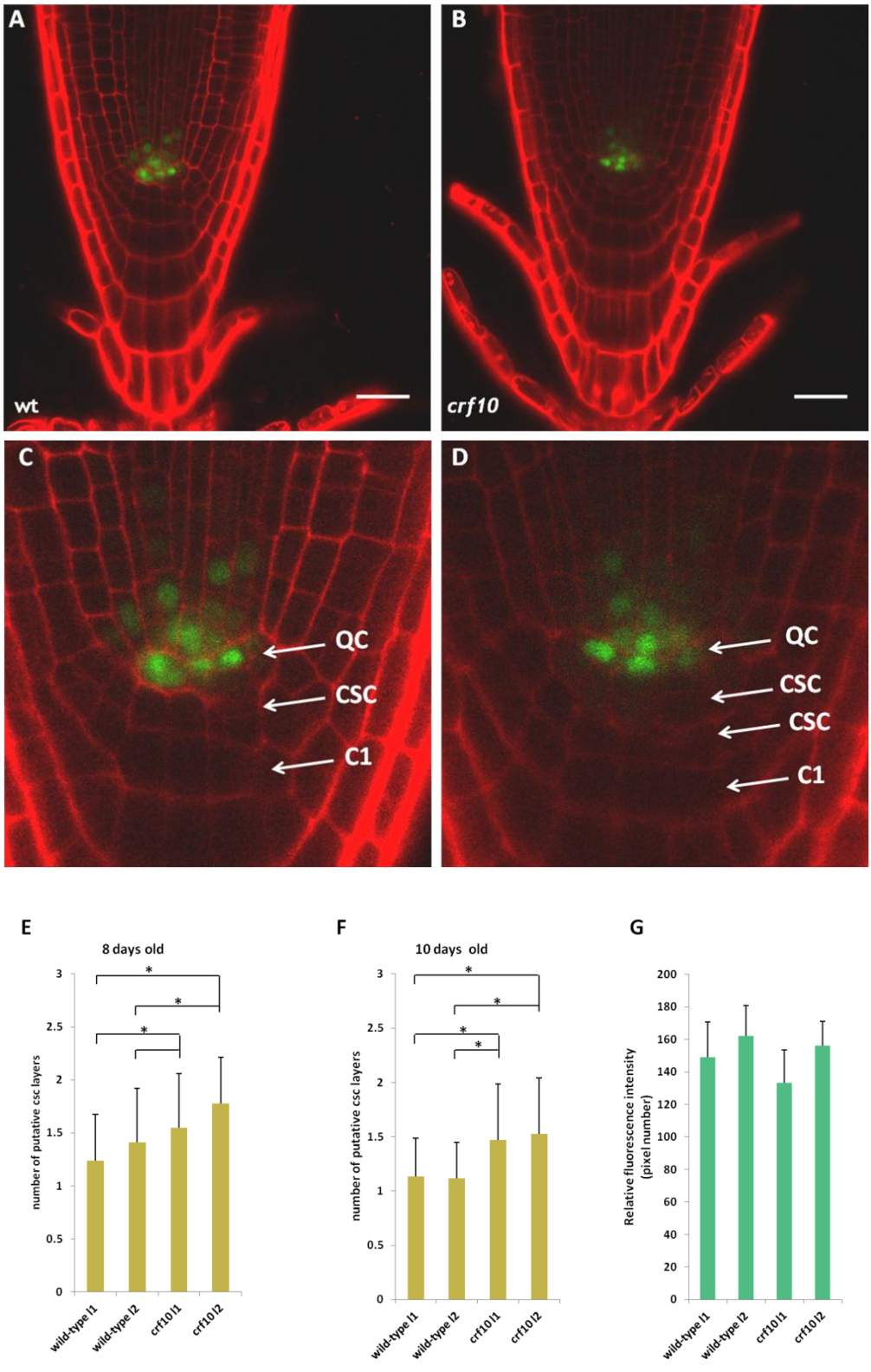

Fig. 3-13. pWOX5-GFP marker line expression in the wild-type **(A)** and the *crf10-1* **(B)** mutant. Arrows indicate layers of the proximal meristem: QC = quiescent center, CSC = columella stem cell layer, C1 = columella layers 1. Number of putative CSC cell layers in pWOX5-GFP plants at 8 days **(E)** and 10 days **(F);** n ≥ 15. GFP fluorescence intensity in 8 days pWOX5-GFP old plants **(G)**; n ≥ 18. Two wild-type and two mutant lines were analyzed (L1 = line 1, l2 = line 2). Plants were grown at 16h light/8h dark conditions in Lyon. The unpaired t-test test was used to calculate significance with *p ≤ 0.05. Bar scale 25 µm.

observed in the *crf10-1* mutant (Suppl. Fig. 2-5). In summary, the mature columella cells do not display obvious developmental defects.

The additional cell layer observed in the mutant could be a second QC layer containing undifferentiated stem cells or a layer with CSC identity. To differentiate between these possibilities, the pWOX5-GFP marker was introduced in the *crf10-1* mutant. WOX5 was shown to be expressed specifically in the QC cell (Sarkar *et al.* 2007). Indeed, in the young seedlings the pWOX5-GFP expression is limited to QC cells, but in the 8 days old seedlings examined in this study the expression was also strong in the vasculature and cortex/endodermis initials (Fig. 3-13A). Despite that, the pWOX5-GFP expression pattern and signal intensity were identical in the wild-type and the *crf10-1* plants (Fig. 3-13). The additional layer at the QC/CSC position was not marked by pWOX5-GFP indicating that this layer may not be a second QC layer (Fig. 3-13C and D). The second additional layer at the QC position might be then a

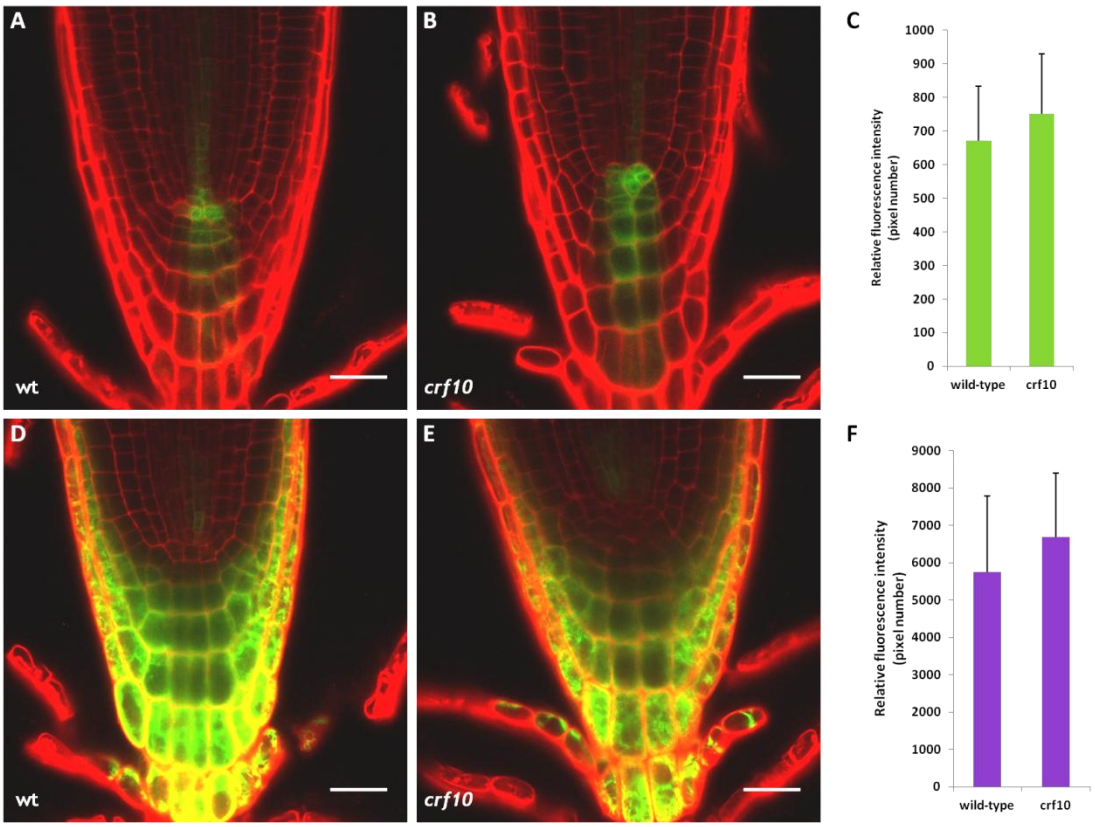

Fig. 3-14. Auxin **(A - C)** and cytokinin **(D - F)** signaling in the RAM of the wild-type and *crf10-1* mutant visualized with the DR5-GFP and TCS-GFP reporter lines respectfully. GFP fluorescence intensity was measured (n ≥ 18) **(C and F)**. Plants were grown for 9 days in 16h light/8h dark conditions in Lyon. The unpaired t-test test was used to calculate significance with *p ≤ 0.05. Bar scale 25 µm.

second CSC identity layer. The number of layers at the putative CSC position (below the pWOX5-GFP marked QC layers and above mature columella layers) was counted in the wild-type and *crf10-1* mutant. Even through the wild-type plants occasionally contained more than one layer at this position, the amount of plants with a double layer was significantly higher in the mutant plant (Fig. 3-13E and F). This suggests that the morphological disorganization of the RAM in the *crf10-1* is based on increased number of cell layers at the columella stem cell position whereas the number of layers with the QC identity remained normal. The result was further validated by looking at the expression of a different QC marker, pSCR:SCR-YFP. SCR protein is found in the QC cells and endodermis (Suppl. Fig. 3-6A). In the *crf10-1* mutant plants this protein localization patterns remained unchanged indicating that the QC and endodermis identity are not disrupted in the mutant background (Suppl. Fig. 3-6B).

Auxin and cytokinin are important regulators of root growth and development. It is therefore conceivable that the disorganization in the proximal meristem could be caused or accompanied by abnormal hormone signaling. This possibility was examined by introducing the auxin signaling reporter DR5-GFP and the cytokinin signaling reporter TCS-GFP into the *crf10-1* mutant. The DR5-GFP expression pattern and intensity were not altered in the mutant background (Fig. 3-14 A-C). Likewise, TCS-GFP showed similar pattern and expression levels in both wild-type and the *crf10* mutant plants (Fig. 3-14 D-F). This suggests that the auxin and cytokinin signaling are not significantly disrupted in the root apical meristem of the *crf10* mutant.

ARF7 is described as a regulator lateral root development (Okushima *et al.* 2005). On the other hand, the role of ARF7 in the development or maintenance of the root apical meristem has not been considered before. However I have shown that ARF7 is expressed in the root apical meristem with strongest expression at the QC position but its expression is absent in the columella stem cells and columella proper (Fig. 1-4A). CRF10 is expressed broadly in the root apical meristem but absent in the QC and columella stem cells (Fig. 3-2A). Thus ARF7 and CRF10 show opposite expression patterns at the QC position but both are absent in the CSC. The compatible expression patterns allow me to speculate that both ARF7 and CRF10 could be involved in RAM development.

To investigate a potential role of ARF7 in the RAM, ARF7 was misexpressed in columella cells using pSMB:ARF7 construct in which ARF7 coding sequence is driven by a columella-specific promoter SMB (Willemsen *et al.* 2008). The control pSMB-mVenus construct containing identical promoter fragment of SMB as the one used in pSMB:ARF7 construct fused to the mVenus fluorescent reporter confirms that this promoter drives expression in the columella and lateral root cap cells but not in

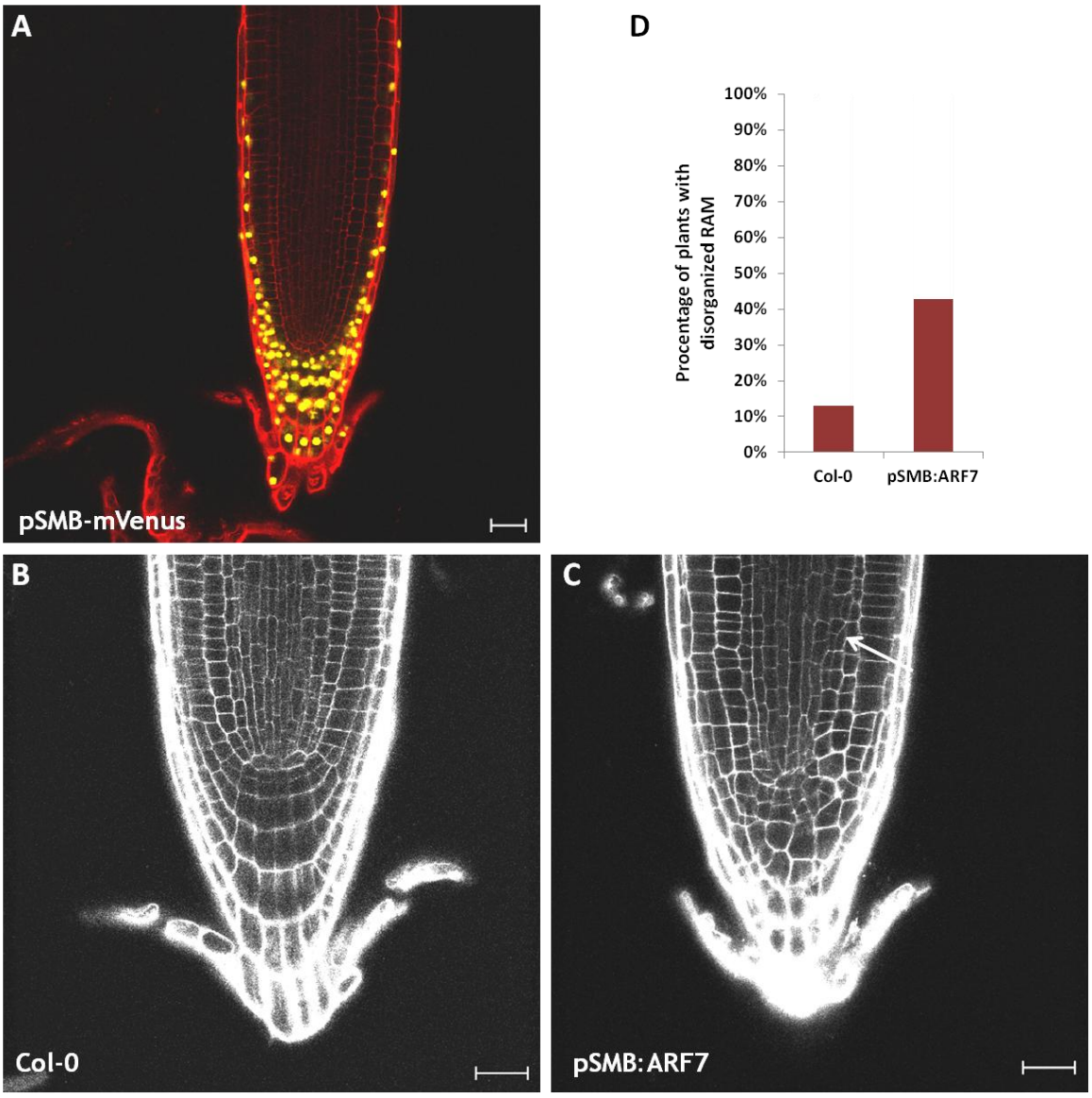

Fig. 3-15. Misexpression of ARF7 in the columella cells under SMB promoter. pSMB-mVenus plants showing expression pattern of the chosen promoter **(A)**. RAM structure in the wild-type **(B)** and the pSMB:ARF7 transgenic plants **(C)**. Arrow indicates abnormal cell division in endodermis layer. Percentage of plants with disorganized RAM in the pSMB:ARF7 line **(D)**. Plants were grown for 9 days in 16h light/8h dark conditions in Lyon. N = 23 roots in Col-0 and 28 roots in pSMB:ARF7. Bar scale 25 µm.

CSC and QC (Fig. 3-15A). As described before, ARF7 is normally not expressed in columella cells thus this experiment shows results of an ectopic expression in proximal meristem. The columella-specific expression of ARF7 resulted in plants that often contained disorganized cellular structure in the QC, CSC and columella region (Fig. 3-15B and C). Nevertheless, not all pSMB:ARF7 plants were affected: 42% of the transgenic plants contained disorganized RAM compared to 13% in the wild-type plants (Fig. 3-15D). In addition, many transgenic pSMB:ARF7 plants displayed abnormal extra periclinal divisions in endodermis layer (Fig. 3-15C). In summary, these results show that misexpression of ARF7 in columella and lateral root cap layers could lead to morphological disorganization in proximal and even distal RAM.

To further investigate the potential interaction between ARF7 and CRF10 in the RAM, the expression of ARF7 was measured using pARF7-mVenus full-length transcriptional reporter line inserted into the *crf10-1* mutant. Preliminary results showed that the fluorescence intensity is approximately 1.4 fold higher in the RAM of the *crf10-1* mutant compared to the wild-type (Fig. 3-16). This experiment was done only once and should be repeated. This result is compatible with the role of CRF10 as a repressor of ARF transcription.

To further investigate the involvement of ARF7 in the control of the RAM morphology, the RAM structure of the *arf7-1* single and *crf10-1 arf7-1* double mutants was examined (Fig. 3-17). Preliminary results (experiment repeated only once) showed no

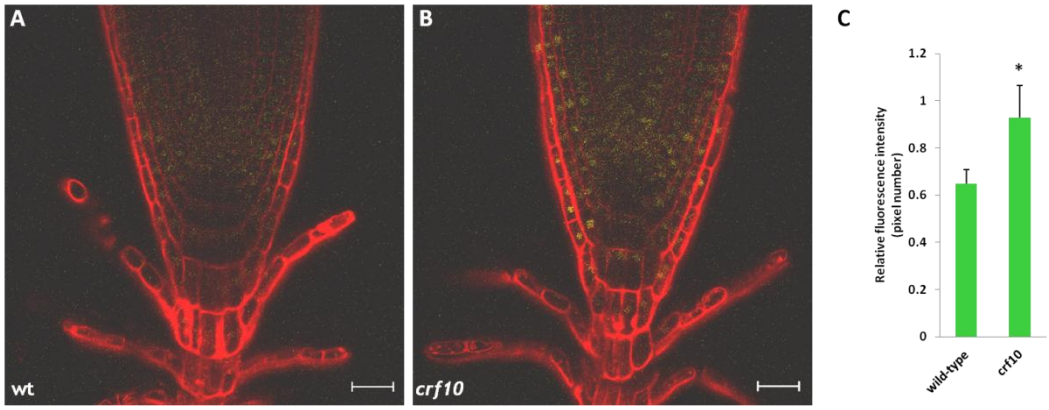

Fig. 3-16. Expression of pARF7-mVenus transcriptional reporter in the root apical meristem of the wild-type **(A)** and *crf10* **(B)** plants. Plants were grown for 8 days in 16h light/8h dark conditions in Lyon. Fluorescence intensity was measured **(C)**. N = 32 roots in the wild-type and 28 roots in *crf10*. The unpaired t-test test was used to calculate significance with *p < 0.0001. Bar scale 25 µm.

abnormally shaped cells in the RAM of the *arf7-1* single mutant and *crf10-1 arf7-1* double mutants. The number of putative columella stem cell layers located at the CSC position below the QC was counted in the 8 days old plants (Fig. 3-17E). Surprisingly, the wild-type had high number of double putative columella stem cell layers in this experiment. Despite that, both *crf10-1* single mutant and the *crf10-1 arf7-1* double mutant have increased number of plants with an additional putative CSC layer but the difference is not statistically significant in this experiment. In the *arf7-1* mutant the number of cell layers is close to the wild-type. These preliminary results need to be confirmed and the plants need to be analyzed also in the 10 days old plants which normally have stronger difference in cell layers between the wild-type and the crf10-1 mutant (Fig. 3-13F).

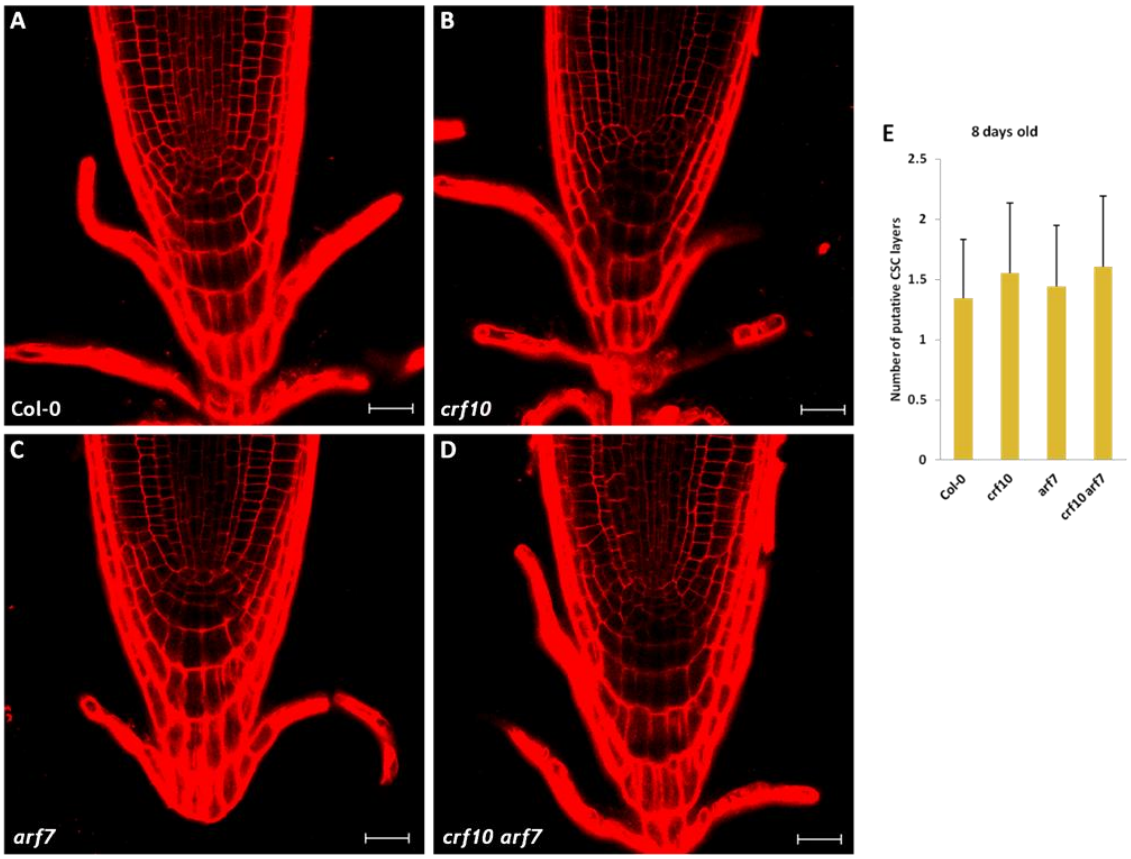

Fig. 3-17. Root apical meristem of the wild-type **(A)**, *crf10-1* **(B)**, *arf7-1* **(C)** and *crf10-1 arf7-1* **(D)** plant. Plants were grown for 8 days at 16h light/8h dark conditions in Lyon. Number of putative CSC cell layers **(E);** n ≥ 23. The unpaired t-test test was used to calculate significance with *p ≤ 0.05. Bar scale 25 µm.

In summary, both CRF10 and ARF7 appear to be involved in control of the RAM meristem morphology. In particular, this control involves cell division and cell differentiation processes in the columella stem cell layer. However, a few of the experiments presented here are needed to be repeated independently to strengthen these conclusions.

Discussion

In this chapter I investigated the regulatory interaction between CRF10 and ARF7. CRF10, a potential repressor of ARF transcription, was shown to control specific developmental processes including senescence of leaves, phototropic response to blue light and the RAM architecture maintenance. Results of this chapter suggest that CRF10 and ARF7 act in the same signaling pathway in some of these processes, and that CRF10 controls these processes through transcriptional regulation of ARF7 expression.

Is *crf10-1* a loss-of-function mutant?

In this chapter I investigated the phenotypes of the single mutant *crf10-1*. For this reason, it is important to understand the molecular nature of this mutant. The T-DNA insertion mutants can be dominant, semi-dominant or loss-of-function mutants. Loss-of-function mutants are the most frequently obtained types of mutants. Often the T-DNA insertion is located close to the 5-prime region of the mRNA within the coding sequence of the gene. This type of insertion hinders production of a stable full-length mRNA and, as a result, the functional protein is not produced (knock-out mutants) or produced to a lesser level (knock-down mutants). These mutations are usually recessive meaning that the phenotype induced by this mutation cannot be observed in heterozygous plants which contain both a functional wild-type allele and a dysfunctional mutant allele of the relevant gene (Slack 2009). Examples of such mutants are *met1-1* and *met1-2* encoding a gene involved in Photosystem II complex formation and repair in *A. thaliana*; these mutants show complete loss of mRNA and protein production (Bhuiyan *et al.* 2015).

On the contrary, gain-of-function mutants often have a dominant phenotype which can be observed even in heterozygous plants. Sometimes an abnormal protein is produced in these mutants, this protein being active constitutively and being resistant to regulations (Slack 2009). Examples of these include gain-of-function mutants of AUX/IAA genes with mutations in domain II that renders the mutated protein insensitive to the auxin-induced degradation and allows for a constitutive repression of auxin signaling (Hamann *et al.* 2002, Nagpal *et al.* 2000, Tian and Reed 1999). Semi-dominant mutants show phenotype in the heterozygous plants but the severity of this phenotype is reduced compared to the one detected in homozygous plants.

For example, heterozygous *phs1-1* mutant encoding the *A. thaliana PHS1* phosphotase shows phenotypes indicative of compromised cortical microtubule functions which are intermediate in severity between the wild-type and the homozygous mutant (Naoi and Hashimoto 2004).

What type of mutant is the *crf10-1* mutant? The T-DNA insertion in this mutant lies within the C-terminal conserved region. A recent publication identified the C-terminal region within CRF5 gene as a trans-activation domain (Striberny *et al.* 2017). One can imagine that the C-terminal region of CRF10 could be important for the activation or repression of its target genes. The T-DNA insertion doesn't prevent production of a truncated mRNA (Fig. 3-1B). Could this lead to production of a truncated CRF10 protein lacking C-terminal conserved region? If functional, such a truncated protein would still be able to bind its target DNA through the AP2 domain and interact with AHP and other CRF proteins through the CRF domain, but it might not be able to activate or repress its target genes due to lack of the C-terminal domain. One can imagine that this truncated CRF10 protein might interfere with the cytokinin signaling machinery by engaging the AHP proteins into direct interactions but this would not result in differential expression of the CRF10 target genes. In this case, the *crf10-1* mutant might be a dominant or a semi-dominant mutant that can block normal cytokinin response.

An alternative scenario would be that the *crf10-1* mutant does not produce a functional protein. In that case, this would be a loss-of-function mutant.

The alternative CRISPR mutants generated in this study should be analyzed and will give a straightforward answer to the question. These mutants contain a small deletion at the start of the gene coding sequence (two CRISPR lines with 59 bp and 58 bp deletions respectively) which is expected to produce complete knock-out mutants due to a frameshift leading to introduction of premature stop codons (after 35 amino acids and 47 amino acid respectively). Finally, a CRISPR mutant of the CRF10 gene in the *crf10-1* background was also created with a mutation site at the start of the coding sequence. If *crf10-1* is not a loss-of-function mutant, then the CRISPR mutation at the start of the gene will effectively attenuate the gain-of-function phenotypes.

Another question would be if the observed phenotypes are due to the T-DNA insertion in the CRF10 locus. The genetic analysis identified at least one more T-

DNA insertion which doesn't disrupt gene coding sequence, but which could still potentially affect gene expression networks in an unpredictable manner. This can be investigated by examining phenotypes in alternative CRF10 mutants. For this reason, the CRISPR mutants constructed in the course of this study will be crucial to prove the connection between the observed phenotypes and the CRF10 mutation. An alternative method would be to complement the *crf10-1* mutant with a genomic CRF10 construct and observe the loss of phenotypes. For this reason, the translational reporter fragment containing CRF10 genomic fragment was inserted both in Col-0 and *crf10-1* backgrounds. Unfortunately, in both cases the extremely weak CRF10 protein levels raises question on the functionality of the construct. Finally, crossing *crf10-1* mutant with the wild-type plants and examining phenotypes in multiple progenies containing homozygous *crf10-1* T-DNA insertion would allow to cross-out additional T-DNA insertion in at least some of these progenies.

Does CRF10 act in cytokinin signaling?

The members of the CRF gene family are acting in the cytokinin signaling pathway. CRF1 to CRF8 directly interact with histidine phosphotransfer proteins (AHPs) and regulate a subset of genes that partially overlaps with the B-type ARR targets (Cutcliffe *et al.* 2011, Raines *et al.* 2016; Rashotte *et al.* 2006). This part of cytokinin signalling pathway is far less studied compared to the cytokinin response transmitted through the B-type ARRs. It is conceivable that cytokinin regulates different aspects of plant development through the ARRs and CRFs signalling pathways.

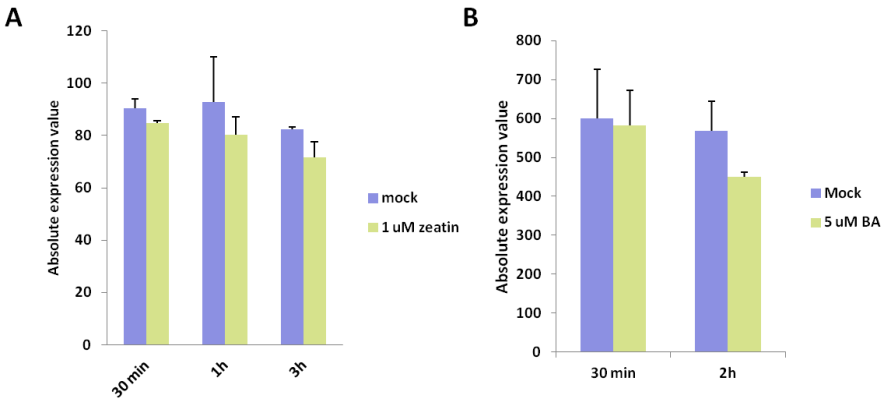

Fig. 3-18. Microarray data showing expression of ARF7 after cytokinin treatment. **(A)** 7 days old seedlings treated with 1 µM zeatin (Winter *et al.* 2007, Goda *et al.* 2008), **(B)** 7 days old seedlings treated with 5 µM BA (Lee *et al.* 2007).

The cytokinin signaling response transmitted through CRFs is based on the protein-protein interactions between CRFs and AHPs. One could presume that CRF10 interacts with certain AHPs through its CRF domain, even through the CRF-AHP interactions were analysed only for the CRF1 to CRF8 proteins (Cutcliffe *et al.* 2011). Nevertheless, if CRF10 and AHPs interact with each other, does it mean that CRF10 requires this interaction to activate or repress its target genes including ARF7? One can question if the AHP proteins are able to phosphorylate CRFs upon interaction and activate them, akin to their ability to activate type-B and type-A ARRs through direct phosphorylation (Hwang *et al.* 2012)? Does phosphorylation status of AHP proteins affect their interaction with CRFs? It cannot be excluded that CRF10 control gene expression independently from AHPs and, thus, independently from the cytokinin signaling. This question can be answered by analyzing if the transcription of CRF10 target genes is dependent from cytokinin treatment. Since ARF7 is the only target gene knows for CRF10, I looked at the expression of ARF7 after cytokinin treatment in publically available microarray datasets. It appears that ARF7 expression might be reduced after a prolonged (greater than 2h) treatment with cytokinin (Fig. 3-18). Presently substantial knowledge is lacking to understand the mechanism of cytokinin response through CRFs and many questions remain unanswered.

CRF10 is a transcription factor; its function would be to activate or repress expression of specific genes. Nevertheless, the target genes of CRF10, with exception of ARF7, are unknown. Binding sites of CRFs in the promoters of their target genes are not well studied. Simaskova *et al.* identified two motifs, AGCAGAC and AGAAGAC, as binding sites for CRF6 in PIN1 and PIN7 promoters respectively (Simaskova *et al.* 2015). An AGCAGAC site is detected at position -606 bp before the start codon in ARF7 promoter. On the contrary, the DAP-seq analysis indicates consensus binding site GGCGG (Suppl. Fig. 3-1B) which can be found in ARF7 promoter at position -217 bp before the start codon. A number of experiments could help to distinguish which of these two potential CRF10 binding sites might be important; the DAP-seq prediction should be considered more probable because this analysis was done on the whole genome level. For example, one can mutate these binding sites in the ARF7 promoter and observe alternations in CRF10-mediated reporter gene repression in the transient protoplast assay. Overall, it remains to be clarified how exactly CRF10 mediates cytokinin response.

CRF10 and ARF7 antagonistically control leaf senescence

My data points towards an antagonistic interaction between CRF10 and ARF7 being important for the timing of leaf senescence. In the *crf10-1* mutant older leaves senescent earlier. One possible explanation for this phenotype could be that the leaves undergo their normal developmental cycle faster and mature earlier in the mutant compared to the wild-type plants. The phenotypical analysis of the shoot growth didn't show accelerated development of the leaves in the mutant background; on the contrary, the mutant produced fewer leaves then the wild-type (Fig. 3-5B). Thus faster development doesn't appear to explain this phenotype.

Perhaps a disrupted hormone signaling in the mutant could account for this phenotype. The onset of senescence in leaves correlates with reduced levels of auxin and cytokinin (Gan and Amasino 1996, Shoji *et al.* 1951). On the contrary, ARF7 was reported to be induced in senescing leaves (Ellis *et al.* 2005); the *arf7* mutant enhanced the *arf2* delay of senescence phenotype indicating that ARF7 is a positive regulator of leaf senescence. Measuring ARF7 levels in the leaves of the *crf10-1* mutant before and after the onset of the early senescence could link this phenotype to alterations in auxin signaling output. One can speculate that if ARF7 levels are increased in senescing leaves, it could it be due to reduced repression by CRF10 gene (Fig. 3-19). In the publically available microarray datasets CRF10 is not

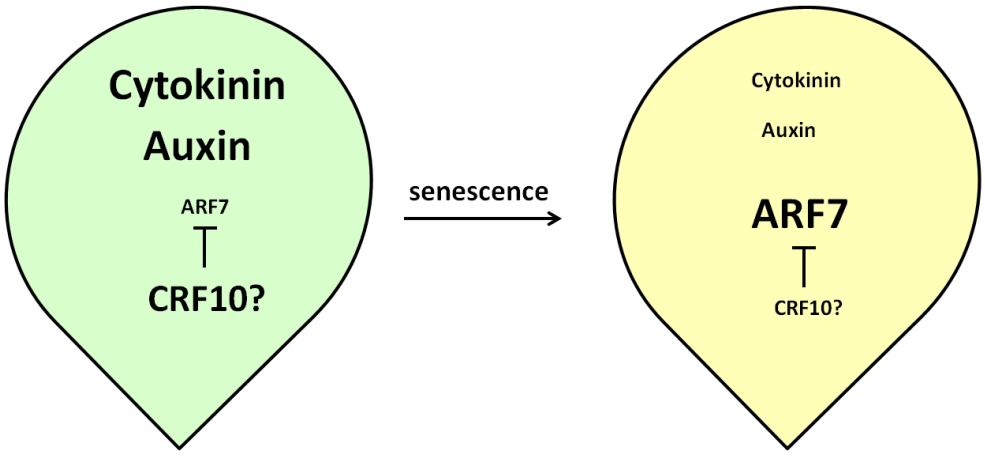

Fig. 3-19. Model of cytokinin and auxin interaction involving CRF10 and ARF7 in senescing leaves. Reduced levels of auxin and cytokinin and the increased levels of ARF7 in senescent leaves are responsible for the onset of leaf senescence.

differentially expressed during leaf senescence (Breeze *et al.* 2011, Lin and Wu 2004). Nevertheless, one can hypothesise that CRF10 could have a reduced ability to repress ARF7 in senescing leaves. Such a mechanism could be, for example, a diminished possibility to interact with active AHP proteins caused by decline of cytokinin signalling in senescing leaves. Alternatively, CRF10 might undergo post-transcriptional modifications which could reduce its ability to repress target genes including ARF7.

Overall, the following model of auxin and cytokinin crosstalk can be speculated: the cytokinin-regulated CRF10 activity is reduced in the senescing leaves where cytokinin levels are low. CRF10 is no longer able to repress ARF7 expression. As a result, ARF7 levels increase and this leads to onset of senescence through an unknown mechanism (Fig. 3-19). This model supports a hypothesis that the *crf10-1* might be a knock-down or a knock-out mutant because such a mutation would result in increased levels of ARF7. This model also explains the identical phenotype in the double *crf10 arf7* and single *arf7* mutants; the ARF7 gene acts downstream of CRF10 in the same pathway. A few questions remain through in connection with this model. Are the reduced levels of auxin sufficient for ARF7 to be able to activate expression of its target genes? What are the target genes of ARF7 during leaf senescence? These could be tested in further experiments. For example, one can express CRF10 gene under the senescence-specific promoter pSAG12; this would result in increased levels of CRF10 in senescing leaves and could subsequently cause reduction of ARF7 expression which then, in turn, might result in delay of senescence phenotype.

CRF10 and ARF7 are acting together in hypocotyl phototropic response

The role of ARF7 in the hypocotyl response to blue light is well-described (Esmon *et al.* 2006, Harper *et al.* 2000, Liscum and Briggs 1996). ARF7 was argued to transmit auxin response in the hypocotyl, promoting faster growth at the shaded side and triggering bending of hypocotyl towards the light source. Preliminary results in this thesis do not show differential expression of ARF7 between the lighted and the shaded side of the hypocotyl. Nevertheless, the differential response could be triggered by asymmetric distribution of auxin (Hohm *et al.* 2014) which could lead to

increased ARF7 transcriptional activity on the side of higher auxin accumulation, thus reinforcing it as a domain of high auxin response.

CRF10 appears to be involved in this process due to the *crf10-1* mutant phenotype with reduced ability to bend its hypocotyl towards the light source. CRF10 is expressed at the hypocotyl epidermis layer of the light-grown seedlings (Fig. 3-2C). Additional experiments could be done to analyze CRF10 expression in the dark-grown seedlings after exposure to the blue light to see if there is any asymmetric expression between the lighted and the shaded side of the hypocotyl. This could be done using my pCRF10-mVenus transcriptional reporter line.

The interaction between CRF10 and ARF7 in this process is incompletely understood. One can imagine that the *crf10-1* phenotype is caused by reduced expression of ARF7 in the mutant background which would lead to slower bending response of the hypocotyl. Preliminary results using pARF7-mVenus reporter line do not show reduced levels of ARF7 expression in the mutant. Multiple tools were made during this study that could be used to further investigate this interaction. These tools include various reporter lines inserted in the *crf10-1* background such as the auxin DR5-GFP reporter, the cytokinin TCS-GFP reporter, the ARF19 and ARF5 transcriptional reporters. These would help to shed more light on role of ARF7 and CRF10 in this response and the interaction between them. With the DR5-GFP reporter one could examine if the asymmetric auxin signaling distribution observed in the wild-type plants is retained the *crf10-1* mutant background. An involvement of the cytokinin signaling in this process could be elucidated by looking at the TCS-GFP reporter in the wild-type and the *crf10-1* mutant backgrounds. If the auxin signaling output is disrupted in the *crf10-1* mutant, one can elucidate if other ARF activators including ARF19 and ARF5 are involved in this process by looking at the expression of these ARFs in the *crf10-1* and the wild-type plants using my transcriptional reporter lines.

CRF10 and ARF7 are involved in the maintenance of the root apical meristem

My results suggest that the CRF10 gene is involved in the maintenance of the root apical meristem based on the interesting phenotype of the *crf10-1* mutant which shows a disorganized morphology around the QC and columella stem cell layers in the RAM. This phenotype is dependent on growth conditions. Often weak

phenotypes displayed by single mutants can be fortified in double mutants with closest homologous genes. In this study *crf10 crf11* and *crf10 crf12* double mutants were created but haven't been analyzed yet. In addition, the alternative CRISPR *crf10* mutants needed to be examined in the future experiments; it is possible that a mutation at the start of the gene in the CRISPR mutant would create a mutant with a stronger phenotype compared to the *crf10-1* mutant.

Another important question is the potential involvement of both CRF10 and its target gene ARF7 in the control of the RAM structure. Both CRF10 and ARF7 are expressed in the RAM with broad but not identical patterns. The biggest difference lies in the expression in the QC: ARF7 has the highest fluorescence precisely in the QC while CRF10 is not expressed there. On the other hand, both genes are not expressed in the columella stem cell layer. This led to speculation that there could be an antagonistic interaction between CRF10 and ARF7 located in the QC. Could it be that ARF7 is expressed in QC because it is not repressed by CRF10 in this tissue? My results show that the *crf10-1* mutant phenotype could result from increased expression levels of ARF7 in the proximal meristem.

The first step to answer this question is to understand the precise nature of the *crf10-1* phenotype. The mutant appears to have additional cell layer and more disorganized cell alignment at the QC and CSC positions. The experimental results with QC marker lines indicate that the QC function is not disrupted in the *crf10-1* mutant. The additional cell layer observed in the mutant is located at the position normally occupied by the QC but doesn't appear to be specified as a QC cell layer as indicated by expression of the QC markers WOX5 and SCR. One can speculate that this additional cell layer rather has columella stem cell identity. A columella stem cell layer marker line such as the J2341 (Ding and Friml 2010, Pi *et al.* 2015) would be useful to confirm this hypothesis.

The columella stem cells are derived from QC cells; these cells can undergo further cell division and differentiation rounds to produce fully mature columella cells which contain gravity-sensing starch granules (Nakajima and Benfey 2002). Auxin can affect the differentiation of the columella stem cells; growth on the medium supplemented either with auxin (NAA) or with an auxin transport inhibitor (NPA) leads to absence of CSC layer which differentiates into a mature columella layer (Ding and Friml 2010). Similarly, a QC- or CSC-specific expression of an auxin biosynthesis

gene IAAM leads to increased differentiation of the CSC layer (Ding and Friml 2010). On the contrary, double layer of undifferentiated columella stem cells was observed in the mutants deficient in auxin biosynthesis (YUCCA and TAA mutants) and transport (*pin3*, *pin4* and *pin7*) (Ding and Friml 2010). This leads to the question that the phenotype observed in the *crf10-1* mutant could be caused by reduced auxin response in the proximal meristem. However, the DR5-GFP marker line displays no clear significant difference between the wild-type and the *crf10-1* mutant suggesting that the auxin signaling output is not strongly affected. Further analysis are required here.

Columella stem cell differentiation is repressed by WOX5 transcription factor (Sarkar *et al.* 2007). One can predict that increased WOX5 levels or the expanded expression pattern could be responsible for the second CSC layer in *crf10-1*. Nevertheless, no difference in WOX5 expression was observed on in *crf10-1* background suggesting that this phenotype is WOX5-independent. Another transcription factor, PLT1, is involved in CSC maintenance acting downstream of WOX5 (Aida *et al.* 2004, Ding and Friml 2010). It would be interesting to see if the expression of PLT1 is affected in the *crf10-1* mutant background.

If auxin signaling is not disrupted in the proximal meristem of the *crf10-1* mutant, could this phenotype be due to abnormal cytokinin signaling? The TCS-GFP marker line showed that the cytokinin output is not disrupted in the mutant. In conclusion, clear connection cannot be established between known regulators of proximal RAM development (auxin, cytokinin, WOX5) and the *crf10-1* mutant phenotype.

ARF7 involvement in the development of the proximal RAM has never been considered before. In this study it was shown that ARF7 misexpression can lead to disorganization of the proximal meristem with ARF7 apparently acting in a non-cell autonomous manner. In addition, preliminary results indicate that ARF7 expression is higher in the RAM of the *crf10-1* mutant. This could mean that increased ARF7 expression levels are responsible for the observed disorganization of the RAM morphology. On the other hand, the auxin signaling output remains unchanged in the *crf10* mutant. One can question if the increased expression of ARF7 could simultaneously lead to reduced expression of other ARF activators, for example, ARF5. This hypothesis is supported by the expression analysis of the whole root tissue using qRT-PCR (Fig. 3-1C) where ARF5 expression is reduced. One can

imagine that a constant auxin output is achieved by rebalancing expression levels of multiple ARFs in the mutant. Nevertheless, ARF activators control expression of different downstream target gene (Nagpal *et al.* 2005, Schlereth *et al.* 2010, Okushima *et al.* 2005), thus such compensation mechanism could lead to different cellular responses and might affect development of the RAM. pARF5-mVenus and pARF19-mVenus transcriptional reporter lines were also crossed in the *crf10-1* mutant during this thesis and the expression will be analyzed in the future to confirm or deny this hypothesis.

A few additional experiments could shed more light on the role of CRF10 and ARF7 in proximal meristem maintenance. For example, misexpression of CRF10 in QC and columella stem cells could potentially lead to interesting phenotypes.

The morphological structure of the root apical meristem is not identical throughout the life cycle of the plant. It was reported that in the older roots the RAM structure can acquire noticeable disorganization and this change was argued to be caused by a reduction of the RAM function (Chapman *et al.* 2003, Rost 2011). One can speculate that the root undergoes an aging process. Is it possible that the disorganization of the RAM structure is a normal event which is activated prematurely in the *crf10-1* mutant? Perhaps the observed phenotype in the *crf10* mutant represents an event of early root senescence.

Material and methods

Plant material

The CRF10 gene ATG number is AT1G68550. T-DNA insertions were analyzed by genotyping using primers listed in Appendix. The *arf7-1* single mutant (SALK_040394), the *arf19-1* single mutant (SALK_009879) and the *arf7-1 arf19-1* double mutants are described elsewhere (Goh *et al.* 2012). The *crf12* (GK_713E09) and *crf11* (GK-355D03) mutants were obtained from NASC. The following double and triple mutants were created during this study: *crf10-1 arf7-1*, *crf10-1 arf19-1*, *crf10-1 arf7-1 arf19-1*, *crf10 crf11*, *crf10 crf12*. The following constructs were crossed with the *crf10-1* mutant: pWOX5-GFP marker for QC line (obtained from University of Nottingham lab collection), DR5-GFP line (obtained from University of Nottingham lab collection), TCS-GFP line (obtained from University of Nottingham lab collection), pARF7-mVenus (transcriptional reporter line described in Chapter I), pSCR:SCR-YFP (obtained from University of Nottingham lab collection).

Analysis of the conserved regions within the CRF10 protein across *A. thaliana* ecotypes

The Arabidopsis 1001 Genomes project was used to download sequences of CRF10 in various ecotypes. SIFT prediction algorithm was used to identified amino acids conserved among ecotypes (http://sift.bii.a-star.edu.sg/).

Genetic analysis of the *crf10-1* mutant

Mutation of the CRF10 gene in the *crf10-1* mutant was confirmed with genotyping using primers indicated in Appendix. The genotyping primers were used to amplify genomic DNA fragments spanning the T-DNA insertion site. The resulting PCR products were sequenced and the precise insertion site was identified.

Expression analysis with qRT-PCR

The expression of ARF activators in the roots and the shoots of 7-days old *crf10-1* and wild-type seedling was done as a part of global analysis of multiple transcription factor mutants. The protocol is described in detail in Chapter II.

Cloning and generation of transgenic lines

The transcriptional and the translational reporter lines of CRF10 were generated using Multisite Gateway cloning technology. For the transcriptional reporter lines the promoter region of the CRF10 locus from -4060 bp to +1 bp was amplified by PCR and inserted into pDONR P4-P1R. The resulting plasmid pCRF10 pDONR P4-P1R was recombined with 3x mVenus-N7 pDONR211 (containing triple mVenus coding sequences and N7 nuclear localization signal), OCS terminator pDONR P2R-P3 (containing the stop codon followed by a octopine synthase (OCS) terminator) and pK7m34GW (the destination vector containing kanamycin resistance gene for *in planta* selection) to produce pCRF10-mVenus construct.

For the translational reporter line, CRF10 genomic DNA fragments from -4060 bp to +972 bp was amplified by PCR. This fragment included the promoter region and the whole coding sequence of CRF10 up to but not including the STOP codon. The resulting CRF10 genomic fragment was inserted into pDONR P4-P1R and recombined with mVenus pDONR211 (none-nuclear localized), OCS terminator pDONR P2R-P3 (containing the stop codon followed by a octopine synthase (OCS) terminator) and pHm43GW (the destination vector containing hygromycin resistance gene for *in planta* selection) to produce pCRF10:CRF10-mVenus construct.

The transcriptional and the translational CRF10 reporter lines were transformed into *Agrobacterium tumefaciens* C58pMP90 strain by electroporation and then transformed into Col-0 plants by floral dip method (Clough and Bent 1998). The translational reporter line was also transformed into *crf10-1* mutant background.

The pSMB:ARF7 and pSMB-3xVenus transgenic lines were also generated using Multisite Gateway cloning technology. SMB promoter fragment from -3330 bp to – 30 bp was amplified by PCR and inserted into pDONR P4-P1R. The ARF coding sequence (without introns) inserted in pENTR/D-TOPO was obtained from Nicola Leftley, University of Nottingham. For the pSMB:ARF7 construct, the following plasmids were recombined together: pSMB pDONR P4-P1R, ARF7 pENTR/D-TOPO, OCS terminator pDONR P2R-P3 (containing the stop codon followed by a octopine synthase (OCS) terminator) and pK7m34GW (the destination vector containing kanamycin resistance gene for *in planta* selection). For pSMB-mVenus construct the following plasmids were recombined: pSMB pDONR P4-P1R, 3x mVenus-N7 pDONR211, OCS terminator pDONR P2R-P3 and pK7m34GW. Both constructs were

transformed into *Agrobacterium tumefaciens* C58pMP90 strain by electroporation and then transformed into Col-0 plants by floral dip method (Clough and Bent 1998).

CRISPR mutants of CRF10 were constructed using the Golden Gate cloning technology with plasmids for simultaneous mutation of two target sgRNAs (Wang *et al.* 2015). The two sites at the start of the CRF10 gene coding sequences were targeted and evaluated for target specificity using Cas-OFFinder (http://www.rgenome.net/cas-offinder/). The sgRNAs expression cassette targeting these two sites was amplified by PCR. The purified PCR fragment was inserted into pHEE401 plasmid (Wang *et al.* 2015). The construct was transformed into *Agrobacterium tumefaciens* C58pMP90 strain by electroporation and then transformed into Col-0 or *crf10-1* plants by floral dip method (Clough and Bent 1998).

Root microscopy

For root microscopy plants were grown on half-strength Murashige and Skoog (MS) medium supplemented with 1% sucrose and 1% agar. The seedlings were grown in either 24h light or 16h light/8h dark conditions and imaged at the time points indicated in the results part for each individual experiment. Plant cell membranes were visualized by staining with 15 µg/ml propidium iodide solution. The roots were examined in the TCS-SP5 (Leica) or LSM710 (Zeiss) confocal microscopes with excitation at 514 nm and emission at 526-560 nm for mVenus, emission 605-745 nm for propidium iodide.

For the BAP treatment, the 5 days pCRF10-3xVenus seedlings grown in 16h light/8h dark conditions were treated with 5 µM BAP or mock for 30 min and 2h.

Fluorescence intensity was measured from confocal images using ImageJ software.

Shoot microscopy

For the shoot microscopy plants were grown in 8h light/16h dark conditions for 6 weeks and then transformed to 16h light/8h light conditions for 2 weeks to induce bolting. The bolted shoots were dissected under a stereomicroscope and planted into an Apex Culture Medium (half-strength MS medium supplemented with 1% sucrose, 0.8% agarose, 1x vitamin solution (myo-Inositol 100 mg/L, nicotinic acid 1 mg/L, pyridoxine hydrochloride 1 mg/L, thiamine hydrochloride 10 mg/L, glycine 2 mg/L)), for overnight incubation at 16h light/8h dark conditions. Cell membranes were visualized by staining the shoot apexes with 100 µg/ml propidium iodide solution. The

shoot apexes were examined in the TCS-SP5 (Leica) confocal microscope with excitation at 514 nm and emission at 526-560 nm for mVenus, and emission 605-745 nm for propidium iodide.

Shoot phenotype analysis

crf10-1 mutant and the wild-type Col-0 were grown in 8h light/16h dark conditions on soil for 43 days. Leaf number was counted every 3 days starting from day 21. Rosette diameter was measured at days 43. After 43 days of growth in the above described conditions, the plants were transferred to 16h light/ 8h dark conditions for bolting. The following parameters were measured at 21 and 27 days in the 16h light/8h dark conditions: length of the main stem, number of cauline branches growing from the main stem, number of axillary branches growing from rosette (the main stem not included). Number of replicates per genotype is 12 plants. For the statistical analysis an unpaired t-test was conducted with $p \leq 0.05$ considered as statistically significant.

Early senescence phenotype analysis

For the early senescence phenotype the plants were grown in 8h light/16h dark conditions on soil for 45 days. The number of green and senescent leaves was counted and the rosette diameter was measured at 45 days. Number of replicates per genotype is 12 plants. For the statistical analysis an unpaired t-test was conducted with $p \leq 0.05$ considered as statistically significant.

Chlorophyll measurement

The leaf 3 (counting from the oldest) of the plant grown in 8h light/16h dark conditions for 40, 45 and 50 days was collected, weighted and incubated in 95% ethanol for 3 hours. The absorbance was measured at A664 and A648. The amount of chlorophyll *a* and *b* was calculated using the following formula: Chl*a* = 13.36 * A664 – 5.19 * A648 [µg/ml] and Chl*b* = 27.43 * A648 – 8.12 * A664 [µg/ml] (Lichtenhalter and Buschmann 2001). Number of replicates per genotype is 3 plants.

Hypocotyl phototropism assay

Seedlings were grown for 4 days in the dark on half-strength Murashige and Skoog (MS) medium supplemented with 1% sucrose and 1% agar and then exposed to blue light for 7h. Images were taken and the hypocotyl bending angle as well as the hypocotyl length was measured using ImageJ software. Number of replicates per

genotype is at least 40 plants. For the statistical analysis an unpaired t-test was conducted with $p \leq 0.05$ considered as statistically significant.

pARF7-mVenus transcriptional reporter line in wild-type and *crf10-1* background were grown as described above. Images of the hypocotyl at the bending site were taken after 7h exposure to the blue light (see Root microscopy).

Root phenotype analysis

For the root phenotype analysis plants were grown on half-strength Murashige and Skoog (MS) medium supplemented with 1% sucrose and 1% agar in 16h light/8h dark conditions. Images were taken at indicated time points; the root length and the lateral root number were measured using ImageJ software (n = 34 plants per genotype). To measure length of the meristematic zone and the number of cells in the meristematic zone, confocal images were taken at indicated time points ($n \geq 14$ plants except 8 plants at the time point 14 days). For the statistical analysis an unpaired t-test was conducted with $p \leq 0.05$ considered as statistically significant.

For the bending assay, plants were grown in 1/2 MS for 3 days in 24h light conditions and then turned at 90°C to induce initiation of a lateral root at the bending site. The plants were examined at 24h and 48h after the bend ($n \geq 13$ plants per genotype). The stage of the lateral root development was determined according to Peret *et al.* 2009 (Fig. In-5).

Lugol's staining was performed by incubating seedlings in Lugol's solution for 45 seconds, washing in water and mounting in clearing solution (8g chloral hydrate, 1 ml glycerin, 2 ml H_2O).

Supplementary information

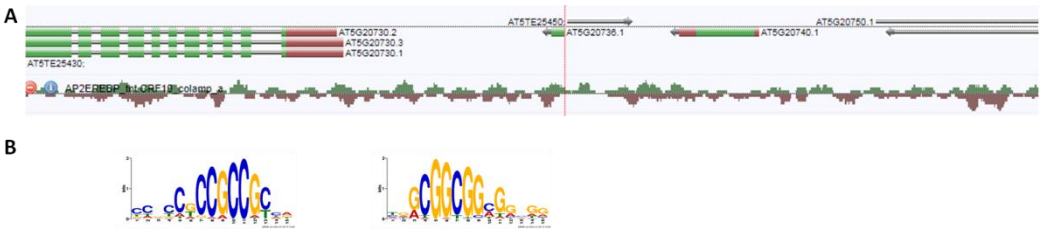

Supplementary Fig. 3-1. *In silico* analysis of the CRF10 binding site in ARF7 promoter using DAP-seq database. DAP-seq peaks of CRF10 in the promoter of ARF7 **(A)** and the consensus binding sequences identified for CRF10 **(B)**.

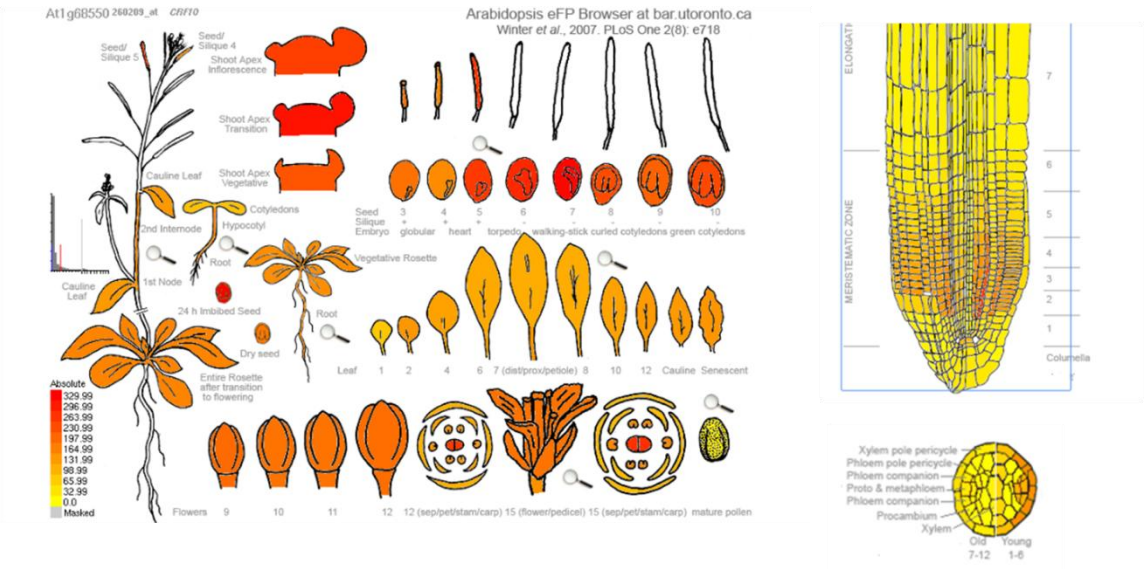

Supplementary Fig. 3-2 Expression profile of the CRF10 gene in the whole plant (left) and the root (right). From Arabidopsis eFP Browser (Winter *et al.* 2007).

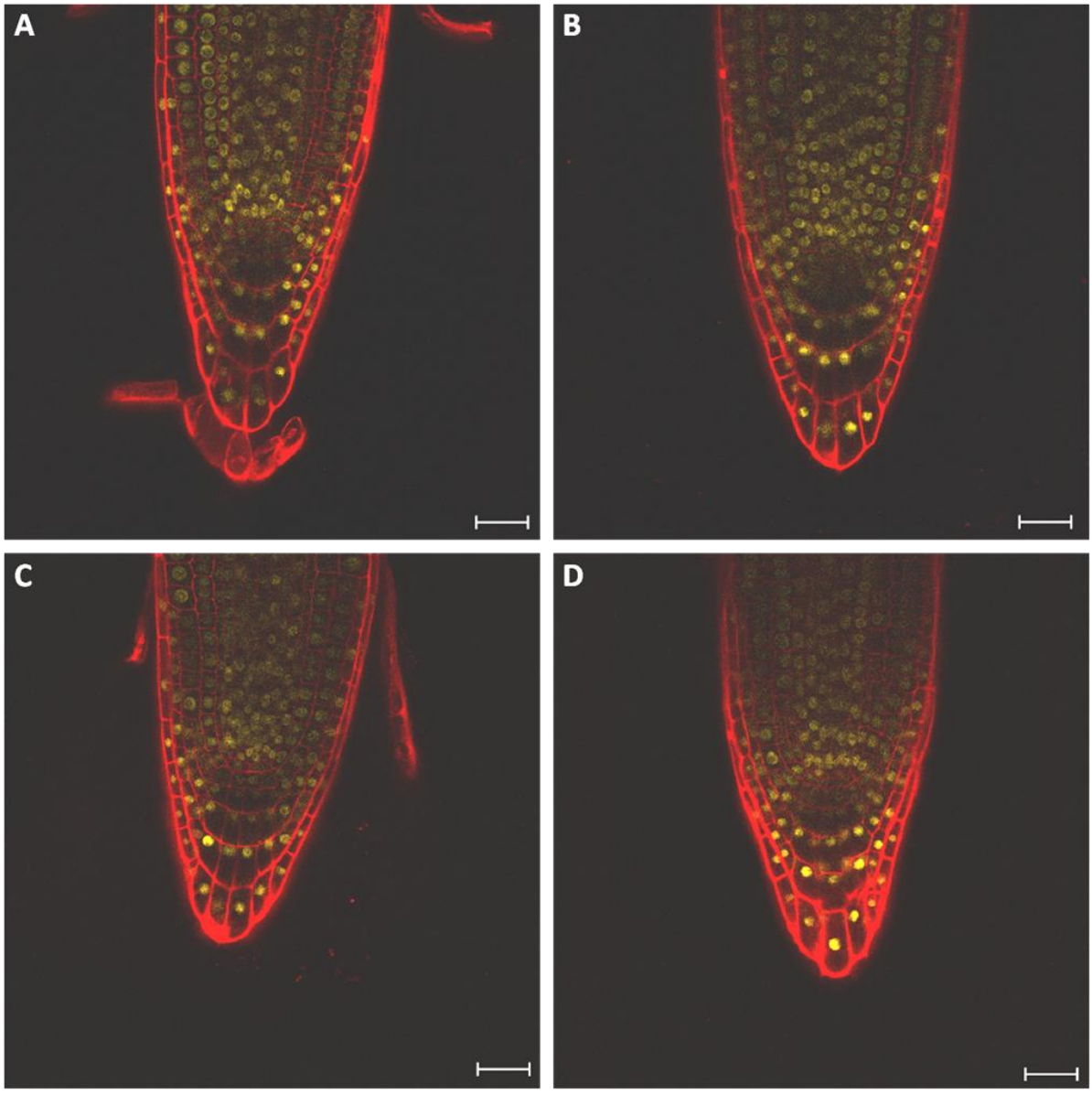

Supplementary Fig. 3-3. Expression of CRF10 gene in the root tip after 30 min of mock **(A)** or 5 µM BAP **(B)** treatment, and after 2h of mock **(C)** or 5 µM BAP **(D)** treatment. Plants were grown for 5 days in 16h light/8h dark conditions. Bar scale 25 µm.

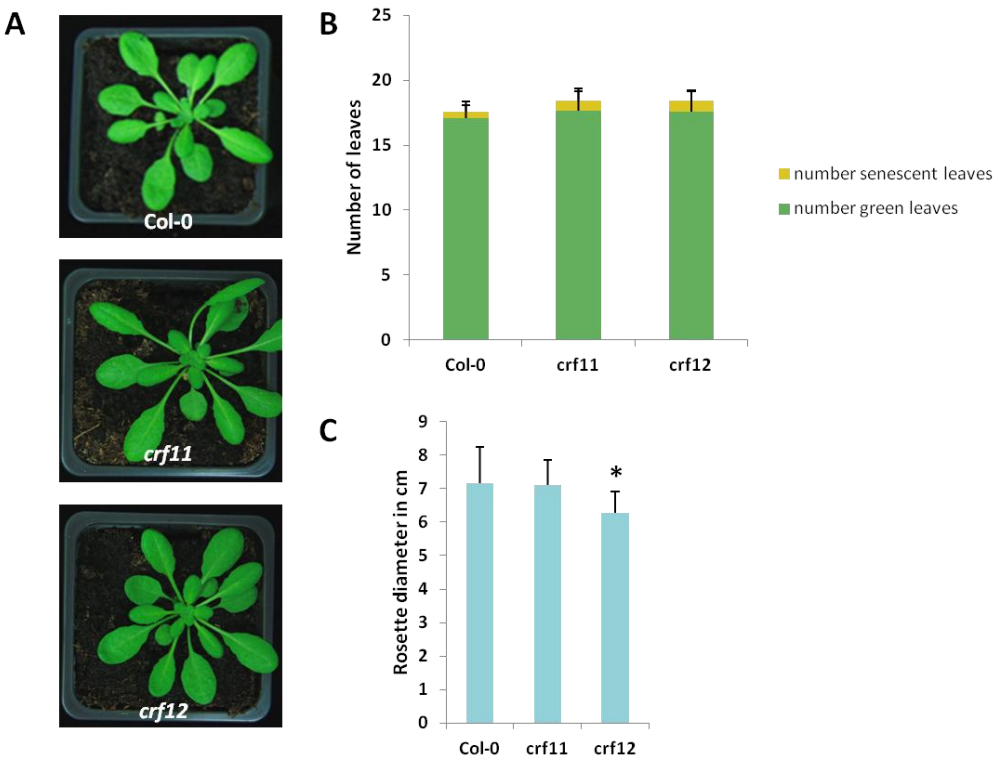

Supplementary Fig. 3-4. The phenotypes of the *crf11* and *crf12* single mutants grown for 45 days in 8h light/16h dark conditions. Images of the rosette **(A)**, the number of green and senescent leaves **(B)** and the rosette size **(C)**. n = 12 plants. The unpaired t-test test was used to calculate significance with *p ≤ 0.05.

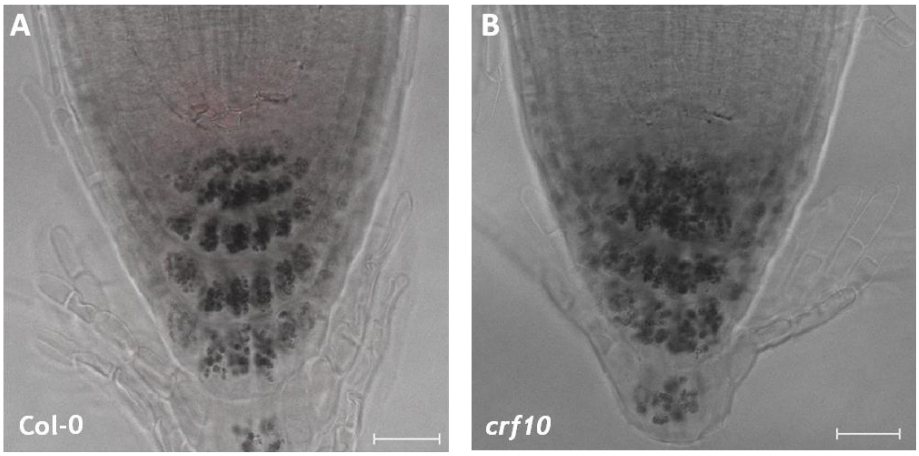

Supplementary Fig. 3-5. Lugol's staining showing accumulation of starch granules in the root tip of the wild-type **(A)** and *crf10-1* mutant **(B)**. Plants were grown for 9 days in 24h light conditions.

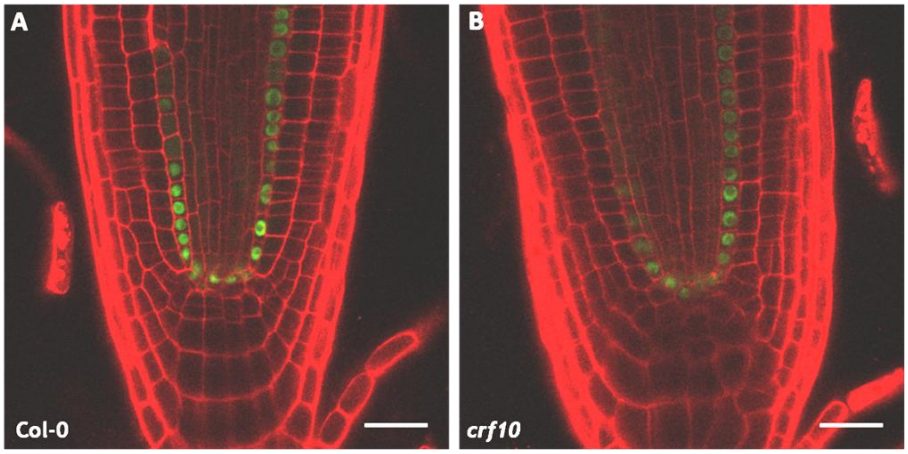

Supplementary Fig. 3-6. pSCR:SCR-YFP marker line expression in the wild-type **(A)** and the *crf10-1* **(B)** mutant. Plants were grown for 9 days in 16h light conditions

General discussion

ARF activators in control of plant development

Multicellular organisms have complicated body structures that often consist of distinct cell populations organized in various tissues, each tissue type having specific functions. For the body to change in response to external or internal stimuli, proper communication between cells and tissues is essential. In plants this communication is transmitted in most part through hormones. Among plant hormones, auxin was shown to control multiple aspects of developmental throughout the life cycle of the plant from embryonic development through to the reproduction, as well as regulating responses to various external stresses.

Auxin has been a subject of plant science research for almost 100 years since its discovery in 1928 by Frits Went (Enders and Strader 2015). Despite its early discovery, the understanding of the molecular mechanism that mediate auxin response only came in the last 20 years. Particularly important advancements came with unraveling the components of the auxin signaling pathway. Auxin signaling is propagated through an elegant and relatively simple molecular mechanism based on auxin-dependant derepression of transcription factors that control expression of multiple auxin-regulated genes. In a simple perspective, this mechanism involves an auxin receptor, a repressor and a transcription factor. Nevertheless, the simple mechanism turned out to be much more complicated due to presence of dozens of homologues genes for each member of this signaling pathway in most land plants. For example, *A. thaliana* contains 6 auxin receptor genes from TIR1/AFB family, 29 AUX/IAA repressors, and 23 ARF transcription factors from which 5 are able to act as activators of auxin response (Dharmasiri *et al.* 2005b, Okushima *et al.* 2005. Remington *et al.* 2004). It is partly through the diversity of these components that tissues and cells are able to respond to auxin in accordance with current plant's needs.

In this thesis I look at the diversity of ARF activators in *Arabidopsis thaliana* with the aim to learn where these five ARFs are expressed in the root and the shoot tissues and to understand how these expression patterns are established. Transcriptional reporters for the 5 activating ARFs have been made previously (Rademacher *et al.*

2011), these contained only ca. 2 kb fragment upstream of the transcriptional start. Through the plethora of data we have in plant genetic studies, there are many examples of well studied genes, such as AGAMOUS, where the elements required for gene transcription are either located in introns or more distantly to the transcriptional start (Busch *et al.* 1999, Jeon *et al.* 2007, Lohman *et al.* 2001, Rose and Last 1997, Vasil *et al.* 1989). Whilst the patterns of some of these published ARF transcriptional reporters matched the patterns observed through *in-situ* hybridizations (Vernoux *et al.* 2011) this was not the case in all occurrences. As this project required a greater knowledge of the sequence required to drive ARF expression, I developed new reporter lines incorporating both longer upstream sequences and the first introns. The patterns observed provided a much closer match with *in-situ* data, indicating that these constructs better represent ARF expression. Of particular note was ARF7 which is required for root gravitropic responses (Okushima *et al.* 2005, Sato *et al.* 2015); this provides strong evidence that ARF7 expression is needed in the root meristem. Constructs lacking the first exon and intron showed limited or no expression in the proximal root meristem, whereas constructs incorporating these elements showed strong expression. Not only did these data provide me with the confidence to use these promoters in the next stage of my project, where I looked for factors regulating these ARFs, but they have also proved to be a valuable source for the community. My ARF19 promoter construct has already been used in one publication investigating the role of auxin in mediating phosphate induced root hair growth (Bhosale *et al.* 2018). My ARF7 construct has been used to test asymmetries in auxin response in response to water availability on the wet and dry side of the root. Data from this study shows that ARF7 is post-transcriptionally regulated to control lateral root patterning in response to water, and my construct helped to rule out any role of asymmetric transcription of ARF7 in this process (Orosa-Puete *et al.* 2018, in preparation).

The next stage of my project was to identify a network of transcription factors that regulate expression of these ARFs using Y1H approach. As discussed in details in chapter II, the Y1H assay is expected to produce false negative results and does not capture all possible interactions due to the limitations forced by using a heterologous organism, and by the size and the content of the prey collection. The gene regulatory network identified with Y1H assay is likely to therefore represent a subset of a bigger true network that functions *in planta*. Despite that, this smaller network is sufficient to

understand many basic principles that govern the expression of ARFs and allows generating new hypothesis. For example, an unproportionally large amount of transcriptional regulators were identified for ARF8 and the fact, that many of them are involved in responses to abiotic and biotic stresses, leads to a new perspective on the role of this ARF as a hub that integrates multiple different environmental inputs into the auxin signaling output.

Identifying genes upstream of the auxin signaling output already contributes to understanding of the auxin signaling pathway. Nevertheless, learning which transcription factors control expression of which ARF is insufficient to draw conclusions about biological significance of these regulations. One key question arising from my network, is how valid are predictions for *in planta* regulations. To address this I tested all the identified interactions in *Arabidopsis thaliana* protoplasts. Protoplasts are plant cells containing the cellular identity of the tissue from which they originate (Faraco *et al.* 2011); this system provides a good ground for *in planta* validation but is still limited by the cell identity as leaf cells. Using the protoplast system I showed that, for the most part, expression of ARF activators is controlled by a set of transcriptional repressors. The subsequent usage of various resources such as the DAP-seq dataset increased the number of validated interactions, and provided further confidence that the identified interactions are not false positives.

The strength of this thesis lies in multiple efforts that were taken to validate the interactions *in planta* and to identify specific developmental processes in which these interactions could be important. Similar studies conducted before with validation of only a few interactions (de Lucas *et al.* 2016, Sparks *et al.* 2016, Taylor-Teeples *et al.* 2015). The validation of the whole gene regulatory network using the transient protoplasts assay allowed me to draw conclusions on the nature of the regulations (repression or activation) and provided the ability to confirm these regulations *in planta* for the whole network. The subsequent phenotypic analysis was limited to 25 out of 42 total transcriptional regulators identified due to limitations in the material available, but this collection represented regulators of all five ARFs and contained no bias in the mutants selected. The results showing auxin-regulate phenotypes in the majority of these mutants further solidified the confidence in the value of the network. Collectively these tests reveal that the identified network describes biologically significant regulations.

In this study I took a different approach from others looking at auxin specificity who have mostly focused on asymmetries in the distribution of the hormone itself, and I looked at the complexity of the auxin signaling pathway at a different level, upstream of the auxin-mediated ARF action. This level of auxin signaling has never been analyzed in this kind of detail, as most of the research has focused on elucidating gene targets downstream of ARFs (Nagpal *et al.* 2005, Okushima *et al.* 2005, Schlereth *et al.* 2010). Indeed, before ARF activators are able to induce expression of their target genes, they have to be first expressed in a given tissue.

Another interesting aspect of this thesis is the integration of knowledge in regards to both the root and the shoot development. This was possible thanks to the collaboration between two laboratories, each of these specializing in either the root (Nottingham) or the shoot (Lyon) development. This approach allowed conducting experiments and drawing conclusions in regards to the growth regulated both at the RAM and the SAM.

Can this work serve as a base to conduct further research into complexity of the auxin signaling pathway? Indeed, further projects can be imagined based on the results obtained in this thesis. In the discussion for chapter II it was mentioned that several identified TF-ARF interactions provide a great potential for further in depth investigations. In accordance with this, the CRF10-ARF7 interaction studied in this thesis led to a few interesting discoveries which are worthy of further study.

Another interesting project arising from this thesis would be to analyze in depth one or two ARF activators for all potential post-transcriptional and post-translational regulations that affect function of this ARF. In this thesis I showed that ARF activators might differ significantly in post-transcriptional and post-translational control mechanisms. Further mechanisms have been described in the literature or could be predicted by bioinformatic methods. For example, ARF7 mRNA must be subjected to alternative splicing because this gene has four different splice variants published (according to the Arabidopsis Information Resource (TAIR)); are these four splice variants produced in separate tissues, and how does this affect the function of ARF7 in these tissues? The activity of ARF7 protein is further modified through phosphorylation during lateral root development (Cho *et al.* 2013), and SUMOylation during lateral root initiation in response to water availability of the soil (Orosa-Puete

et al. 2018, in preparation). Such thorough analysis would enable to look at all aspects of regulation combined and permit to judge on the activity of this ARF.

In this study multiple TFs binding a single promoter were identified; it could be interesting to study potential combinatorial binding of ARF regulators on a single ARF promoter. For example, one can investigate if some of these transcription factors can interact with each other and bind the ARF promoter together, perhaps building transcriptional regulatory protein complexes. Does preventing one transcription factor form binding its target promoter will affect the binding affinity of another TF? Could multiple repressors of ARF transcription recruit a common co-repressor such as TOPLESS? Such a project would focus on studying the relationships between individual transcriptional regulators and their modes of action using a single ARF as an example.

ARF activators diversify and specialize during evolution

One can question why does *Arabidopsis thaliana* require five ARF activators to mediate auxin response. It can be presumed that the advantage of having multiple ARF activators lies in the increased specificity of auxin response due to specialization of individual ARFs in controlling particular aspects of plant development. Indeed in this thesis I showed that all five ARFs have discrete expression patterns in the root and the shoot that suggests that each ARF specializes to transmit auxin responses in specific tissues or cells. In correlation to this, expression of each ARF activator was shown to be regulated by a discrete set of transcription factors.

On the other hand, it was shown that a deficiency in one ARF activator can be compensated by another ARF. For example, Nagpal *et al.* were able to complement reduced production of seeds in *arf8* mutant by introducing extra copies of ARF6 gene into this mutant (Nagpal *et al.* 2005). In this case closely related ARFs, ARF6 and ARF8, might have identical function in seed development; it appears that a correct copy number of those two ARFs combined is more important that the specific function of each ARF. Perhaps this ability is limited to homologous ARFs, or could non-homologous ARFs also successfully substitute functions of each other? One can further investigate this by misexpressing one ARF activator under promoter of a different ARF. For example, would the pARF7:ARF5 construct complement *arf7* mutant phenotypes?

Looking at the evolution of the ARFs could provide clues on the necessity and advantages of having multiple ARF activators with diverse functions. ARF-like proteins appear first in charophytes, the green algae. The function of these proto-ARFs is unclear because charophytes lack other components required for the auxin signaling response such as the AUX/IAAs repressors and TIR1/AFB auxin receptors (Finet *et al.* 2013, Mutte *et al.* 2018). On the contrary, land plants contain all required components of the auxin signaling pathway including ARFs which are divided into three phylogenetic lineages (Fig. 4-1). One of the lineages includes ARF activators whereas the other two lineages consist of ARF repressors. Interestingly, ARF activators already form a separate group from the ARF repressors in all land plants (Class A in Fig. 4-1). In liverworts, mosses and lycophytes ARF activators consist of two separate branches: one canonical and one non-cannonical ARF. The hornworts contain only one canonical ARF activator. The non-cannonical ARF activator was eventually lost during evolution and it is not found in ferns, gymnosperms and angiosperms. On the other hand, the canonical ARF activator

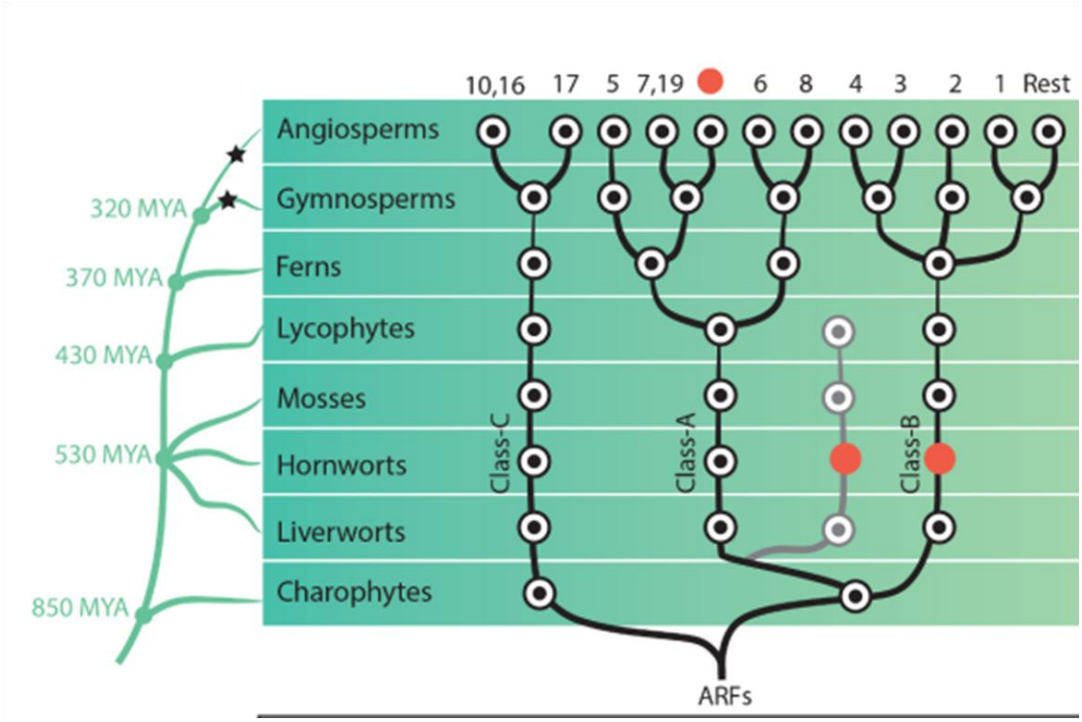

Fig. 4-1. Reconstruction of ancestral state of ARFs in plant evolution. Phylogenetic tree shows the copy number and phylogenetic relationship of each ARF in the common ancestors. Numbers on the top indicate ARF genes in *Arabidopsis thaliana*. Black circle: ARF gene; grey circle: non-canonical ARF; red circle: ascent ARF subfamily (Mutte *et al.* 2018).

underwent a duplication event producing an ARF5/7/19 precursor and an ARF6/8 precursor in ferns (Fig. 4-1). Subsequently, the ARF5/7/19 precursor underwent another duplication event ending up with three ARF activators in gymnosperms: ARF5, ARF7/19 and ARF6/8. Finally, two additional duplication events resulted in five ARFs present in angiosperms: ARF5, ARF7/19, paralogue of ARF7/19 which was later lost in *A. thaliana*, ARF6 and ARF8. (Fig. 4-1) (Mutte *et al.* 2018). It appears that the number of ARF activators increased during evolution as a consequence of a few duplication events. This increased number of ARFs might correspond to increased complexity of the life-style and the body structure of the plants. One can argue that these duplication events allowed ARFs to diversify and specialize in particular aspects of plant development. Perhaps, following the duplication event, one of the progeny ARF could keep the original function of its ancestral ARF whereas the other progeny ARF could adopt a new function and thus participate in development of new evolutionary innovations.

Indeed, the duplication of ARF6/8 ancestral locus into separate loci for ARF6 and ARF8 occurred in angiosperms and may be associated with acquisition of an elaborate reproductive system in form of flowers. In connection to this, ARF6 and ARF8 were shown to be absolutely necessary for the development of flowers in *A. thaliana* (Nagpal *et al.* 2005). In addition, ARF8 controls development of the fruits which are also specific for the angiosperm reproduction system (Goetz *et al.* 2006, Goetz *et al.* 2007). Thus this duplication event might have contributed to the evolution of the reproductive system in plants.

One can only speculate on the significance of other duplication events during evolution. Perhaps the development of the separate ARF5 and ARF7/19 proteins in gymnosperms could be important for the development of the elaborate root systems characteristic for the gymnosperms and angiosperms or, alternatively, could be important for wood development.

Looking at the conservation of ARF activators in other species could provide clues on importance of having multiple ARFs for evolutional adaptations associated with various group of plants. Unfortunately, characterization of ARF activators in species other than *Arabidopsis thaliana* has not been performed extensively. Among dicots, tomato has been reported to contain seven ARF activators: ARF5, 6A, 7A, 7B, 8A, 8B and 19 (Zouine *et al.* 2014). Interestingly, similarly to *A. thaliana*, SpARF6A,

SpARF8A, and SpARF8B are important for flower development in tomato (Liu *et al.* 2014). It would be interesting to investigate why tomato requires three ARF activators in this process when *A. thaliana* uses only two.

In monocots, rice was shown to contain 9 different ARF activators: ARF5, 6, 11, 12, 16, 17, 19, 21 and 25 (Shen *et al.* 2010). An alignment of these ARF activators showed that AtARF6 and AtARF8 has four homologues in rice with OsARF25, OsARF12, OsARF6 and OsARF17; AtARF7 and AtARF19 together have four

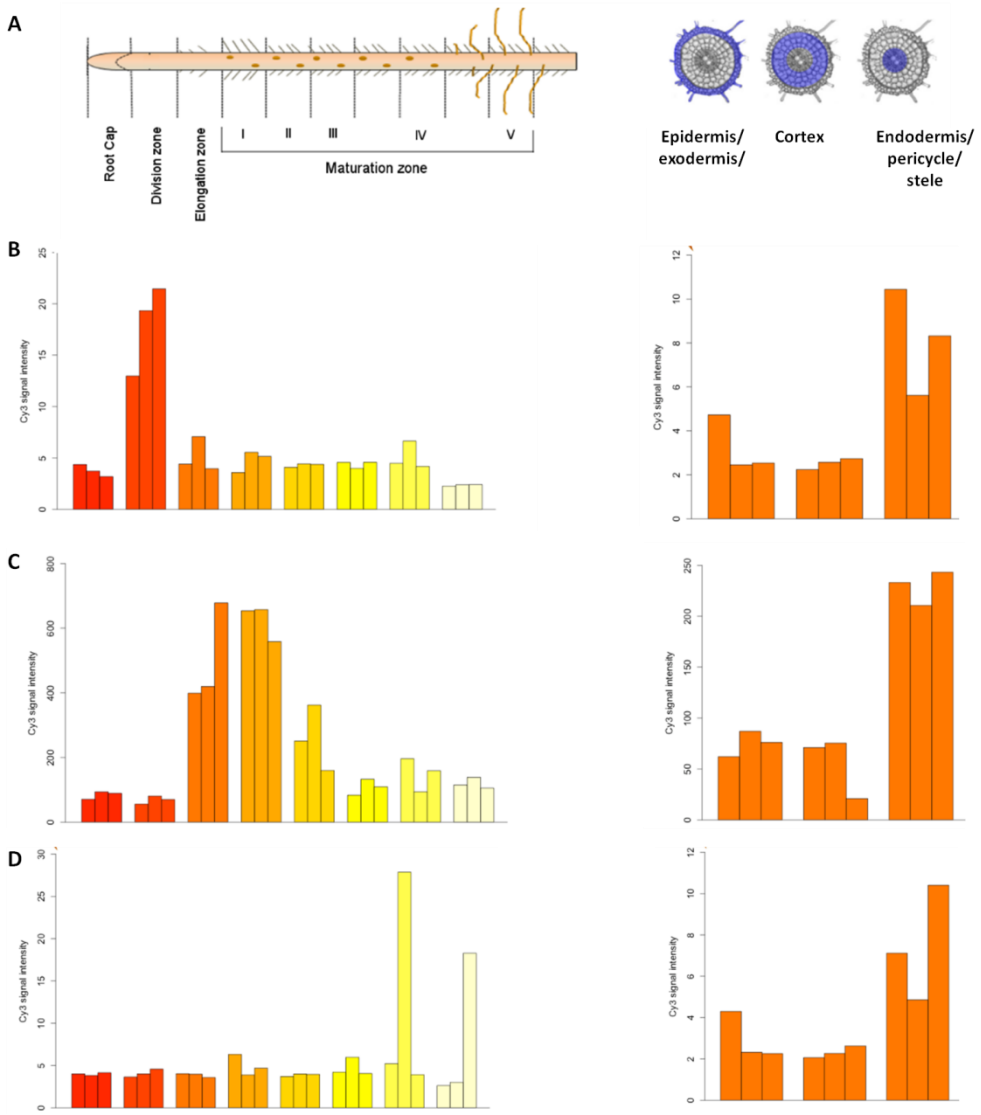

Fig. 4-2. Expression of rice ARF activators in the crown roots. Laser microdissection was used to collect samples from different zones of the crown root of 10 days root seedlings. Schematic of root sections with tissues collected separately **(A)**. Expression profiles of OsARF11 **(B)**, OsARF21 **(C)** and OsARF6 **(D)** in the corresponding tissues of the root (Data from Rice Expression Profile Database RiceXPro).

homologues with OsARF5, OsARF21, OsARF16 and OsARF19; AtARF5 has one homologue OsARF11 (Wang *et al.* 2007). Similarly to *A. thaliana*, these ARFs also show differential expression patterns in the root (Fig. 4-2) indicating their divergent functions. The presence of 9 ARF activators leads to question if an increased number of ARF activator in rice result in further diversification of their functions.

Surprisingly, the ARF6/8 homologues OsARF12 and OsARF25 were shown to be involved in control of root elongation (Qi *et al.* 2012) whereas the involvement in flower development hasn't been demonstrated yet. Could it be that these two ARF6/8 homologues acquired new functions in control of the root growth leaving other two homologues to regulate flower development?

The evolution of ARF activators requires further investigations to draw clear correlation between the increased number of ARFs and the increased complexity of developmental organization. In particular, the roles of ARF activators in mosses, lycophytes, ferns and gymnosperms are needed to be described in more details.

Component of auxin signaling pathway show specificity in expression patterns

The diversity and specificity of ARFs is argued to be a major factor controlling auxin response. In addition, other components of the auxin signaling pathway might contribute as well. In particular, *Arabidopsis thaliana* the auxin signaling pathway includes 6 TIR1/AFBs, 29 AUX/IAAs and 23 ARFs (Dharmasiri *et al.* 2005b, Okushima *et al.* 2005, Remington *et al.* 2004). The ARF activators were shown to have specific expression in both the RAM and the SAM in this study. In addition to ARF activators, ARF repressors also show tissue-specific expression patterns in the root and the shoot apical meristems and during embryonic development (Rademacher *et al.* 2011, Vernoux *et al.* 2011). *Arabidopsis thaliana* contains 18 putative ARF repressors (Okushima *et al.* 2005). Contrary to ARF activators, the majority of ARF repressors do not interact with other ARFs or AUX/IAA repressors (Vernoux *et al.* 2011). Thus it is possible that many ARF repressors do not participate in oligomer complexes between ARFs and AUX/IAA that control expression of auxin-induced genes (Korasick *et al.* 2014, Nanao *et al.* 2014). In that case, the role of ARF repressors might be to block ARF binding sites in the promoters of the auxin-

responsive genes preventing binding of ARF activators and thus repressing the auxin response. One can conclude that a high expression of an ARF activator in a given tissue might not lead to increased auxin response due to repressive action of the ARF repressors acting in the same tissue.

In addition to ARFs, other components of the auxin signaling pathway show specificity in their expression patterns. This specificity was observed in the SAM (Vernoux *et al.* 2011). In particular, among 6 TIR1/AFB auxin receptors, only three (TIR1, AFB1 and AFB6) are considered to be important for the auxin signaling in the SAM based on their expression patterns. Similarly, only 13 ARFs and 12AUX/IAAs are expressed in the SAM with variable degree of overlap in their expression patterns (Vernoux *et al.* 2011). This global expression analysis of all auxin signaling components allowed identifying domains of higher and lower auxin sensitivity within the SAM and provided insight into stability and robustness of the auxin signaling output. How the diversity in expression patterns of individual auxin signaling pathway components leads to high specificity of auxin response remains to be studied in greater detail.

One final factor that influences the specificity of auxin responses is the distribution of auxin itself. Both the RAM and the SAM have domains of higher and lower auxin (Fig. In-3 and In-7). One should consider that AUX/IAAs expressed in the domains of high auxin are expected to be subjected to constant degradation. It is proposed that ARF activators might be able to induce expression of their target genes only in these domains of high auxin. The domains of lower auxin might remain insensitive to auxin response despite expression of ARF activators in these tissues. All these points are should be considered when looking globally at the auxin signaling output.

ARF activator expression is predominantly regulated by gene repression mechanism

Auxin regulates growth and development through reprogramming of gene expression in a cell and tissue specific manner. This reprogramming is based on activation and repression of multiple genes in a given cell which ultimately leads to functional changes within this cell; often the cell adopts a new cell fate and differentiates to a different cell type. ARF activators are responsible for switching on these gene expression changes in response to high auxin levels.

It is clear that ARFs are able to induce a very powerful cellular response that should only be activated when and where necessary. In that case it would be advantageous for the plant to strictly control the action of these ARF activators by spatially and temporally restricting their expression. In this study it was shown that the expression of ARF activators is controlled by multiple transcriptional repressors *in planta*. It appears that repression and derepression could be the mechanism that restricts ARF action during development or in response to environment.

Interestingly, ARF activator action is already restricted by other repressive mechanisms which include repression through oligomerization with the AUX/IAAs and through the competitive binding of the target DNA sequences by ARF repressors. Nevertheless, these mechanisms are not necessary redundant and might serve different purposes. As such, the repression by AUX/IAAs is auxin-dependant and serves to control ARF activator response in dependence to auxin levels in the tissue.

On the other hand, the competitive binding with ARF repressors is auxin-independent, but might depend on the protein concentrations of both ARF repressors and ARF activators in the tissue and on the affinity of these to their target DNA. Thus the mechanism of repression by ARF repressors could serve to fine-tune severity of auxin response in a given tissue.

The repression of ARF transcription by specific transcription factors is in many cases independent from auxin levels. These transcription factors can be members of the signaling pathway from the different plant hormones or belong to gene signaling networks that act independently from auxin. The repression by the regulatory transcription factors could then provide a link between the auxin signaling pathway and other hormonal pathways or gene regulatory networks.

Auxin and cytokinin interactions regulate many aspects of plant development

Auxin and cytokinin were shown to mutually regulate a plethora of developmental processes (Schaller *et al.* 2015). In many processes these hormones appear to have antagonistic roles often conferring distinct developmental fates to precursor cells during cell differentiation; these include patterning of the root vasculature (Bishopp *et al.* 2011) and lateral organ initiation in the shoot apical meristem (Besnard *et al.*

2014). The cross-talk between these two hormones is detected for the components of their signaling pathways. In many cases the bridge signaling molecules are negative regulators of the respective pathways such as AHP6 (Besnard *et al.* 2014, Bishopp *et al.* 2011) or type-A ARRs (Zhao *et al.* 2010) from the cytokinin signaling pathway and the AUX/IAA proteins such as SHY2 from the auxin signaling pathway (Moubayidin *et al.* 2010). The interaction is therefore based on repressing hormone signaling output in specific cells by these negative regulators.

In this thesis the cross-talk between auxin and cytokinin once again appears to be based on the negative regulation: the expression of ARF7, one of the main components of the auxin signaling pathway, is repressed by CRF10, a member of the cytokinin signaling pathway. Interestingly, this interaction involves a gene from the CRF transcription factor family those role in the cytokinin signaling pathway is poorly characterized. Despite that, the control of the auxin signaling by CRFs has been shown before with CRF2 and CRF6 regulating expression of the auxin efflux carriers PIN1 and PIN7 in the root (Simaskova *et al.* 2015). This interaction affects the polar auxin transport and thus auxin levels in the root. On the other hand, CRF10-ARF7 interaction might not affect hormone levels or distribution but could modulate auxin output in specific tissues by reducing auxin responsiveness through down-regulation of ARF7 levels. This additional link between cytokinin and auxin appears to be specific for a few developmental processes which haven't been considered before as potential points of cross-talk between these hormones.

Appendix

Overview of primers used in this study

Primers used in this study are indicated by their number from the following list of primers

1. Cloning full-length transcriptional reporters of ARFs

ARF5: 239 + 240; ARF6: 243 + 245; ARF7: 237 + 238; ARF8: 250 + 251; ARF19: 252 + 253

2. Cloning shorter transcriptional reporters of ARFs (without downstream region)

ARF5: 239 + 241; ARF6: 243 + 244; ARF7: 246 + 247; ARF8: 249 + 250; ARF19: 252 + 254

3. Cloning ARF translational fusions (C-terminal mVenus)

ARF5: 258 + 259; ARF6: 243 + 256; ARF7: 260 + 261; ARF8: 262 + 263; ARF19: 252 + 257

4. Cloning ARF7 and ARF19 translational fusions (N-terminal mTQ2)

mTQ2 pDONR211: 528 + 529; ARF7 pDONR P2R-P3: 530 + 531;

ARF19 pDONR P2R-P3: 532 + 533

5. Cloning bait (promoter) constructs for yeast one-hybrid assay

ARF5: 1 + 2, 3 + 4; ARF6: 5 + 6; ARF7: 7 + 8; ARF8: 9 + 10, 11 + 12; ARF19: 13 + 14; 15 + 16

6. Sequencing of the transcriptional reporters, translational reporters, protoplast promoter constructs and Y1H bait constructs

Primers: 17 – 61 and 264 – 287

7. Cloning shoot-specific transcription factors (preys) for Y1H assay

Primers: 62 – 236

8. Cloning promoter constructs for the protoplast assay

ARF5: 242 + 240, 242 + 241; ARF6: 243 + 245, 243 + 244; ARF7: 8 + 7, 246 + 247; ARF8: 248 + 251; 255 + 256, 11 + 12; ARF19: 252 + 253, 255 + 254

9. Cloning transcription factor constructs for the protoplast assay

Primers: 307 – 395

10. Genotyping T-DNA insertion mutants of the transcription factors

Primers: 396 – 451

11. qRT-PCR primers used in this study

Primers: 452 – 527

12. Cloning CRF10 transcriptional and translational fusions

Transcriptional fusion: 534 + 535; translational fusion: 534 + 536

13. Identifying off-target T-DNA insertion in *crf10* mutant

Primers: 537– 540

14. Genotyping additional mutants

crf11: 541 + 542; crf12: 543 + 544; arf7-1: 545 + 546; arf19-1: 547 + 548

15. Cloning pSMB-mVenus and pSMB:ARF7 constructs

Primers:549 + 550

16. Cloning CRISPR mutation of CRF10 gene

Primers: 551 – 554

List of primers

1	ARF5_F1_for3	gtttggcaggagagagaggt	pARF5 cloning for Y1H
2	ARF5_F1_rev3	cctgactggtctttcaacagc	pARF5 cloning for Y1H
3	ARF5_F2_for	ggggacaactttgtatagaaaagttggatgttcctagtctctcctgctg	pARF5 cloning for Y1H
4	ARF5_F2_rev	ggggactgctttttttgtacaaacttgttccgaatccttcctaaacgtt	pARF5 cloning for Y1H
5	ARF6_for2	cacgtgtggattcagtgtgg	pARF6 cloning for Y1H
6	ARF6_rev3	agtgagacaagaggaccagc	pARF6 cloning for Y1H
7	ARF7_for	ggggacaactttgtatagaaaagttggaaagagatgtcgcaaaccagc	pARF7 cloning for Y1H and for protoplasts
8	ARF7_rev	ggggactgctttttttgtacaaacttgtcctttctcctgcattcacaca	pARF7 cloning for Y1H and for protoplasts
p	ARF8_F1_for	ggggacaactttgtatagaaaagttggaggacaatttcttccgaccct	pARF8 cloning for Y1H
10	ARF8_F1_rev	ggggactgctttttttgtacaaacttgttcatgaccctgttgacccaa	pARF8 cloning for Y1H
11	ARF8_F2_for3	ccaaaccgaaccgatccaaa	pARF8 cloning for Y1H and for protoplasts
12	ARF8_F2_rev3	agccagcctcagttctcatt	pARF8 cloning for Y1H and for protoplasts
13	ARF19_F1_for3	gtcggagtctagagcctgtc	pARF19 cloning for Y1H
14	ARF19_F1_rev3	cttacttgctcgctgtgtcc	pARF19 cloning for Y1H
15	ARF19_F2_for3	aaatgatcccaaagcctagagt	pARF19 cloning for Y1H
16	ARF19_F2_rev3	tgcgcgtggagagtatatgt	pARF19 cloning for Y1H
17	M13 forward	tgt aaa acg acg gcc agt	Gateway plasmids sequencing primers
18	M13 reverse	cag gaa aca gct atg acc	Gateway plasmids sequencing primers
19	ARF5_seq1	tggtatccttttctttgcatgtg	Sequencing of pARF5
20	ARF5_seq2	tgtgataatgtggattgtgtact	Sequencing of pARF5
21	ARF5_seq3	tggaggtggtcttaactctt	Sequencing of pARF5
22	ARF5_seq4	agaagcctcctcctttgtca	Sequencing of pARF5
23	ARF5_seq5	ccatttccaagcaaaataaaacc	Sequencing of pARF5 and yeast genotyping
24	ARF5_seq6	aggaatgtggtttgagagct	Sequencing of pARF5
25	ARF5_seq7	tcgaacagaacataccaacga	Sequencing of pARF5
26	ARF5_seq8	atcgacggtcaggagagatc	Sequencing of pARF5
27	ARF5_seq9	tccgttctttgaattgtttactt	Sequencing of pARF5
28	ARF5_seq10	tgtacgacaccaattaccttca	Sequencing of pARF5 and yeast genotyping
29	ARF6_seq1	tttgacgtcgaaaatctatcct	Sequencing of pARF6
30	ARF6_seq2	tgacatataatcgatgatgcctt	Sequencing of pARF6
31	ARF6_seq3	agctacgtttctaatttgtcgca	Sequencing of pARF6
32	ARF6_seq4	ccaaacgaggaagtgtgtat	Sequencing of pARF6
33	ARF6_seq5	ggtcatccactagctgaaaa	Sequencing of pARF6
34	ARF6_seq6	attatagcaccgtcacgtcg	Sequencing of pARF6 and yeast genotyping
35	ARF7_seq1	tctcctaaagcaaagtaacgtt	Sequencing of pARF7
36	ARF7_seq2	aaccggttctgaaatgcgtc	Sequencing of pARF7
37	ARF7_seq3	tggaggttcagtctttggtaga	Sequencing of pARF7
38	ARF7_seq4	aagttccattctcgtttaaaaca	Sequencing of pARF7

39	ARF7_seq5	aatcgtggccagtttgctag	Sequencing of pARF7
40	ARF7_seq6	aggtcgtatgctttgtttgtct	Sequencing of pARF7 and yeast genotyping
41	ARF8_seq1	aattcatcctcaaagccagc	Sequencing of pARF8
42	ARF8_seq2	atgagaactgaggctggctt	Sequencing of pARF8
43	ARF8_seq3	agcagcagagaaaatatttgatg	Sequencing of pARF8
44	ARF8_seq4	tgttggattatcgggcatct	Sequencing of pARF8
45	ARF8_seq5	ccttctctccactgtatcgga	Sequencing of pARF8 and yeast genotyping
46	ARF8_seq6	ccaaaccgaaccgataaccc	Sequencing of pARF8
47	ARF8_seq7	aatgccctttccatgatgcc	Sequencing of pARF8
48	ARF8_seq8	ttccgtcaaaagtttcccgc	Sequencing of pARF8 and yeast genotyping
49	ARF8_seq9	agggtcttcttgtaaatccttg	Sequencing of pARF8
50	ARF8_seq10	ttgtccgtgttagaattgtgt	Sequencing of pARF8
51	ARF8_seq11	tcatcatgggcacaaaacaa	Sequencing of pARF8
52	ARF19_seq1	gcaggatgcgtggatcaaat	Sequencing of pARF19
53	ARF19_seq2	cggtatttcttgtttaaccgcg	Sequencing of pARF19
54	ARF19_seq3	gaaagatcggcgttgaaagga	Sequencing of pARF19
55	ARF19_seq4	gggacatcttttctggtaacca	Sequencing of pARF19
56	ARF19_seq5	tgagaatctgcagaaacacgag	Sequencing of pARF19 and yeast genotyping
57	ARF19_seq6	cccaaagcctagagtataagtct	Sequencing of pARF19
58	ARF19_seq7	cacggtgacatataaaatttgga	Sequencing of pARF19
59	ARF19_seq8	tgcatagcttttgtggagaa	Sequencing of pARF19
60	ARF19_seq9	cagtagctgccaaagttaaga	Sequencing of pARF19
61	ARF19_seq10	agtgaaatttctccccacaagt	Sequencing of pARF19 and yeast genotyping
62	AttB1_adaptor_fw	ggggacaagtttgtacaaaaaagcaggct	Adaptor primer for TF library cloning
63	AttB2_adaptor_rv	ggggaccactttgtacaagaaagctgggt	Adaptor primer for TF library cloning
64	ARF13_for	aaaaagcaggcttcatggaaaataatggagaaatg	ARF13
65	ARF13_rev	agaaagctgggtcttagttatctgtgacgtttgg	ARF13
66	ARF14_for	aaaaagcaggcttcatggaaagtggcaacgtt	ARF14
67	ARF14_rev	agaaagctgggtctcaacttgagagactcttcct	ARF14
68	ARF20_for	aaaaagcaggcttcatggaaactggcaacgt	ARF20
69	ARF17_for	aaaaagcaggcttcatgtcaccgccgtcg	ARF17
70	ARF17_rev	agaaagctgggtcttaaccttgggagctagaac	ARF17
71	ARF22_for	aaaaagcaggcttcatggaaagtggcaacatt	ARF22
72	ARF20_rev	agaaagctgggtctcaacttgagagactcttactgg	ARF20
73	ARF22_rev	agaaagctgggtcttactggacttcaagtttttgac	ARF22
74	ARF23_for	aaaaagcaggcttcatggaaagtggcaatgtt	ARF23
75	ARF23_rev	agaaagctgggtctcatctgataccaactcgtaact	ARF23
76	SPL4_for	aaaaagcaggcttcatggagggtaagagatcaca	SPL4
77	SPL4_rev	agaaagctgggtcctatctaatctgtggtcgctt	SPL4
78	LAS_for	aaaaagcaggcttcatgcttacttccttcaaatcc	LAS
79	LAS_rev	agaaagctgggtctcatttccacgacgaaa	LAS
80	CAL_for	aaaaagcaggcttcatgggaaggggtagg	CAL
81	CAL_rev	agaaagctgggtctcaagcggcgtaaca	CAL
82	YAB1_for	aaaaagcaggcttcatgtctatgtcgtctatgtcc	YAB1

83	YAB1_rev	agaaagctgggtcttaataaggagtcacaccaac	YAB1
84	YAB2_for	aaaaagcaggcttcatgtctgtagatttctcatctgag	YAB2
85	YAB2_rev	agaaagctgggtcttagtaatagccattagacttttgg	YAB2
86	YAB3_for	aaaaagcaggcttcatgtcgagcatgtccat	YAB3
87	YAB3_rev	agaaagctgggtcctagttatgggccaccc	YAB3
88	YAB5_for	aaaaagcaggcttcatggctaactctgtgatgg	YAB5
89	YAB5_rev	agaaagctgggtcttaggctatcttagcttgctt	YAB5
90	STM_for	aaaaagcaggcttcatggagagtggttccaac	STM
91	STM_rev	agaaagctgggtctcaaagcatggtggagg	STM
92	WUS_for	aaaaagcaggcttcatggagccgccac	WUS
93	WUS_rev	agaaagctgggtcctagttcagacgtagctcaag	WUS
94	PRS_for	aaaaagcaggcttcatgagtcctgtggcttc	PRS
95	PRS_rev	agaaagctgggtcttaaagtttggtactgtcttgtttg	PRS
96	KAN1_for	aaaaagcaggcttcatgtctatggaaggtgtttttcta	KAN1
97	KAN1_rev	agaaagctgggtctcatttctcgtgccaatc	KAN1
98	KAN4_rev	agaaagctgggtcttagcacttgagaagggttaaat	KAN4
99	CONSTANS_for	aaaaagcaggcttcatgttgaaacaagagagtaacg	CONSTANS
100	CONSTANS_rev	agaaagctgggtctcagaatgaaggaacaatcc	CONSTANS
101	LUH_for	aaaaagcaggcttcatggctcagagtaattggg	LUH
102	LUH_rev	agaaagctgggtcctacttccaaatctttacggattt	LUH
103	DRNL_for	aaaaagcaggcttcatggaagaagcaatcatgag	DRNL
104	DRNL_rev	agaaagctgggtcctaataatcatcatgaaagcaatact	DRNL
105	DRN_for	aaaaagcaggcttcatggaaaaagccttgagaaa	DRN
106	DRN_rev	agaaagctgggtcctatccccacgatcttcg	DRN
107	SOC1_for	aaaaagcaggcttcatggtgaggggcaaaa	SOC1
108	SOC1_rev	agaaagctgggtctcactttcttgaagaacaagg	SOC1
109	AGL24_for	aaaaagcaggcttcatggcgagagagaagataa	AGL24
110	AGL24_rev	agaaagctgggtctcattcccaagatggaag	AGL24
111	SVP_for	aaaaagcaggcttcatggcgagagaaaagattc	SVP
112	SVP_rev	agaaagctgggtcctaaccaccatacggtaag	SVP
113	LMI_for	aaaaagcaggcttcatggagtggtcaacaacg	LMI
114	LMI_rev	agaaagctgggtctcaggggtatgacggc	LMI
115	LMI2_for	aaaaagcaggcttcatgggaagaacaccttgt	LMI2
116	PAN_for	aaaaagcaggcttcatgcagagcagcttca	PAN
117	PAN_rev	agaaagctgggtcttagtctctaggtctggcta	PAN
118	JAG_for	aaaaagcaggcttcatgaggcatgaggagaatta	JAG
119	JAG_rev	agaaagctgggtctcagagcgagtgatgatc	JAG
120	CUC3_for	aaaaagcaggcttcatgatgcttgcggtg	CUC3
121	CUC3_rev	agaaagctgggtcctacagctggaatcctaaag	CUC3
122	KAN3_for	aaaaagcaggcttcatggagcttttcccttca	KAN3
123	KAN3_rev	agaaagctgggtcttagggagagaggtttgg	KAN3
124	KAN4_for	aaaaagcaggcttcatgatgatgttagagtcaagaaac	KAN4
125	LMI2_rev	agaaagctgggtcctagaatttggaaaccatggaa	LMI2
126	CUC1_for	aaaaagcaggcttcatggatgttgatgtgtttaac	CUC1
127	CUC1_rev	agaaagctgggtctcagagagtaaacggcc	CUC1
128	CUC2_for	aaaaagcaggcttcatggacattccgtattacca	CUC2

129	CUC2_rev	agaaagctgggtctcagtagttccaaatacagtca	CUC2
130	SEP1_for	aaaaagcaggcttcatgggaagaggaagagtag	SEP1
131	SEP1_rev	agaaagctgggtctcagagcatccaccc	SEP1
132	KNAT1_for	aaaaagcaggcttcatggaagaataccagcatga	KNAT1
133	KNAT1_rev	agaaagctgggtcttatggaccgagacgataa	KNAT1
134	KNAT2_for	aaaaagcaggcttcatggatagaatgtgtggtttc	KNAT2
135	KNAT2_rev	agaaagctgggtcttactcggtaaagaatgtttcatta	KNAT2
136	KNAT3_for	aaaaagcaggcttcatggcgtttcatcacaatc	KNAT3
137	KNAT3_rev	agaaagctgggtcctacgcgaaccgc	KNAT3
138	KNAT4_for	aaaaagcaggcttcatggcgtttcataacaatca	KNAT4
139	KNAT4_rev	agaaagctgggtctcaacggtctcttccg	KNAT4
140	JLO_for	aaaaagcaggcttcatgagcagtagcggaaa	JLO
141	JLO_rev	agaaagctgggtctcattctcgttttatcactga	JLO
142	LOB_for	aaaaagcaggcttcatggcgtcgtcatcaa	LOB
143	LOB_rev	agaaagctgggtctcacatgttacctccttgc	LOB
144	FD_for	aaaaagcaggcttcatgttgtcatcagctaagc	FD
145	FD_rev	agaaagctgggtctcaaaatggagctgtgg	FD
146	PLT5_for	aaaaagcaggcttcatgaagaacaataacaacaaatcttc	PLT5
147	PLT5_rev	agaaagctgggtctcattccaacccaaaaacc	PLT5
148	PLT7_for	aaaaagcaggcttcatggctcctccaatgac	PLT7
149	PLT7_rev	agaaagctgggtcttagtaagactggttaggcc	PLT7
150	PLT2_for	aaaaagcaggcttcatgaattctaacaactggctc	PLT2
151	PLT2_rev	agaaagctgggtcttattcattccacatcgtgaaaa	PLT2
152	TPC10_for	aaaaagcaggcttcatgggacttaaaggatatagcg	TPC10
153	TPC10_rev	agaaagctgggtcttagaggtgtgagtttgga	TPC10
154	Flo10_for	aaaaagcaggcttcatggagagatcaaacagcata	FLO10
155	Flo10_rev	agaaagctgggtcttaagcgaaacccaaacg	FLO10
156	KNU_for	aaaaagcaggcttcatggcggaaccacc	KNU
157	KNU_rev	agaaagctgggtcttataaacggagagaaaggtcta	KNU
158	ARR1_for	aaaaagcaggcttcatgatgaatccgagtcacg	ARR1
159	ARR1_rev	agaaagctgggtctcaaaccggaatgttatcgat	ARR1
160	ARR10_for	aaaaagcaggcttcatgactatggagcaagaaattga	ARR10
161	ARR10_rev	agaaagctgggtctcaagctgacaaagaaaagg	ARR10
162	ARR11_for	aaaaagcaggcttcatggagaaaagcggct	ARR11
163	ARR11_rev	agaaagctgggtcttaagatatgaataaaccttggtctac	ARR11
164	ARR12_for	aaaaagcaggcttcatgactgttgaacaaaatttagaag	ARR12
165	ARR12_rev	agaaagctgggtctcatatgcatgttctgagtga	ARR12
166	ARR14_for	aaaaagcaggcttcatgccgatcaacgatca	ARR14
167	ARR14_rev	agaaagctgggtcctatctttgtcttgaagatctttcc	ARR14
168	ARR18_for	aaaaagcaggcttcatgagggttcttgctgt	ARR18
169	ARR18_rev	agaaagctgggtcctaaggtggaggaaatgaatc	ARR18
170	ARR20_for	aaaaagcaggcttcatggctttcttgatgaagaataag	ARR20
171	ARR20_rev	agaaagctgggtctcaattgtgaccaatctgatc	ARR20
172	TOC1_for	aaaaagcaggcttcatggatttgaacggtgagt	TOC1
173	TOC1_rev	agaaagctgggtctcaagttcccaaagcatc	TOC1
174	PRR2_for	aaaaagcaggcttcatggtcattaccgctaacg	PRR2

175	PRR2_rev	agaaagctgggtctcagcggagacgatg	PRR2
176	PRR8_for	aaaaagcaggcttcatgatacgcaaatgcgg	PRR8
177	PRR8_rev	agaaagctgggtcttaaggtttaagctctttggc	PRR8
178	CRF4_for	aaaaagcaggcttcatgatgatggatgagtttatgg	CRF4
179	CRF4_rev	agaaagctgggtctcacacaagtaagagatcgg	CRF4
180	CRF10_for	aaaaagcaggcttcatggttgcgattagaaagga	CRF10
181	CRF10_rev	agaaagctgggtcctatgaagctgcaaaacttttaat	CRF10
182	CRF11_for	aaaaagcaggcttcatggctgaacgaaagaaac	CRF11
183	CRF11_rev	agaaagctgggtcttatgggcacgcgatatta	CRF11
184	CRF12_for	aaaaagcaggcttcatgaagtcctttgtgaaacc	CRF12
185	CRF12_rev	agaaagctgggtcttaaaccaaaccgagaggc	CRF12
186	RGL1_for	aaaaagcaggcttcatgaagagagagcacaacc	RGL1
187	RGL1_rev	agaaagctgggtcttattccacacgattgattcg	RGL1
188	SHI_for	aaaaagcaggcttcatggcaggatttttctcgt	SHI
189	SHI_rev	agaaagctgggtctcaagatcttgagttggagaa	SHI
190	SPL3_for	aaaaagcaggcttcatgagtatgagaagaagcaaag	SPL3
191	SPL3_rev	agaaagctgggtcttagtcagttgtgcttttcc	SPL3
192	ALC_for	aaaaagcaggcttcatgggtgattctgacgtc	ALC
193	ALC_rev	agaaagctgggtctcaaagcagagtggct	ALC
194	MYB33_for	aaaaagcaggcttcatgagttacacgagcact	MYB33
195	MYB33_rev	agaaagctgggtcttagggtagttctgtcatttga	MYB33
196	PIF1_for	aaaaagcaggcttcatgcatcattttgtccctg	PIF1
197	PIF1_rev	agaaagctgggtcttaacctgttgtgtggtttc	PIF1
198	PIF4_for	aaaaagcaggcttcatggaacaccaaggttg	PIF4
199	PIF4_rev	agaaagctgggtcctagtggtccaaacgaga	PIF4
200	PIF5_for	aaaaagcaggcttcatggaacaagtgtttgctg	PIF5
201	PIF5_rev	agaaagctgggtctcagcctattttacccatatga	PIF5
202	EIL2_for	aaaaagcaggcttcatggatatgtataacaacaatataggg	EIL2
203	EIL2_rev	agaaagctgggtcttactgaatccaagatgtgg	EIL2
204	ABI5_for	aaaaagcaggcttcatggtaactagagaaacgaagtt	ABI5
205	ABI5_rev	agaaagctgggtcttagagtggacaactcgg	ABI5
206	ABF2_for	aaaaagcaggcttcatggatggtagtatgaatttggg	ABF2
207	ABF2_rev	agaaagctgggtctcaccaaggtcccg	ABF2
208	BZR1_for	aaaaagcaggcttcatgacttcggatggagc	BZR1
209	BZR1_rev	agaaagctgggtctcaaccacgagccttc	BZR1
210	BZR2_for	aaaaagcaggcttcatgaaaagattcttctataattccagc	BZR2
211	BZR2_rev	agaaagctgggtctcaactatgagctttaccatttc	BZR2
212	MYB30_for	aaaaagcaggcttcatggtgaggcctcct	MYB30
213	MYB30_rev	agaaagctgggtctcagaagaaattagtgttttcatcc	MYB30
214	IWS1_for	aaaaagcaggcttcatgggtttcgaggatgatc	IWS1
215	IWS1_rev	agaaagctgggtcctagaggtacttgatcataccc	IWS1
216	ARF4_for	aaaaagcaggcttcatggaatttgacttgaatactgag	ARF4
217	ARF4_rev	agaaagctgggtctcaaaccctagtgattgtagg	ARF4
218	ARF11_for	aaaaagcaggcttcatgagccaaacaagcttaga	ARF11
219	ARF11_rev	agaaagctgggtcttaaacgtgaactgtcctct	ARF11
220	SEP3_for	aaaaagcaggcttcatgggaagagggagagt	SEP3

221	SEP3_rev	agaaagctgggtctcaaatagagttggtgtcataag	SEP3
222	ARF13_seq1	tgacgtcagtttaagtggtgg	Sequencing forward primer
223	ARF13_seq2	tggaaggattcagaatggcg	Sequencing forward primer
224	LUH_seq1	tctccaagacaactgccagt	Sequencing forward primer
225	LUH_seq2	accatgtgaatagcatgcca	Sequencing forward primer
226	ARF14_seq1	agacgagcaggacatcaaca	Sequencing forward primer
227	ARF17_seq1	gtcagagtagcgttgccaag	Sequencing forward primer
228	ARF20_seq1	catggggtaattgcttccgc	Sequencing forward primer
229	PLT2_seq1	acaagacatagatggaccggt	Sequencing forward primer
230	ARR18_seq1	gggagtgaacaggatggtga	Sequencing forward primer
231	TOC1_seq1	ggtcttggtgctgatggaac	Sequencing forward primer
232	ARF4_seq1	gacacaagcacacatggagg	Sequencing forward primer
233	ARF4_seq2	ggtgcgatgggatgagtctt	Sequencing forward primer
234	ARF11_seq1	acacaacctacaccgactca	Sequencing forward primer
235	ARF4_seq3	gctctcctccttcgtctctc	Sequencing reverse primer
236	IWS1_seq1	tgcttctttccaagtacatcgg	Sequencing reverse primer
237	ARF7_for2	aagagatgtcgcaaaccagc	pARF7_fl
238	ARF7_rev2	cctttctcctgcattcacaca	pARF7_fl
239	ARF5_pr_for	gggg aca act ttg tat aga aaa gtt ggatgttcctagtctctcctgctg	pARF5_fl, pARF5_pr
240	ARF5_fl_rev	gggg ac tgc ttt ttt gta caa act tgt acctgactggtctttcaacagc	pARF5_fl
241	ARF5_F1_pr_rev	gggg ac tgc ttt ttt gta caa act tgt acagagagatttttcaatgttctgtt	pARF5_pr
242	ARF5_F1_pr_for	gggg aca act ttg tat aga aaa gtt gga gtttggcaggagagagaggt	pARF5_fl and pARF5_pr protoplasts
243	ARF6_pr_for	gggg aca act ttg tat aga aaa gtt gga cacgtgtggattcagtgtgg	pARF6_fl and pARF6_pr, ARF6 translational fusion
244	ARF6_pr_rev	gggg ac tgc ttt ttt gta caa act tgt tttttattctaacttaaaaagcaaacaacaaa	pARF6_pr
245	ARF6_fl_rev	gggg ac tgc ttt ttt gta caa act tgt tagtgagacaagaggaccag	pARF6_fl
246	ARF7_pr_for	gggg aca act ttg tat aga aaa gtt gga aagagatgtcgcaaaccagc	pARF7_pr
247	ARF7_pr_rev	gggg ac tgc ttt ttt gta caa act tgt gatcactcaactttactttctctgaa	pARF7_pr
248	ARF8_F1_pr_for	gggg aca act ttg tat aga aaa gtt gga ggacaatttcttccgaccct	pARF8_fl and pARF8_pr for protoplasts
249	ARF8_F1_pr_rev	gggg ac tgc ttt ttt gta caa act tgt gtctaattcaacttcaagaaaccaaa	pARF8_pr
250	ARF8_pr_for	gggg aca act ttg tat aga aaa gtt ggaccaaaccgaaccgatccaaa	pARF8_fl, pARF8_pr
251	ARF8_fl_rev	gggg ac tgc ttt ttt gta caa act tgt ttcatgaccctgttgaccca	pARF8_fl
252	ARF19_pr_for	gggg aca act ttg tat aga aaa gtt gga aaatgatcccaaagcctagagt	pARF19_fl, pARF19_pr, ARF19 tranlational fusion
253	ARF19_fl_rev	gggg ac tgc ttt ttt gta caa act tgt ttgctcgctgtgtccttgag	pARF19_fl
254	ARF19_F1_pr_rev	gggg ac tgc ttt ttt gta caa act tgt ggtttatagaaagaacgaaaaaattggt	pARF19_pr
255	ARF19_F1_pr_for	gggg aca act ttg tat aga aaa gtt gga gtcggagtctagagcctgtc	pARF19-F1_pr construct for protoplasts
256	ARF6_tf_attB1r_rev	gggg ac tgc ttt ttt gta caa act tgtgtagttgaatgaacccccaa	ARF6 translational fusion
257	ARF19_tf_attB1r_rev	gggg ac tgc ttt ttt gta caa act tgttctgttgaaagaagctgca	ARF19 translational fusion
258	ARF5_tf_topo_for	tgttcctagtctctcctgctg	ARF5 translational fusion
259	ARF5_tf_topo_rev	tgaaacagaagtcttaagatcgttaa	ARF5 translational fusion
260	ARF7_tf_topo_for	aagagatgtcgcaaaccagc	ARF7 translational fusion
261	ARF7_tf_topo_rev	ccggttaaacgaagtggc	ARF7 translational fusion
262	ARF8_tf_topo_for	ccaaaccgaaccgatcc	ARF8 translational fusion
263	ARF8_tf_topo_rev	gagatgggtcgggttttg	ARF8 translational fusion

264	ARF19_cDNA_seq1	ttcaggttgcagcatcgatg	sequencing of ARF19 translational fusion construct
265	ARF19_cDNA_seq2	gcagaattggactttcatcttct	sequencing of ARF19 translational fusion construct
266	ARF19_cDNA_seq3	gcacagagttcgatgttccc	sequencing of ARF19 translational fusion construct
267	ARF19_cDNA_seq4	cagcagacacaaagccatca	sequencing of ARF19 translational fusion construct
268	ARF6_cDNA_seq1	tcagctgggtttaatcctcaac	sequencing of ARF6 translational fusion construct
269	ARF6_cDNA_seq2	ccgagctgctgagaaagttt	sequencing of ARF6 translational fusion construct
270	ARF6_cDNA_seq3	gcgagtccatcagagtttgt	sequencing of ARF6 translational fusion construct
271	ARF6_cDNA_seq4	cagctgcccttcaagacatg	sequencing of ARF6 translational fusion construct
272	ARF6_cDNA_seq5	gcaacctgaaaaccacaaaaca	sequencing of ARF6 translational fusion construct
273	arf5_seq11	cgacgaaataattgacatgcgg	sequencing of ARF5 promoter
274	ARF5_tf_seq1	agctgttgaaagaccagtcag	sequencing of ARF5 translational fusion construct
275	ARF5_tf_seq2	tcctattgctttaactgctgct	sequencing of ARF5 translational fusion construct
276	ARF5_tf_seq3	cagcgatttggatccgttga	sequencing of ARF5 translational fusion construct
277	ARF5_tf_seq4	accaaccacagtctgatcca	sequencing of ARF5 translational fusion construct
278	ARF7_tf_seq1	cccgaatcttccttccaagc	sequencing of ARF7 translational fusion construct
279	ARF7_tf_seq2	atggaaaggcgcaacttctg	sequencing of ARF7 translational fusion construct
280	ARF7_tf_seq3	tgaagagagcaatgccatgg	sequencing of ARF7 translational fusion construct
281	ARF7_tf_seq4	tccgtccagctcccttaatc	sequencing of ARF7 translational fusion construct
282	ARF8_tf_seq1	cacagtgaacaggtttgggt	sequencing of ARF8 translational fusion construct
283	ARF8_tf_seq2	ggctgttaagtatgtctgaagca	sequencing of ARF8 translational fusion construct
284	ARF8_tf_seq3	cagtggcatggggaactttc	sequencing of ARF8 translational fusion construct
285	ARF8_tf_seq4	aacatcggcggtggagatc	sequencing of ARF8 translational fusion construct
286	ARF8_tf_seq5	tgtacttccggagctaaagagt	sequencing of ARF8 translational fusion construct
287	pARF8_seq12	tttgttttgtgcccatgatgat	sequencing of the ARF8 promoter
288	attB2r_2A_F	ggggacagctttcttgtacaaagtgggccagctgttgaattttgaccttc	Cloning of 2A-mCherry-NLS-tnos plasmid for protoplast assay
289	2A-CH-R	cttgctcactttaaagggcccagggttggactcgac	Cloning of 2A-mCherry-NLS-tnos plasmid for protoplast assay
290	2A-CH-F	tttaaagtgagcaagggcgaggagg	Cloning of 2A-mCherry-NLS-tnos plasmid for protoplast assay
291	CH-NLSR	tttaaacttgtacagctcgtccatgc	Cloning of 2A-mCherry-NLS-tnos plasmid for protoplast assay
292	CH-NLSF	aagtttaaacctgaacctcctaagaagaagag	Cloning of 2A-mCherry-NLS-tnos plasmid for protoplast assay
293	attB3_tnos	ggggacaactttgtataataaagttgactgtcgaggcgggatcaattc	Cloning of 2A-mCherry-NLS-tnos and VP16-2A-mCherry-NLS-tnos
294	RPS5a_seq1	tctgcatttgacactgccaa	sequencing of RPS5a promoter
295	RPS5a_seq2	aagcccatgtagacagctcc	sequencing of RPS5a promoter
296	RPS5a_for	ggg cca taa tcg tga gta g	pRPS5a cloning
297	RPS5a_rev	cgg ctg tgg tga gag aaa c	pRPS5a cloning
298	attB2_term35S	gggg ac cac ttt gta caa gaa agc tgg gta atttaggtgacactatagaatatgc	cloning NLS-mVenus-term construct for protoplast assay
299	CG_attb2 NLS F	ggg gac aag ttt gta caa aaa agc agg ctg cat gac tcc tcc taa gaa aaa gag aaa ggt t	cloning NLS-mVenus-term construct for protoplast assay

300	VP16_2A_rev2	gaaggtcaaaattcaacagctg cccaccgtactcgtca	cloning VP16-2A-mCherry-NLS-tenos plasmid for protoplast assay
301	VP16_2A_for2	tgacgagtacggtggg cagctgttgaattttgaccttc	cloning VP16-2A-mCherry-NLS-tenos plasmid for protoplast assay
302	VP16_for_attB2r	gggg aca gct ttc ttg tac aaa gtg gac agcctgggggacgag	cloning VP16-2A-mCherry-NLS-tenos plasmid for protoplast assay
303	mCherry_seq_rev	caccttgaagcgcatgaact	sequencing primer binding in mCherry
304	G4S4_seq_rev	ccaccagaaccaccacctc	sequencing primer binding in G4S4 linker
305	NLS-tnos-rev	tga acg atc gct agg tac cc	sequencing primer binding in tnos terminator
306	35S-term_rev	gcggtaaggatctgagctaca	sequencing primer binding in 35S terminator
307	KNAT1_PR_for	gggg aca agt ttg tac aaa aaa gca ggc ttc atggaagaataccagcatga	Cloning KNAT1 cDNA
308	KNAT1_PR_rev	gggg ac cac ttt gta caa gaa agc tgg gtc tggaccgagacgataag	Cloning KNAT1 cDNA
309	WUS_PR_for	gggg aca agt ttg tac aaa aaa gca ggc ttc atggagccgccac	Cloning WUS cDNA
310	WUS_PR_rev	gggg ac cac ttt gta caa gaa agc tgg gtc gttcagacgtagctcaag	Cloning WUS cDNA
311	KNU_PR_for	gggg aca agt ttg tac aaa aaa gca ggc ttc atggcggaaccacc	Cloning KNU cDNA
312	KNU_PR_rev	gggg ac cac ttt gta caa gaa agc tgg gtc taaacggagagaaaggtctag	Cloning KNU cDNA
313	CRF10_PR_for	gggg aca agt ttg tac aaa aaa gca ggc ttc atggttgcgattagaaagga	Cloning CRF10 cDNA
314	CRF10_PR_rev	gggg ac cac ttt gta caa gaa agc tgg gtc tgaagctgcaaaacttttaatg	Cloning CRF10 cDNA
315	CUC2_PR_for	gggg aca agt ttg tac aaa aaa gca ggc ttc atggacattccgtattacca	Cloning CUC2 cDNA
316	CUC2_PR_rev	gggg ac cac ttt gta caa gaa agc tgg gtc gtagttccaaatacagtcaagt	Cloning CUC2 cDNA
317	LBD3_PR_for	gggg aca agt ttg tac aaa aaa gca ggc ttc atgagacaaaagggtcaca	Cloning LBD3 cDNA
318	LBD3_PR_rev	gggg ac cac ttt gta caa gaa agc tgg gtc gcaagaccaaaggaagtc	Cloning LBD3 cDNA
319	DOF1.8_PR_for	gggg aca agt ttg tac aaa aaa gca ggc ttc atggacactgctaaatgg	Cloning Dof1.8 cDNA
320	DOF1.8_PR_rev	gggg ac cac ttt gta caa gaa agc tgg gtc ttgccatgaaccacca	Cloning Dof1.8 cDNA
321	ZFP7_PR_for	gggg aca agt ttg tac aaa aaa gca ggc ttc atgacggaatctgatgatg	Cloning ZFP7 cDNA
322	ZFP7_PR_rev	gggg ac cac ttt gta caa gaa agc tgg gtc gagtcttaaggtaagatcagg	Cloning ZFP7 cDNA
323	At2g26940_PR_for	gggg aca agt ttg tac aaa aaa gca ggc ttc atgaagagaacaagagacctt	Cloning At2g26940 cDNA
324	At2g26940_PR_rev	gggg ac cac ttt gta caa gaa agc tgg gtc aggatgatcttcatggtaag	Cloning At2g26940 cDNA
325	JAM2_PR_for	gggg aca agt ttg tac aaa aaa gca ggc ttc atgaatattggtcgcctagt	Cloning JAM2 cDNA
326	JAM2_PR_rev	gggg ac cac ttt gta caa gaa agc tgg gtc tctacctgatgatgttcttga	Cloning JAM2 cDNA
327	NFYB13_PR_for	gggg aca agt ttg tac aaa aaa gca ggc ttc atggatccaatggatatagtcg	Cloning NFYB13 cDNA
328	NFYB13_PR_rev	gggg ac cac ttt gta caa gaa agc tgg gtc gctttgcggacttctc	Cloning NFYB13 cDNA
329	SMZ_PR_for	gggg aca agt ttg tac aaa aaa gca ggc ttc atgttggatcttaacctaaagatc	Cloning SMZ cDNA
330	SMZ_PR_rev	gggg ac cac ttt gta caa gaa agc tgg gtc tggatcaaaacaattggaca	Cloning SMZ cDNA
331	SPL2_PR_for	gggg aca agt ttg tac aaa aaa gca ggc ttc atggagtgtaatgcaaagc	Cloning SPL2 cDNA
332	SPL2_PR_rev	gggg ac cac ttt gta caa gaa agc tgg gtc gttataaaactggttcaagctga	Cloning SPL2 cDNA
333	SPL13B_PR_for	gggg aca agt ttg tac aaa aaa gca ggc ttc atggactggaatttcaaacttag	Cloning SPL13b cDNA
334	SPL13B_PR_rev	gggg ac cac ttt gta caa gaa agc tgg gtc ctcccaatgaaacggg	Cloning SPL13b cDNA

335	HFR1_PR_for	gggg aca agt ttg tac aaa aaa gca ggc ttc atgtcgaataatcaagctttcat	Cloning HFR1 cDNA
336	HFR1_PR_rev	gggg ac cac ttt gta caa gaa agc tgg gtc tagtcttctcatcgcatgg	Cloning HFR1 cDNA
337	NTL4_PR_for	gggg aca agt ttg tac aaa aaa gca ggc ttc atgggtcgtggctc	Cloning NTL4 cDNA
338	NTL4_PR_rev	gggg ac cac ttt gta caa gaa agc tgg gtc cctggaagagaccaaaatg	Cloning NTL4 cDNA
339	TGA1_PR_for	gggg aca agt ttg tac aaa aaa gca ggc ttc atgaattcgacatcgacacat	Cloning TGA1 cDNA
340	TGA1_PR_rev	gggg ac cac ttt gta caa gaa agc tgg gtc cgttggttcacgatgtc	Cloning TGA1 cDNA
341	ARF9_PR_for	gggg aca agt ttg tac aaa aaa gca ggc ttc atggcaaatcgcgg	Cloning ARF9 cDNA
342	ARF9_PR_rev	gggg ac cac ttt gta caa gaa agc tgg gtc gttggaatgattatctgttttgg	Cloning ARF9 cDNA
343	IAA30_PR_for	aaaaagcaggcttc atgggaagagggagaag	Cloning IAA30 cDNA
344	IAA30_PR_rev	agaaagctgggtc gtagtgataagctcttgagatc	Cloning IAA30 cDNA
345	ABS2_PR_for	aaaaagcaggcttc atgtcaataaaccaatactcaag	Cloning ABS2 cDNA
346	ABS2_PR_rev	agaaagctgggtc gctcgtccggttca	Cloning ABS2 cDNA
347	ASIL1_PR_for	aaaaagcaggcttc atggaggacgacgac	Cloning ASIL1 cDNA
348	ASIL1_PR_rev	agaaagctgggtc gctacttacattgccgttat	Cloning ASIL1 cDNA
349	AT2G44730_PR_for	aaaaagcaggcttc atgtccgatccggatt	Cloning At2g44730 cDNA
350	AT2G44730_PR_rev	agaaagctgggtc tctagctttcttcttcttgtc	Cloning At2g44730 cDNA
351	AT1G61730_PR_for	aaaaagcaggcttc atgacgaagaaactcaatcc	Cloning At1g61730 cDNA
352	AT1G61730_PR_rev	agaaagctgggtc tgtatctaatggcttgttcttag	Cloning At1g61730 cDNA
353	AT1G26610_PR_for	aaaaagcaggcttc atggagcagttcaaagag	Cloning At1g26610 cDNA
354	AT1G26610_PR_rev	agaaagctgggtc ttcatcaataggagcaggaa	Cloning At1g26610 cDNA
355	ABF4_PR_for	aaaaagcaggcttc atgggaactcacatcaatttc	Cloning ABF4 cDNA
356	ABF4_PR_rev	agaaagctgggtc ccatggtccggttaatg	Cloning ABF4 cDNA
357	DREB2A_PR_for	aaaaagcaggcttc atggcagtttatgatcagag	Cloning DREB2A cDNA
358	DREB2A_PR_rev	agaaagctgggtc gttctccagatccaagtaac	Cloning DREB2A cDNA
359	DREB26_PR_for	aaaaagcaggcttc atggtgaaacaagaacgc	Cloning DREB26 cDNA
360	DREB26_PR_rev	agaaagctgggtc attgaaactccaaagcgg	Cloning DREB26 cDNA
361	DDF1_PR_for	aaaaagcaggcttc atgaataatgatgatattattctggc	Cloning DDF1 cDNA
362	DDF1_PR_rev	agaaagctgggtc atatctgtaactccacaatgac	Cloning DDF1 cDNA
363	AL3_PR_for	aaaaagcaggcttc atggaaggtggagct	Cloning AL3 cDNA
364	AL3_PR_rev	agaaagctgggtc agctcgagctcttttgt	Cloning AL3 cDNA
365	ATERF15_PR_for	aaaaagcaggcttc atggaatattcccaatcttcc	Cloning ATERF15 cDNA
366	ATERF15_PR_rev	agaaagctgggtc acatgagctcataagaagttg	Cloning ATERF15 cDNA
367	MYB65_PR_for	aaaaagcaggcttc atgagttacacgacggc	Cloning MYB65 cDNA
368	MYB65_PR_rev	agaaagctgggtc cagcgaccaaacagg	Cloning MYB65 cDNA
369	NLP5_PR_for	aaaaagcaggcttc atggaaaacaattctcttcctat	Cloning NLP5 cDNA
370	NLP5_PR_rev	agaaagctgggtc tgaaagacatccactgaca	Cloning NLP5 cDNA
371	WRKY38_PR_for	aaaaagcaggcttc atggaaatgaactcccc	Cloning WRKY38 cDNA
372	WRKY38_PR_rev	agaaagctgggtc aaagtaaaactgatcataacgatc	Cloning WRKY38 cDNA
373	ZAP1_PR_for	aaaaagcaggcttc atggctgaggtggg	Cloning ZAP1 cDNA
374	ZAP1_PR_rev	agaaagctgggtc gctttgggcaggc	Cloning ZAP1 cDNA
375	WRKY4_PR_for	aaaaagcaggcttc atgtcggaaaaggaagaag	Cloning WRKY4 cDNA
376	WRKY4_PR_rev	agaaagctgggtc agttgtttgctcttcttaag	Cloning WRKY4 cDNA
377	WRKY11_PR_for	aaaaagcaggcttc atggccgtcgatctaat	Cloning WRKY11 cDNA
378	WRKY11_PR_rev	agaaagctgggtc agccgaggcaaaca	Cloning WRKY11 cDNA

379	WRKY17_PR_for	aaaaagcaggcttc atgaccgttgatattatgcg	Cloning WRKY17 cDNA
380	WRKY17_PR_rev	agaaagctgggtc agccgaaccaaacac	Cloning WRKY17 cDNA
381	WRKY20_PR_for	aaaaagcaggcttc atgaaccctcaagctaatg	Cloning WRKY20 cDNA
382	WRKY20_PR_rev	agaaagctgggtc cggacccgattgtact	Cloning WRKY20 cDNA
383	WRKY21_PR_for	aaaaagcaggcttc atggaggagatagaaggaac	Cloning WRKY21 cDNA
384	WRKY21_PR_rev	agaaagctgggtc agttgttatagcttgagatgg	Cloning WRKY21 cDNA
385	WRKY33_PR_for	aaaaagcaggcttc atggctgcttcttttcttac	Cloning WRKY33 cDNA
386	WRKY33_PR_rev	agaaagctgggtc gggcataaacgaatcgaa	Cloning WRKY33 cDNA
387	ZFP5_PR_for	aaaaagcaggcttc atgtctataaatccgacaatgtc	Cloning ZFP5 cDNA
388	ZFP5_PR_rev	agaaagctgggtc tgccgcatctccg	Cloning ZFP5 cDNA
389	ZFP6_PR_for	aaaaagcaggcttc atggcgactgaaacatc	Cloning ZFP6 cDNA
390	ZFP6_PR_rev	agaaagctgggtc tggcccaaggcttaaa	Cloning ZFP6 cDNA
391	ARF7_PR_for	aaaaagcaggcttcatgaaagctccttcatca	Cloning ARF7 cDNA
392	ARF7_PR_rev	agaaagctgggtcccggttaaacgaagtg	Cloning ARF7 cDNA
393	ARF9_seq1	tattgacgacagggtggagc	sequencing of ARF9 cDNA
394	JAM2_seq1	ctcgaggtgaaggtggtcc	sequencing of JAM2 cDNA
395	NLP5_seq1	tgaacaaggtagtcagatttgct	sequencing of NLP5 cDNA
396	Dof1_8_gen_for	tgtacacgttcatcaaatggg	genotyping Dof1.8 mutant SALK_130584
397	Dof1_8_gen_rev	aaagctccaaagacgaggaag	genotyping Dof1.8 mutant SALK_130584
398	NF_YB13_gen_for	atttggtttggttttggttcc	genotyping NF-YB13 mutant SALK_042710C
399	NF_YB13_gen_rev	ctcctgagcatgttctcaagg	genotyping NF-YB13 mutant SALK_042710C
400	MYB65_gen_for	CCAATGCAAGAAGAAGTTTGC	genotyping MYB65 mutant SALK_063552
401	MYB65_gen_rev	catcgcaggtagaggagtcag	genotyping MYB65 mutant SALK_063552
402	NLP5_gen_for	agctcaaacatgggtctcatg	genotyping NLP5 mutant SALK_027488C
403	NLP5_gen_rev	ttgtagggatgatgcttctgg	genotyping NLP5 mutant SALK_027488C
404	AL3_gen_for	gagtcaagtcgtgagagaccg	genotyping AL3 mutant SALK_080056C
405	AL3_gen_rev	ggaatggctaaagcaaaggac	genotyping AL3 mutant SALK_080056C
406	WRKY38_gen_for	tcttgtccggcaataaaaatg	genotyping WRKY38 mutant SAIL_749_B02
407	WRKY38_gen_rev	aattaagtgagccgcgtactg	genotyping WRKY38 mutant SAIL_749_B02
408	HFR1_gen_for	aataaggattcacccccactg	genotyping HFR1 mutant SALK_037727C
409	HFR1_gen_rev	ctaaaatggggctacggctac	genotyping HFR1 mutant SALK_037727C
410	NTL4_gen_for	tcttcatttcccatcagttgc	genotyping NTL4 mutant SALK_009578C
411	NTL4_gen_rev	tggtgggaaatagacaagtcg	genotyping NTL4 mutant SALK_009578C
412	IAA30_gen_for1	cggaacaattgtaatatctccg	genotyping IAA30 mutant SALK_065384C
413	IAA30_gen_rev1	agggagaagctcatcgtcttc	genotyping IAA30 mutant SALK_065384C
414	ABS2_gen_for	tttttccaaccatttagctcg	genotyping ABS2 mutant SALK_146872C
415	ABS2_gen_rev	gaatctagctggcactccatg	genotyping ABS2 mutant SALK_146872C
416	ASIL1_gen_for	ccttgaaagttattccaggcc	genotyping ASIL1 mutant SALK_124095C
417	ASIL1_gen_rev	attcctcaggagaagcctcag	genotyping ASIL1 mutant SALK_124095C

418	At1g61730_gen_for	catattttcatcaacaaggccc	genotyping At1g61730 mutant SALK_065296C
419	At1g61730_gen_rev	ttttgttcctgatttcatcgc	genotyping At1g61730 mutant SALK_065296C
420	DDF1_gen_for	atgtgtcctacgcgcgtatac	genotyping DDF1 mutant SALK_137015
421	DDF1_gen_rev	taacgcctgggacacatctac	genotyping DDF1 mutant SALK_137015
422	WRKY4_gen_for	aattaatgggatcgaaattcaac	genotyping WRKY4 mutant SALK_082016
423	WRKY4_gen_rev	gaaaagacccaaaaagcttgg	genotyping WRKY4 mutant SALK_082016
424	WRKY17_gen_for	tggattttggttaaagaccttc	genotyping WRKY17 mutant SALK_076337C
425	WRKY17_gen_rev	agcaagaaagatcgaagagcc	genotyping WRKY17 mutant SALK_076337C
426	ZFP6_gen_for	tatgtggatgcatgccataag	genotyping ZFP6 mutant SALK_200865C
427	ZFP6_gen_rev	tgaaatcgacttggtatgcatc	genotyping ZFP6 mutant SALK_200865C
428	WRKY20_gen_for	ttttggtcaattgcttccaag	genotyping WRKY20 mutant SALK_056001
429	WRKY20_gen_rev	tgttgcattgaatgaaccaag	genotyping WRKY20 mutant SALK_056001
430	WRKY21_gen_for	gaaagttttgttttctggggg	genotyping WRKY21 mutant WiscDsLox477-480H13
431	WRKY21_gen_rev	aaggatggttctttgcatgtg	genotyping WRKY21 mutant WiscDsLox477-480H13
432	At1g26610_gen_for	ttgccttgatggtaggatctg	genotyping At1g26610 mutant GK-910E04
433	At1g26610_gen_rev	tcttcaccagacctcatctgg	genotyping At1g26610 mutant GK-910E04
434	CRF10_gen_for	tcagaatctaacgcccaactg	genotyping CRF10 mutant SALK_084716C
435	CRF10_gen_rev	tggtgttaggcaaaggaaatg	genotyping CRF10 mutant SALK_084716C
436	At2g26940_gen_for	gaggtcgtatccctttccaag	genotyping At2g26940 mutant SALK_112806
437	At2g26940_gen_rev	caattgctgcatttgaatgtg	genotyping At2g26940 mutant SALK_112806
438	WRKY11_gen_for	tgtcgtattgatgaatcgctg	genotyping WRKY11 mutant SALK_141511C
439	WRKY11_gen_rev	gtcagtgatctcggagcagtc	genotyping WRKY11 mutant SALK_141511C
440	ABF4_gen_for	tcctcgattaagcacatacgg	genotyping ABF4 mutant SALK_069523
441	ABF4_gen_rev	gaacaagggttttagggcttg	genotyping ABF4 mutant SALK_069523
442	At2g44730_gen_for	tgacgcgtacagagacaaatg	genotyping At2g44730 mutant GABI_104F06
443	At2g44730_gen_rev	cactgtcggaaactgaggaac	genotyping At2g44730 mutant GABI_104F06
444	LBD3_gen_for	ATCATCCGTATACGCAACAGC	genotyping LBD3 mutant WiscDsLoxHs070_10G
445	LBD3_gen_rev	TTTGGGATTTTAGCCACTTTG	genotyping LBD3 mutant WiscDsLoxHs070_10G
446	LBb1.3	attttgccgatttcggaac	genotyping SALK T-DNA insertion lines
447	LB3	tagcatctgaatttcataaccaatctcgatacac	genotyping SAIL T-DNA insertion lines
448	pSKTAIL-L1	ttctcatctaagcccccatttgg	genotyping SK T-DNA insertion lines
449	WiscDsLox_LP	aacgtccgcaatgtgttattaagttg	genotyping WiscDsLox T-DNA insertion lines
450	LB4	cgtgtgccaggtgcccacggaatagt	genotyping FLAG T-DNA insertion lines
451	WsDsLox B2	ctgaaagcgacgttggatgt	genotyping LBD3 mutant WiscDsLoxHs070_10G
452	TUB4_for	CTCTCCGGCTGTAGCATCTT	qRT-PCR of ARFs in mutants of TFs

453	TUB4_rev	AAGGCTTTCCTTCATTGGTACA	qRT-PCR of ARFs in mutants of TFs
454	ARF5_qRT_for	gttctgcttgtaggagatgatcc	qRT-PCR of ARFs in mutants of TFs
455	ARF5_qRT_rev	tccttatgcaccttacgcatc	qRT-PCR of ARFs in mutants of TFs
456	ARF6_qRT_for	ctcgcgtctctgttggtatg	qRT-PCR of ARFs in mutants of TFs
457	ARF6_qRT_rev	ccagttattgtacccatgtaccg	qRT-PCR of ARFs in mutants of TFs
458	ARF7_qRT_for	cgccatttcgaacgatct	qRT-PCR of ARFs in mutants of TFs
459	ARF7_qRT_rev	agcctcgtttttgcaccttt	qRT-PCR of ARFs in mutants of TFs
460	ARF8_qRT_for	tgtctttgtcagtgccaagc	qRT-PCR of ARFs in mutants of TFs
461	ARF8_qRT_rev	aagagttgattcttttcattcctga	qRT-PCR of ARFs in mutants of TFs
462	ARF19_qRT_for	cctaagtacccgaggcaacc	qRT-PCR of ARFs in mutants of TFs
463	ARF19_qRT_rev	ctctgtgcgtccttcatcc	qRT-PCR of ARFs in mutants of TFs
464	CRF10_qRT_for1	tcgaagataacggtccaagtg	qRT-PCR of TF mutants (gene specific primers)
465	CRF10_qRT_rev1	gggcaagagatgttgataggag	qRT-PCR of TF mutants (gene specific primers)
466	CRF10_qRT_for2	gaaacactctatcgtcccttcc	qRT-PCR of TF mutants (gene specific primers)
467	CRF10_qRT_rev2	cgtttcattttccttggcttagg	qRT-PCR of TF mutants (gene specific primers)
468	AL3_qRT_for	ccaacaatgtgaccctgaga	qRT-PCR of TF mutants (gene specific primers)
469	AL3_qRT_rev	gcccatccctagcaaagtta	qRT-PCR of TF mutants (gene specific primers)
470	WRKY38_qRT_for	tgctaaaccagaaaccgaaga	qRT-PCR of TF mutants (gene specific primers)
471	WRKY38_qRT_rev	tccctccaattctcacttgaa	qRT-PCR of TF mutants (gene specific primers)
472	Dof1.8_qRT_for	agtatcccagagtttctgcaagtag	qRT-PCR of TF mutants (gene specific primers)
473	Dof1.8_qRT_rev	gaagttgagaccagtgggttg	qRT-PCR of TF mutants (gene specific primers)
474	LBD3_qRT_for	gtccacaagatttttggtgct	qRT-PCR of TF mutants (gene specific primers)
475	LBD3_qRT_rev	tcgtacaccatcgaatccac	qRT-PCR of TF mutants (gene specific primers)
476	NFYB13_qRT_for1	gagcaacataagtatgaaacaatgc	qRT-PCR of TF mutants (gene specific primers)
477	NFYB13_qRT_rev1	ctgctgcttcctcctcagtc	qRT-PCR of TF mutants (gene specific primers)
478	NFYB13_qRT_for2	aactgaaaccgtaagggtaagtgt	qRT-PCR of TF mutants (gene specific primers)
479	NFYB13_qRT_rev2	cgcatttgcaacttacaagg	qRT-PCR of TF mutants (gene specific primers)
480	MYB65_qRT_for1	gtggcagcgaaaacctga	qRT-PCR of TF mutants (gene specific primers)
481	MYB65_qRT_rev1	aacattccctgcaaaagctg	qRT-PCR of TF mutants (gene specific primers)
482	MYB65_qRT_for2	ttcatgcacctggcttacat	qRT-PCR of TF mutants (gene specific primers)
483	MYB65_qRT_rev2	ccaaatttttaccaagtccacaa	qRT-PCR of TF mutants (gene specific primers)
484	NLP5_qRT_for1	gttggtttgcctggaagagt	qRT-PCR of TF mutants (gene specific primers)
485	NLP5_qRT_rev1	cctcacatcaggagtccattc	qRT-PCR of TF mutants (gene specific primers)
486	NLP5_qRT_for2	ggatgattttctgagggtaaagg	qRT-PCR of TF mutants (gene specific primers)
487	NLP5_qRT_rev2	ctatgcgagtttctcatcttaaacc	qRT-PCR of TF mutants (gene specific primers)

488	NTL4_qRT_for1	gatgtatacaaatctgagccttgg	qRT-PCR of TF mutants (gene specific primers)
489	NTL4_qRT_rev1	gtctctacttttcagcctcgactt	qRT-PCR of TF mutants (gene specific primers)
490	NTL4_qRT_for2	gcaacagagtttgagccaga	qRT-PCR of TF mutants (gene specific primers)
491	NTL4_qRT_rev2	gcaggaatagcacccaacat	qRT-PCR of TF mutants (gene specific primers)
492	IAA30_qRT_for1	ttcaatgcttcaatcctttgg	qRT-PCR of TF mutants (gene specific primers)
493	IAA30_qRT_rev1	cgtacgttagcacgtgactctt	qRT-PCR of TF mutants (gene specific primers)
494	IAA30_qRT_for2	gaatctaggattgaccaatacagtca	qRT-PCR of TF mutants (gene specific primers)
495	IAA30_qRT_rev2	cgaacaagtgatttacattcagaca	qRT-PCR of TF mutants (gene specific primers)
496	ABS2_qRT_for	catttctaccctcaacaacaacac	qRT-PCR of TF mutants (gene specific primers)
497	ABS2_qRT_rev	ccggttcatatctcctgtgaa	qRT-PCR of TF mutants (gene specific primers)
498	ASIL1_qRT_for	tctgagtctgatcctgaacctg	qRT-PCR of TF mutants (gene specific primers)
499	ASIL1_qRT_rev	aggtgggagactctcagcag	qRT-PCR of TF mutants (gene specific primers)
500	At1g61730_qRT_for	cgacttcaacgaaacgagtg	qRT-PCR of TF mutants (gene specific primers)
501	At1g61730_qRT_rev	aagatttcgtcttcttcactcca	qRT-PCR of TF mutants (gene specific primers)
502	WRKY4_qRT_for	atgagcctgatcccaagaga	qRT-PCR of TF mutants (gene specific primers)
503	WRKY4_qRT_rev	tctgtcacagttctatgtgaagca	qRT-PCR of TF mutants (gene specific primers)
504	WRKY17_qRT_for	gaccactctgaaggcttttcc	qRT-PCR of TF mutants (gene specific primers)
505	WRKY17_qRT_rev	gcttttcttgcaatggcact	qRT-PCR of TF mutants (gene specific primers)
506	WRKY20_qRT_for	gaatcaatccagacttcccaaa	qRT-PCR of TF mutants (gene specific primers)
507	WRKY20_qRT_rev	atcagccaagatggatggag	qRT-PCR of TF mutants (gene specific primers)
508	WRKY21_qRT_for	gcttaaaatgcgggagctcta	qRT-PCR of TF mutants (gene specific primers)
509	WRKY21_qRT_rev	ctcctaacccgatgtttcctc	qRT-PCR of TF mutants (gene specific primers)
510	At1g26610_qRT_for	tggtgatgttcattatgattcagata	qRT-PCR of TF mutants (gene specific primers)
511	At1g26610_qRT_rev	ccaacttctttggtccattcc	qRT-PCR of TF mutants (gene specific primers)
512	At2g26940_qRT_for	ccggaagaaagaagtgaagatg	qRT-PCR of TF mutants (gene specific primers)
513	At2g26940_qRT_rev	caaatcacacaaaagtgcttcc	qRT-PCR of TF mutants (gene specific primers)
514	WRKY11_qRT_for	ccggcgataagtgcaaag	qRT-PCR of TF mutants (gene specific primers)
515	WRKY11_qRT_rev	atcctctgaatgtactgcacttgta	qRT-PCR of TF mutants (gene specific primers)
516	ABF4_qRT_for	gctagatcaagagctcgaaagc	qRT-PCR of TF mutants (gene specific primers)
517	ABF4_qRT_rev	ccaccatttcagcctgtttt	qRT-PCR of TF mutants (gene specific primers)
518	At2g44730_qRT_for	tcctgaaggaggagggaaac	qRT-PCR of TF mutants (gene specific primers)
519	At2g44730_qRT_rev	gctatctccaccattggatca	qRT-PCR of TF mutants (gene specific primers)
520	ARF8-2_qRT_for	cgtccaaccaaaccaagaac	qRT-PCR of TF mutants (gene specific primers)
521	ARF8-2_qRT_rev	ccctaactcttctcgcagctc	qRT-PCR of TF mutants (gene specific primers)
522	ZFP6_qRT_for	ccggagaagtaaagactcatgg	qRT-PCR of TF mutants (gene specific primers)

523	ZFP6_qRT_rev	actatctccggcgaacctc	qRT-PCR of TF mutants (gene specific primers)
524	HFR1_qRT_for	cagttactcgaaaaggttccaag	qRT-PCR of TF mutants (gene specific primers)
525	HFR1_qRT_rev	accgaaaccttgtccgtct	qRT-PCR of TF mutants (gene specific primers)
526	DDF1_qRT_for	tctcaacgacgatgatgagact	qRT-PCR of TF mutants (gene specific primers)
527	DDF1_qRT_rev	aggagtcatgtcttccatatacga	qRT-PCR of TF mutants (gene specific primers)
528	mTQ2_BOX2_attB1	GGGG ACA AGT TTG TAC AAA AAA GCA GGC TCA atgGTGAGCAAGGGCGAG	N-terminal translational fusion mTQ2
529	mTQ2_BOX2_attB2	GGGG AC CAC TTT GTA CAA GAA AGC TGG GTGGGCCGCAGCTGCCTTGTACAGCTCGTCCATG	N-terminal translational fusion mTQ2
530	ARF7_BOX3_attB2r	GGGG ACA GCT TTC TTG TAC AAA GTG GAC AAAGCTCCTTCATCAAATG	N-terminal translational fusion ARF7 genomic
531	ARF7_BOX3_attB3	GGGG AC AAC TTT GTA TAA TAA AGT TGA TCACCGGTTAAACGAAGT	N-terminal translational fusion ARF7 genomic
532	ARF19_BOX3_attB2r	GGGG ACA GCT TTC TTG TAC AAA GTG GAC AAAGCTCCATCAAATGGAT	N-terminal translational fusion ARF19 genomic
533	ARF19_BOX3_attB3	GGGG AC AAC TTT GTA TAA TAA AGT TGA CTATCTGTTGAAAGAAGCTGC	N-terminal translational fusion ARF19 genomic
534	pCRF10_for	GGGG ACA ACT TTG TAT AGA AAA GTT GGA GTGATAGAGCTGCAGGA	CRF10 transcriptional and translational reporter
535	pCRF10_rev	GGGG AC TGC TTT TTT GTA CAA ACT TGT TGTTAAACCCACTCCTCAAA	CRF10 transcriptional reporter
536	CRF10_tf_rev	GGGG AC TGC TTT TTT GTA CAA ACT TGT TGAAGCTGCAAAACTTTTTAATG	CRF10 translational reporetr
537	SALK084716_gen_for	GGAAATCAACCATGCCTTGC	offtarget T-DNA insertions
538	SALK084716_gen_rev	CGAAGCTGAACAAACGTGGA	offtarget T-DNA insertions
539	SALK084716_gen2_for	ATATGATTGGCACGACTCTGG	offtarget T-DNA insertions
540	SALK084716_gen2_rev	TCTAGTCGGATTGTTGATGGG	offtarget T-DNA insertions
541	CRF11_gen_LP	TCGCTTTCTGCTCTGTTTTTC	genotyping crf11 mutant
542	CRF11_gen_RP	ATCAAGCTCACAAGCATTTGG	genotyping crf11 mutant
543	CRF12_gen_LP	CTGCGATTTCGTCTCTGTTTC	genotyping crf12 mutant
544	CRF12_gen_RP	GTCTAGCTCTGCACCATTTGC	genotyping crf12 mutant
545	arf7-1_gen_LP	CAGCTAGATCGTTCGAAATGG	genotyping arf7-1 mutant
546	arf7-1_gen_RP	AGCACATCACCATTTAGGTGC	genotyping arf7-1 mutant
547	arf19-1_gen_LP	TGAGACTGAGGATTGTGGGG	genotyping arf19-1 mutant
548	arf19-1_gen_RP	CTGGTTGTGCTTGCATCTGT	genotyping arf19-1 mutant
549	pSMB_for	GGGG ACA ACT TTG TAT AGA AAA GTT GGA cctatctttgttgacggctcg	pSMB:ARF7 and pSMB-mVenus constructs
550	pSMB_rev	GGGG AC TGC TTT TTT GTA CAA ACT TGT cgctttcttttcgacctttgc	pSMB:ARF7 and pSMB-mVenus constructs
551	C2_DT1-BsF_2_n	ATATATGGTCTCGATTGTCAAGAAACCCAACCTTTGGTT	CRISPR cloning CRF10
552	C2_DT1_F0_2_n	TGTCAAGAAACCCAACCTTTGGTTTTAGAGCTAGAAATAGC	CRISPR cloning CRF10
553	C2_DT2_R0_2_n	AACCATCACTAGAGGAATCATCCAATCTCTTAGTCGACTCTAC	CRISPR cloning CRF10
554	C2_DT2_BsR_2_n	ATTATTGGTCTCGAAACCATCACTAGAGGAATCATCCAA	CRISPR cloning CRF10
555	35Sprom_AccIII_for	AAGCATCCGGACAAGTGGATTGATGTGATATC	35S promoter fragment in pARF8 for protoplast assay
556	35Sprom_AccIII_rev	TGCAATCCGGACCTCTCCAAATGAAATGAAC	35S promoter fragment in pARF8 for protoplast assay

References

Abel, S., Oeller, P.W., and Theologis, A. (1994). Early auxin-induced genes encode short-lived nuclear proteins. Proc Natl Acad Sci U S A *91*, 326–330.

Adamowski, M., and Friml, J. (2015). PIN-dependent auxin transport: action, regulation, and evolution. Plant Cell *27*, 20–32.

Adibi, M., Yoshida, S., Weijers, D., and Fleck, C. (2016). Centering the organizing center in the *Arabidopsis thaliana* shoot apical meristem by a combination of cytokinin signaling and self-organization. PLoS ONE *11*, e0147830.

Aida, M., Beis, D., Heidstra, R., Willemsen, V., Blilou, I., Galinha, C., Nussaume, L., Noh, Y.-S., Amasino, R., and Scheres, B. (2004). The PLETHORA genes mediate patterning of the *Arabidopsis* root stem cell niche. Cell *119*, 109–120.

Alon, U. (2007). Network motifs: theory and experimental approaches. Nat. Rev. Genet. *8*, 450–461.

An, L., Zhou, Z., Sun, L., Yan, A., Xi, W., Yu, N., Cai, W., Chen, X., Yu, H., Schiefelbein, J., et al. (2012). A zinc finger protein gene ZFP5 integrates phytohormone signaling to control root hair development in *Arabidopsis*. Plant J. *72*, 474–490.

Argueso, C.T., Ferreira, F.J., and Kieber, J.J. (2009). Environmental perception avenues: the interaction of cytokinin and environmental response pathways. Plant Cell Environ. *32*, 1147–1160.

Bainbridge, K., Guyomarc'h, S., Bayer, E., Swarup, R., Bennett, M., Mandel, T., and Kuhlemeier, C. (2008). Auxin influx carriers stabilize phyllotactic patterning. Genes Dev. *22*, 810–823.

Balkunde, R., Kitagawa, M., Xu, X.M., Wang, J., and Jackson, D. (2017). SHOOT MERISTEMLESS trafficking controls axillary meristem formation, meristem size and organ boundaries in *Arabidopsis*. Plant J. *90*, 435–446.

Band, L.R., Wells, D.M., Larrieu, A., Sun, J., Middleton, A.M., French, A.P., Brunoud, G., Sato, E.M., Wilson, M.H., Péret, B., et al. (2012). Root gravitropism is regulated by a transient lateral auxin gradient controlled by a tipping-point mechanism. Proc. Natl. Acad. Sci. U.S.A. *109*, 4668–4673.

Bartlett, M.E., and Thompson, B. (2014). Meristem identity and phyllotaxis in inflorescence development. Front Plant Sci *5*, 508.

Barton, M.K. (2010). Twenty years on: the inner workings of the shoot apical meristem, a developmental dynamo. Dev. Biol. *341*, 95–113.

Basu, S., Mehreja, R., Thiberge, S., Chen, M.-T., and Weiss, R. (2004). Spatiotemporal control of gene expression with pulse-generating networks. Proc. Natl. Acad. Sci. U.S.A. *101*, 6355–6360.

Bate, N.J., Straus, N.A., and Thompson, J.E. (1991). Expression of chloroplast photosynthesis genes during leaf senescence. Physiologia Plantarum *80*, 217–225.

Bates, T.R., and Lynch, J.P. (1996). Stimulation of root hair elongation in *Arabidopsis thaliana* by low phosphorus availability. Plant, Cell & Environment *19*, 529–538.

Bates, T.R., and Lynch, J.P. (2001). Root hairs confer a competitive advantage under low phosphorus availability. Plant and Soil *236*, 243–250.

Baum, S.F., Dubrovsky, J.G., and Rost, T.L. (2002). Apical organization and maturation of the cortex and vascular cylinder in *Arabidopsis thaliana* (*Brassicaceae*) roots. Am. J. Bot. *89*, 908–920.

Beaulieu, E., Green, L., Elsby, L., Alourfi, Z., Morand, E.F., Ray, D.W., and Donn, R. (2011). Identification of a novel cell type-specific intronic enhancer of macrophage migration inhibitory factor (MIF) and its regulation by mithramycin. Clin. Exp. Immunol. *163*, 178–188.

Becskei, A., and Serrano, L. (2000). Engineering stability in gene networks by autoregulation. Nature *405*, 590–

593.

Bellini, C., Pacurar, D.I., and Perrone, I. (2014). Adventitious roots and lateral roots: similarities and differences. Annu Rev Plant Biol *65*, 639–666.

Benková, E., Michniewicz, M., Sauer, M., Teichmann, T., Seifertová, D., Jürgens, G., and Friml, J. (2003). Local, efflux-dependent auxin gradients as a common module for plant organ formation. Cell *115*, 591–602.

Bennett, T., and Leyser, O. (2006). Something on the side: axillary meristems and plant development. Plant Mol. Biol. *60*, 843–854.

Bentsink, L., and Koornneef, M. (2008). Seed dormancy and germination. Arabidopsis Book *6*.

van den Berg, C., Willemsen, V., Hendriks, G., Weisbeek, P., and Scheres, B. (1997). Short-range control of cell differentiation in the *Arabidopsis* root meristem. Nature *390*, 287–289.

Berkel, K. van, Boer, R.J. de, Scheres, B., and Tusscher, K. ten (2013). Polar auxin transport: models and mechanisms. Development *140*, 2253–2268.

Berleth, T., and Jurgens, G. (1993). The role of the monopteros gene in organising the basal body region of the *Arabidopsis* embryo. Development *118*, 575–587.

Besnard, F., Refahi, Y., Morin, V., Marteaux, B., Brunoud, G., Chambrier, P., Rozier, F., Mirabet, V., Legrand, J., Lainé, S., et al. (2014). Cytokinin signalling inhibitory fields provide robustness to phyllotaxis. Nature *505*, 417–421.

Besseau, S., Li, J., and Palva, E.T. (2012). WRKY54 and WRKY70 co-operate as negative regulators of leaf senescence in *Arabidopsis thaliana*. J. Exp. Bot. *63*, 2667–2679.

Bhosale, R., Giri, J., Pandey, B.K., Giehl, R.F.H., Hartmann, A., Traini, R., Truskina, J., Leftley, N., Hanlon, M., Swarup, K., et al. (2018). A mechanistic framework for auxin dependent *Arabidopsis* root hair elongation to low external phosphate. Nat Commun *9*, 1409.

Bhuiyan, N.H., Friso, G., Poliakov, A., Ponnala, L., and van Wijk, K.J. (2015). MET1 is a thylakoid-associated TPR protein involved in photosystem II supercomplex formation and repair in *Arabidopsis*. Plant Cell *27*, 262–285.

Bianchi, M., Crinelli, R., Giacomini, E., Carloni, E., and Magnani, M. (2009). A potent enhancer element in the 5'-UTR intron is crucial for transcriptional regulation of the human ubiquitin C gene. Gene *448*, 88–101.

Bielach, A., Podlesáková, K., Marhavy, P., Duclercq, J., Cuesta, C., Müller, B., Grunewald, W., Tarkowski, P., and Benková, E. (2012). Spatiotemporal regulation of lateral root organogenesis in *Arabidopsis* by cytokinin. Plant Cell *24*, 3967–3981.

Bielach, A., Hrtyan, M., and Tognetti, V.B. (2017). Plants under stress: involvement of auxin and cytokinin. Int J Mol Sci *18*.

Birkenbihl, R.P., Diezel, C., and Somssich, I.E. (2012). *Arabidopsis* WRKY33 is a key transcriptional regulator of hormonal and metabolic responses toward *Botrytis cinerea* infection. Plant Physiol. *159*, 266–285.

Bishopp, A., Help, H., El-Showk, S., Weijers, D., Scheres, B., Friml, J., Benková, E., Mähönen, A.P., and Helariutta, Y. (2011). A mutually inhibitory interaction between auxin and cytokinin specifies vascular pattern in roots. Curr. Biol. *21*, 917–926.

Blancaflor, E.B., Fasano, J.M., and Gilroy, S. (1998). Mapping the functional roles of cap cells in the response of *Arabidopsis* primary roots to gravity. Plant Physiol *116*, 213–222.

Blilou, I., Xu, J., Wildwater, M., Willemsen, V., Paponov, I., Friml, J., Heidstra, R., Aida, M., Palme, K., and Scheres, B. (2005). The PIN auxin efflux facilitator network controls growth and patterning in *Arabidopsis* roots. Nature *433*, 39–44.

Boer, D.R., Freire-Rios, A., van den Berg, W.A.M., Saaki, T., Manfield, I.W., Kepinski, S., López-Vidrieo, I., Franco-Zorrilla, J.M., de Vries, S.C., Solano, R., et al. (2014). Structural basis for DNA binding specificity by the auxin-dependent ARF transcription factors. Cell *156*, 577–589.

Bornstein, P., McKay, J., Liska, D.J., Apone, S., and Devarayalu, S. (1988). Interactions between the promoter

and first intron are involved in transcriptional control of alpha 1(I) collagen gene expression. Mol. Cell. Biol. *8*, 4851–4857.

Bradnam, K.R., and Korf, I. (2008). Longer first introns are a general property of eukaryotic gene structure. PLoS ONE *3*, e3093.

Brady, S.M., Zhang, L., Megraw, M., Martinez, N.J., Jiang, E., Yi, C.S., Liu, W., Zeng, A., Taylor-Teeples, M., Kim, D., et al. (2011). A stele-enriched gene regulatory network in the *Arabidopsis* root. Mol. Syst. Biol. *7*, 459.

Brand, U., Fletcher, J.C., Hobe, M., Meyerowitz, E.M., and Simon, R. (2000). Dependence of stem cell fate in *Arabidopsis* on a feedback loop regulated by CLV3 activity. Science *289*, 617–619.

Braybrook, S.A., and Peaucelle, A. (2013). Mechano-chemical aspects of organ formation in *Arabidopsis thaliana*: the relationship between auxin and pectin. PLoS ONE *8*, e57813.

Breeze, E., Harrison, E., McHattie, S., Hughes, L., Hickman, R., Hill, C., Kiddle, S., Kim, Y.-S., Penfold, C.A., Jenkins, D., et al. (2011). High-resolution temporal profiling of transcripts during *Arabidopsis* leaf senescence reveals a distinct chronology of processes and regulation. Plant Cell *23*, 873–894.

Brown, L.K., George, T.S., Thompson, J.A., Wright, G., Lyon, J., Dupuy, L., Hubbard, S.F., and White, P.J. (2012). What are the implications of variation in root hair length on tolerance to phosphorus deficiency in combination with water stress in barley (*Hordeum vulgare*)? Ann. Bot. *110*, 319–328.

Brunoud, G., Wells, D.M., Oliva, M., Larrieu, A., Mirabet, V., Burrow, A.H., Beeckman, T., Kepinski, S., Traas, J., Bennett, M.J., et al. (2012). A novel sensor to map auxin response and distribution at high spatio-temporal resolution. Nature *482*, 103–106.

Buchanan-Wollaston, V., Page, T., Harrison, E., Breeze, E., Lim, P.O., Nam, H.G., Lin, J.-F., Wu, S.-H., Swidzinski, J., Ishizaki, K., et al. (2005). Comparative transcriptome analysis reveals significant differences in gene expression and signalling pathways between developmental and dark/starvation-induced senescence in *Arabidopsis*. Plant J. *42*, 567–585.

Busch, M.A., Bomblies, K., and Weigel, D. (1999). Activation of a floral homeotic gene in Arabidopsis. Science *285*, 585–587.

Byrne, M.E., Simorowski, J., and Martienssen, R.A. (2002). ASYMMETRIC LEAVES1 reveals knox gene redundancy in *Arabidopsis*. Development *129*, 1957–1965.

Cai, S., Zhou, P., and Liu, Z. (2013). Functional characteristics of a double negative feedback loop mediated by microRNAs. Cogn Neurodyn *7*, 417–429.

Calderon-Villalobos, L.I.A., Lee, S., De Oliveira, C., Ivetac, A., Brandt, W., Armitage, L., Sheard, L.B., Tan, X., Parry, G., Mao, H., et al. (2012). A combinatorial TIR1/AFB-Aux/IAA co-receptor system for differential sensing of auxin. Nat. Chem. Biol. *8*, 477–485.

Calderon-Villalobos, L.I., Tan, X., Zheng, N., and Estelle, M. (2010). Auxin perception--structural insights. Cold Spring Harb Perspect Biol *2*, a005546.

Camas, F.M., Blázquez, J., and Poyatos, J.F. (2006). Autogenous and nonautogenous control of response in a genetic network. Proc. Natl. Acad. Sci. U.S.A. *103*, 12718–12723.

Cao, J., Jiang, F., Sodmergen, null, and Cui, K. (2003). Time-course of programmed cell death during leaf senescence in *Eucommia ulmoides*. J. Plant Res. *116*, 7–12.

Capron, A., Chatfield, S., Provart, N., and Berleth, T. (2009). Embryogenesis: pattern formation from a single cell. Arabidopsis Book *7*.

Causier, B., Ashworth, M., Guo, W., and Davies, B. (2012). The TOPLESS interactome: a framework for gene repression in *Arabidopsis*. Plant Physiol. *158*, 423–438.

Cha, J.-Y., Kim, W.-Y., Kang, S.B., Kim, J.I., Baek, D., Jung, I.J., Kim, M.R., Li, N., Kim, H.-J., Nakajima, M., et al. (2015). A novel thiol-reductase activity of *Arabidopsis* YUC6 confers drought tolerance independently of auxin biosynthesis. Nature Communications *6*, 8041.

Chaiwanon, J., Wang, W., Zhu, J.-Y., Oh, E., and Wang, Z.-Y. (2016). Information integration and communication

in plant growth regulation. Cell *164*, 1257–1268.

Chapman, K., Groot, E.P., Nichol, S.A., and Rost, T.L. (2002). Primary root growth and the pattern of root apical meristem organization are coupled. J Plant Growth Regul *21*, 287–295.

Chen, H., Xu, Z., Mei, C., Yu, D., and Small, S. (2012). A system of repressor gradients spatially organizes the boundaries of “morphogen-dependent” target genes. Cell *149*, 618–629.

Chickarmane, V.S., Gordon, S.P., Tarr, P.T., Heisler, M.G., and Meyerowitz, E.M. (2012). Cytokinin signaling as a positional cue for patterning the apical-basal axis of the growing *Arabidopsis* shoot meristem. Proc. Natl. Acad. Sci. U.S.A. *109*, 4002–4007.

Cho, H., Ryu, H., Rho, S., Hill, K., Smith, S., Audenaert, D., Park, J., Han, S., Beeckman, T., Bennett, M.J., et al. (2014). A secreted peptide acts on BIN2-mediated phosphorylation of ARFs to potentiate auxin response during lateral root development. Nature Cell Biology *16*, 66–76.

Chorev, M., and Carmel, L. (2012). The function of introns. Front Genet *3*, 55.

Christie, J.M., Blackwood, L., Petersen, J., and Sullivan, S. (2015). Plant flavoprotein photoreceptors. Plant Cell Physiol. *56*, 401–413.

Ciftci-Yilmaz, S., and Mittler, R. (2008). The zinc finger network of plants. Cell. Mol. Life Sci. *65*, 1150–1160.

Clough, S.J., and Bent, A.F. (1998). Floral dip: a simplified method for *Agrobacterium*-mediated transformation of *Arabidopsis thaliana*. Plant J. *16*, 735–743.

Clowes, F. a. L. (1956). Nucleic acids in root apical meristems of *Zea*. New Phytologist *55*, 29–34.

Cole, M., Chandler, J., Weijers, D., Jacobs, B., Comelli, P., and Werr, W. (2009). DORNROSCHEN is a direct target of the auxin response factor MONOPTEROS in the *Arabidopsis* embryo. Development *136*, 1643–1651.

Cui, H., Levesque, M.P., Vernoux, T., Jung, J.W., Paquette, A.J., Gallagher, K.L., Wang, J.Y., Blilou, I., Scheres, B., and Benfey, P.N. (2007). An evolutionarily conserved mechanism delimiting SHR movement defines a single layer of endodermis in plants. Science *316*, 421–425.

Cutcliffe, J.W., Hellmann, E., Heyl, A., and Rashotte, A.M. (2011). CRFs form protein–protein interactions with each other and with members of the cytokinin signalling pathway in *Arabidopsis* via the CRF domain. J Exp Bot *62*, 4995–5002.

D’Alessio, A.C., Fan, Z.P., Wert, K.J., Baranov, P., Cohen, M.A., Saini, J.S., Cohick, E., Charniga, C., Dadon, D., Hannett, N.M., et al. (2015). A systematic approach to identify candidate transcription factors that control cell identity. Stem Cell Reports *5*, 763–775.

De Michele, R., Formentin, E., Todesco, M., Toppo, S., Carimi, F., Zottini, M., Barizza, E., Ferrarini, A., Delledonne, M., Fontana, P., et al. (2009). Transcriptome analysis of *Medicago truncatula* leaf senescence: similarities and differences in metabolic and transcriptional regulations as compared with *Arabidopsis*, nodule senescence and nitric oxide signalling. New Phytol. *181*, 563–575.

De Rybel, B., Vassileva, V., Parizot, B., Demeulenaere, M., Grunewald, W., Audenaert, D., Van Campenhout, J., Overvoorde, P., Jansen, L., Vanneste, S., et al. (2010). A novel aux/IAA28 signaling cascade activates GATA23-dependent specification of lateral root founder cell identity. Curr. Biol. *20*, 1697–1706.

De Rybel, B., Möller, B., Yoshida, S., Grabowicz, I., Barbier de Reuille, P., Boeren, S., Smith, R.S., Borst, J.W., and Weijers, D. (2013). A bHLH complex controls embryonic vascular tissue establishment and indeterminate growth in *Arabidopsis*. Dev. Cell *24*, 426–437.

De Rybel, B., Adibi, M., Breda, A.S., Wendrich, J.R., Smit, M.E., Novák, O., Yamaguchi, N., Yoshida, S., Van Isterdael, G., Palovaara, J., et al. (2014). Plant development. Integration of growth and patterning during vascular tissue formation in *Arabidopsis*. Science *345*, 1255215.

De Smet, I., Tetsumura, T., De Rybel, B., Frei dit Frey, N., Laplaze, L., Casimiro, I., Swarup, R., Naudts, M., Vanneste, S., Audenaert, D., et al. (2007). Auxin-dependent regulation of lateral root positioning in the basal meristem of *Arabidopsis*. Development *134*, 681–690.

De Smet, I., Lau, S., Voss, U., Vanneste, S., Benjamins, R., Rademacher, E.H., Schlereth, A., De Rybel, B.,

Vassileva, V., Grunewald, W., et al. (2010). Bimodular auxin response controls organogenesis in *Arabidopsis*. Proc. Natl. Acad. Sci. U.S.A. *107*, 2705–2710.

De Tullio, M.C., Jiang, K., and Feldman, L.J. (2010). Redox regulation of root apical meristem organization: Connecting root development to its environment. Plant Physiology and Biochemistry *48*, 328–336.

Dello Ioio, R., Linhares, F.S., Scacchi, E., Casamitjana-Martinez, E., Heidstra, R., Costantino, P., and Sabatini, S. (2007). Cytokinins determine *Arabidopsis* root-meristem size by controlling cell differentiation. Curr. Biol. *17*, 678–682.

Dello Ioio, R., Nakamura, K., Moubayidin, L., Perilli, S., Taniguchi, M., Morita, M.T., Aoyama, T., Costantino, P., and Sabatini, S. (2008). A genetic framework for the control of cell division and differentiation in the root meristem. Science *322*, 1380–1384.

Deplancke, B., Mukhopadhyay, A., Ao, W., Elewa, A.M., Grove, C.A., Martinez, N.J., Sequerra, R., Doucette-Stamm, L., Reece-Hoyes, J.S., Hope, I.A., et al. (2006). A gene-centered *C. elegans* protein-DNA interaction network. Cell *125*, 1193–1205.

Desclos, M., Etienne, P., Coquet, L., Jouenne, T., Bonnefoy, J., Segura, R., Reze, S., Ourry, A., and Avice, J.-C. (2009). A combined 15N tracing/proteomics study in Brassica napus reveals the chronology of proteomics events associated with N remobilisation during leaf senescence induced by nitrate limitation or starvation. Proteomics *9*, 3580–3608.

Dharmasiri, N., Dharmasiri, S., and Estelle, M. (2005a). The F-box protein TIR1 is an auxin receptor. Nature *435*, 441–445.

Dharmasiri, N., Dharmasiri, S., Weijers, D., Lechner, E., Yamada, M., Hobbie, L., Ehrismann, J.S., Jürgens, G., and Estelle, M. (2005b). Plant development is regulated by a family of auxin receptor F box proteins. Dev. Cell *9*, 109–119.

Di Mambro, R., De Ruvo, M., Pacifici, E., Salvi, E., Sozzani, R., Benfey, P.N., Busch, W., Novak, O., Ljung, K., Di Paola, L., et al. (2017). Auxin minimum triggers the developmental switch from cell division to cell differentiation in the *Arabidopsis* root. Proc. Natl. Acad. Sci. U.S.A. *114*, E7641–E7649.

Diepenbruck, M., Tiede, S., Saxena, M., Ivanek, R., Kalathur, R.K.R., Lüönd, F., Meyer-Schaller, N., and Christofori, G. (2017). miR-1199-5p and Zeb1 function in a double-negative feedback loop potentially coordinating EMT and tumour metastasis. Nat Commun *8*, 1168.

Ding, Z., and Friml, J. (2010). Auxin regulates distal stem cell differentiation in *Arabidopsis* roots. Proc. Natl. Acad. Sci. U.S.A. *107*, 12046–12051.

Dolan, L., Janmaat, K., Willemsen, V., Linstead, P., Poethig, S., Roberts, K., and Scheres, B. (1993). Cellular organisation of the *Arabidopsis thaliana* root. Development *119*, 71–84.

Donner, T.J., Sherr, I., and Scarpella, E. (2009). Regulation of preprocambial cell state acquisition by auxin signaling in *Arabidopsis* leaves. Development *136*, 3235–3246.

van Doorn, W.G., and Woltering, E.J. (2004). Senescence and programmed cell death: substance or semantics? J. Exp. Bot. *55*, 2147–2153.

Dubrovsky, J.G., and Barlow, P.W. (2015). The origins of the quiescent centre concept. New Phytologist *206*, 493–496.

Dyer, T.A., and Osborne, D.J. (1971). Leaf nucleic acids:II. metabolism during senescence and the effect of kinetin. J Exp Bot *22*, 552–560.

Ellis, C.M., Nagpal, P., Young, J.C., Hagen, G., Guilfoyle, T.J., and Reed, J.W. (2005). AUXIN RESPONSE FACTOR1 and AUXIN RESPONSE FACTOR2 regulate senescence and floral organ abscission in *Arabidopsis thaliana*. Development *132*, 4563–4574.

Enders, T.A., and Strader, L.C. (2015). Auxin activity: Past, present, and future. Am. J. Bot. *102*, 180–196.

Esau, K. (1977). Anatomy of Seed Plants (Wiley).

Esmon, C.A., Tinsley, A.G., Ljung, K., Sandberg, G., Hearne, L.B., and Liscum, E. (2006). A gradient of auxin and

auxin-dependent transcription precedes tropic growth responses. Proc Natl Acad Sci U S A *103*, 236–241.

Fankhauser, C., and Christie, J.M. (2015). Plant phototropic growth. Curr. Biol. *25*, R384-389.

Faraco, M., Di Sansebastiano, G.P., Spelt, K., Koes, R.E., and Quattrocchio, F.M. (2011). One protoplast is not the other! Plant Physiol *156*, 474–478.

Feng, Z., Zhu, J., Du, X., and Cui, X. (2012). Effects of three auxin-inducible LBD members on lateral root formation in Arabidopsis thaliana. Planta *236*, 1227–1237.

Finet, C., Berne-Dedieu, A., Scutt, C.P., and Marlétaz, F. (2013). Evolution of the ARF gene family in land plants: old domains, new tricks. Mol. Biol. Evol. *30*, 45–56.

Fletcher, J.C., Brand, U., Running, M.P., Simon, R., and Meyerowitz, E.M. (1999). Signaling of cell fate decisions by CLAVATA3 in *Arabidopsis* shoot meristems. Science *283*, 1911–1914.

Forzani, C., Aichinger, E., Sornay, E., Willemsen, V., Laux, T., Dewitte, W., and Murray, J.A.H. (2014). WOX5 suppresses CYCLIN D activity to establish quiescence at the center of the root stem cell niche. Curr. Biol. *24*, 1939–1944.

Franks, R.G., Wang, C., Levin, J.Z., and Liu, Z. (2002). SEUSS, a member of a novel family of plant regulatory proteins, represses floral homeotic gene expression with LEUNIG. Development *129*, 253–263.

Frébort, I., Kowalska, M., Hluska, T., Frébortová, J., and Galuszka, P. (2011). Evolution of cytokinin biosynthesis and degradation. J. Exp. Bot. *62*, 2431–2452.

Friml, J., Benková, E., Blilou, I., Wisniewska, J., Hamann, T., Ljung, K., Woody, S., Sandberg, G., Scheres, B., Jürgens, G., et al. (2002a). AtPIN4 mediates sink-driven auxin gradients and root patterning in *Arabidopsis*. Cell *108*, 661–673.

Friml, J., Wiśniewska, J., Benková, E., Mendgen, K., and Palme, K. (2002b). Lateral relocation of auxin efflux regulator PIN3 mediates tropism in *Arabidopsis*. Nature *415*, 806–809.

Fu, J., and Wang, S. (2011). Insights into auxin signaling in plant-pathogen interactions. Front Plant Sci *2*, 74.

Fujita, H., Toyokura, K., Okada, K., and Kawaguchi, M. (2011). Reaction-diffusion pattern in shoot apical meristem of plants. PLoS ONE *6*, e18243.

Fukaki, H., Tameda, S., Masuda, H., and Tasaka, M. (2002). Lateral root formation is blocked by a gain-of-function mutation in the SOLITARY-ROOT/IAA14 gene of *Arabidopsis*. Plant J. *29*, 153–168.

Fukaki, H., Nakao, Y., Okushima, Y., Theologis, A., and Tasaka, M. (2005). Tissue-specific expression of stabilized SOLITARY-ROOT/IAA14 alters lateral root development in *Arabidopsis*. Plant J. *44*, 382–395.

Galbiati, F., Sinha Roy, D., Simonini, S., Cucinotta, M., Ceccato, L., Cuesta, C., Simaskova, M., Benkova, E., Kamiuchi, Y., Aida, M., et al. (2013). An integrative model of the control of ovule primordia formation. Plant J. *76*, 446–455.

Galvan-Ampudia, C.S., Chaumeret, A.M., Godin, C., and Vernoux, T. (2016). Phyllotaxis: from patterns of organogenesis at the meristem to shoot architecture. Wiley Interdiscip Rev Dev Biol *5*, 460–473.

Gälweiler, L., Guan, C., Müller, A., Wisman, E., Mendgen, K., Yephremov, A., and Palme, K. (1998). Regulation of polar auxin transport by AtPIN1 in *Arabidopsis* vascular tissue. Science *282*, 2226–2230.

Gan, S., and Amasino, R.M. (1995). Inhibition of leaf senescence by autoregulated production of cytokinin. Science *270*, 1986–1988.

Gan, S., and Amasino, R.M. (1996). Cytokinins in plant senescence: From spray and pray to clone and play. BioEssays *18*, 557–565.

Gan, S., and Amasino, R.M. (1997). Making sense of senescence (molecular genetic regulation and manipulation of leaf senescence). Plant Physiol *113*, 313–319.

Gao, M.-J., Lydiate, D.J., Li, X., Lui, H., Gjetvaj, B., Hegedus, D.D., and Rozwadowski, K. (2009). Repression of seed maturation genes by a trihelix transcriptional repressor in *Arabidopsis* seedlings. Plant Cell *21*, 54–71.

Gaudinier, A., Zhang, L., Reece-Hoyes, J.S., Taylor-Teeples, M., Pu, L., Liu, Z., Breton, G., Pruneda-Paz, J.L., Kim, D., Kay, S.A., et al. (2011). Enhanced Y1H assays for *Arabidopsis*. Nat. Methods *8*, 1053–1055.

Gaunitz, F., Heise, K., and Gebhardt, R. (2004). A silencer element in the first intron of the glutamine synthetase gene represses induction by glucocorticoids. Mol. Endocrinol. *18*, 63–69.

Gaunitz, F., Deichsel, D., Heise, K., Werth, M., Anderegg, U., and Gebhardt, R. (2005). An intronic silencer element is responsible for specific zonal expression of glutamine synthetase in the rat liver. Hepatology *41*, 1225–1232.

Gepstein, S., Sabehi, G., Carp, M.-J., Hajouj, T., Nesher, M.F.O., Yariv, I., Dor, C., and Bassani, M. (2003). Large-scale identification of leaf senescence-associated genes. Plant J. *36*, 629–642.

Germanguz, I., Listgarten, J., Cinkornpumin, J., Solomon, A., Gaeta, X., and Lowry, W.E. (2016). Identifying gene expression modules that define human cell fates. Stem Cell Res *16*, 712–724.

Giehl, R.F.H., and von Wirén, N. (2014). Root nutrient foraging. Plant Physiol. *166*, 509–517.

Gifford, M.L., Dean, A., Gutierrez, R.A., Coruzzi, G.M., and Birnbaum, K.D. (2008). Cell-specific nitrogen responses mediate developmental plasticity. Proc. Natl. Acad. Sci. U.S.A. *105*, 803–808.

Gladish, D.K., and Rost, T.L. (1993). The effects of temperature on primary root growth dynamics and lateral root distribution in garden pea (*Pisum sativum* L., cv. "Alaska"). Environmental and Experimental Botany *33*, 243–258.

Goda, H., Sasaki, E., Akiyama, K., Maruyama-Nakashita, A., Nakabayashi, K., Li, W., Ogawa, M., Yamauchi, Y., Preston, J., Aoki, K., et al. (2008). The AtGenExpress hormone and chemical treatment data set: experimental design, data evaluation, model data analysis and data access. Plant J. *55*, 526–542.

Goetz, M., Vivian-Smith, A., Johnson, S.D., and Koltunow, A.M. (2006). AUXIN RESPONSE FACTOR8 is a negative regulator of fruit initiation in *Arabidopsis.* Plant Cell *18*, 1873–1886.

Goetz, M., Hooper, L.C., Johnson, S.D., Rodrigues, J.C.M., Vivian-Smith, A., and Koltunow, A.M. (2007). Expression of aberrant forms of AUXIN RESPONSE FACTOR8 stimulates parthenocarpy in *Arabidopsis* and tomato. Plant Physiol. *145*, 351–366.

Goh, T., Joi, S., Mimura, T., and Fukaki, H. (2012). The establishment of asymmetry in *Arabidopsis* lateral root founder cells is regulated by LBD16/ASL18 and related LBD/ASL proteins. Development *139*, 883–893.

Goldsmith, M.H.M. (1977). The polar transport of auxin. Annual Review of Plant Physiology *28*, 439–478.

Gordon, S.P., Chickarmane, V.S., Ohno, C., and Meyerowitz, E.M. (2009). Multiple feedback loops through cytokinin signaling control stem cell number within the *Arabidopsis* shoot meristem. Proc. Natl. Acad. Sci. U.S.A. *106*, 16529–16534.

Grierson, C., Nielsen, E., Ketelaarc, T., and Schiefelbein, J. (2014). Root hairs. Arabidopsis Book *12*.

Groot, E.P., Doyle, J.A., Nichol, S.A., and Rost, T.L. (2004). Phylogenetic distribution and evolution of root apical meristem organization in dicotyledonous angiosperms. International Journal of Plant Sciences *165*, 97–105.

Gruel, J., Landrein, B., Tarr, P., Schuster, C., Refahi, Y., Sampathkumar, A., Hamant, O., Meyerowitz, E.M., and Jönsson, H. (2016). An epidermis-driven mechanism positions and scales stem cell niches in plants. Sci Adv *2*, e1500989.

Guilfoyle, T.J. (2015). The PB1 domain in auxin response factor and Aux/IAA proteins: a versatile protein interaction module in the auxin response. Plant Cell *27*, 33–43.

Guo, Y., Cai, Z., and Gan, S. (2004). Transcriptome of *Arabidopsis* leaf senescence. Plant, Cell & Environment *27*, 521–549.

Guss, K.A., Nelson, C.E., Hudson, A., Kraus, M.E., and Carroll, S.B. (2001). Control of a genetic regulatory network by a selector gene. Science *292*, 1164–1167.

Gutierrez, L., Bussell, J.D., Pacurar, D.I., Schwambach, J., Pacurar, M., and Bellini, C. (2009). Phenotypic plasticity of adventitious rooting in *Arabidopsis* is controlled by complex regulation of AUXIN RESPONSE FACTOR transcripts and microRNA abundance. Plant Cell *21*, 3119–3132.

Gutierrez, L., Mongelard, G., Floková, K., Pacurar, D.I., Novák, O., Staswick, P., Kowalczyk, M., Pacurar, M., Demailly, H., Geiss, G., et al. (2012). Auxin controls *Arabidopsis* adventitious root initiation by regulating jasmonic acid homeostasis. Plant Cell *24*, 2515–2527.

Hamann, T., Benkova, E., Bäurle, I., Kientz, M., and Jürgens, G. (2002). The *Arabidopsis* BODENLOS gene encodes an auxin response protein inhibiting MONOPTEROS-mediated embryo patterning. Genes Dev. *16*, 1610–1615.

Han, Y., Yang, H., and Jiao, Y. (2014). Regulation of inflorescence architecture by cytokinins. Front Plant Sci *5*.

Hardtke, C.S., and Berleth, T. (1998). The *Arabidopsis* gene MONOPTEROS encodes a transcription factor mediating embryo axis formation and vascular development. EMBO J. *17*, 1405–1411.

Hardtke, C.S., Ckurshumova, W., Vidaurre, D.P., Singh, S.A., Stamatiou, G., Tiwari, S.B., Hagen, G., Guilfoyle, T.J., and Berleth, T. (2004). Overlapping and non-redundant functions of the *Arabidopsis* auxin response factors MONOPTEROS and NONPHOTOTROPIC HYPOCOTYL 4. Development *131*, 1089–1100.

Harper, R.M., Stowe-Evans, E.L., Luesse, D.R., Muto, H., Tatematsu, K., Watahiki, M.K., Yamamoto, K., and Liscum, E. (2000). The NPH4 locus encodes the auxin response factor ARF7, a conditional regulator of differential growth in aerial *Arabidopsis* tissue. Plant Cell *12*, 757–770.

Hattori, T., Totsuka, M., Hobo, T., Kagaya, Y., and Yamamoto-Toyoda, A. (2002). Experimentally determined sequence requirement of ACGT-containing abscisic acid response element. Plant Cell Physiol. *43*, 136–140.

Hayashi, K. (2012). The interaction and integration of auxin signaling components. Plant Cell Physiol. *53*, 965–975.

Heidstra, R., and Sabatini, S. (2014). Plant and animal stem cells: similar yet different. Nat. Rev. Mol. Cell Biol. *15*, 301–312.

Heimsch, C., and Seago, J.L. (2008). Organization of the root apical meristem in angiosperms. Am. J. Bot. *95*, 1–21.

Heisler, M.G., Ohno, C., Das, P., Sieber, P., Reddy, G.V., Long, J.A., and Meyerowitz, E.M. (2005). Patterns of auxin transport and gene expression during primordium development revealed by live imaging of the *Arabidopsis* inflorescence meristem. Curr. Biol. *15*, 1899–1911.

Helariutta, Y., Fukaki, H., Wysocka-Diller, J., Nakajima, K., Jung, J., Sena, G., Hauser, M.T., and Benfey, P.N. (2000). The SHORT-ROOT gene controls radial patterning of the *Arabidopsis* root through radial signaling. Cell *101*, 555–567.

Hensel, L.L., Grbić, V., Baumgarten, D.A., and Bleecker, A.B. (1993). Developmental and age-related processes that influence the longevity and senescence of photosynthetic tissues in *Arabidopsis*. Plant Cell *5*, 553–564.

Hirai, H., Tani, T., and Kikyo, N. (2010). Structure and functions of powerful transactivators: VP16, MyoD and FoxA. Int. J. Dev. Biol. *54*, 1589–1596.

Hirose, N., Takei, K., Kuroha, T., Kamada-Nobusada, T., Hayashi, H., and Sakakibara, H. (2008). Regulation of cytokinin biosynthesis, compartmentalization and translocation. J. Exp. Bot. *59*, 75–83.

Ho, S.H., So, G.M., and Chow, K.L. (2001). Postembryonic expression of *Caenorhabditis elegans* mab-21 and its requirement in sensory ray differentiation. Dev. Dyn. *221*, 422–430.

Hohm, T., Demarsy, E., Quan, C., Allenbach Petrolati, L., Preuten, T., Vernoux, T., Bergmann, S., and Fankhauser, C. (2014). Plasma membrane H^+ -ATPase regulation is required for auxin gradient formation preceding phototropic growth. Mol. Syst. Biol. *10*, 751.

ten Hove, C.A., Lu, K.-J., and Weijers, D. (2015). Building a plant: cell fate specification in the early *Arabidopsis* embryo. Development *142*, 420–430.

Husbands, A., Bell, E.M., Shuai, B., Smith, H.M.S., and Springer, P.S. (2007). LATERAL ORGAN BOUNDARIES defines a new family of DNA-binding transcription factors and can interact with specific bHLH proteins. Nucleic Acids Res *35*, 6663–6671.

Hwang, I., Sheen, J., and Müller, B. (2012). Cytokinin signaling networks. Annu Rev Plant Biol *63*, 353–380.

Inostroza, J.A., Mermelstein, F.H., Ha, I., Lane, W.S., and Reinberg, D. (1992). Dr1, a TATA-binding protein-associated phosphoprotein and inhibitor of class II gene transcription. Cell *70*, 477–489.

Jakobsen, J.S., Braun, M., Astorga, J., Gustafson, E.H., Sandmann, T., Karzynski, M., Carlsson, P., and Furlong, E.E.M. (2007). Temporal ChIP-on-chip reveals Biniou as a universal regulator of the visceral muscle transcriptional network. Genes Dev. *21*, 2448–2460.

Je, B.I., Gruel, J., Lee, Y.K., Bommert, P., Arevalo, E.D., Eveland, A.L., Wu, Q., Goldshmidt, A., Meeley, R., Bartlett, M., et al. (2016). Signaling from maize organ primordia via FASCIATED EAR3 regulates stem cell proliferation and yield traits. Nat. Genet. *48*, 785–791.

Jeon, J., Cho, C., Lee, M.R., Van Binh, N., and Kim, J. (2016). CYTOKININ RESPONSE FACTOR2 (CRF2) and CRF3 regulate lateral root development in response to cold stress in *Arabidopsis*. Plant Cell *28*, 1828–1843.

Jeon, J.S., Lee, S., Jung, K.H., Jun, S.H., Kim, C., and An, G. (2000). Tissue-preferential expression of a rice alpha-tubulin gene, OsTubA1, mediated by the first intron. Plant Physiol. *123*, 1005–1014.

Jeong, Y.-M., Mun, J.-H., Kim, H., Lee, S.-Y., and Kim, S.-G. (2007). An upstream region in the first intron of petunia actin-depolymerizing factor 1 affects tissue-specific expression in transgenic *Arabidopsis* (*Arabidopsis thaliana*). Plant J. *50*, 230–239.

Jiang, C.Z., Rodermel, S.R., and Shibles, R.M. (1993). Photosynthesis, rubisco activity and amount, and their regulation by transcription in senescing soybean leaves. Plant Physiol *101*, 105–112.

Johnston, R.J., Chang, S., Etchberger, J.F., Ortiz, C.O., and Hobert, O. (2005). MicroRNAs acting in a double-negative feedback loop to control a neuronal cell fate decision. Proc. Natl. Acad. Sci. U.S.A. *102*, 12449–12454.

Jones, A., Forero-Vargas, M., Withers, S.P., Smith, R.S., Traas, J., Dewitte, W., and Murray, J.A.H. (2017). Cell-size dependent progression of the cell cycle creates homeostasis and flexibility of plant cell size. Nat Commun *8*, 15060.

Jönsson, H., Heisler, M.G., Shapiro, B.E., Meyerowitz, E.M., and Mjolsness, E. (2006). An auxin-driven polarized transport model for phyllotaxis. PNAS *103*, 1633–1638.

Jonsson, J.J., Foresman, M.D., Wilson, N., and McIvor, R.S. (1992). Intron requirement for expression of the human purine nucleoside phosphorylase gene. Nucleic Acids Res. *20*, 3191–3198.

Joseph, M.P., Papdi, C., Kozma-Bognár, L., Nagy, I., López-Carbonell, M., Rigó, G., Koncz, C., and Szabados, L. (2014). The Arabidopsis ZINC FINGER PROTEIN3 interferes with abscisic acid and light signaling in seed germination and plant development. Plant Physiol. *165*, 1203–1220.

Journot-Catalino, N., Somssich, I.E., Roby, D., and Kroj, T. (2006). The transcription factors WRKY11 and WRKY17 act as negative regulators of basal resistance in *Arabidopsis thaliana*. Plant Cell *18*, 3289–3302.

Kang, H.-G., Kim, J., Kim, B., Jeong, H., Choi, S.H., Kim, E.K., Lee, H.-Y., and Lim, P.O. (2011). Overexpression of FTL1/DDF1, an AP2 transcription factor, enhances tolerance to cold, drought, and heat stresses in *Arabidopsis thaliana*. Plant Sci. *180*, 634–641.

Kang, J.G., Pyo, Y.J., Cho, J.W., and Cho, M.H. (2004). Comparative proteome analysis of differentially expressed proteins induced by K+ deficiency in *Arabidopsis thaliana*. Proteomics *4*, 3549–3559.

Katagiri, F., Lam, E., and Chua, N.H. (1989). Two tobacco DNA-binding proteins with homology to the nuclear factor CREB. Nature *340*, 727–730.

Kazan, K., and Manners, J.M. (2009). Linking development to defense: auxin in plant-pathogen interactions. Trends Plant Sci. *14*, 373–382.

Kepinski, S., and Leyser, O. (2005). The *Arabidopsis* F-box protein TIR1 is an auxin receptor. Nature *435*, 446–451.

Kieber, J.J., and Schaller, G.E. (2014). Cytokinins. Arabidopsis Book *12*, e0168.

Kierzkowski, D., Nakayama, N., Routier-Kierzkowska, A.-L., Weber, A., Bayer, E., Schorderet, M., Reinhardt, D., Kuhlemeier, C., and Smith, R.S. (2012). Elastic domains regulate growth and organogenesis in the plant shoot apical meristem. Science *335*, 1096–1099.

Kilian, J., Whitehead, D., Horak, J., Wanke, D., Weinl, S., Batistic, O., D'Angelo, C., Bornberg-Bauer, E., Kudla, J., and Harter, K. (2007). The AtGenExpress global stress expression data set: protocols, evaluation and model data analysis of UV-B light, drought and cold stress responses. Plant J. *50*, 347–363.

Kim, H.J., Ryu, H., Hong, S.H., Woo, H.R., Lim, P.O., Lee, I.C., Sheen, J., Nam, H.G., and Hwang, I. (2006). Cytokinin-mediated control of leaf longevity by AHK3 through phosphorylation of ARR2 in *Arabidopsis*. Proc. Natl. Acad. Sci. U.S.A. *103*, 814–819.

Kim, J.H., Lee, S.-R., Li, L.-H., Park, H.-J., Park, J.-H., Lee, K.Y., Kim, M.-K., Shin, B.A., and Choi, S.-Y. (2011a). High cleavage efficiency of a 2A peptide derived from porcine teschovirus-1 in human cell lines, zebrafish and mice. PLoS ONE *6*, e18556.

Kim, J.I., Murphy, A.S., Baek, D., Lee, S.-W., Yun, D.-J., Bressan, R.A., and Narasimhan, M.L. (2011b). YUCCA6 over-expression demonstrates auxin function in delaying leaf senescence in *Arabidopsis thaliana*. J. Exp. Bot. *62*, 3981–3992.

Kim, K., Ryu, H., Cho, Y.-H., Scacchi, E., Sabatini, S., and Hwang, I. (2012). Cytokinin-facilitated proteolysis of ARABIDOPSIS RESPONSE REGULATOR 2 attenuates signaling output in two-component circuitry. Plant J. *69*, 934–945.

Kim, K.-C., Lai, Z., Fan, B., and Chen, Z. (2008). Arabidopsis WRKY38 and WRKY62 transcription factors interact with histone deacetylase 19 in basal defense. Plant Cell *20*, 2357–2371.

Kim, S.-Y., Kim, S.-G., Kim, Y.-S., Seo, P.J., Bae, M., Yoon, H.-K., and Park, C.-M. (2007). Exploring membrane-associated NAC transcription factors in *Arabidopsis*: implications for membrane biology in genome regulation. Nucleic Acids Res. *35*, 203–213.

Konishi, M., and Yanagisawa, S. (2010). Identification of a nitrate-responsive cis-element in the *Arabidopsis* NIR1 promoter defines the presence of multiple cis-regulatory elements for nitrogen response. Plant J. *63*, 269–282.

Konishi, M., and Yanagisawa, S. (2013). *Arabidopsis* NIN-like transcription factors have a central role in nitrate signalling. Nat Commun *4*, 1617.

Konishi, M., Donner, T.J., Scarpella, E., and Yanagisawa, S. (2015). MONOPTEROS directly activates the auxin-inducible promoter of the Dof5.8 transcription factor gene in *Arabidopsis thaliana* leaf provascular cells. J Exp Bot *66*, 283–291.

Korasick, D.A., Enders, T.A., and Strader, L.C. (2013). Auxin biosynthesis and storage forms. J. Exp. Bot. *64*, 2541–2555.

Korasick, D.A., Westfall, C.S., Lee, S.G., Nanao, M.H., Dumas, R., Hagen, G., Guilfoyle, T.J., Jez, J.M., and Strader, L.C. (2014). Molecular basis for AUXIN RESPONSE FACTOR protein interaction and the control of auxin response repression. Proc. Natl. Acad. Sci. U.S.A. *111*, 5427–5432.

Krishnaswamy, S., Verma, S., Rahman, M.H., and Kav, N.N.V. (2011). Functional characterization of four APETALA2-family genes (RAP2.6, RAP2.6L, DREB19 and DREB26) in *Arabidopsis*. Plant Mol. Biol. *75*, 107–127.

Krysan, P.J., Young, J.C., and Sussman, M.R. (1999). T-DNA as an insertional mutagen in *Arabidopsis*. Plant Cell *11*, 2283–2290.

Kudo, T., Kiba, T., and Sakakibara, H. (2010). Metabolism and long-distance translocation of cytokinins. J Integr Plant Biol *52*, 53–60.

Kuhlemeier, C. (2007). Phyllotaxis. Trends Plant Sci. *12*, 143–150.

Lai, Z., Vinod, K., Zheng, Z., Fan, B., and Chen, Z. (2008). Roles of *Arabidopsis* WRKY3 and WRKY4 transcription factors in plant responses to pathogens. BMC Plant Biol. *8*, 68.

Lamarche, M.G., Wanner, B.L., Crépin, S., and Harel, J. (2008). The phosphate regulon and bacterial virulence: a regulatory network connecting phosphate homeostasis and pathogenesis. FEMS Microbiol. Rev. *32*, 461–473.

Laplaze, L., Benkova, E., Casimiro, I., Maes, L., Vanneste, S., Swarup, R., Weijers, D., Calvo, V., Parizot, B., Herrera-Rodriguez, M.B., et al. (2007). Cytokinins act directly on lateral root founder cells to inhibit root initiation. The Plant Cell *19*, 3889–3900.

Lau, S., Jürgens, G., and De Smet, I. (2008). The evolving complexity of the auxin pathway. Plant Cell *20*, 1738–1746.

Laufs, P., Grandjean, O., Jonak, C., Kiêu, K., and Traas, J. (1998). Cellular parameters of the shoot apical meristem in *Arabidopsis*. Plant Cell *10*, 1375–1390.

Lavenus, J., Goh, T., Roberts, I., Guyomarc'h, S., Lucas, M., De Smet, I., Fukaki, H., Beeckman, T., Bennett, M., and Laplaze, L. (2013). Lateral root development in *Arabidopsis*: fifty shades of auxin. Trends Plant Sci. *18*, 450–458.

Laxa, M. (2016). Intron-mediated enhancement: a tool for heterologous gene expression in plants? Front Plant Sci *7*, 1977.

Lee, H.-H., and Frasch, M. (2005). Nuclear integration of positive Dpp signals, antagonistic Wg inputs and mesodermal competence factors during *Drosophila* visceral mesoderm induction. Development *132*, 1429–1442.

Lee, D.J., Park, J.-Y., Ku, S.-J., Ha, Y.-M., Kim, S., Kim, M.D., Oh, M.-H., and Kim, J. (2007). Genome-wide expression profiling of ARABIDOPSIS RESPONSE REGULATOR 7(ARR7) overexpression in cytokinin response. Mol. Genet. Genomics *277*, 115–137.

Lee, S., Park, J.H., Lee, M.H., Yu, J., and Kim, S.Y. (2010). Isolation and functional characterization of CE1 binding proteins. BMC Plant Biol. *10*, 277.

Lee, S., Seo, P.J., Lee, H.-J., and Park, C.-M. (2012). A NAC transcription factor NTL4 promotes reactive oxygen species production during drought-induced leaf senescence in Arabidopsis. Plant J. *70*, 831–844.

Lee, T.I., Rinaldi, N.J., Robert, F., Odom, D.T., Bar-Joseph, Z., Gerber, G.K., Hannett, N.M., Harbison, C.T., Thompson, C.M., Simon, I., et al. (2002). Transcriptional regulatory networks in *Saccharomyces cerevisiae*. Science *298*, 799–804.

Leibfried, A., To, J.P.C., Busch, W., Stehling, S., Kehle, A., Demar, M., Kieber, J.J., and Lohmann, J.U. (2005). WUSCHEL controls meristem function by direct regulation of cytokinin-inducible response regulators. Nature *438*, 1172–1175.

Lenhard, M., and Laux, T. (2003). Stem cell homeostasis in the *Arabidopsis* shoot meristem is regulated by intercellular movement of CLAVATA3 and its sequestration by CLAVATA1. Development *130*, 3163–3173.

Levesque, M.P., Vernoux, T., Busch, W., Cui, H., Wang, J.Y., Blilou, I., Hassan, H., Nakajima, K., Matsumoto, N., Lohmann, J.U., et al. (2006). Whole-genome analysis of the SHORT-ROOT developmental pathway in *Arabidopsis*. PLoS Biol. *4*, e143.

Li, J., Dai, X., and Zhao, Y. (2006a). A role for Auxin Response Factor 19 in auxin and ethylene signaling in *Arabidopsis*. Plant Physiol *140*, 899–908.

Li, W., Zhang, H., Li, X., Zhang, F., Liu, C., Du, Y., Gao, X., Zhang, Z., Zhang, X., Hou, Z., et al. (2017). Intergrative metabolomic and transcriptomic analyses unveil nutrient remobilization events in leaf senescence of tobacco. Sci Rep *7*, 12126.

Li, X., Mo, X., Shou, H., and Wu, P. (2006b). Cytokinin-mediated cell cycling arrest of pericycle founder cells in lateral root initiation of *Arabidopsis*. Plant Cell Physiol. *47*, 1112–1123.

Liang, X., Nazarenus, T.J., and Stone, J.M. (2008). Identification of a consensus DNA-binding site for the *Arabidopsis thaliana* SBP domain transcription factor, AtSPL14, and binding kinetics by surface plasmon resonance. Biochemistry *47*, 3645–3653.

Licausi, F., Ohme-Takagi, M., and Perata, P. (2013). APETALA2/Ethylene Responsive Factor (AP2/ERF) transcription factors: mediators of stress responses and developmental programs. New Phytol. *199*, 639–649.

Lichtenthaler, H., and Buschmann, C. (2001). Chlorophylls and Carotenoids: Measurement and Characterization by UV-VIS Spectroscopy. In Current Protocols in Food Analytical Chemistry.

Lim, P.O., Kim, H.J., and Nam, H.G. (2007). Leaf senescence. Annu Rev Plant Biol *58*, 115–136.

Lim, P.O., Lee, I.C., Kim, J., Kim, H.J., Ryu, J.S., Woo, H.R., and Nam, H.G. (2010). Auxin response factor 2 (ARF2) plays a major role in regulating auxin-mediated leaf longevity. J. Exp. Bot. *61*, 1419–1430.

Lin, J.-F., and Wu, S.-H. (2004). Molecular events in senescing *Arabidopsis* leaves. Plant J. *39*, 612–628.

Lin, M., Pang, C., Fan, S., Song, M., Wei, H., and Yu, S. (2015). Global analysis of the *Gossypium hirsutum* L. Transcriptome during leaf senescence by RNA-Seq. BMC Plant Biol. *15*, 43.

Lindemose, S., Jensen, M.K., de Velde, J.V., O'Shea, C., Heyndrickx, K.S., Workman, C.T., Vandepoele, K., Skriver, K., and Masi, F.D. (2014). A DNA-binding-site landscape and regulatory network analysis for NAC transcription factors in *Arabidopsis thaliana*. Nucleic Acids Res *42*, 7681–7693.

Liscum, E., and Briggs, W.R. (1996). Mutations of *Arabidopsis* in potential transduction and response components of the phototropic signaling pathway. Plant Physiol *112*, 291–296.

Liu, Z., and Meyerowitz, E.M. (1995). LEUNIG regulates AGAMOUS expression in *Arabidopsis* flowers. Development *121*, 975–991.

Liu, N., Wu, S., Van Houten, J., Wang, Y., Ding, B., Fei, Z., Clarke, T.H., Reed, J.W., and van der Knaap, E. (2014). Down-regulation of AUXIN RESPONSE FACTORS 6 and 8 by microRNA 167 leads to floral development defects and female sterility in tomato. J. Exp. Bot. *65*, 2507–2520.

Ljung, K., Bhalerao, R.P., and Sandberg, G. (2001). Sites and homeostatic control of auxin biosynthesis in *Arabidopsis* during vegetative growth. Plant J. *28*, 465–474.

Ljung, K., Hull, A.K., Celenza, J., Yamada, M., Estelle, M., Normanly, J., and Sandberg, G. (2005). Sites and regulation of auxin biosynthesis in *Arabidopsis* roots. Plant Cell *17*, 1090–1104.

Lohmann, J.U., Hong, R.L., Hobe, M., Busch, M.A., Parcy, F., Simon, R., and Weigel, D. (2001). A molecular link between stem cell regulation and floral patterning in *Arabidopsis*. Cell *105*, 793–803.

López-Bucio, J., Hernández-Abreu, E., Sánchez-Calderón, L., Nieto-Jacobo, M.F., Simpson, J., and Herrera-Estrella, L. (2002). Phosphate availability alters architecture and causes changes in hormone sensitivity in the *Arabidopsis* root system. Plant Physiol. *129*, 244–256.

Lucas, W.J., Groover, A., Lichtenberger, R., Furuta, K., Yadav, S.-R., Helariutta, Y., He, X.-Q., Fukuda, H., Kang, J., Brady, S.M., et al. (2013). The plant vascular system: evolution, development and functions. J Integr Plant Biol *55*, 294–388.

de Lucas, M., Pu, L., Turco, G., Gaudinier, A., Morao, A.K., Harashima, H., Kim, D., Ron, M., Sugimoto, K., Roudier, F., et al. (2016). Transcriptional Regulation of Arabidopsis Polycomb Repressive Complex 2 coordinates cell-type proliferation and differentiation. Plant Cell *28*, 2616–2631.

Luo, J., Zhou, J.-J., and Zhang, J.-Z. (2018). Aux/IAA gene family in plants: molecular structure, regulation, and function. Int J Mol Sci *19*.

Ma, H.-W., Kumar, B., Ditges, U., Gunzer, F., Buer, J., and Zeng, A.-P. (2004). An extended transcriptional regulatory network of *Escherichia coli* and analysis of its hierarchical structure and network motifs. Nucleic Acids Res. *32*, 6643–6649.

Maeda, Y.T., and Sano, M. (2006). Regulatory dynamics of synthetic gene networks with positive feedback. J. Mol. Biol. *359*, 1107–1124.

Mähönen, A.P., Bishopp, A., Higuchi, M., Nieminen, K.M., Kinoshita, K., Törmäkangas, K., Ikeda, Y., Oka, A., Kakimoto, T., and Helariutta, Y. (2006). Cytokinin signaling and its inhibitor AHP6 regulate cell fate during vascular development. Science *311*, 94–98.

Majda, M., and Robert, S. (2018). The role of auxin in cell wall expansion. International Journal of Molecular Sciences *19*, 951.

Malamy, J.E., and Benfey, P.N. (1997). Organization and cell differentiation in lateral roots of *Arabidopsis thaliana*. Development *124*, 33–44.

Mangan, S., Zaslaver, A., and Alon, U. (2003). The coherent feedforward loop serves as a sign-sensitive delay element in transcription networks. J. Mol. Biol. *334*, 197–204.

Mannhaupt, G., Schnall, R., Karpov, V., Vetter, I., and Feldmann, H. (1999). Rpn4p acts as a transcription factor by binding to PACE, a nonamer box found upstream of 26S proteasomal and other genes in yeast. FEBS Lett.

450, 27–34.

Martin, R.C., Asahina, M., Liu, P.-P., Kristof, J.R., Coppersmith, J.L., Pluskota, W.E., Bassel, G.W., Goloviznina, N.A., Nguyen, T.T., Martínez-Andújar, C., et al. (2010). Regulation of post-germinative transition from the cotyledon- to vegetative-leaf stages by microRNA-targeted SQUAMOSA PROMOTER-BINDING PROTEIN LIKE13 in *Arabidopsis*. Seed Science Research.

Mathieu, J., Yant, L.J., Mürdter, F., Küttner, F., and Schmid, M. (2009). Repression of flowering by the miR172 target SMZ. PLoS Biol. *7*, e1000148.

Mayer, K.F., Schoof, H., Haecker, A., Lenhard, M., Jürgens, G., and Laux, T. (1998). Role of WUSCHEL in regulating stem cell fate in the *Arabidopsis* shoot meristem. Cell *95*, 805–815.

McCabe, M.S., Garratt, L.C., Schepers, F., Jordi, W.J., Stoopen, G.M., Davelaar, E., van Rhijn, J.H., Power, J.B., and Davey, M.R. (2001). Effects of P(SAG12)-IPT gene expression on development and senescence in transgenic lettuce. Plant Physiol. *127*, 505–516.

Mellor, N., Adibi, M., El-Showk, S., De Rybel, B., King, J., Mähönen, A.P., Weijers, D., and Bishopp, A. (2017). Theoretical approaches to understanding root vascular patterning: a consensus between recent models. J. Exp. Bot. *68*, 5–16.

Michniewicz, M., Brewer, P.B., and Friml, J.Í. (2007). Polar auxin transport and asymmetric auxin distribution. Arabidopsis Book *5*, e0108.

Milani, P., Gholamirad, M., Traas, J., Arnéodo, A., Boudaoud, A., Argoul, F., and Hamant, O. (2011). In vivo analysis of local wall stiffness at the shoot apical meristem in *Arabidopsis* using atomic force microscopy. Plant J. *67*, 1116–1123.

Milani, P., Mirabet, V., Cellier, C., Rozier, F., Hamant, O., Das, P., and Boudaoud, A. (2014). Matching patterns of gene expression to mechanical stiffness at cell resolution through quantitative tandem epifluorescence and nanoindentation. Plant Physiol. *165*, 1399–1408.

Millar, A.A., and Gubler, F. (2005). The Arabidopsis GAMYB-like genes, MYB33 and MYB65, are microRNA-regulated genes that redundantly facilitate anther development. Plant Cell *17*, 705–721.

Morello, L., Bardini, M., Sala, F., and Breviario, D. (2002). A long leader intron of the Ostub16 rice beta-tubulin gene is required for high-level gene expression and can autonomously promote transcription both in vivo and in vitro. Plant J. *29*, 33–44.

Moreno-Risueno, M.A., Van Norman, J.M., Moreno, A., Zhang, J., Ahnert, S.E., and Benfey, P.N. (2010). Oscillating gene expression determines competence for periodic *Arabidopsis* root branching. Science *329*, 1306–1311.

Moubayidin, L., Perilli, S., Dello Ioio, R., Di Mambro, R., Costantino, P., and Sabatini, S. (2010). The rate of cell differentiation controls the *Arabidopsis* root meristem growth phase. Curr. Biol. *20*, 1138–1143.

Müller, B., and Sheen, J. (2008). Cytokinin and auxin interaction in root stem-cell specification during early embryogenesis. Nature *453*, 1094–1097.

Müller, D., and Leyser, O. (2011). Auxin, cytokinin and the control of shoot branching. Ann Bot *107*, 1203–1212.

Müller, A., Guan, C., Gälweiler, L., Tänzler, P., Huijser, P., Marchant, A., Parry, G., Bennett, M., Wisman, E., and Palme, K. (1998). AtPIN2 defines a locus of *Arabidopsis* for root gravitropism control. EMBO J. *17*, 6903–6911.

Murray, J.A.H., Jones, A., Godin, C., and Traas, J. (2012). Systems analysis of shoot apical meristem growth and development: integrating hormonal and mechanical signaling. Plant Cell *24*, 3907–3919.

Mutte, S.K., Kato, H., Rothfels, C., Melkonian, M., Wong, G.K.-S., and Weijers, D. (2018). Origin and evolution of the nuclear auxin response system. eLife Sciences *7*, e33399.

Nagpal, P., Walker, L.M., Young, J.C., Sonawala, A., Timpte, C., Estelle, M., and Reed, J.W. (2000). AXR2 encodes a member of the Aux/IAA protein family. Plant Physiol. *123*, 563–574.

Nagpal, P., Ellis, C.M., Weber, H., Ploense, S.E., Barkawi, L.S., Guilfoyle, T.J., Hagen, G., Alonso, J.M., Cohen, J.D., Farmer, E.E., et al. (2005). Auxin response factors ARF6 and ARF8 promote jasmonic acid production and

flower maturation. Development *132*, 4107–4118.

Naito, T., Yamashino, T., Kiba, T., Koizumi, N., Kojima, M., Sakakibara, H., and Mizuno, T. (2007). A link between cytokinin and ASL9 (ASYMMETRIC LEAVES 2 LIKE 9) that belongs to the AS2/LOB (LATERAL ORGAN BOUNDARIES) family genes in *Arabidopsis thaliana*. Biosci. Biotechnol. Biochem. *71*, 1269–1278.

Nakajima, K., and Benfey, P.N. (2002). Signaling in and out: control of cell division and differentiation in the shoot and root. Plant Cell *14 Suppl*, S265-276.

Nakajima, K., Sena, G., Nawy, T., and Benfey, P.N. (2001). Intercellular movement of the putative transcription factor SHR in root patterning. Nature *413*, 307–311.

Nakata, M., and Ohme-Takagi, M. (2013). Two bHLH-type transcription factors, JA-ASSOCIATED MYC2-LIKE2 and JAM3, are transcriptional repressors and affect male fertility. Plant Signal Behav *8*, e26473.

Nanao, M.H., Vinos-Poyo, T., Brunoud, G., Thévenon, E., Mazzoleni, M., Mast, D., Lainé, S., Wang, S., Hagen, G., Li, H., et al. (2014). Structural basis for oligomerization of auxin transcriptional regulators. Nat Commun *5*, 3617.

Naoi, K., and Hashimoto, T. (2004). A semidominant mutation in an *Arabidopsis* mitogen-activated protein kinase phosphatase-like gene compromises cortical microtubule organization. Plant Cell *16*, 1841–1853.

Niu, Y.F., Chai, R.S., Jin, G.L., Wang, H., Tang, C.X., and Zhang, Y.S. (2013). Responses of root architecture development to low phosphorus availability: a review. Ann Bot *112*, 391–408.

Noodén, L.D., Kahanak, G.M., and Okatan, Y. (1979). Prevention of monocarpic senescence in soybeans with auxin and cytokinin: an antidote for self-destruction. Science *206*, 841–843.

Oh, E., Zhu, J.-Y., Bai, M.-Y., Arenhart, R.A., Sun, Y., and Wang, Z.-Y. (2014a). Cell elongation is regulated through a central circuit of interacting transcription factors in the *Arabidopsis* hypocotyl. Elife *3*.

Oh, E., Zhu, J.-Y., Ryu, H., Hwang, I., and Wang, Z.-Y. (2014b). TOPLESS mediates brassinosteroid-induced transcriptional repression through interaction with BZR1. Nat Commun *5*, 4140.

Ohashi-Ito, K., and Bergmann, D.C. (2007). Regulation of the *Arabidopsis* root vascular initial population by LONESOME HIGHWAY. Development *134*, 2959–2968.

Ohashi-Ito, K., Saegusa, M., Iwamoto, K., Oda, Y., Katayama, H., Kojima, M., Sakakibara, H., and Fukuda, H. (2014). A bHLH complex activates vascular cell division via cytokinin action in root apical meristem. Curr. Biol. *24*, 2053–2058.

Okushima, Y., Overvoorde, P.J., Arima, K., Alonso, J.M., Chan, A., Chang, C., Ecker, J.R., Hughes, B., Lui, A., Nguyen, D., et al. (2005). Functional genomic analysis of the AUXIN RESPONSE FACTOR gene family members in *Arabidopsis thaliana*: unique and overlapping functions of ARF7 and ARF19. Plant Cell *17*, 444–463.

Okushima, Y., Fukaki, H., Onoda, M., Theologis, A., and Tasaka, M. (2007). ARF7 and ARF19 regulate lateral root formation via direct activation of LBD/ASL genes in *Arabidopsis*. Plant Cell *19*, 118–130.

O'Malley, R.C., Huang, S.-S.C., Song, L., Lewsey, M.G., Bartlett, A., Nery, J.R., Galli, M., Gallavotti, A., and Ecker, J.R. (2016). Cistrome and epicistrome features shape the regulatory DNA landscape. Cell *165*, 1280–1292.

Ori, N., Juarez, M.T., Jackson, D., Yamaguchi, J., Banowetz, G.M., and Hake, S. (1999). Leaf senescence is delayed in tobacco plants expressing the maize homeobox gene knotted1 under the control of a senescence-activated promoter. Plant Cell *11*, 1073–1080.

Overvoorde, P., Fukaki, H., and Beeckman, T. (2010). Auxin control of root development. Cold Spring Harb Perspect Biol *2*.

Palmiter, R.D., Sandgren, E.P., Avarbock, M.R., Allen, D.D., and Brinster, R.L. (1991). Heterologous introns can enhance expression of transgenes in mice. Proc. Natl. Acad. Sci. U.S.A. *88*, 478–482.

Pandey, S.P., and Somssich, I.E. (2009). The role of WRKY transcription factors in plant immunity. Plant Physiol. *150*, 1648–1655.

Panne, D., Maniatis, T., and Harrison, S.C. (2007). An atomic model of enhanceosome structure in the vicinity of DNA. Cell *129*, 1111–1123.

Park, S.G., Hannenhalli, S., and Choi, S.S. (2014). Conservation in first introns is positively associated with the number of exons within genes and the presence of regulatory epigenetic signals. BMC Genomics *15*, 526.

Pattanaik, S., Patra, B., Singh, S.K., and Yuan, L. (2014). An overview of the gene regulatory network controlling trichome development in the model plant, *Arabidopsis*. Front Plant Sci *5*, 259.

Pauwels, L., Barbero, G.F., Geerinck, J., Tilleman, S., Grunewald, W., Pérez, A.C., Chico, J.M., Bossche, R.V., Sewell, J., Gil, E., et al. (2010). NINJA connects the co-repressor TOPLESS to jasmonate signalling. Nature *464*, 788–791.

Payne, T., Johnson, S.D., and Koltunow, A.M. (2004). KNUCKLES (KNU) encodes a C2H2 zinc-finger protein that regulates development of basal pattern elements of the *Arabidopsis gynoecium*. Development *131*, 3737–3749.

Peaucelle, A., Braybrook, S.A., Le Guillou, L., Bron, E., Kuhlemeier, C., and Höfte, H. (2011). Pectin-induced changes in cell wall mechanics underlie organ initiation in *Arabidopsis*. Curr. Biol. *21*, 1720–1726.

Perales, M., Rodriguez, K., Snipes, S., Yadav, R.K., Diaz-Mendoza, M., and Reddy, G.V. (2016). Threshold-dependent transcriptional discrimination underlies stem cell homeostasis. Proc. Natl. Acad. Sci. U.S.A. *113*, E6298–E6306.

Péret, B., De Rybel, B., Casimiro, I., Benková, E., Swarup, R., Laplaze, L., Beeckman, T., and Bennett, M.J. (2009). *Arabidopsis* lateral root development: an emerging story. Trends Plant Sci. *14*, 399–408.

Péret, B., Li, G., Zhao, J., Band, L.R., Voß, U., Postaire, O., Luu, D.-T., Da Ines, O., Casimiro, I., Lucas, M., et al. (2012a). Auxin regulates aquaporin function to facilitate lateral root emergence. Nat. Cell Biol. *14*, 991–998.

Péret, B., Swarup, K., Ferguson, A., Seth, M., Yang, Y., Dhondt, S., James, N., Casimiro, I., Perry, P., Syed, A., et al. (2012b). AUX/LAX genes encode a family of auxin influx transporters that perform distinct functions during *Arabidopsis* development. Plant Cell *24*, 2874–2885.

Perrot-Rechenmann, C. (2010). Cellular responses to auxin: division versus expansion. Cold Spring Harb Perspect Biol *2*, a001446.

Petricka, J.J., Winter, C.M., and Benfey, P.N. (2012). Control of *Arabidopsis* root development. Annu Rev Plant Biol *63*, 563–590.

Pi, L., Aichinger, E., van der Graaff, E., Llavata-Peris, C.I., Weijers, D., Hennig, L., Groot, E., and Laux, T. (2015). Organizer-derived WOX5 signal maintains root columella stem cells through chromatin-mediated repression of CDF4 expression. Dev. Cell *33*, 576–588.

Prigge, M.J., Greenham, K., Zhang, Y., Santner, A., Castillejo, C., Mutka, A.M., O'Malley, R.C., Ecker, J.R., Kunkel, B.N., and Estelle, M. (2016). The *Arabidopsis* auxin receptor F-Box proteins AFB4 and AFB5 are required for response to the synthetic auxin picloram. G3 (Bethesda) *6*, 1383–1390.

Przemeck, G.K., Mattsson, J., Hardtke, C.S., Sung, Z.R., and Berleth, T. (1996). Studies on the role of the *Arabidopsis* gene MONOPTEROS in vascular development and plant cell axialization. Planta *200*, 229–237.

Qi, J., Wang, Y., Yu, T., Cunha, A., Wu, B., Vernoux, T., Meyerowitz, E., and Jiao, Y. (2014). Auxin depletion from leaf primordia contributes to organ patterning. Proc. Natl. Acad. Sci. U.S.A. *111*, 18769–18774.

Qi, Y., Wang, S., Shen, C., Zhang, S., Chen, Y., Xu, Y., Liu, Y., Wu, Y., and Jiang, D. (2012). OsARF12, a transcription activator on auxin response gene, regulates root elongation and affects iron accumulation in rice (*Oryza sativa*). New Phytol. *193*, 109–120.

Rackham, O.J.L., Firas, J., Fang, H., Oates, M.E., Holmes, M.L., Knaupp, A.S., FANTOM Consortium, Suzuki, H., Nefzger, C.M., Daub, C.O., et al. (2016). A predictive computational framework for direct reprogramming between human cell types. Nat. Genet. *48*, 331–335.

Rademacher, E.H., Möller, B., Lokerse, A.S., Llavata-Peris, C.I., van den Berg, W., and Weijers, D. (2011). A cellular expression map of the *Arabidopsis* AUXIN RESPONSE FACTOR gene family. Plant J. *68*, 597–606.

Raines, T., Shanks, C., Cheng, C.-Y., McPherson, D., Argueso, C.T., Kim, H.J., Franco-Zorrilla, J.M., López-Vidriero, I., Solano, R., Vaňková, R., et al. (2016). The cytokinin response factors modulate root and shoot growth and promote leaf senescence in *Arabidopsis*. Plant J. *85*, 134–147.

Rashotte, A.M., and Goertzen, L.R. (2010). The CRF domain defines cytokinin response factor proteins in plants. BMC Plant Biol. *10*, 74.

Rashotte, A.M., Mason, M.G., Hutchison, C.E., Ferreira, F.J., Schaller, G.E., and Kieber, J.J. (2006). A subset of *Arabidopsis* AP2 transcription factors mediates cytokinin responses in concert with a two-component pathway. Proc. Natl. Acad. Sci. U.S.A. *103*, 11081–11085.

Raven, J.A. (1975). Transport of indoleacetic acid in plant cells in relation to pH and electrical potential gradients, and its significance for polar IAA transport. New Phytologist *74*, 163–172.

Rayle, D.L., Evans, M.L., and Hertel, R. (1970). Action of auxin on cell elongation. Proc Natl Acad Sci U S A *65*, 184–191.

Reddy, G.V., Heisler, M.G., Ehrhardt, D.W., and Meyerowitz, E.M. (2004). Real-time lineage analysis reveals oriented cell divisions associated with morphogenesis at the shoot apex of *Arabidopsis thaliana*. Development *131*, 4225–4237.

Reece-Hoyes, J.S., and Walhout, A.J.M. (2012). Gene-centered yeast one-hybrid assays. Methods Mol. Biol. *812*, 189–208.

Reece-Hoyes, J.S., Barutcu, A.R., McCord, R.P., Jeong, J.S., Jiang, L., MacWilliams, A., Yang, X., Salehi-Ashtiani, K., Hill, D.E., Blackshaw, S., et al. (2011). Yeast one-hybrid assays for gene-centered human gene regulatory network mapping. Nat Methods *8*, 1050–1052.

Reinhardt, D., Mandel, T., and Kuhlemeier, C. (2000). Auxin regulates the initiation and radial position of plant lateral organs. Plant Cell *12*, 507–518.

Reinhardt, D.H., and Rost, T.L. (1995). On the correlation of primary root growth and tracheary element size and distance from the tip in cotton seedlings grown under salinity. Environmental and Experimental Botany *35*, 575–588.

Reinhardt, D., Pesce, E.-R., Stieger, P., Mandel, T., Baltensperger, K., Bennett, M., Traas, J., Friml, J., and Kuhlemeier, C. (2003). Regulation of phyllotaxis by polar auxin transport. Nature *426*, 255–260.

Remington, D.L., Vision, T.J., Guilfoyle, T.J., and Reed, J.W. (2004). Contrasting modes of diversification in the Aux/IAA and ARF gene families. Plant Physiol. *135*, 1738–1752.

Richmond, A.E., and Lang, A. (1957). Effect of kinetin on protein content and survival of detached *Xanthium* leaves. Science *125*, 650–651.

Rose, A.B., and Last, R.L. (1997). Introns act post-transcriptionally to increase expression of the *Arabidopsis thaliana* tryptophan pathway gene PAT1. Plant J. *11*, 455–464.

Rose, A.B. (2008). Intron-Mediated Regulation of Gene Expression. In Nuclear Pre-mRNA Processing in Plants, (Springer, Berlin, Heidelberg), pp. 277–290.

Rose, A.B., Elfersi, T., Parra, G., and Korf, I. (2008). Promoter-proximal introns in *Arabidopsis thaliana* are enriched in dispersed signals that elevate gene expression. Plant Cell *20*, 543–551.

Rosenfeld, N., Elowitz, M.B., and Alon, U. (2002). Negative autoregulation speeds the response times of transcription networks. J. Mol. Biol. *323*, 785–793.

Rost, T.L. (2011). The organization of roots of dicotyledonous plants and the positions of control points. Ann. Bot. *107*, 1213–1222.

Rousseaux, M.C., Hall, A.J., and Sánchez, R.A. (1996). Far-red enrichment and photosynthetically active radiation level influence leaf senescence in field-grown sunflower. Physiologia Plantarum *96*, 217–224.

Rozier, F., Mirabet, V., Vernoux, T., and Das, P. (2014). Analysis of 3D gene expression patterns in plants using whole-mount RNA in situ hybridization. Nat Protoc *9*, 2464–2475.

Rubery, P.H., and Sheldrake, A.R. (1973). Effect of pH and surface charge on cell uptake of auxin. Nature New Biol. *244*, 285–288.

Rubery, P.H., and Sheldrake, A.R. (1974). Carrier-mediated auxin transport. Planta *118*, 101–121.

Ruegger, M., Dewey, E., Gray, W.M., Hobbie, L., Turner, J., and Estelle, M. (1998). The TIR1 protein of *Arabidopsis* functions in auxin response and is related to human SKP2 and yeast grr1p. Genes Dev. *12*, 198–207.

Sabatini, S., Heidstra, R., Wildwater, M., and Scheres, B. (2003). SCARECROW is involved in positioning the stem cell niche in the Arabidopsis root meristem. Genes Dev. *17*, 354–358.

Sakai, T., and Haga, K. (2012). Molecular genetic analysis of phototropism in *Arabidopsis*. Plant Cell Physiol. *53*, 1517–1534.

Sakakibara, H. (2006). Cytokinins: activity, biosynthesis, and translocation. Annu Rev Plant Biol *57*, 431–449.

Sakuma, Y., Liu, Q., Dubouzet, J.G., Abe, H., Shinozaki, K., and Yamaguchi-Shinozaki, K. (2002). DNA-binding specificity of the ERF/AP2 domain of *Arabidopsis* DREBs, transcription factors involved in dehydration- and cold-inducible gene expression. Biochem. Biophys. Res. Commun. *290*, 998–1009.

Sakuma, Y., Maruyama, K., Osakabe, Y., Qin, F., Seki, M., Shinozaki, K., and Yamaguchi-Shinozaki, K. (2006). Functional analysis of an *Arabidopsis* transcription factor, DREB2A, involved in drought-responsive gene expression. Plant Cell *18*, 1292–1309.

Salehin, M., Bagchi, R., and Estelle, M. (2015). SCFTIR1/AFB-based auxin perception: mechanism and role in plant growth and development. Plant Cell *27*, 9–19.

Salopek-Sondi, B., Pavlović, I., Smolko, A., and Šamec, D. (2017). Auxin as a mediator of abiotic stress responses. In mechanism of plant hormone signaling under stress, (Wiley-Blackwell), pp. 1–36.

Sánchez-Calderón, L., López-Bucio, J., Chacón-López, A., Cruz-Ramírez, A., Nieto-Jacobo, F., Dubrovsky, J.G., and Herrera-Estrella, L. (2005). Phosphate starvation induces a determinate developmental program in the roots of *Arabidopsis thaliana*. Plant Cell Physiol. *46*, 174–184.

Sandmann, T., Girardot, C., Brehme, M., Tongprasit, W., Stolc, V., and Furlong, E.E.M. (2007). A core transcriptional network for early mesoderm development in *Drosophila melanogaster*. Genes Dev *21*, 436–449.

Sarkar, A.K., Luijten, M., Miyashima, S., Lenhard, M., Hashimoto, T., Nakajima, K., Scheres, B., Heidstra, R., and Laux, T. (2007). Conserved factors regulate signalling in *Arabidopsis thaliana* shoot and root stem cell organizers. Nature *446*, 811–814.

Sasaki-Sekimoto, Y., Jikumaru, Y., Obayashi, T., Saito, H., Masuda, S., Kamiya, Y., Ohta, H., and Shirasu, K. (2013). Basic helix-loop-helix transcription factors JASMONATE-ASSOCIATED MYC2-LIKE1 (JAM1), JAM2, and JAM3 are negative regulators of jasmonate responses in *Arabidopsis*. Plant Physiol. *163*, 291–304.

Sasaki-Sekimoto, Y., Saito, H., Masuda, S., Shirasu, K., and Ohta, H. (2014). Comprehensive analysis of protein interactions between JAZ proteins and bHLH transcription factors that negatively regulate jasmonate signaling. Plant Signal Behav *9*, e27639.

Sato, E.M., Hijazi, H., Bennett, M.J., Vissenberg, K., and Swarup, R. (2015). New insights into root gravitropic signalling. J. Exp. Bot. *66*, 2155–2165.

Sauer, M., Robert, S., and Kleine-Vehn, J. (2013). Auxin: simply complicated. J Exp Bot *64*, 2565–2577.

Schaller, G.E., Bishopp, A., and Kieber, J.J. (2015). The yin-yang of hormones: cytokinin and auxin interactions in plant development. Plant Cell *27*, 44–63.

Schlereth, A., Möller, B., Liu, W., Kientz, M., Flipse, J., Rademacher, E.H., Schmid, M., Jürgens, G., and Weijers, D. (2010). MONOPTEROS controls embryonic root initiation by regulating a mobile transcription factor. Nature *464*, 913–916.

Schoof, H., Lenhard, M., Haecker, A., Mayer, K.F., Jürgens, G., and Laux, T. (2000). The stem cell population of *Arabidopsis* shoot meristems in maintained by a regulatory loop between the CLAVATA and WUSCHEL genes. Cell *100*, 635–644.

Scohy, S., Gabant, P., Szpirer, C., and Szpirer, J. (2000). Identification of an enhancer and an alternative promoter in the first intron of the alpha-fetoprotein gene. Nucleic Acids Res. *28*, 3743–3751.

Sebastian, J., Ryu, K.H., Zhou, J., Tarkowská, D., Tarkowski, P., Cho, Y.-H., Yoo, S.-D., Kim, E.-S., and Lee, J.-Y. (2015). PHABULOSA controls the quiescent center-independent root meristem activities in *Arabidopsis thaliana*. PLOS Genetics *11*, e1004973.

Serrano-Mislata, A., Schiessl, K., and Sablowski, R. (2015). Active control of cell size generates spatial detail during plant organogenesis. Curr. Biol. *25*, 2991–2996.

Shen, C., Wang, S., Bai, Y., Wu, Y., Zhang, S., Chen, M., Guilfoyle, T.J., Wu, P., and Qi, Y. (2010). Functional analysis of the structural domain of ARF proteins in rice (*Oryza sativa* L.). J. Exp. Bot. *61*, 3971–3981.

Shen-Orr, S.S., Milo, R., Mangan, S., and Alon, U. (2002). Network motifs in the transcriptional regulation network of *Escherichia coli*. Nat. Genet. *31*, 64–68.

Shi, B., Zhang, C., Tian, C., Wang, J., Wang, Q., Xu, T., Xu, Y., Ohno, C., Sablowski, R., Heisler, M.G., et al. (2016). Two-Step regulation of a meristematic cell population acting in shoot branching in *Arabidopsis*. PLoS Genet *12*.

Shi, H., Zhong, S., Mo, X., Liu, N., Nezames, C.D., and Deng, X.W. (2013). HFR1 sequesters PIF1 to govern the transcriptional network underlying light-initiated seed germination in *Arabidopsis*. Plant Cell *25*, 3770–3784.

Shikata, M., Koyama, T., Mitsuda, N., and Ohme-Takagi, M. (2009). Arabidopsis SBP-box genes SPL10, SPL11 and SPL2 control morphological change in association with shoot maturation in the reproductive phase. Plant Cell Physiol. *50*, 2133–2145.

Shimizu-Sato, S., Tanaka, M., and Mori, H. (2009). Auxin-cytokinin interactions in the control of shoot branching. Plant Mol. Biol. *69*, 429–435.

Shirozu, R., Yashiroda, H., and Murata, S. (2015). Identification of minimum Rpn4-responsive elements in genes related to proteasome functions. FEBS Lett. *589*, 933–940.

Shoji, K., Addicott, F.T., and Swets, W.A. (1951). Auxin in relation to leaf blade abscission. Plant Physiol *26*, 189–191.

Siemens, H., Jackstadt, R., Hünten, S., Kaller, M., Menssen, A., Götz, U., and Hermeking, H. (2011). miR-34 and SNAIL form a double-negative feedback loop to regulate epithelial-mesenchymal transitions. Cell Cycle *10*, 4256–4271.

Šimášková, M., O'Brien, J.A., Khan, M., Van Noorden, G., Ötvös, K., Vieten, A., De Clercq, I., Van Haperen, J.M.A., Cuesta, C., Hoyerová, K., et al. (2015). Cytokinin response factors regulate PIN-FORMED auxin transporters. Nat Commun *6*, 8717.

Simon, S., and Petrášek, J. (2011). Why plants need more than one type of auxin. Plant Sci. *180*, 454–460.

Singh, S., Letham, D.S., and Palni, L.M.S. (1992). Cytokinin biochemistry in relation to leaf senescence. VIII. Translocation, metabolism and biosynthesis of cytokinins in relation to sequential leaf senescence of tobacco. Physiologia Plantarum *86*, 398–406.

Slack, J.M.W. (2009). Essential Developmental Biology (John Wiley & Sons).

Smith, R.S., Guyomarc'h, S., Mandel, T., Reinhardt, D., Kuhlemeier, C., and Prusinkiewicz, P. (2006). A plausible model of phyllotaxis. Proc. Natl. Acad. Sci. U.S.A. *103*, 1301–1306.

Song, S., Qi, T., Fan, M., Zhang, X., Gao, H., Huang, H., Wu, D., Guo, H., and Xie, D. (2013). The bHLH subgroup IIId factors negatively regulate jasmonate-mediated plant defense and development. PLoS Genet. *9*, e1003653.

Sparks, E.E., Drapek, C., Gaudinier, A., Li, S., Ansariola, M., Shen, N., Hennacy, J.H., Zhang, J., Turco, G., Petricka, J.J., et al. (2016). Establishment of expression in the SHORTROOT-SCARECROW transcriptional cascade through opposing activities of both activators and repressors. Dev. Cell *39*, 585–596.

Sridhar, V.V., Surendrarao, A., Gonzalez, D., Conlan, R.S., and Liu, Z. (2004). Transcriptional repression of target genes by LEUNIG and SEUSS, two interacting regulatory proteins for *Arabidopsis* flower development. Proc Natl

Acad Sci U S A *101*, 11494–11499.

Srinivasan, K., Leone, D.P., Bateson, R.K., Dobreva, G., Kohwi, Y., Kohwi-Shigematsu, T., Grosschedl, R., and McConnell, S.K. (2012). A network of genetic repression and derepression specifies projection fates in the developing neocortex. Proc. Natl. Acad. Sci. U.S.A. *109*, 19071–19078.

Stals, H., and Inzé, D. (2001). When plant cells decide to divide. Trends Plant Sci. *6*, 359–364.

Stewart, A.J., Hannenhalli, S., and Plotkin, J.B. (2012). Why transcription factor binding sites are ten nucleotides long. Genetics *192*, 973–985.

Stoma, S., Lucas, M., Chopard, J., Schaedel, M., Traas, J., and Godin, C. (2008). Flux-based transport enhancement as a plausible unifying mechanism for auxin transport in meristem development. PLoS Comput. Biol. *4*, e1000207.

Striberny, B., Melton, A.E., Schwacke, R., Krause, K., Fischer, K., Goertzen, L.R., and Rashotte, A.M. (2017). Cytokinin Response Factor 5 has transcriptional activity governed by its C-terminal domain. Plant Signal Behav *12*, e1276684.

Su, Y.-H., Liu, Y.-B., and Zhang, X.-S. (2011). Auxin-cytokinin interaction regulates meristem development. Mol Plant *4*, 616–625.

Sumimoto, H., Kamakura, S., and Ito, T. (2007). Structure and function of the PB1 domain, a protein interaction module conserved in animals, fungi, amoebas, and plants. Sci. STKE *2007*, re6.

Sun, B., Xu, Y., Ng, K.-H., and Ito, T. (2009). A timing mechanism for stem cell maintenance and differentiation in the *Arabidopsis* floral meristem. Genes Dev. *23*, 1791–1804.

Svistoonoff, S., Creff, A., Reymond, M., Sigoillot-Claude, C., Ricaud, L., Blanchet, A., Nussaume, L., and Desnos, T. (2007). Root tip contact with low-phosphate media reprograms plant root architecture. Nat. Genet. *39*, 792–796.

Szemenyei, H., Hannon, M., and Long, J.A. (2008). TOPLESS mediates auxin-dependent transcriptional repression during *Arabidopsis* embryogenesis. Science *319*, 1384–1386.

Szymanski, P., and Levine, M. (1995). Multiple modes of dorsal-bHLH transcriptional synergy in the *Drosophila* embryo. EMBO J. *14*, 2229–2238.

Takahashi, K., and Yamanaka, S. (2006). Induction of pluripotent stem cells from mouse embryonic and adult fibroblast cultures by defined factors. Cell *126*, 663–676.

Tan, X., Calderon-Villalobos, L.I.A., Sharon, M., Zheng, C., Robinson, C.V., Estelle, M., and Zheng, N. (2007). Mechanism of auxin perception by the TIR1 ubiquitin ligase. Nature *446*, 640–645.

Taylor-Teeples, M., Lin, L., de Lucas, M., Turco, G., Toal, T.W., Gaudinier, A., Young, N.F., Trabucco, G.M., Veling, M.T., Lamothe, R., et al. (2015). An *Arabidopsis* gene regulatory network for secondary cell wall synthesis. Nature *517*, 571–575.

Thanos, D., and Maniatis, T. (1995). Virus induction of human IFN beta gene expression requires the assembly of an enhanceosome. Cell *83*, 1091–1100.

Tian, Q., and Reed, J.W. (1999). Control of auxin-regulated root development by the *Arabidopsis thaliana* SHY2/IAA3 gene. Development *126*, 711–721.

Tian, C.-E., Muto, H., Higuchi, K., Matamura, T., Tatematsu, K., Koshiba, T., and Yamamoto, K.T. (2004). Disruption and overexpression of Auxin Response Factor 8 gene of *Arabidopsis* affect hypocotyl elongation and root growth habit, indicating its possible involvement in auxin homeostasis in light condition. Plant J. *40*, 333–343.

Tiwari, S.B., Hagen, G., and Guilfoyle, T. (2003). The roles of auxin response factor domains in auxin-responsive transcription. Plant Cell *15*, 533–543.

To, J.P.C., and Kieber, J.J. (2008). Cytokinin signaling: two-components and more. Trends Plant Sci. *13*, 85–92.

Tourmente, S., Chapel, S., Dreau, D., Drake, M.E., Bruhat, A., Couderc, J.L., and Dastugue, B. (1993). Enhancer and silencer elements within the first intron mediate the transcriptional regulation of the beta 3 tubulin gene by 20-

hydroxyecdysone in *Drosophila* Kc cells. Insect Biochem. Mol. Biol. *23*, 137–143.

Traas, J. (2013). Phyllotaxis. Development *140*, 249–253.

Tréhin, C., Planchais, S., Glab, N., Perennes, C., Tregear, J., and Bergounioux, C. (1998). Cell cycle regulation by plant growth regulators: involvement of auxin and cytokinin in the re-entry of *Petunia* protoplasts into the cell cycle. Planta *206*, 215–224.

Trichas, G., Begbie, J., and Srinivas, S. (2008). Use of the viral 2A peptide for bicistronic expression in transgenic mice. BMC Biol *6*, 40.

Truskina, J., and Vernoux, T. (2018). The growth of a stable stationary structure: coordinating cell behavior and patterning at the shoot apical meristem. Curr. Opin. Plant Biol. *41*, 83–88.

Ubeda-Tomás, S., Beemster, G.T.S., and Bennett, M.J. (2012). Hormonal regulation of root growth: integrating local activities into global behaviour. Trends Plant Sci. *17*, 326–331.

Ulmasov, T., Liu, Z.B., Hagen, G., and Guilfoyle, T.J. (1995). Composite structure of auxin response elements. The Plant Cell *7*, 1611–1623.

Ulmasov, T., Murfett, J., Hagen, G., and Guilfoyle, T.J. (1997). Aux/IAA proteins repress expression of reporter genes containing natural and highly active synthetic auxin response elements. The Plant Cell *9*, 1963–1971.

Ulmasov, T., Hagen, G., and Guilfoyle, T.J. (1999). Activation and repression of transcription by auxin-response factors. Proc. Natl. Acad. Sci. U.S.A. *96*, 5844–5849.

Uyttewaal, M., Burian, A., Alim, K., Landrein, B., Borowska-Wykręt, D., Dedieu, A., Peaucelle, A., Ludynia, M., Traas, J., Boudaoud, A., et al. (2012). Mechanical stress acts via katanin to amplify differences in growth rate between adjacent cells in *Arabidopsis.* Cell *149*, 439–451.

Van Norman, J.M., Breakfield, N.W., and Benfey, P.N. (2011). Intercellular communication during plant development. Plant Cell *23*, 855–864.

Vanneste, S., Maes, L., Smet, I.D., Himanen, K., Naudts, M., Inzé, D., and Beeckman, T. (2005). Auxin regulation of cell cycle and its role during lateral root initiation. Physiologia Plantarum *123*, 139–146.

Vasil, V., Clancy, M., Ferl, R.J., Vasil, I.K., and Hannah, L.C. (1989). Increased gene expression by the first intron of maize shrunken-1 locus in grass species. Plant Physiol. *91*, 1575–1579.

Vaughan-Hirsch, J., Goodall, B., and Bishopp, A. (2018). North, East, South, West: mapping vascular tissues onto the *Arabidopsis* root. Curr. Opin. Plant Biol. *41*, 16–22.

Vermeirssen, V., Barrasa, M.I., Hidalgo, C.A., Babon, J.A.B., Sequerra, R., Doucette-Stamm, L., Barabási, A.-L., and Walhout, A.J.M. (2007). Transcription factor modularity in a gene-centered *C. elegans* core neuronal protein-DNA interaction network. Genome Res. *17*, 1061–1071.

Vernoux, T., Besnard, F., and Traas, J. (2010). Auxin at the shoot apical meristem. Cold Spring Harb Perspect Biol *2*, a001487.

Vernoux, T., Brunoud, G., Farcot, E., Morin, V., Van den Daele, H., Legrand, J., Oliva, M., Das, P., Larrieu, A., Wells, D., et al. (2011). The auxin signalling network translates dynamic input into robust patterning at the shoot apex. Mol. Syst. Biol. *7*, 508.

Vierbuchen, T., Ostermeier, A., Pang, Z.P., Kokubu, Y., Südhof, T.C., and Wernig, M. (2010). Direct conversion of fibroblasts to functional neurons by defined factors. Nature *463*, 1035–1041.

Vieten, A., Vanneste, S., Wisniewska, J., Benková, E., Benjamins, R., Beeckman, T., Luschnig, C., and Friml, J. (2005). Functional redundancy of PIN proteins is accompanied by auxin-dependent cross-regulation of PIN expression. Development *132*, 4521–4531.

Wang, D., Pei, K., Fu, Y., Sun, Z., Li, S., Liu, H., Tang, K., Han, B., and Tao, Y. (2007). Genome-wide analysis of the auxin response factors (ARF) gene family in rice (*Oryza sativa*). Gene *394*, 13–24.

Wang, J., Zhuang, J., Iyer, S., Lin, X., Whitfield, T.W., Greven, M.C., Pierce, B.G., Dong, X., Kundaje, A., Cheng, Y., et al. (2012). Sequence features and chromatin structure around the genomic regions bound by 119 human

transcription factors. Genome Res. *22*, 1798–1812.

Wang, L., Kim, J., and Somers, D.E. (2013). Transcriptional corepressor TOPLESS complexes with pseudoresponse regulator proteins and histone deacetylases to regulate circadian transcription. Proc. Natl. Acad. Sci. U.S.A. *110*, 761–766.

Wang, Q., Kohlen, W., Rossmann, S., Vernoux, T., and Theres, K. (2014a). Auxin depletion from the leaf axil conditions competence for axillary meristem formation in *Arabidopsis* and tomato. Plant Cell *26*, 2068–2079.

Wang, Y., Wang, J., Shi, B., Yu, T., Qi, J., Meyerowitz, E.M., and Jiao, Y. (2014b). The stem cell niche in leaf axils is established by auxin and cytokinin in *Arabidopsis*. Plant Cell *26*, 2055–2067.

Wang, Z.-P., Xing, H.-L., Dong, L., Zhang, H.-Y., Han, C.-Y., Wang, X.-C., and Chen, Q.-J. (2015). Egg cell-specific promoter-controlled CRISPR/Cas9 efficiently generates homozygous mutants for multiple target genes in *Arabidopsis* in a single generation. Genome Biol. *16*, 144.

von Wangenheim, D., Fangerau, J., Schmitz, A., Smith, R.S., Leitte, H., Stelzer, E.H.K., and Maizel, A. (2016). Rules and self-organizing properties of post-embryonic plant organ cell division patterns. Curr. Biol. *26*, 439–449.

Watahiki, M.K., and Yamamoto, K.T. (1997). The *massugu1* mutation of *Arabidopsis* identified with failure of auxin-induced growth curvature of hypocotyl confers auxin insensitivity to hypocotyl and leaf. Plant Physiol. *115*, 419–426.

Wei, S., Xi, Y.-Z., Song, D.-P., Wei, H., Gruber, M.Y., Gao, M.-J., Parkin, I., Kachatourians, G., and Hannoufa, A. (2015). Quantitative and structural analyses of T-DNA tandem repeats in transgenic SK mutant lines. Plant Cell Tiss Organ Cult *123*, 183–192.

Weijers, D., Schlereth, A., Ehrismann, J.S., Schwank, G., Kientz, M., and Jürgens, G. (2006). Auxin triggers transient local signaling for cell specification in *Arabidopsis* embryogenesis. Dev. Cell *10*, 265–270.

Willemsen, V., Bauch, M., Bennett, T., Campilho, A., Wolkenfelt, H., Xu, J., Haseloff, J., and Scheres, B. (2008). The NAC domain transcription factors FEZ and SOMBRERO control the orientation of cell division plane in *Arabidopsis* root stem cells. Dev. Cell *15*, 913–922.

Williamson, L.C., Ribrioux, S.P.C.P., Fitter, A.H., and Leyser, H.M.O. (2001). Phosphate availability regulates root system architecture in *Arabidopsis*. Plant Physiology *126*, 875–882.

Willis, L., Refahi, Y., Wightman, R., Landrein, B., Teles, J., Huang, K.C., Meyerowitz, E.M., and Jönsson, H. (2016). Cell size and growth regulation in the *Arabidopsis thaliana* apical stem cell niche. Proc. Natl. Acad. Sci. U.S.A. *113*, E8238–E8246.

Wilmoth, J.C., Wang, S., Tiwari, S.B., Joshi, A.D., Hagen, G., Guilfoyle, T.J., Alonso, J.M., Ecker, J.R., and Reed, J.W. (2005). NPH4/ARF7 and ARF19 promote leaf expansion and auxin-induced lateral root formation. Plant J. *43*, 118–130.

Winkler, M., Niemeyer, M., Hellmuth, A., Janitza, P., Christ, G., Samodelov, S.L., Wilde, V., Majovsky, P., Trujillo, M., Zurbriggen, M.D., et al. (2017). Variation in auxin sensing guides AUX/IAA transcriptional repressor ubiquitylation and destruction. Nat Commun *8*, 15706.

Winter, D., Vinegar, B., Nahal, H., Ammar, R., Wilson, G.V., and Provart, N.J. (2007). An “Electronic Fluorescent Pictograph” browser for exploring and analyzing large-scale biological data sets. PLoS ONE *2*, e718.

Woo, H.R., Chung, K.M., Park, J.H., Oh, S.A., Ahn, T., Hong, S.H., Jang, S.K., and Nam, H.G. (2001). ORE9, an F-box protein that regulates leaf senescence in *Arabidopsis*. Plant Cell *13*, 1779–1790.

Woolhouse, H.W. (1984). The biochemistry and regulation of senescence in chloroplasts. Can. J. Bot. *62*, 2934–2942.

Wu, M.-F., Tian, Q., and Reed, J.W. (2006). Arabidopsis microRNA167 controls patterns of ARF6 and ARF8 expression, and regulates both female and male reproduction. Development *133*, 4211–4218.

Xie, Y., and Varshavsky, A. (2001). RPN4 is a ligand, substrate, and transcriptional regulator of the 26S proteasome: a negative feedback circuit. Proc. Natl. Acad. Sci. U.S.A. *98*, 3056–3061.

Xie, Y., Huhn, K., Brandt, R., Potschin, M., Bieker, S., Straub, D., Doll, J., Drechsler, T., Zentgraf, U., and Wenkel,

S. (2014). REVOLUTA and WRKY53 connect early and late leaf development in *Arabidopsis*. Development *141*, 4772–4783.

Xin, W., Wang, Z., Liang, Y., Wang, Y., and Hu, Y. (2017). Dynamic expression reveals a two-step patterning of WUS and CLV3 during axillary shoot meristem formation in *Arabidopsis*. J. Plant Physiol. *214*, 1–6.

Xing, S., Salinas, M., Höhmann, S., Berndtgen, R., and Huijser, P. (2010). miR156-targeted and nontargeted SBP-box transcription factors act in concert to secure male fertility in *Arabidopsis*. Plant Cell *22*, 3935–3950.

Xiong, W., and Ferrell, J.E. (2003). A positive-feedback-based bistable "memory module" that governs a cell fate decision. Nature *426*, 460–465.

Xiong, Y., Contento, A.L., and Bassham, D.C. (2005). AtATG18a is required for the formation of autophagosomes during nutrient stress and senescence in *Arabidopsis thaliana*. Plant J. *42*, 535–546.

Yadav, R.K., Girke, T., Pasala, S., Xie, M., and Reddy, G.V. (2009). Gene expression map of the *Arabidopsis* shoot apical meristem stem cell niche. Proc. Natl. Acad. Sci. U.S.A. *106*, 4941–4946.

Yadav, R.K., Perales, M., Gruel, J., Girke, T., Jönsson, H., and Reddy, G.V. (2011). WUSCHEL protein movement mediates stem cell homeostasis in the *Arabidopsis* shoot apex. Genes Dev. *25*, 2025–2030.

Yadav, R.K., Perales, M., Gruel, J., Ohno, C., Heisler, M., Girke, T., Jönsson, H., and Reddy, G.V. (2013). Plant stem cell maintenance involves direct transcriptional repression of differentiation program. Mol. Syst. Biol. *9*, 654.

Yadav, R.K., Tavakkoli, M., Xie, M., Girke, T., and Reddy, G.V. (2014). A high-resolution gene expression map of the *Arabidopsis* shoot meristem stem cell niche. Development *141*, 2735–2744.

Yamaguchi, N., Wu, M.-F., Winter, C.M., Berns, M.C., Nole-Wilson, S., Yamaguchi, A., Coupland, G., Krizek, B.A., and Wagner, D. (2013). A molecular framework for auxin-mediated initiation of flower primordia. Dev. Cell *24*, 271–282.

Yanagisawa, S., and Schmidt, R.J. (1999). Diversity and similarity among recognition sequences of Dof transcription factors. Plant J. *17*, 209–214.

Yang, M., and Jiao, Y. (2016). Regulation of axillary meristem initiation by transcription factors and plant hormones. Front Plant Sci *7*.

Yang, M., Li, S.-N., Anjum, K.M., Gui, L.-X., Zhu, S.-S., Liu, J., Chen, J.-K., Liu, Q.-F., Ye, G.-D., Wang, W.-J., et al. (2013). A double-negative feedback loop between Wnt-β-catenin signaling and HNF4α regulates epithelial-mesenchymal transition in hepatocellular carcinoma. J. Cell. Sci. *126*, 5692–5703.

Yeger-Lotem, E., Sattath, S., Kashtan, N., Itzkovitz, S., Milo, R., Pinter, R.Y., Alon, U., and Margalit, H. (2004). Network motifs in integrated cellular networks of transcription-regulation and protein-protein interaction. Proc. Natl. Acad. Sci. U.S.A. *101*, 5934–5939.

Yokoyama, A., Yamashino, T., Amano, Y.-I., Tajima, Y., Imamura, A., Sakakibara, H., and Mizuno, T. (2007). Type-B ARR transcription factors, ARR10 and ARR12, are implicated in cytokinin-mediated regulation of protoxylem differentiation in roots of *Arabidopsis thaliana*. Plant Cell Physiol. *48*, 84–96.

Yoshida, S., Ito, M., Nishida, I., and Watanabe, A. (2002). Identification of a novel gene HYS1/CPR5 that has a repressive role in the induction of leaf senescence and pathogen-defence responses in *Arabidopsis thaliana*. Plant J. *29*, 427–437.

Yoshida, S., Saiga, S., and Weijers, D. (2013). Auxin regulation of embryonic root formation. Plant Cell Physiol. *54*, 325–332.

Yoshida, S., Barbier de Reuille, P., Lane, B., Bassel, G.W., Prusinkiewicz, P., Smith, R.S., and Weijers, D. (2014). Genetic control of plant development by overriding a geometric division rule. Dev. Cell *29*, 75–87.

Yoshida, T., Fujita, Y., Sayama, H., Kidokoro, S., Maruyama, K., Mizoi, J., Shinozaki, K., and Yamaguchi-Shinozaki, K. (2010). AREB1, AREB2, and ABF3 are master transcription factors that cooperatively regulate ABRE-dependent ABA signaling involved in drought stress tolerance and require ABA for full activation. Plant J. *61*, 672–685.

Yu, C.-P., Lin, J.-J., and Li, W.-H. (2016). Positional distribution of transcription factor binding sites in *Arabidopsis*

thaliana. Sci Rep *6*, 25164.

Zhang, G., Li, X., Cao, H., Zhao, H., and Geller, A.I. (2011). The vesicular glutamate transporter-1 upstream promoter and first intron each support glutamatergic-specific expression in rat postrhinal cortex. Brain Res. *1377*, 1–12.

Zhang, J.-Y., He, S.-B., Li, L., and Yang, H.-Q. (2014). Auxin inhibits stomatal development through MONOPTEROS repression of a mobile peptide gene STOMAGEN in mesophyll. PNAS *111*, E3015–E3023.

Zhang, W., Swarup, R., Bennett, M., Schaller, G.E., and Kieber, J.J. (2013). Cytokinin induces cell division in the quiescent center of the *Arabidopsis* root apical meristem. Curr. Biol. *23*, 1979–1989.

Zhang, Z., Tucker, E., Hermann, M., and Laux, T. (2017). A molecular framework for the embryonic initiation of shoot meristem stem cells. Dev. Cell *40*, 264–277.e4.

Zhao, Y. (2012). Auxin biosynthesis: a simple two-step pathway converts tryptophan to indole-3-acetic acid in plants. Mol Plant *5*, 334–338.

Zhao, Z., Andersen, S.U., Ljung, K., Dolezal, K., Miotk, A., Schultheiss, S.J., and Lohmann, J.U. (2010). Hormonal control of the shoot stem-cell niche. Nature *465*, 1089–1092.

Zheng, Z., Qamar, S.A., Chen, Z., and Mengiste, T. (2006). *Arabidopsis* WRKY33 transcription factor is required for resistance to necrotrophic fungal pathogens. Plant J. *48*, 592–605.

Zhou, Z., Sun, L., Zhao, Y., An, L., Yan, A., Meng, X., and Gan, Y. (2013). Zinc Finger Protein 6 (ZFP6) regulates trichome initiation by integrating gibberellin and cytokinin signaling in *Arabidopsis thaliana*. New Phytol. *198*, 699–708.

Zhu, T., O'Quinn, R.L., Lucas, W.J., and Rost, T.L. (1998). Directional cell-to-cell communication in the *Arabidopsis* root apical meristem II. Dynamics of plasmodesmatal formation. Protoplasma *204*, 84–93.

Zhu, Z., Xu, F., Zhang, Y., Cheng, Y.T., Wiermer, M., Li, X., and Zhang, Y. (2010). *Arabidopsis* resistance protein SNC1 activates immune responses through association with a transcriptional corepressor. Proc. Natl. Acad. Sci. U.S.A. *107*, 13960–13965.

Zinzen, R.P., Senger, K., Levine, M., and Papatsenko, D. (2006). Computational models for neurogenic gene expression in the *Drosophila* embryo. Curr. Biol. *16*, 1358–1365.

Zouine, M., Fu, Y., Chateigner-Boutin, A.-L., Mila, I., Frasse, P., Wang, H., Audran, C., Roustan, J.-P., and Bouzayen, M. (2014). Characterization of the tomato ARF gene family uncovers a multi-levels post-transcriptional regulation including alternative splicing. PLoS ONE *9*, e84203.

Zürcher, E., Tavor-Deslex, D., Lituiev, D., Enkerli, K., Tarr, P.T., and Müller, B. (2013). A robust and sensitive synthetic sensor to monitor the transcriptional output of the cytokinin signaling network in planta. Plant Physiol. *161*, 1066–1075.

Zwack, P.J., and Rashotte, A.M. (2013). Cytokinin inhibition of leaf senescence. Plant Signal Behav *8*, e24737.

Zwack, P.J., Robinson, B.R., Risley, M.G., and Rashotte, A.M. (2013). Cytokinin response factor 6 negatively regulates leaf senescence and is induced in response to cytokinin and numerous abiotic stresses. Plant Cell Physiol. *54*, 971–981.